AN ABSTRACT OF THE THESIS OF

Endalkachew Sahle-Demessie for the degree of Doctor of Philosophy in Chemical Engineering presented on May 6, 1994.

Title: Deposition of Chemicals in Semi-porous Solids Using Supercritical Fluid Carriers.

Abstract approved: _____

Keith L. Levien

Supercritical chemical deposition is a novel concept that uses a fluid above its critical point to deliver a chemical into semi-porous solid and offers the potential for producing unique high-value products. Pure or modified supercritical carbon dioxide was used to first dissolve organic and organo-metallic biocides. A saturated supercritical fluid (SCF) mixture was then allowed to permeate into a semi-porous matrix (wood). The solubility of the solute was subsequently reduced, by decreasing pressure or temperature, which caused depositing the solute within the porous matrix.

Solubilities of nine commonly used biocides were measured and SCF deposition of four of them: IPBC *(3-Iodo-2-propynyl butyl carbamate)*, PCP *(pentachlorophenol)*, TCMTB *(2-(Thiocyanomethylthio) benzothiazole)*, and tebuconazole *(α-[2-(4-chlorophenyl)ethyl] -α- (1,1-dimethylethyl)-1H-1,2,4-triazole-1-ethanol)*, in Douglas-fir heartwood and ponderosa pine sapwood were studied. Distributions of IPBC and PCP in the treated wood were analyzed using neutron activation analysis and x-ray fluorescence analysis, respectively. Samples taken from different portions of TCMTB or tebuconazole treated

wood were ground, extracted and analyzed using HPLC to determine levels of loading.

Deposition amounts were influenced by the solvent properties (density, temperature and composition), solute chemistry and the porous solid characteristics for a fixed treatment period. Biocide distribution in treated wood blocks was strongly affected by fluid pressure and the permeability and size of the wood pieces. For example, increasing the treatment pressure from 140 to 270 bar increased retention of TCMTB at the center of Douglas-fir heartwood blocks (38x38 mm) by 700%. A 30 minute treatment period was sufficient to completely impregnate a 38 x 38 mm Douglas-fir block.

A simple rate model was developed to predict deposition amounts within wood. The model was based on compressible flow through porous media and assumed fast precipitation kinetics prevented any supersaturation. Simulations agreed, at least qualitatively, with the data without fitting.

DEPOSITION OF CHEMICALS IN SEMI-POROUS SOLIDS USING SUPERCRITICAL FLUID CARRIERS

by

Endalkachew Sahle-Demessie

A THESIS
submitted to
Oregon State University

in partial fulfillment of
the requirements for the
degree of

Doctor of Philosophy

Completed May 6, 1994
Commencement June 1994

APPROVED:

Redacted for Privacy

Assistant Professor of Chemical Engineering in charge of major

Redacted for Privacy

Head of Department of Chemical Engineering

Redacted for Privacy

Dean of Graduate School

Date thesis is presented May 6, 1994

Typed by Endalkachew Sahle-Demessie

Acknowledgment

I am deeply indebted to Dr. Keith L. Levien for the assistance and guidance he gave me while doing this study and for lots of other things that I learned from him. A special note of thanks is also due to Dr. Jeffrey J. Morrell for his advice, his critical reading of this manuscript and for his helpful criticism and encouragement.

I am most graciously indebted to my wife, Hinsa Mariam Tesfaye, without whose aid my graduate study would have been impossible. I am indebted to her for her encouragement when progress seemed to be at a standstill. I am indebted to my family for their encouragements and supports. Sincere appreciation and heartfelt thanks to the graduate students in the Chemical Engineering Department, specially to Ali Hassan, Sarawadee Junsophonsri and Jung-Seok Yi for the good discussions and cuisine dining.

I am indebted to the Chemical Engineering Department, OSU, for giving me an assistantship and for the Electric Power Research Institute for financial support of this project.

TABLE OF CONTENTS

Page

LIST OF FIGURES

Figure Page

Figure Page

Figure Page

Figure Page

Figure **Page**

Figure | Page

LIST OF TABLES

TABLE OF APPENDICES

LIST OF APPENDICES FIGURES

LIST OF APPENDICES TABLES

LIST OF APPENDICES TABLES

NOMENCLATURE

a	van der Waals attractive parameter
b	van der Waals repulsive parameter
C	concentration, mol/cm^3
D_{21}	molecular diffusion coefficient, cm^2/s
E	solubility enhancement factor
f	fugacity
G	specific gravity
h	enthaply, J
J	number of parallel capillary tubes per unit area in eqn. (7.8)
k	interaction coefficient
K	specific permeability, cm^2
K_g	superficial gas permeability, m^2
L	length, cm
M_w	molecular weight, g/mol
n	total number of moles
N	flux , mol/cm^2.s
P	total pressure, bar
q	heat flow, J
r	pore radius, m
R	universal gas constant, J mol^{-1} K^{-1}
R^*	retention, gm
S	supersaturation = w/w^*
t	time , min
T	temperature, K
w	concentration, gm/cm^3
w_s	deposited solute concentration per unit area, gm/cm^2
u	superficial velocity of fluid, m/s

U internal energy, J

V volume, m^3

x distance, cm

y mass fraction of solute in gas phase

X dimensionless distance, x/L

W moisture content, wt %

z distance, cm

z' dimensionless distance, z/L

Z compressibility coefficient

Greek symbols

α slope of the relationship in eqn. (4.15)

β intercept of the relationship in eqn. (4.15)

σ isothermal spacing constant in eqn. (4.15)

δ solubility parameter $(cal/cm^3)^{1/2}$

Δ reduced solubility parameter, $\delta_{co2}/\delta_{biocide}$ (-)

γ constant $(= \Delta H_{vap} + \Delta H_{sol})/R$ for eqn. (4.11)

ε porosity

ε^* dimensionless energy parameter $(=H^{Lvap}/2.3RT)$

ε' specific surface area per unit volume of solid matrix, cm^{-1}

ϕ fugacity coefficient

Φ solvent volume fraction

Γ mean free path of a gas molecule, m

ξ fluid characteristics defined by eqn. (7.28)

κ_T isothermal compressibility, bar^{-1}

κ_1, κ_2 and κ_3 constants that depends on fluid and porous matrix in eqn. (7.30)

ζ flow coefficient in eqn. (7.18), cm^2/s

ζ^* the variable $\delta^2 v^L/(2.3RT)$ in eqn. (4.20)

μ viscosity, $N\ s/m^2$

ρ density, mol/L

χ fraction of mean free path and pore radius

ω intercept parameter in eqn. (4.22)

Ω dynamic flow coefficient, s^{-1}

Subscript

c critical property

e effective

m mean

R reduced property, ratio of actual to critical values

v constant volume

p constant pressure

o original (initial)

ref reference

1 solvent

2 solute

Superscript

\- average

* saturated

id ideal

s solid

sat saturated

F fluid

o reference

∞ ambient

^ property measure in solution

CAUTION

Most of the chemicals used for this study are toxic and can cause health hazard. For anyone who wants to reproduce or continue this work, care must be taken to handle those chemicals as recommended by the respective Material Safety Data Sheets.

DEPOSITION OF CHEMICALS IN SEMI-POROUS SOLIDS USING SUPERCRITICAL FLUID CARRIERS

CHAPTER 1

INTRODUCTION

1.1 General

Supercritical fluids are employed in a variety of applications in the food, chemical and pharmaceutical industries and have been acclaimed as a solution to various technological challenges. Supercritical fluid (SCF) technology offers unusual possibilities for selective extraction and fractionation, separation and purification, impregnation and surface deposition, nucleation and particle size regulation, and chemical reactions and synthesis. Some of the newly commercialized applications of supercritical fluids include: extraction of coffee and hops, catalytic regeneration and supercritical chromatography.

Supercritical fluids offer a novel combination of liquid-like and gas-like properties, which makes them unique as solvents and reaction media. Compared to conventional techniques, processes based on supercritical technology benefit from such desirable characteristics as high mass transfer rates, ease of solvent regeneration, potential energy savings and lower pressure drops in flow systems.

The solvent power of a SCF has been known for over 100 years (Hanny,1880; Hanny and Hogerth,1887). However, only in the past 15 years

has interest in supercritical fluid technology been renewed by researchers looking for energy efficient and environmentally acceptable technologies. Various applications and capabilities have been proposed and some processes have been commercialized (Table 1.1).

A supercritical fluid is formed when a liquid or vapor is heated and pressurized beyond its critical point. Unlike liquid-gas or solid-gas phase transitions, which involve discontinuous changes of density and other molar properties, a transition from gas or liquid to SCF conditions is not accompanied by abrupt property changes. This kind of transition is called second-order since discontinuities appear only in the second derivative of Gibbs free energy. Depending on the fluid density, the behavior of a SCF may vary from gas-like (possessing low density, low viscosity and a high diffusion coefficient) to liquid-like (high density, high viscosity and a low diffusion coefficient). The density, viscosity and diffusivity for a typical supercritical fluid, a liquid and a gas are shown in Table 1.2. A pressure-temperature phase diagram and some pressure-density isotherms for pure CO_2 at subcritical and supercritical conditions are shown in Figures 1.1 and 1.2, respectively. For temperatures above the critical temperature, the density increases rapidly with rising pressure and the slope of the critical temperature isotherm at the critical point, i.e. the compressibility $[-1/v(\partial v/\partial p)_T]$, is very high - approaching infinity at the critical point. Therefore, density changes near the critical point on a T_c

Table 1.1 Applications of supercritical fluids*

Chemical Purification and Separation with SCF
- Separation of chemicals from renewable resources, i.e.(nonpolar from polar compounds, aromatic isomer separation, isotope separation)
- Separation of aromatic and paraffinic hydrocarbons, or oxygenated organics from water,
- Purification of organometallic compounds or potable water from seawater
- Regeneration of activated carbon, adsorbents, filters, catalysts

Rate Processes in SCF
- Decaffeination of coffee and tea
- Deoderization of oils and fats
- Extraction of:
  - Nicotine from tobacco,
  - Drugs from plant material
  - Food coloring from plant material, hops and spices
  - Flavors, fragrances, aromas, perfumes

Chemical Reactions in and with SCF
- Waste detoxification in supercritical water
- Carboxylic acid extraction from water
- Hydrogenation of SC-CO_2 to make formic acid

Material Processing using Supercritical Fluids
- Impregnation and spray coating
- Deposition of materials in microporous substrates
- Densification of ceramics of wood with monomers
- Comminution via precipitation from supercritical fluids
- Polymer fractionation,extraction of monomers of oligomer from polymers

Processing Heavy Hydrocarbons
- Deasphalting petroleum fractions or coal liquefaction
- Recovery and purification of used oils and lubricants
- Processing low-vapor-pressure oils
- Tertiary oil recovery

Supercritical Chromatography

(*) *Adapted from Hoyer (1985) and Bruno and Ely, (1991)*

Table 1.2 Order of magnitude comparison of physico-chemical properties of a typical gas, liquid and supercritical fluid

Property	Gas	SCF	Liquid
Viscosity, Ns/m^2	10^{-5}	10^{-5} - 10^{-4}	10^{-3}
Density, Kg/m^3	1	300 - 900	1000
Kinematic Viscosity, m^2/s	10^{-5}	10^{-7}	10^{-6}
Diffusion Coefficient cm^2/s	10^{-1}	10^{-5} - 10^{-3}	10^{-5}

isotherm are very significant. However at temperatures above T_c, a larger pressure increase is required to produce an equivalent density increase.

The density and the dielectric constant of CO_2 rise steeply between 70 and 200 bar and reach values similar to those of liquids (Stahl et al., 1978, Hubert and Vitzthum, 1979). The dielelectric constant measures the fluid's electrical properties that are responsible for the solubility enhancement and arises from the interaction of solute molecules with solvent molecules due to increase polarity. The Hilderbrand solubility parameter, δ, (the square root of the cohesive energy molar density) is a qualitative measure of solvent strength. It has frequently been pointed out that changes in the solubility parameter with pressure resemble changes of density (Figure 1.3). On a log-log scale, the plot of the solubility parameter versus density is approximately linear with all isotherms collapsing to a line (except near the critical point where calculated values contain significant errors) (Figure 1.4). Therefore, in the critical region the solvent strength may be manipulated by making small changes in temperature or pressure, which is a unique property of SCFs.

Many common substances have critical temperatures near ambient (Table 1.3). Carbon dioxide has been attractive for supercritical fluid treatments because it is cheap, nonflammable, nontoxic and readily available. Supercritical carbon dioxide processes are increasingly employed in various

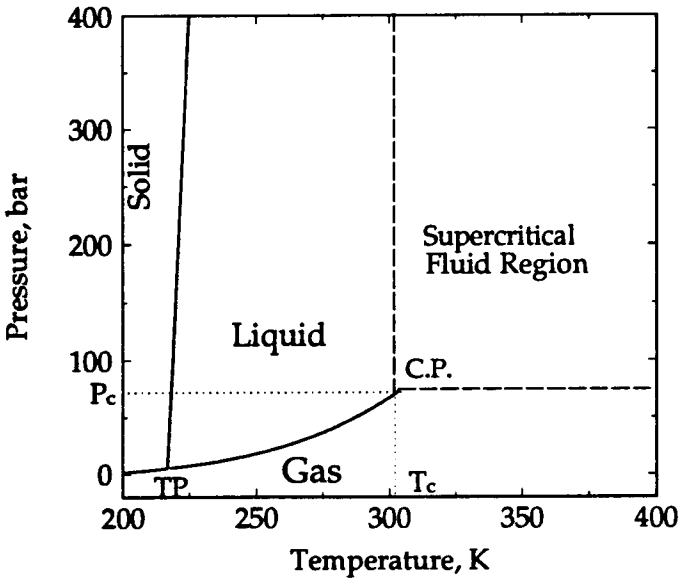

Figure 1.1 *P-T* Phase diagram for pure carbon dioxide (Angus et al., 1976).

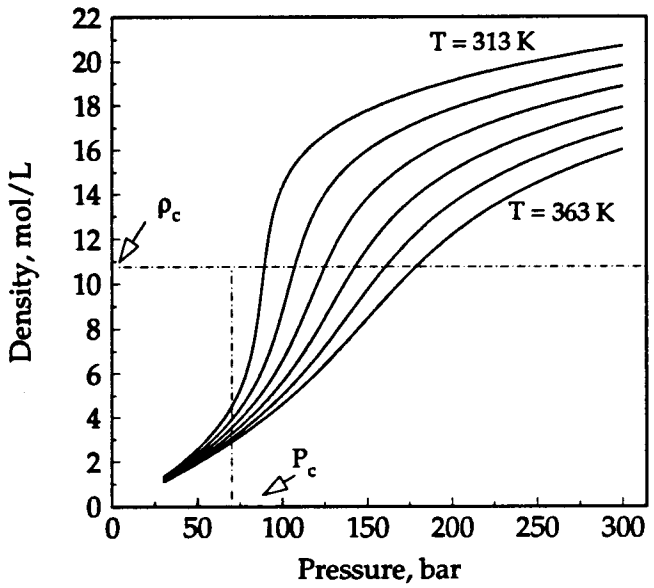

Figure 1.2 Density *vs.* pressure relationship for CO_2 (Ely, 1986).

process industries. The adjustability in solvent density is the basis for almost all operations.

Supercritical fluids typically have solute molecular diffusivities orders of magnitude greater than those of liquids, giving improved mass-transfer across a boundary or through a solid matrix (Tsekhanskaya, 1971; Swaid and Schneider, 1979; Saad and Gularii, 1984). The binary diffusion coefficient, D_{AB}, of a SCF increases with temperature, but in general the product ρD_{AB} is approximately constant for a given system and temperature (Balenovic et al., 1970; Bartman and Schneider, 1973). Viscosities of SCFs are almost as low as those of gases, facilitating both pumping, natural convection and enhanced solid settling rates during precipitation (Reichenenberg, 1975; Stephen and Lucas, 1979). Viscosities of dense gases increase with pressure and decrease with temperature near the critical pressure (Figure 1.5). The range of greatest interest for most SCF operations is near the critical point, T_r = 1.01 - 1.2 and P_r = 1.01 - 3.0. Transport and thermal properties undergo large changes within the critical region, which can be useful for optimizing a supercritical process. Many thermodynamic properties of a system, such as heat capacity, thermal conductivity or sonic velocity, become either indefinitely large or zero at the critical point (Figure 1.6). The underlying thermodynamic causes for this anomalous behavior are not fully understood. On the other hand, the solubility of solids has been observed to be continuous near the critical point of the solution (Booth and Bildwell, 1949; Rowlinson and Richardson, 1958).

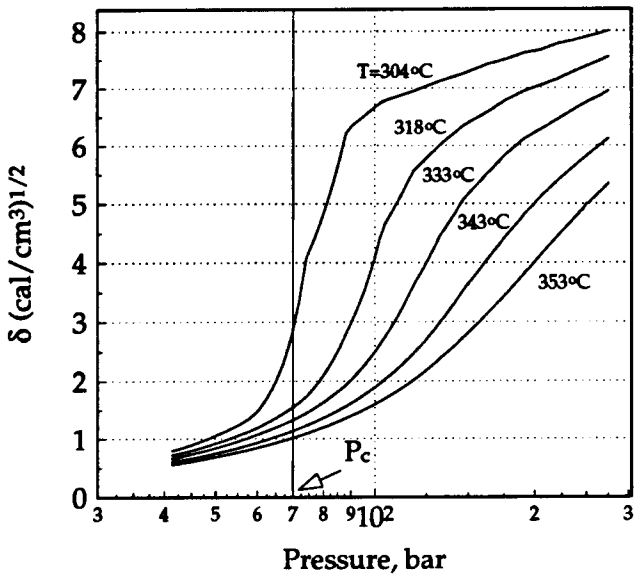

Figure 1.3 Solubility parameter *vs* pressure for CO_2 (Giddings, et al., 1968).

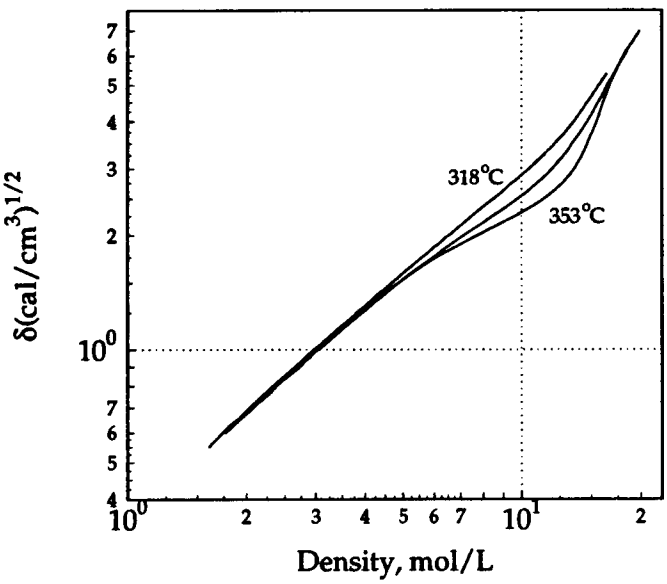

Figure 1.4 Solubility parameter *vs* density of CO_2.

Table 1.3 Critical parameters of common fluids

Compound	Critical Temperature °C	Critical Pressure bar	Critical density g/cm^3
Carbon dioxide	31.0	73.8	0.468
Ethane	32.2	48.8	0.203
Ethylene	9.2	50.4	0.218
Propane	96.7	42.5	0.217
Propylene	91.9	45.6	0.232
Chlorotrifluoromethane	28.8	38.2	0.58
Tetrafluoroethylene	33.3	38.9	0.58
Methyl fluoride	44.6	58.0	0.31
Sulfur hexafluoride	45.6	37.1	0.53
Nitrous oxide	36.5	72.4	0.452
Hydrogen chloride	51.45	83	0.42
Hydrogen sulfide	100.4	88.9	0.345
Carbon disulfide	104.8	65.0	0.45
Dichlorodifluoro-methane (Freon-12)	111.5	39.56	0.555

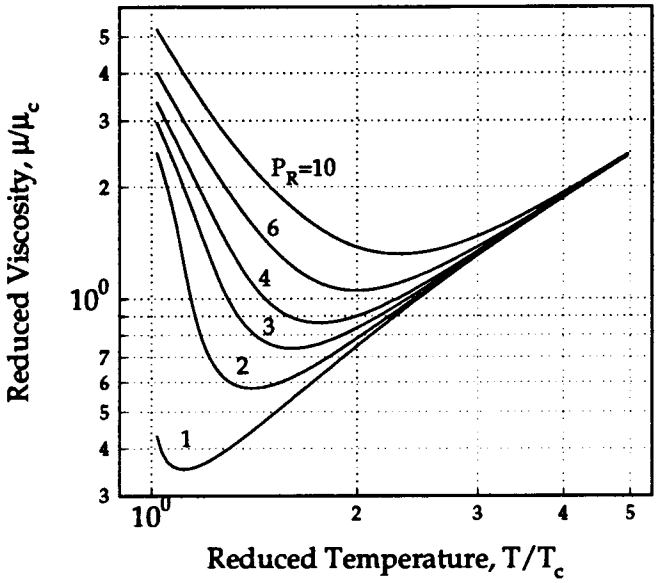

Figure 1.5 Reduced viscosity *vs* reduced temperature for CO_2 (Yoon and Thodos,1970, Ely, 1986).

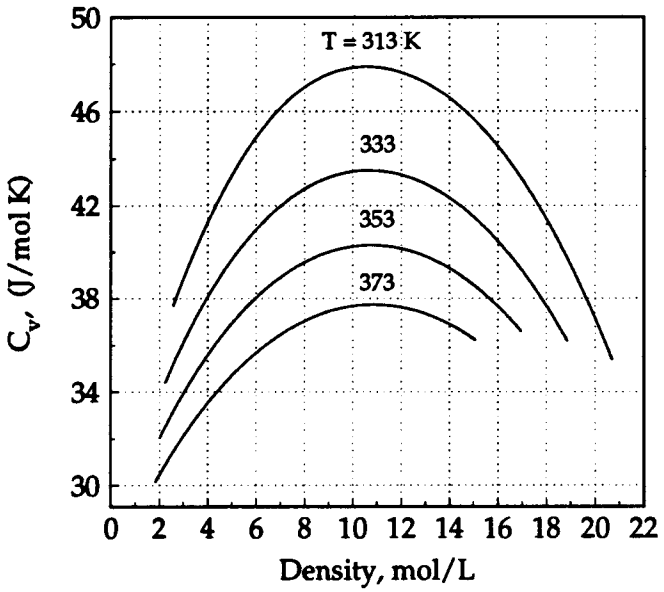

Figure 1.6 Constant volume heat capacity *vs* density of CO_2 (Angus et al., 1976).

1.2 Supercritical Fluids and Wood Processing

Wood is a cellular material that consists of polymeric and low-molecular-weight constituents. The weight proportions of the polymeric constituents of wood include cellulose (40 - 45 %), hemicellulose (20 - 30 %) and lignin (20 - 30 %). Low molecular weight constituents are extractives (2 - 4 % by weight) and inorganic matter (<1%). Wood processing operations may be chemical or mechanical or a combination of both.

Previous studies made of potential applications of supercritical fluids to the processing of wood include: liquefaction, delignification, extraction, and impregnation with monomers that polymerize within the wood structure. Early studies were primarily focused on liquefaction or gasification of wood. Liquefaction of biomass (wood) entails pyrolysis conducted in a supercritical solvent. The process includes swelling of the wood structure followed by solubilization of the pyrolytic breakdown products of lignin and carbohydrates (Hansen and April, 1982). A caging effect of the SCF solvent molecules surrounding the mid-size fragments protects them from secondary reactions (Larecque et al., 1984). Supercritical fluid extraction (SFE) of pyrolytic oils from wood was performed using organic solvents (Calimli and Olcay, 1983; McDoland et al., 1982 and 1983; Labercque et al., 1984, Stahl, et al, 1978) or with supercritical water (Modell, 1982). SFE has advantages over conventional thermochemical liquefaction techniques because it uses no

gaseous reducing reactant, no catalyst, and no acidic reactants which might degrade the material (Labrecque, 1984).

Supercritical carbon dioxide has been suggested for the removal of resinous extractives from wood chips prior to pulping or other wood conversion processes (Ritter and Campbell, 1991). These wood extractives can hinder the pulping process and lower the final product quality (Casey 1960; Dorek and Allen 1978; Hillis 1980; Worster et al. 1986). The use of a SCF to remove resinous extractives from wood prior to pulping reduces the chemical consumption during pulping, increases the quality of paper, and reduces air and water pollution problems (Ritter and Campbell, 1991). McDonald et al. (1982, 1983) showed that the yield from southern pine chips extracted first with SC-CO_2 and then with petroleum ether was more than petroleum ether extraction alone. These results suggest that extraction using SC-CO_2 can sometimes open the structure of wood particles, to allow greater penetration of other fluids. Puri and Haners (1983) have reported that lignocellulose residues can be explosively opened with high pressure CO_2. It was similarly reported that tobacco leaves expanded after extraction with SC-CO_2 (Williams, 1981; Zosel, 1979; Hubert and Vitzthum, 1978). The extent of the volume expansion depended on various factors such as temperature, moisture content and the structure of the solid. However, scanning electron microscopy of wood surfaces extracted with SCF revealed no significant alteration of the wood surface (Ritter and Campbell, 1991).

Kiran and Li (1988) studied SCF pulping using different species of wood and lignocellulosic model compounds (such as xylose, glucose, xylene, cellulose and kraft lignin) at low temperatures and pressures up to 300 bar. Supercritical carbon dioxide was found to have little effect on wood, even at extreme conditions (Table 1.3).

Non-cellulosic components of wood can be extracted and precipitated in solvent-free forms (Li and Kiran, 1989). Extraction of lignin can be performed from either wood or from black liquor, producing extracts that are free of inorganic loadings (such as NaOH and NaS that are present in black liquor from conventional pulping process). These materials can be used as chemical feed stocks or even fuels, significantly reducing pollution since they can be burned directly in ordinary power boilers. Preliminary studies show that supercritical pulping can save energy, reduce capital costs and reduce waste streams (Li and Kiran, 1989a).

In a different application, SC-CO_2 was used to load small Douglas-fir blocks with methyl methacrylate to make a wood-polymer composite within short treatment periods (Ward, et al., 1990). After the monomers were deposited in the wood matrix, polymerization was completed using heat to activate a Vazo catalyst. Such processes could be used to modify strength, surface characteristics, biological properties, or the dimensional stability of wood. Although, their work was exploratory and lacked rigorous analysis, Sunol et al. 1989, have demonstrated the potential for SCF deposition of

monomers. However, little simultaneous experimental and theoretical work has been done on the use of supercritical fluids to deliver material into semi-porous solids.

Table 1.4 Weight loss of wood components in supercritical fluids (Li and Kiran, 1988)

Wood Species	Solvent	SC Critical Properties T_c °C	P_c bar	Extraction Condition T °C	P bar	Weight Loss, %	
Spruce	acetone	235.5	47.6	250	81	35	[a]
	THF	267	52.6	290	81	62	
	toluene	320.8	42.2	340	81	68	
Birch	diethyl ether	192.6	36.6	250	101	20.8	[b]
	acetone	235.5	47.6	250	101	22.8	
	methanol	240	80.6	250	101	25.3	
	ethanol	243	64.6	250	101	21.8	
	1-propanol	263.6	52.4	270	101	32.4	
Pine	CO_2	31	73.9	40	81	3.9	[c]
Western red cedar	acetone	235.5	47.8	260	100	41	[d]
				350	100	75	
				350	280	91	
	methanol	240	79.5	260	100	28	
				350	100	72	
				350	100	96	
Southern pine	CO_2	31	73.9	40	210	2.1	
			40	620	5.6		
90%brich	SO_2 +	100.4	78.8	170	79.2	89.2	[e]
10%maple	H_2O	374.1	221.2	180	87.4	94.4	
	80% methyl amine +H_2O	157	74.6	180	100	40	[f]

[a] Calimli and Olcay, 1978, [b] Koll et al., 1979, [c] Froment, 1981, [d] McDonald et al.,1983, [e] Vick Roy and Converse, 1985, [f] Beer and Peter, 1985

1.3 Wood Preservation and Supercritical Fluids

The wood preservation industry uses liquids as solvents and carriers of biocides. The risks of spills, soil pollution from the drippage from treated wood and the difficulty of reducing waste generation are typical features of liquid solvents. The other major difficulty in the practice of wood preservation is that all wood is not uniformly permeable and it may be nearly impossible to adequately impregnate this material with liquid preservatives.

Many species of wood require long treating periods to produce relatively thin bands of protection, leaving an untreated core of heartwood despite the use of pressure periods that may be up to 20 times longer than those used for more easily treated species (Hunt and Garratt, 1967). Thin bands of treatment are more easily compromised exposing the untreated inner core to fungal decay or insect attack.

Progress in the wood preserving industry has been slow. Previous processes have depended on the movement of liquid preservatives in the wood at pressures less than 14 bar (200 psi). Lateral fluid movement beyond the wood surface is primarily dictated by the permeability of pit membranes (Hunt and Garratt, 1967). Fluid movement through encrusted and aspirated pits is often difficult and nearly impossible (Baines, 1985; Blew, 1967; Gjovik, 1983; Ruddick, 1980; Thompson, 1981). Surface tension effects result in a need for considerably higher pressures to force a gas-liquid interface through a capillary tube than is required to cause flow of fluid alone. The use of surfactants to

reduce surface tension or sound waves to break trapped air bubbles may affect flow but test trials with these applications have yielded marginal success (Kumar and Morrell, 1992). Incising may also improve fluid flow but has an impact on the mechanical properties of the finished product and does not overcome the basic treatability problems (Morris et al., 1994).

A more versatile method for wood impregnation would be to alter fluid characteristics to allow penetration into refractory wood using supercritical fluids. The concept of employing supercritical fluids to treat refractory wood species was first proposed in a Japanese patent (Ito,1984). Other US patents of similar applications include supercritical fluid-aided impregnation of wood with monomers (Sunol et al., 1992), perfusion of porous solid with chemicals (Kayihan, 1992) and densification of ceramics (Berneburg et al. 1985). Supercritical treatment of wood involves dissolving a biocide in a SCF, carrying it into the wood, and changing operating conditions to deposit the biocide. Rapid pressure reduction after the supercritical fluid solution has penetrated through the wood substrate should encourage nucleation and precipitate the biocide on the lumen surfaces and, possibly, within the wood cell wall.

Previous investigations suggest that extraction using SC-CO_2 can open the structure of wood particles to allow greater penetration of other fluids. The extent of volume expansion depends on factors such as temperature, moisture content and the structure of the solid. In summary, the advantages

that supercritical fluid technology promises over that of liquid solvents in the treatment of wood include:

- solvent density and its dissolving power depend on pressure and temperature and can be quickly varied throughout the system. Once sufficient penetration has been achieved, a change in these conditions can precipitate the dissolved chemicals, immobilizing them in the wood.
- density, temperature and composition offer considerable flexibility to the process.
- faster diffusion leads to more efficient permeation.
- the absence of surface tension in supercritical fluids enhances the passage of the solvent into the interstices of the solid matrix. In the conventional liquid treatment, the presence of small gas-liquid interfaces in pit pores results in back pressures which oppose penetration.
- low viscosities make SCFs virtually ideal fluids for enhancing mass transfer across a boundary, increasing flow through porous solids and facilitating pumping and fluid flow in the process.
- supercritical fluids can also change the physical structure of the wood to allow increased mass transfer.
- essentially complete separation of solvent /solute with high solvent recovery can be accomplished by isothermal decompression or isobaric heating.

However, the limited data and lack of adequate mathematical models in a relatively new technology make process design and scaling-up difficult.

CHAPTER 2

OBJECTIVES AND SIGNIFICANCE OF RESEARCH

The ultimate goal of this thesis was to contribute to the understanding of processes that use supercritical fluid carriers to deliver substances into semi-porous media. Accomplishing this goal would help to develop a method for complete and satisfactory penetration of semi-porous structures that would otherwise be impossible to impregnate. For wood treatment, this technology also promises to reduce or avoid the high rate of ground and water pollution and other environmental concerns that are associated with the current technologies using liquid carriers.

The supercritical impregnation process incorporates several phenomena: solubility, compressible flow through porous media, heterogenous crystallization and interaction of solvents and solutes with the porous medium. Although some of these phenomena have been individually studied, a quantitative understanding of their simultaneous effects poses a significant challenge.

There are practically no available thermodynamic data in the open literature for commercially potential biocides. Therefore, original solubility studies, were conducted, new methods of analysis for the dissolved biocides

were developed and a system to treat wood using SCF had to be designed and built. The success of this technology depends on selecting the best biocide-solvent-cosolvent system and optimizing operating conditions and techniques that result in deeper and uniform distribution of biocides in the wood matrix.

The objective of this thesis was to identify process parameters and solvent properties that influence the precipitation and distribution of solute in a porous matrix without breakdown or loss of the mechanical strength. Biocides were solubilized in a supercritical solvent, and the mixture was allowed to permeate into the wood matrix. The biocides were deposited in the wood cell structure when the operating conditions were changed. The two primary problems in wood treatment are the inability to obtain even distribution of the chemical in the wood structure and the difficulty in achieving a desired level of chemical retention in the wood. The goal was to find a solute-solvent system and operating conditions that result in obtaining the required solute retention and distribution in the wood.

Experiments began with a saturated supercritical solution and followed one of two operational modes. In the first mode, nucleation was triggered by an abrupt reduction of pressure. The second mode attempted to initiate nucleation by reducing temperature and subsequently controlling precipitation with pressure manipulation in the treatment vessel. The macrodistribution of biocides in wood was determined by analyzing different portions of each piece.

This study included two stages. The first stage involved studying solubilities of potential biocides in supercritical fluids. The second stage included studying the influence of the various factors that affect retention and distribution.

2.1 Experimental Objectives

Experimental studies of equilibrium solubilities of candidate biocides were performed in pure and modified SC-CO_2 between 45 and 80 °C and 100 to 300 bar. For this purpose, a high pressure experimental system was assembled and the reliability of equilibrium measurements made by the apparatus were tested by comparing them to solubility data from literature.

Several cosolvents that could potentially enhance the solvent power of SC-CO_2 were evaluated using gas chromatographic techniques and two or three of the most promising cosolvents for each biocide were selected for high pressure studies. Detailed solubility studies for each selected biocide were done to investigate the effects of pressure, temperature and cosolvent amount.

Impregnation studies were conducted to establish the significance of process parameters and to understand their effects on distribution of biocides within wood. Other factors that influence the process, such as solvent the mixing pattern and flow directions in the treatment vessel, the scale of the process and wood species characteristics were also investigated.

2.2 Theoretical Objectives

For process development, experimental equilibrium data must be correlated to establish the dependence of solute solubility solvent density. The solubility enhancement factor, *E*, defined as the ratio of the observed equilibrium solubility to that predicted from the ideal gas law at the same temperature and pressure, was correlated to solute reduced solubility parameter term as suggested by Ziger and Eckert (1986). Values of *E* can also be correlated with solvent reduced density as first proposed by Johnston and Eckert (1981).

A mathematical model was needed to understand the complex transient phenomena in a wood block during treatment. This model could be used to predict which variable(s) have significant effects on the distribution of chemicals and to develop a theoretical relationship between changes in properties of the supercritical fluid solution in the wood pores and the retention and distribution of biocides. Predictions of biocide distribution in wood and measurements from the real system were used to validate the model.

CHAPTER 3

BIOCIDE SOLUBILITY IN SUPERCRITICAL FLUIDS

3.1 Background

As a first step in developing a SCF treatment process for wood, it was necessary to find biocides that are soluble in SCFs. Nine organic biocides were selected for initial screening based upon considerations such as large production volume, inclusion of a variety of organic classes in the screening, future market potential, environmental acceptance and reasonable safety in handling in laboratory tests. The biocides of interest differed with respect to both their relative molecular weights and the number and nature of functional groups. The biocides selected were: IPBC *(3-Iodo-2-propynyl butyl carbamate)*, tebuconazole *(α-[2-(4-chlorophenyl)ethyl]-α- (1,1-dimethylethyl)-1H-1,2,4-triazole-1-ethanol*, TCMTB *(2-(Thiocyanomethylthio) benzothiazole*, propiconazole *(1-(2-(2',4'-dichlorophenyl)-4-propyl-1,3-dioxolan-2-methyl)-1H-1,2,4-triazole)*, pentachlorophenol, copper naphthenate, Amical-48 *(diiodomethyl p-tolyl sulfone)*, chlorothalonil *(tetrachloro- isophthalonitrile)*, and Cu-8-quinolinolate. Technical data are given in Table 3.1, physical properties are listed in Tables 3.2 and molecular structures are shown in Table 3.3 and 3.4.

The solubility of solids and liquids in supercritical solvents is strongly

Table 3.1 Biocides selected for screening studies

	Biocide	Class	Trade Name	Toxicity LD_{50} (mg/kg)	Purity %
1	IPBC	Carbamate	Troysan Polyphase P100	1470	97
2	Tebuconazole	Triazole	NA	5000	95
3	TCMTB	Thiazole	NA	2000	85
4	Propiconazole	Triazole	WOCOSEN	4000	88
5	Pentachlorophenol	chlorinated phenol	Penta	360	99.8
6	Copper Naphthenate	Naphthenic acid + CuO	Cuprinol	NA	74
7	Diiodomethyl p-tolyl sulphone	NA	AMICAL-48	NA	96
8	Chlorothalonil	NA	Nipcocide N-96	10,000	95
9	Cu-8-quinolinolate	Organo metallic complex	NA	NA	NA

NA - not available

Table 3.2 Properties of biocides tested for solubility

Biocide	Mol Wt	State*	P^{vap} @ 20°C mmHg	B.P. °C	M.P °C	δ^1 $(J/cm^3)^{1/2}$
IPBC	281	Solid	$2x10^{-5}$	NA	63	23.1
Tebuconazole	308	Solid	$5.5x10^{-9}$	140	103	29.4
TCMTB	238	Liquid	5.5	80	32	23.4
Propiconazole	342	Liquid	10^{-6}	180	32	22.54
Pentachlorophenol	266	Solid	$5x10^{-4}$	310	188	29.86
Copper Naphthenate	mixture	Liquid	$3.4x10^{-3}$	NA	NA	NA
AMICAL-48	417	Solid	NA	NA	180	24.32
Chlorothalonil	266	Solid	NA	NA	250	42.71
Cu-8-Quinolinolate	376	Solid	NA	NA	375	NA

[1] Evaluated using atomic and group contribution method of Fedros, (1974)

* Above the CO_2 critical temperature.

Table 3.3 Molecular structure of biocides evaluated for solubility (Part 1)

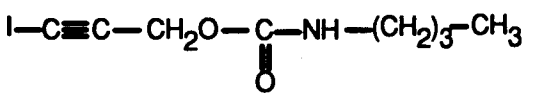

IPBC

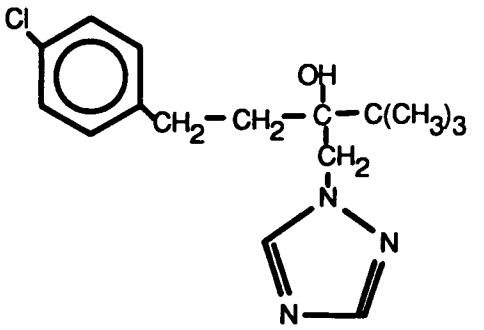

Tebuconazole

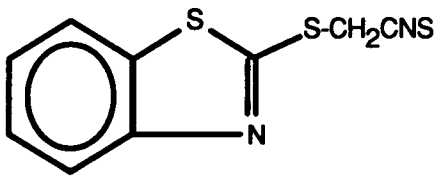

TCMTB

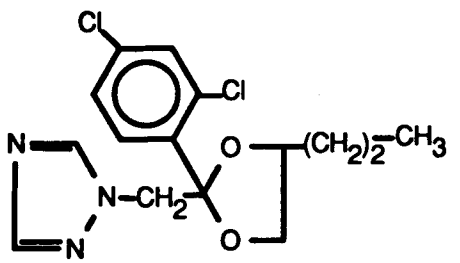

Propiconazole

Table 3.4 Molecular structure of biocides evaluated for solubility (Part 2)

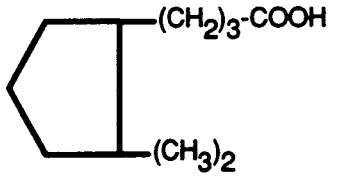

Copper Naphthenate-typical naphthenic acid shown

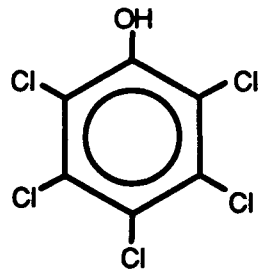

Pentachlorophenol

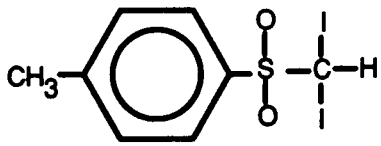

AMICAL-48

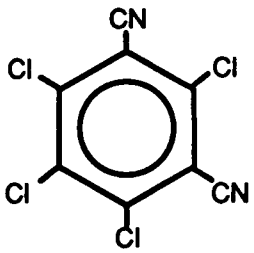

Chlorothalonil

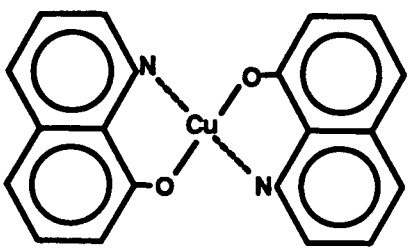

Cu-8-Quinolinolate

affected by pressure and temperature in the near critical region where the isothermal compressibility is large. Solubility of a solid near the critical point varies exponentially with the solvent density and the functionality of the solute is relatively less important (Diepen, et al., 1953; Christal et al. 1982 ; Johnston, 1981).

The process of dissolving a solid or a liquid molecule in a supercritical phase can be characterized either as vaporization, when the solute molecules simply move from a condensed (dense) phase into an expanded phase, or as a dissolution, when these are strong solute-solvent interactions (Hoyer, 1985). Solvent-solute interactions are responsible for enhancements of condensed phase solubility in SCF as great as 10^{10} (Williams, 1981).

The influence of temperature on solubility varies depending on the pressure range. Solubility changes associated with increasing temperature are dependent on solute vapor pressure and solvent density. If the solvent density remains constant, the solubility increases with increasing temperature, as does the vapor pressure of the solute. However, for pressures just above the critical pressure, the carbon dioxide density is much more sensitive to temperature than is the vapor pressure. At constant pressure, a decreases in density at higher temperature counters the effect of the increased solute vapor pressure (or sublimation pressure) and can result in lower solubility. At even higher pressures, the effect of the solute vapor pressure dominates the solvent density

effect leading to a higher solubility. This effect is called retrograde vaporization.

Solubilities of a solute in SC-CO_2 are determined by both vapor pressure and intermolecular forces. At constant temperatures, as pressure rises, density increases and the solubility of less volatile components in the fluid generally increases. The effects of pressure on the density and the dielectric constant of CO_2 helps to explain the greater solvent power of SC-CO_2 for low-volatility compounds at elevated pressures. The solubility and dielectric constant increases more sharply for CO_2 than other gases. As a result, the solvent power of the SCF phase cannot solely be attributed to the corresponding density increase (Lira, 1988).

Solubility of a solute is hindered by the presence of polar functional groups, such as carbonyl and hydroxyl groups. A high molecular weight for a solute also tends to inhibit solubility in SC-CO_2, to a degree that few molecules above 400 g mol^{-1} show appreciable solubility in SC-CO_2 (Stahl et al., 1978). Solubility of polar solutes may be enhanced by adding a small amount of cosolvent. Thus, a multicomponent fluid mixture can be tailor-made to have a specific solvent strength and selectivity for dissolution or separation.

3.1.1 Cosolvent Effect

Although SC-CO_2 has many desirable properties, its polarizability is lower than any hydrocarbon except methane. A pressure of 200 bar is

required at 35°C to attain a solubility parameter of 7.3 $(cal/cm^3)^{1/2}$, a value that is very close to that of liquid hexane. Therefore, pure SC-CO_2 is similar to hexane and has limited ability to dissolve polar solutes even at very high densities.

The idea of adding a small amount of miscible organic compound to supercritical solvent was first suggested by Peter et al., 1974, who used benzene as an entrainer (cosolvent) in a propane-ethylene-steric acid-oleic acid system. A cosolvent is a subcritical component added in relatively small amounts whose volatility is between that of the SCF and the solute. Extending this definition, volatile solids that are mixed with less volatile solids may also act as cosolvents (Krunik and Reid, 1982).

Biocide solubility may be increased by adding a small amount of a cosolvent. Near the critical point, SCFs have high compressibility and it has been postulated that the large free volume allows the attractive forces to move molecules to energetically favorable locations to form clusters around the relatively large solute molecules (Eckert et al., 1986; Debenedetti, 1987; Kajimoto et al., 1988; Cochran and Lee, 1989; Debenedetti et al., 1989; Brennecke et al., 1990; Morita and Kajimoto, 1990). Local and bulk compositions can be modified by adding a cosolvent which increases the polarizability of the SC-CO_2 and the interactions with functional groups on the solute molecules.

Most liquid cosolvents have solubility parameters that are larger than that of carbon dioxide which allows their use to increase solubility of the solute, or to decrease operating pressure. Cosolvent effects may be caused by either an increase in the mixture molar density at lower pressures or a modification of the chemical environment for solute molecules in solution. These modifications increase physical interactions with nonpolar cosolvents or enhance chemical association between a polar cosolvent and the solute. Solubility enhancement due to a cosolvent effect depends primarily on the amount of the cosolvent and is relatively constant over a wide range of pressures or densities (Dobbs, 1986). However, maximizing solubility depends on selecting cosolvents specific for the solute.

Volatile organic solvents, such as acetone or methanol, are common examples of cosolvents. Methanol may act as either a Lewis base or acid, while acetone is a weak Lewis base and very slightly acidic (Kamlet et al., 1983). Acid-base interactions are a secondary cosolvent effect superimposed on a primary effect determined by cosolvent concentration (Van Alsten, 1986).

Solubility of nonfunctional compounds is also enhanced by cosolvents, but the enhancements are more dependent on the cosolvent concentration than the cosolvent functionality (Brunner and Peter, 1982, Brunner, 1983;Van Alsten 1986). The addition of a cosolvent shifts the critical properties from those of the pure solvent, and the extent of this shift indicates the degree of interaction between the solvent and the cosolvent (Gurdial et al., 1993).

Our objective in this work was to understand how different cosolvents affected solubility of organic biocides, with the possibility that the supercritical solution may be tailored for different levels of biocide solubility, retention and distribution in a porous solid. Solvent-cosolvent systems had to be identified for each biocide so that the required impregnation and retention of the biocide was achieved.

3.2 Cosolvent Screening Using Gas Chromatograph

The selection of a suitable cosolvent is the initial step in using SCF technology. Although there has been considerable effort to understand solute/solvent and solute/cosolvent interactions, the choice of a potential cosolvent for a given solute/SCF system remains largely empirical. The objective of this part of our study was to systematically screen potential cosolvents using a gas chromatograph operated near atmospheric pressure to reduce the screening required in subsequent high pressure experiments (Tavanan, 1989a). The method measures the ability of a solute in a packed GC column to reduce the retention time of a cosolvent peak. A relatively large reduction in the retention time would indicate significant potential for the cosolvent to improve the solubility of the solute.

3.2.1 Materials and Methods

An initial cosolvent screening study was conducted using an HP model 5840A gas chromatograph. Teflon GC columns (1.2 m long by 3 mm inner diameter) were filled with an inert packing (80 - 100 mesh CHROMOSORB G AW) coated with one of the candidate biocides. A measured amount (0.2 g) of each biocide was first dissolved in acetone and mixed with 5.5 g of the support material. This amount of solution was estimated to be adequate to create a monolayer over the support. The mixture was allowed to stand in a fume hood

for 3 days, with occasional stirring while the solvent evaporated. Biocide coated solids were then packed in the columns which were installed in the GC and purged with helium carrier gas overnight at temperatures higher than the operating temperature to remove traces of the solvent and volatile impurities.

All gas chromatographic experiments were performed at low pressures (4 bar) and at temperatures low enough to ensure that no solute dissociation would occur during the experiment (50-80) °C. A small volume of each cosolvent (0.2-0.3 µl depending on the volatility of the cosolvent) was injected into the inert mobile phase (He) as a pulse, and the retention times as measured by detection of the cosolvent using either a thermal conductivity or a flame ionization detector were measured. To ensure that the solid did not irreversibly adsorb certain compounds (which could result in surface property changes), the experiment was repeated, changing the order of the injected cosolvents. Three to four trials were performed for each cosolvent-biocide combination. Each experiment was repeated using a column packed with the inert packing without biocide. The retention time ratio, RTR, was equal to the peak retention time in the presence of biocide divided by the retention time without biocide. Larger ratios indicated the stronger biocide-cosolvent interactions.

3.2.2 Results of Cosolvent Screening

The retention time ratios (RTRs) varied from one, for no increase with chlorothalonil, to more than 14, for propiconazole. These values are comparable to results from previous studies using different stationary phases (Tavanan et al., 1989a). The strongest three interacting cosolvents for each biocide are shown in Table 3.5. Acetone, ethanol and methanol, as a group, consistently interacted with the biocide, indicating polarity and hydrogen bonding are important properties for cosolvent/biocide interactions. In some cases, however, specific functional group interactions appeared to be dominant. This gas chromatographic affinity test was a fast screening technique to predict potentially good cosolvent candidates and appeared to be more reproducible for column temperatures in the range of 30 to 60°C (results not shown).

Table 3.5 Retention time ratios (RTRs) of cosolvents in biocide coated and uncrated materials as shown by gas chromatograph

	Biocide	Form at Room Temp.	RTR for Strongly interacting Cosolvent *
1	TCMTB	Liquid	M 34.1, E 32.4, A 26.8
2	Propiconazole	Liquid	E 16.5, B 14.6, M 8.5
3	Tebuconazole	Solid	E 14.6, B 8.0, M 6.2
4	Copper Naphthenate	Solid	H 12.6, E 12.1, B 10.4
5	Copper-8-Quinolinolate	Solid	E 12.6, B 11.9, H 11.2
6	AMICAL-48	Solid	M 3.3, B 3.3, E 3.1
7	IPBC	Solid	E 2.2, M 1.2, T 1.1
8	Chlorothalonil	Solid	E 1.8, M 1.5, B 1.3

* A= Acetone
B= Benzene
E= Ethanol
H= Heptane
M= Methanol
T= Toluene

3.3 Experimental Solubility Studies

The solubility of biocides in supercritical fluids is an important thermophysical property that should be fully understood and modeled for successful development of supercritical fluid treatment processes. The dependence of solubility on pressure and temperature can be used to determine the best operating conditions to dissolve, carry, and deposit chemicals.

Experimental techniques for measuring solubilities in supercritical fluids can be either static (equilibrium) or dynamic (flow). Researchers have also used chromatographic and spectroscopic methods and various combinations of these techniques. A flow (dynamic) method was used in the present study.

3.3.1 Materials and Methods

The equipment used to measure solubility of the biocides was a modified dual-pump Isco Series 2200 SFE system (Isco, Inc. Lincoln, NE) which consisted of two syringe pumps, heating coils, an equilibrium cell, a metering valve and a cold trap for sample collection. The basic concept was to measure the amount of biocide used to create a saturated solution with a known amount of SC-CO_2 with and with out cosolvent. The amount of biocide used was determined by one of two methods: weight loss from a saturator vessel or gravimetric analysis of a recovered solution of solute in a collection trap. The

sources and purity of the various compounds used are given in Table 3.5. All were used without further purification. Characteristics of cosolvents used in this study is listed in Table 3.6.

Solid biocides were ground and charged to the saturator with glass beads (1.5 mm o.d.), to increase the porosity of the bed and to facilitate efficient SCF-solute contact. Glass wool and metal frits (1 μm) were used at the inlet and exit of the saturator to prevent entrainment of biocide droplets or particles. To ensure a saturated solution was obtained, solvent flow rates of 0.5 to 0.7 ml/min were used for all experiments. Solvent flow rates were at liquid conditions in the syringe pump. This flow range was low enough that the solubility measurements were independent of solvent flow rates. At the beginning of a run, the saturator was operated for 30 minutes to obtain thermal equilibrium and a constant flow.

Schematics for operation with SC-CO_2 or SC-CO_2 plus cosolvent are shown in Figures 3.1 and 3.2. In both configurations, liquid CO_2 was drawn through a dip tube from a supply cylinder by syringe pump A, which had a range of 1 to 517 bar, a total capacity of 260 ml, and a maximum flow rate of 90 ml/min. The pump cylinder-jacket was cooled by a chiller (VWR 1156) to keep the CO_2 at a constant temperature of 4 (± 0.1) °C. After each complete refill stroke, the CO_2 was allowed to thermally equilibrate with the jacket liquid for about 30 minutes, after which it was compressed to the desired

Table 3.6 Purity and source of biocides, solvents and cosolvents used to study SCF solubility

Biocide	Purity	Source
IPBC	97 %	Troy Chemicals
Tebuconazole	95 %	Mobay Corporation
Propiconazole	88 %	Jassen Pharmaceutical
Pentachlorophenol	99 %	Sigma Chemical Company
Copper naphthenate	74 %	OMG
Diiodomethyl p-tolyl sulfone	96 %	Abbott Laboratories
Chlorothalonil	95 %	ISK Biotech
Cu-8-quinolinolate	Active powder form	ISK Biotech
TCMTB	80 %	Buckman Lab. Inc.
Carbon dioxide	99 %	Industrial Welding Supply Inc.
Methanol	HPLC grade	Mallinckrodt Specialty Chemical
Ethanol	HPLC grade	Mallinckrodt Specialty Chemical
Acetone	99.99 %	Mallinckrodt Specialty Chemical

Table 3.7 Characteristics of cosolvents used to study solubility (Lory and Richardson, 1981)

Solvent	Type	Dipole Moment D,debyes	Dielectric constant, ε	Solubility parameter, δ,$(cal/cm^3)^{1/2}$	Polarizability ($cm^3 \times 10^{24}$)	π^*
Ethanol	Protic	1.66	24.55	12.7	5.13	0.54
Methanol	Protic	2.87	33.70	14.3	3.26	0.60
Acetone	Aprotic	2.69	20.70	9.6	6.41	0.71
DMF	Aprotic	3.86	38.0	11.8	7.90	0.88
DMSO	Aprotic	3.9	46.68	13.0	7.99	1.00

Configuration 1 - Single Solvent

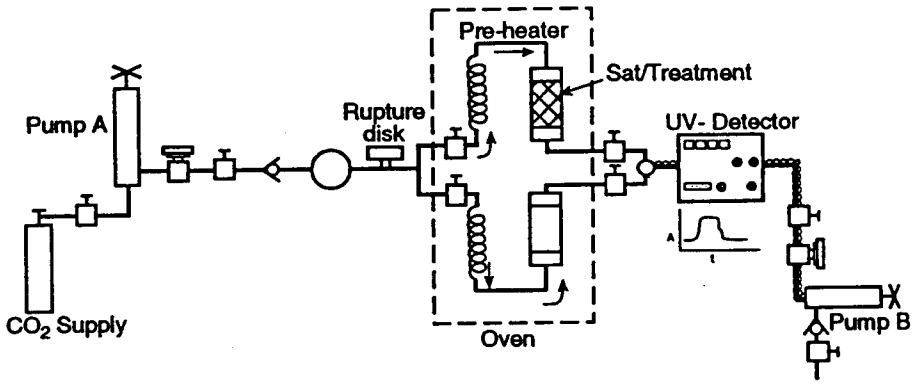

Configuration 2 - Dual Solvent

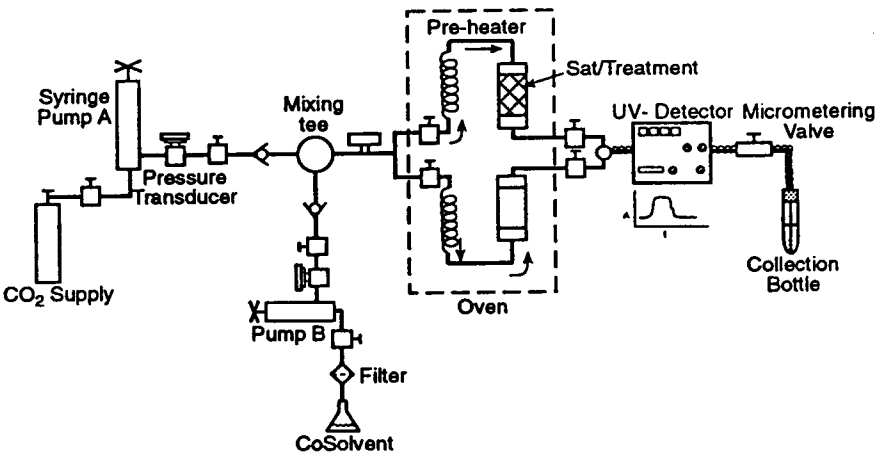

Figure 3.1 and 3.2 Schematics of the flow apparatus used for measuring biocide solubility in SC-CO_2 (Configuration 1) and in SC-CO_2 with cosolvent (Configuration 2)

pressure. The system was purged with CO_2 at low pressure before being brought to the required temperature and pressure.

Method for Solutes that are Solid at Solution Conditions

In Configuration 1 in Figure 3.1 pure SC-CO_2 flowed from pump A through a preheater coil to attain the desired temperature. It then passed through the saturator and dissolved the biocide. This saturated solution passed through an on-line UV-detector to a second syringe pump B, which was controlled to maintain a constant flow rate through the system. Pump B had a pressure range of 0.69 to 689.6 bar, a total capacity of 100 ml, and a maximum flow rate 25 ml/min. Use of both pumps enabled independent control of pressure and flow rates of to within 1 psi and 10 µl/min, respectively. The dissolved amount of solute was determined from the weight loss of the saturator. In this configuration, the fluid was always in the supercritical state and the transfer tubing did not become plugged with the solute. However, nonequilibrium conditions could exist during venting. The initial CO_2 in the saturator was allowed to equilibrate for 30 minutes after pressurization and before establishing flow. After establishing steady flow, the two pumps were run until at least more than 100 mg of solute were dissolved. This measured volume of CO_2 used was then converted to mass units based on the jacket temperature, the cylinder pressure and a modifier BWR equation of state for CO_2 (Ely, 1986).

In Configuration 2 the pump controller was used to maintain both a constant ratio of cosolvent to CO_2 and the pressure. The flow rate was controlled by adjusting micrometering valve (Autoclave model 10VRMM2812) based on the measured flow of the CO_2 at ambient conditions from a flow meter (McMillan Co., 310-3). The micrometering valve and the connecting tubing were heated to about 15 to 20 °C above the melting point of the any solute to minimize clogging by solid biocides precipitating inside and to compensate for the Joule-Thompson effect upon depressurization. The precipitated solute was recovered in a collection bottle that was placed in an ice bath. Glass wool was inserted at the tubing outlet to eliminate solid entrainment. The collected solute was weighed using a precision balance (Mettler, AE 200). The difficulty with this configuration is that precipitation of solute between the saturator and the trap inlet can lead to significant errors. Excessive heating of the tubing between the saturator and the micrometering valve can, however, lead to retrograde precipitation at lower pressures (Diepen, 1953), which would cause similar errors. The tubing between the saturator and the cold trap was flushed with liquid solvent after each run.

Method for Liquid Solutes

For biocides that are liquid at SC-CO_2 conditions, a Jerguson gauge series 40 view cell was connected in series with the saturator which contained biocides coated on inert supports (diatomaceous earth) or cellulose sponge

(Figure 3.3). The sight gauge (40 ml) ensured that the sampling was performed from the gaseous phase with no visible liquid entrainment.

The system was filled to the midpoint of the sight gauge with a liquid solute and then brought to the required pressure and temperature. The flow system was allowed to thermally equilibrate for 30 minutes. The system was then equilibrated for 3-4 hours by continuously flowing through SCF at about 0.2 lt/min (at ambient conditions) using the metering valve for flow control. The flow was measured with digital flow indicator (McMillan Co., 310-3) which was connected to a flow totalizer (Kessler-Ellis Co., INT-69).

Solubilities in mixed solvents were studied using the pump controller to maintain a constant ratio of cosolvent to CO_2 as well as the pressure. To check consistency, a mixture composition containing 1 mole % acetone was monitored using an on-line UV-detector. The mixture composition did not show significant detectable fluctuation over a two hour period.

Because of potential limits mass transfer on concentration due to rates, in all dynamic methods it is important to choose a low enough flow rate which allows the solution to reach equilibrium while in contact with the solute in the saturator. Tests must be conducted for each solute at each temperature of study. For these studies it was found that for all solutes and supercritical solvent mixtures, a CO_2 flow rate of 0.6 ml/min, measured at the syringe pump conditions, was low enough that measured solubilities were independent of flow rate.

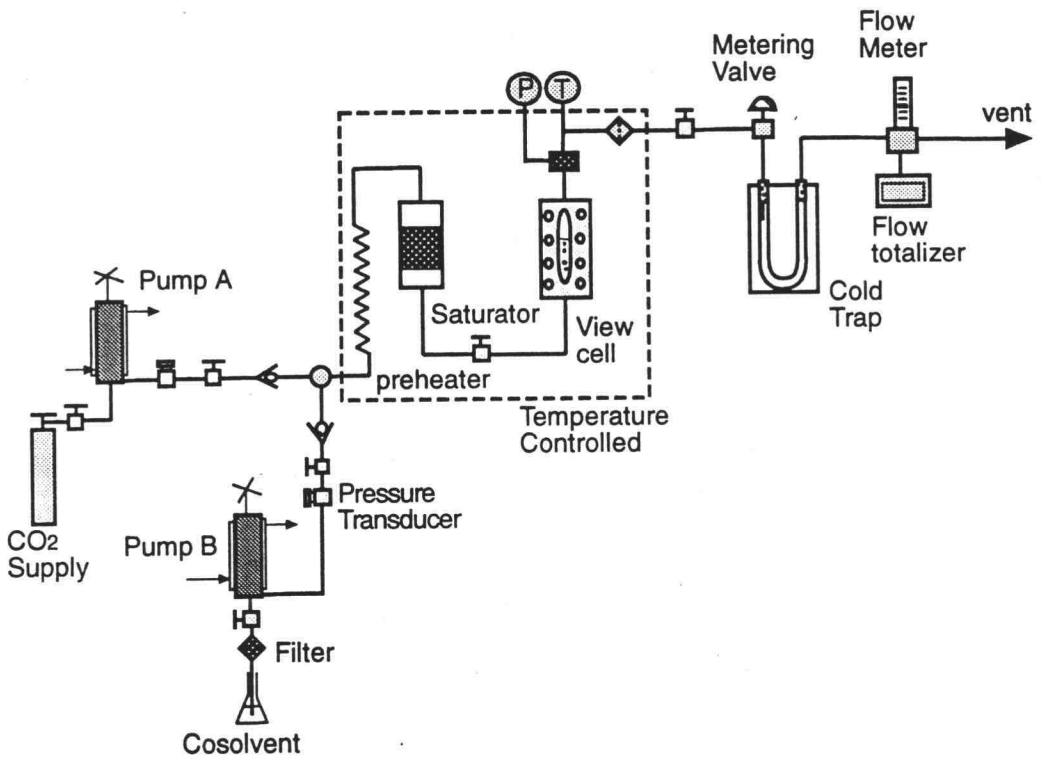

Figure 3.3 Schematics of the modified setup of Configuration 2 used to evaluate solubility of liquid solutes

3.3.2 Accuracy of Measurement and Validation of Method

Pressure: The pressure of the syringe pumps was measured using a pressure transducer placed at the head of the cylinder. The pressure signal was amplified by a circuit board and sent to the controller. These pressure traducers had an accuracy of ± 2 % of full scale or ± 1 bar and repeatability of ±1% of full scale. The pressure range was 0.69 bar to 487 bar.

Temperature: The syringe pump jacket temperature was controlled by a water circulating chiller with an accuracy of ± 0.5 K. The saturator oven temperature was measured using a J type thermocouple located in the heater block. The oven controller had a digital display that showed the set point and measured temperature values. The interior chamber thermocouple was recalibrated using a thermocouple and a mercury thermometer.

Volume Flow Rate: The flow rate was measured based on the rate of piston displacement, which was measured using a tachometer disk and a sensor CBA (Isco 60-2255-029). Flow rate ranges were 0.1 µm/min to 90 ml/min for the larger 260D pump and 0.1 µm/min to 25 ml/min for the smaller 100D pump. Each had an accuracy of ± 0.3%. The flow rate display resolution on the controller front panel was 0.1 µl/min.

Solute Mass: The balance used for weighing the dissolved amount of solute had an accuracy of ±0.01 mg for weights under 100g.

The methods employed for solubility measurements were validated by measuring the solubility of naphthalene, the most common solute used in previous SC-CO_2 solubility studies, and comparing those values with those of Tsekhanskaya et al., (1962, 1964). Measurements were performed at 35 and 45 °C. The results are presented with those of Tsekhanskaya (1962) and others (McHugh et al.,1980; King et al., 1983; Dobbs et al., 1986) in Figures 3.4 and 3.5. The differences in solubility using our this flow method and the data of Tsekhanskaya, which is widely considered to be reliable, did not exceed 5%. However, errors in the method can be considerably higher if the net gas volume used for a run was less than 0.02 m^3 measured at atmospheric condition or if the amount of solute collected was less than 0.05 g.

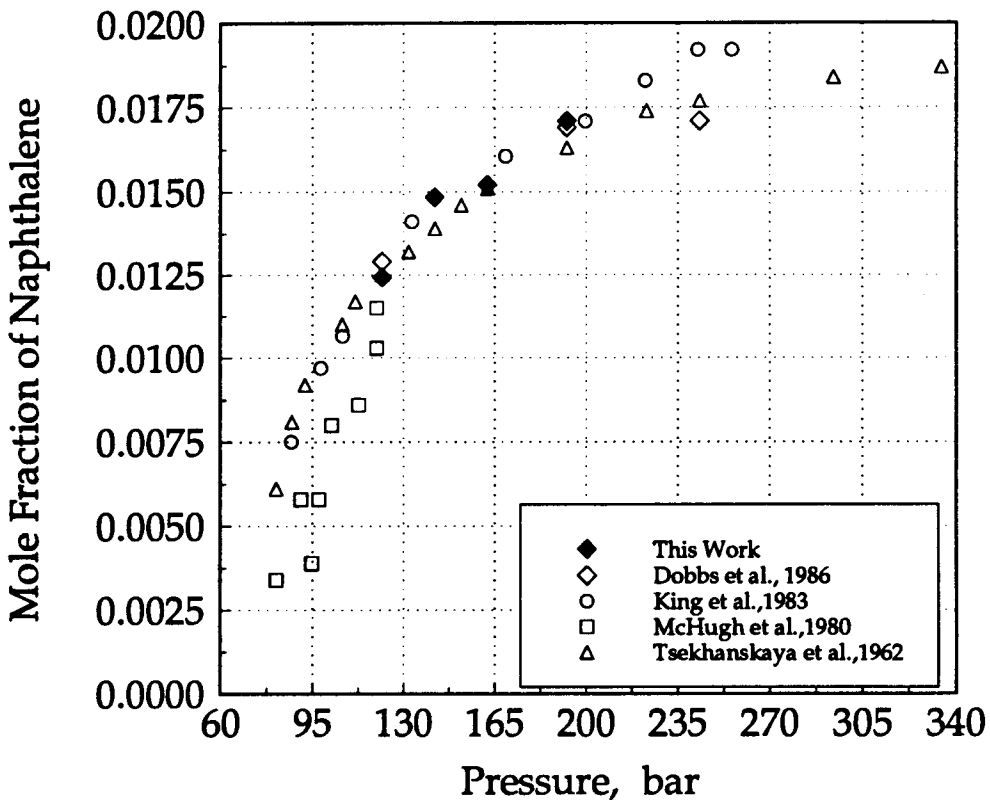

Figure 3.4 Solubility of naphthalene in CO_2 at 35°C.

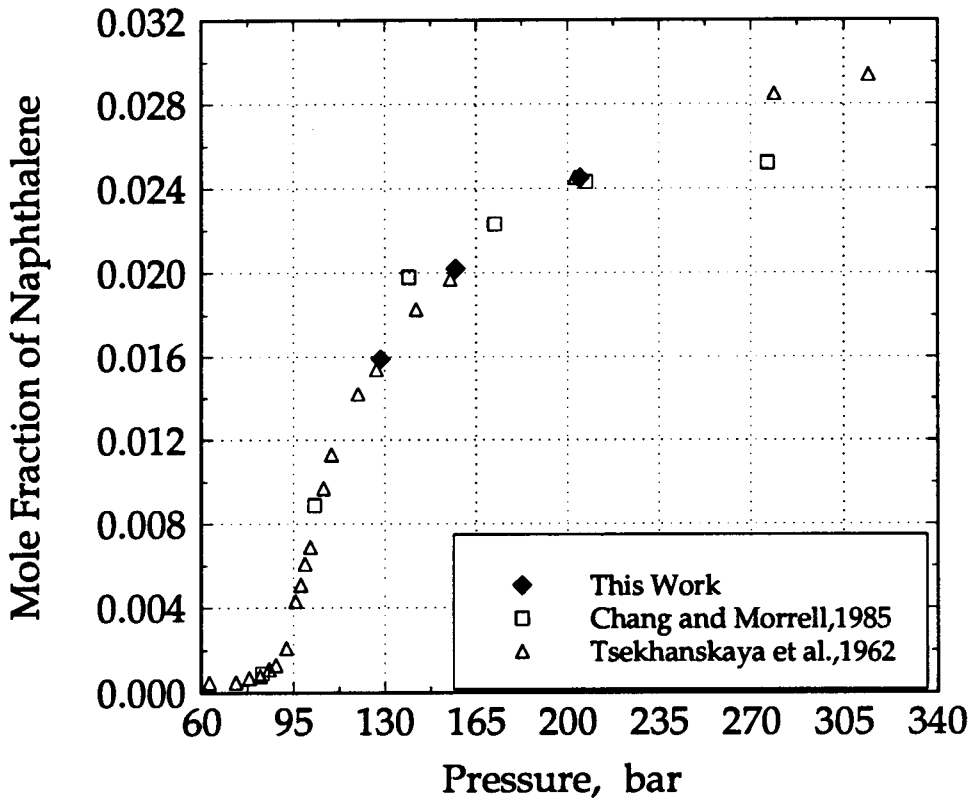

Figure 3.5 Solubility of naphthalene in CO_2 at 45°C.

3.4 Results of Solubility Study

3.4.1 Binary Systems

The solubilities of nine biocides in SC-CO_2 were measured at a constant pressure of 250 bar and temperatures ranging from 40 to 80 °C as shown in Figure 3.6. The solubilities of the biocides varied over a range of more than three orders of magnitude. The results demonstrate that solute volatility was the dominant solubility factor when using pure CO_2 , i.e. solutes with higher vapor pressures or lower melting/boiling temperatures had higher solubilities. The relative solubilities of these biocides were consistent with the postulates of other workers, since increasing polarity, high molecular weights or low vapor pressure corresponded to low solubility (Stahl et al., 1978; Dandge et al., 1985). The biocides were classified according to their maximum observed solubilities (Table 3.8).

Temperature affects solute vapor pressure, solvent density and intermolecular interactions in the fluid phase. The effect of temperature on solubility of chlorothalonil is shown in Figure 3.7. At pressures below 180 bar solubility deceased with increasing temperatures (retrograde vaporization). Therefore, the effect of an increase in temperature causing a decrease in solvent density was stronger than the positive effect to increase the solute vapor pressure. Above 200 bar, vapor pressure effects were more dominant since solubility increased with temperature. Similar phenomena have been documented in previous studies (Johnston and Eckert, 1981; Hoyer, 1985)

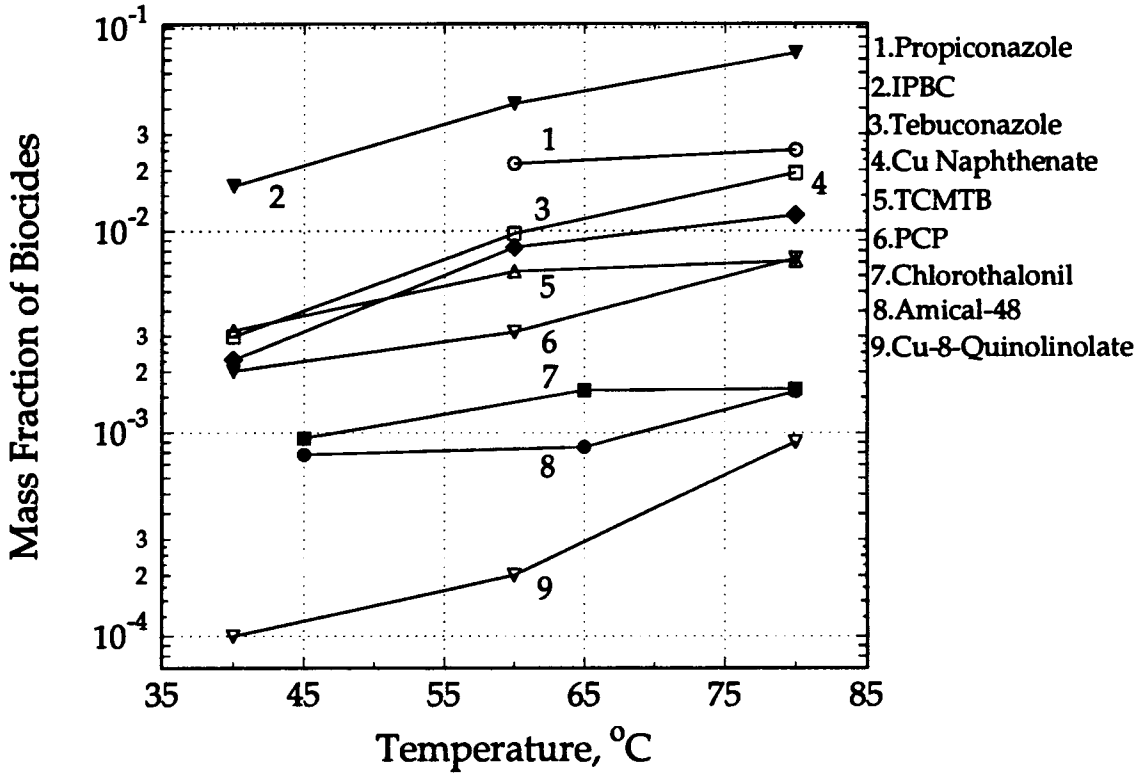

Figure 3.6 Solubility levels of biocides in SC-CO_2 at 250 bar and selected temperatures.

Table 3.8 Maximum observed solubilities of selected biocides in supercritical CO_2 (mass %)

High	Intermediate	Low
y > 2 %	y = 0.8 - 2 %	y < 0.8%
IPBC Tebuconazole TCMTB Propiconazole	PCP Cu-naphthenate	Cu-8- quinolinolate Chlorotaonil Amical-48

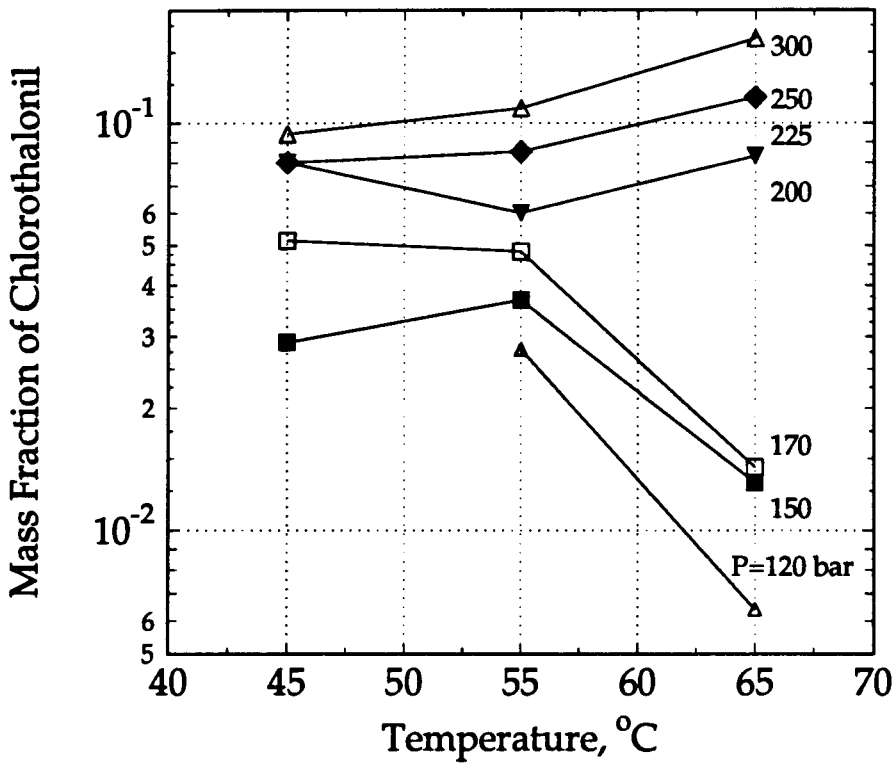

Figure 3.7 Solubility of chlorothalonil in SC-CO_2 at selected temperatures and pressures.

Solubilities of three biocides, pentachlorophenol, Amical-48 and TCMTB, in SC-CO_2 are shown at constant temperature and selected pressures (Figures 3.8, 3.9 and 3.10). Tabulated values are given in Appendix A. Solubility increased with a rise in pressure at all three temperatures (40, 60, 80 °C). With an increase in pressure, the density of CO_2 rises, decreasing the intermolecular mean distance of molecules and thereby increasing the specific interactions between the solute and solvent molecules.

Since there was no previously reported work done on the solubility of these solutes, comparison of data with literature values was not possible, except for pentachlorophenol. DeFillipi et al. (1980) found that the logarithm of the measured solubility of pentachlorophenol at 275 bar increased linearly from 0.7 to 1.01 wt % for temperatures between 80 and 125 °C. The data presented here show that the solubility of PCP at 250 bar increased from 0.2 to 0.7 wt % for temperatures from 40 to 80 °C. Although the two sets of data were measured at different temperatures, they are reasonable similar.

3.4.2 Ternary Systems

Solubilities of biocides in SC-CO_2 with 3.5 mole percent acetone, methanol and ethanol, at 250 bar, are shown in Figures 3.11, 3.12 and 3.13 respectively. Cosolvents usually produced increased solubility. The size of increase depended strongly on the structure of the solute and the type of the cosolvent. Cosolvent induced solubility enhancements, measured as the ratio of solubility

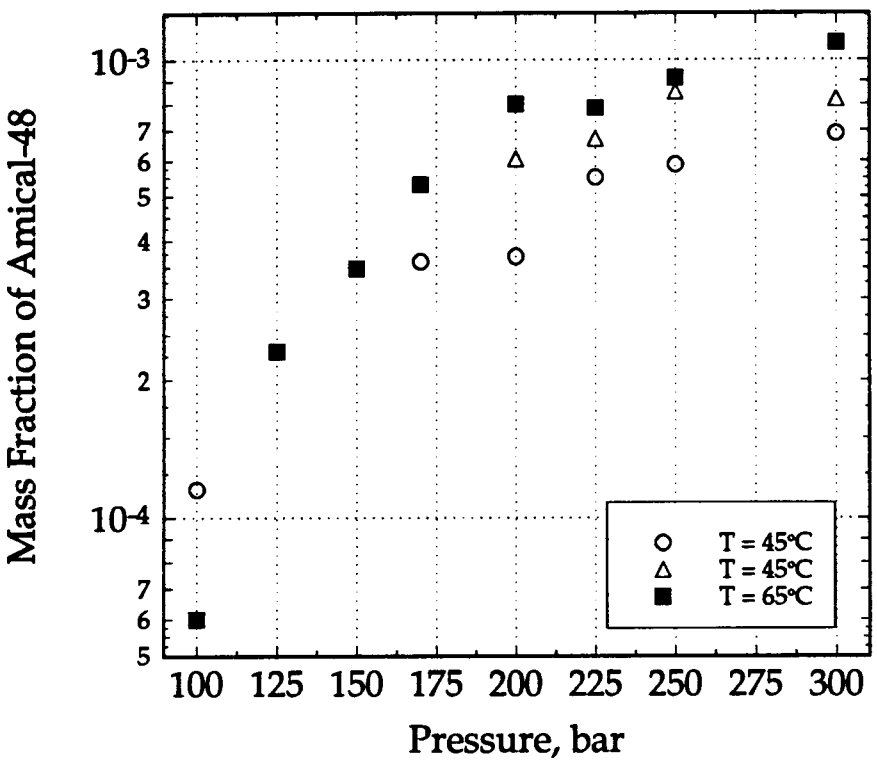

Figure 3.8 Solubility isotherms of Amical-48 in SC-CO_2 at selected temperatures and pressures.

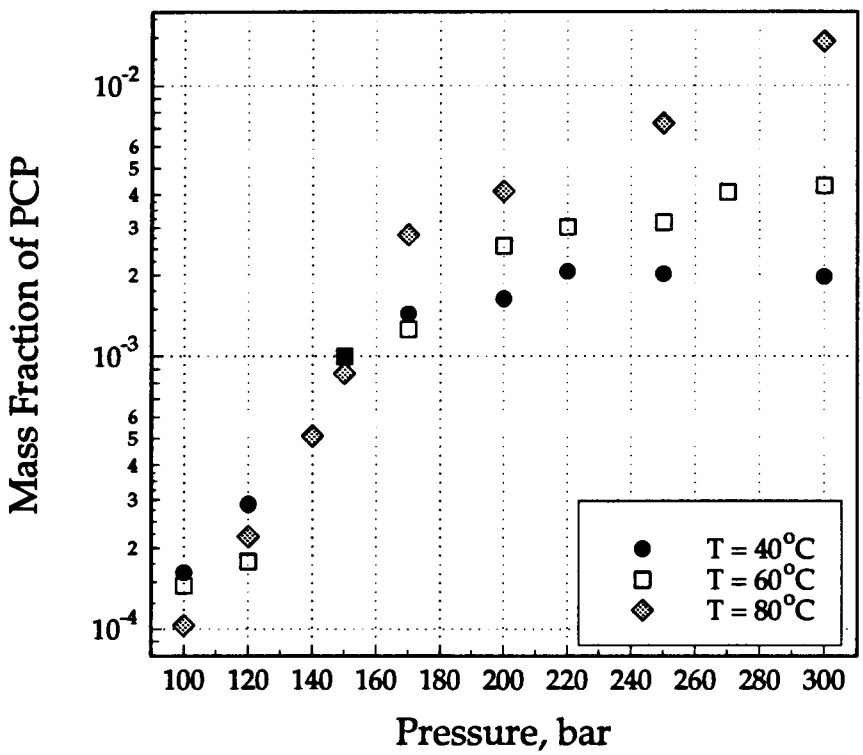

Figure 3.9 Solubility isotherms of pentachlorophenol in SC-CO_2 selected temperatures and pressures.

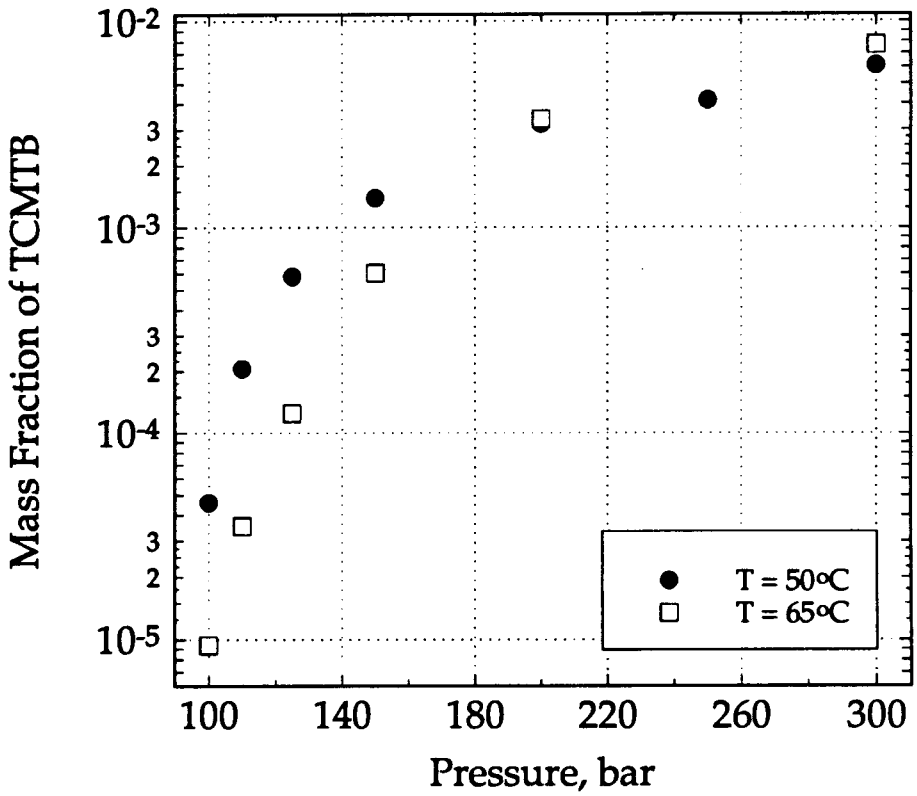

Figure 3.10 Solubility of TCMTB in SC-CO_2 at selected pressures. (adapted from Sarawadee Junsophonsri, 1994, with permission)

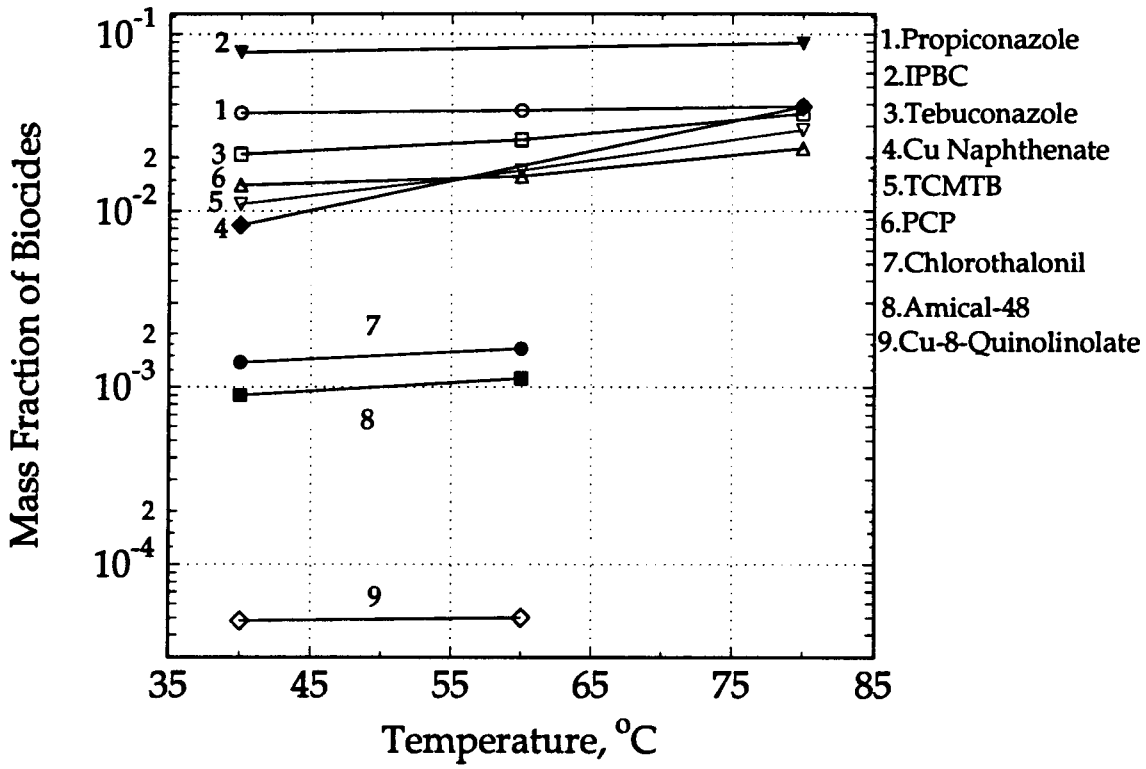

Figure 3.11 Solubility levels of biocides in SC-CO_2/3.5 mole % acetone at 250 bar and selected temperatures.

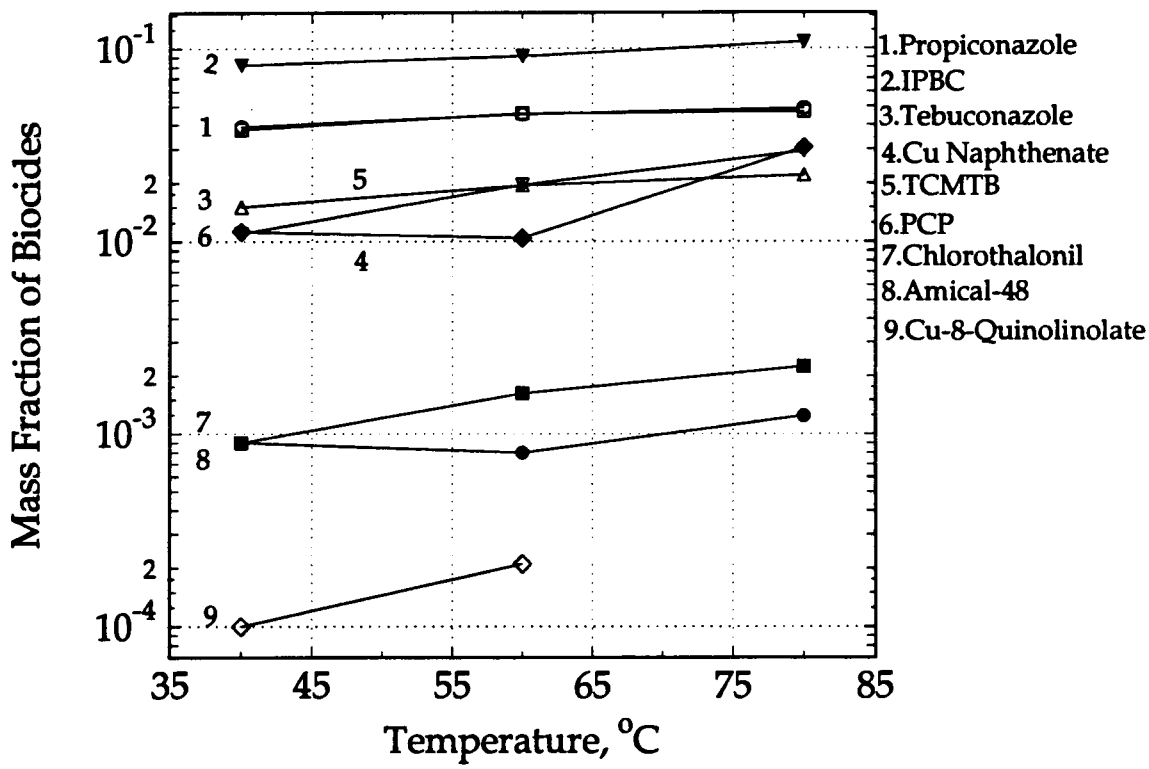

Figure 3.12 Solubility levels of biocides in SC-CO_2/3.5 mole % methanol at 250 bar and selected temperatures.

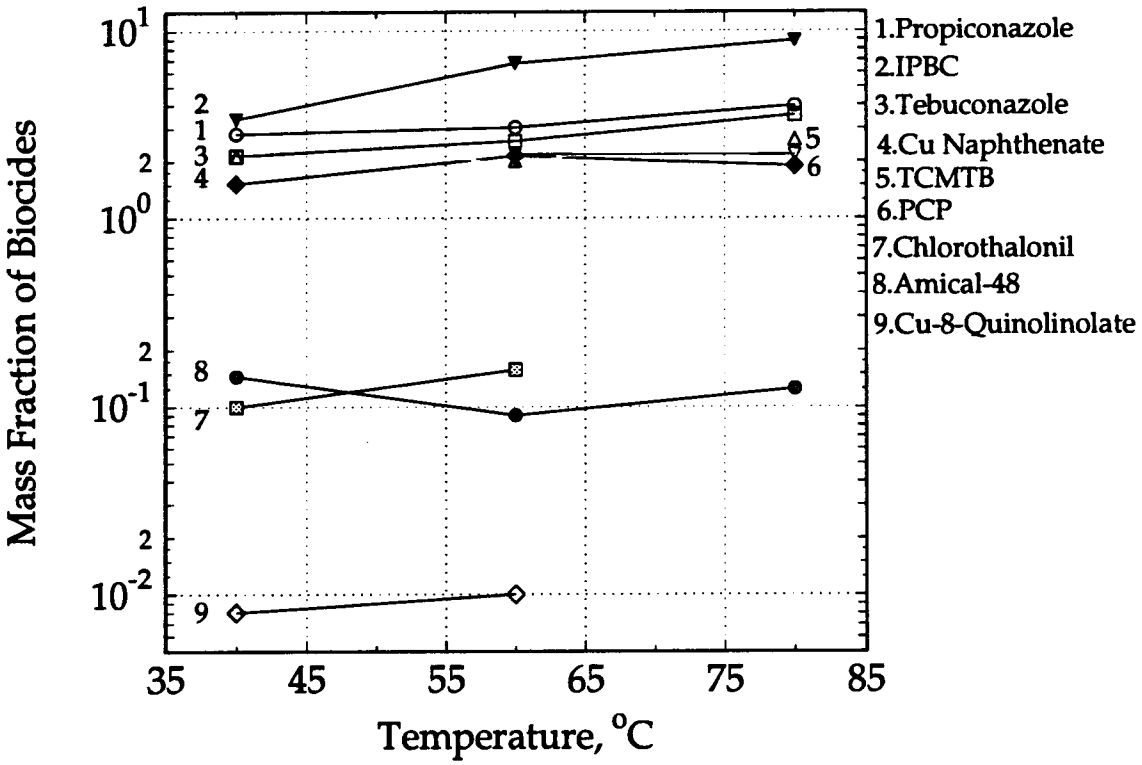

Figure 3.13 Solubility levels of biocides in SC-CO_2/3.5 mole % ethanol at 250 bar and selected temperatures.

in the cosolvent/CO_2 mixture to solubility in CO_2 under the same conditions, are summarized in Tables 3.9. These ratios varied from 1 for chlorothalonil to 16 for tebuconazole.

The effect of four different cosolvents (at 3.5 mol %) on the solubility of pentachlorophenol at selected temperatures are shown in Figures 3.14 and 3.15. In all cases, the solubility of PCP was increased by a factor of two to four through the use of a cosolvent. Methanol and ethanol produced larger increases than acetone. These large enhancements can be attributed to the hydrogen bonding between the hydroxyl functional groups of the biocides and the cosolvent or to the polarizability and acidic nature of acetone. Further studies have shown that cosolvent effects on solubility were even more significant at lower temperatures (Figures 3.16 and 3.18) enabling one to operate at lower temperatures and more moderate pressures to obtain the required solubility. In the presence of a high-pressure fluid, some solutes can experience significant freezing point depressions (Brennecke and Eckert, 1989; Dobbs et al, 1987, McHugh and Yogan, 1984; Chang and Morrell, 1985). The very high solubility increases of tebuconazole and IPBC when a cosolvent was added to SC-CO_2 may be due to similar phenomena where some of the cosolvents and CO_2 move into the solute rich phase. Chromatographic and spectroscopic analysis on two of the biocides (tebuconazole and IPBC) confirmed that the measured solubility enhancements with cosolvents were not due to chemical changes of the biocides (Figures 3.19, 3.20, 3.21 and 3.22).

Table 3.9 **Cosolvent induced solubility enhancements at 250 bar and 3.5 mol % cosolvent**

	Biocide	Temper. °C	$\frac{y^{ternary}}{y^{binary}}$		
			Methanol	Ethanol	Acetone
1	IPBC	40 55 80	4.91 2.17 1.44	2.0 1.59 1.17	4.72 na 1.18
2	Tebuconazole	40 55 80	16.39 6.73 6.41	9.30 3.08 2.92	9.04 3.02 2.94
3	TCMTB	40 55 80	4.68 3.08 3.09	6.65 3.74 3.67	4.375 2.47 3.16
4	Propiconazole	40 55 80	na 3.0 2.76	na 1.74 1.57	na 1.76 1.55
5	Copper Naphthenate	40 55 80	3.78 1.07 1.57	5.12 2.18 1.01	2.79 na 1.99
6	Pentachlorophenol	40 55 80	5.47 6.21 4.00	na 6.94 2.96	5.44 5.37 3.92
7	AMICAL-48	45 65 80	1.15 0.94 0.77	1.86 1.06 0.78	1.77 1.94 na
8	Chlorothalonil	45 65 80	0.96 1.01 1.35	1.06 0.97 na	0.96 0.71 na
9	Cu-8-Quinolinolate	40 60 80	10.01 10.0	8.08 5.04	4.8 2.5

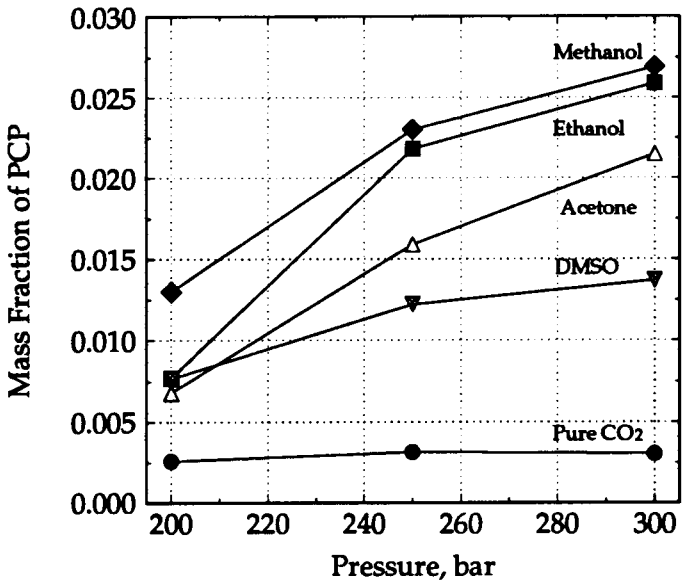

Figure 3.14 Solubility of pentachlorophenol in SC-CO_2 mixed with 3.5 mole % of a cosolvent at 333 K and selected pressures.

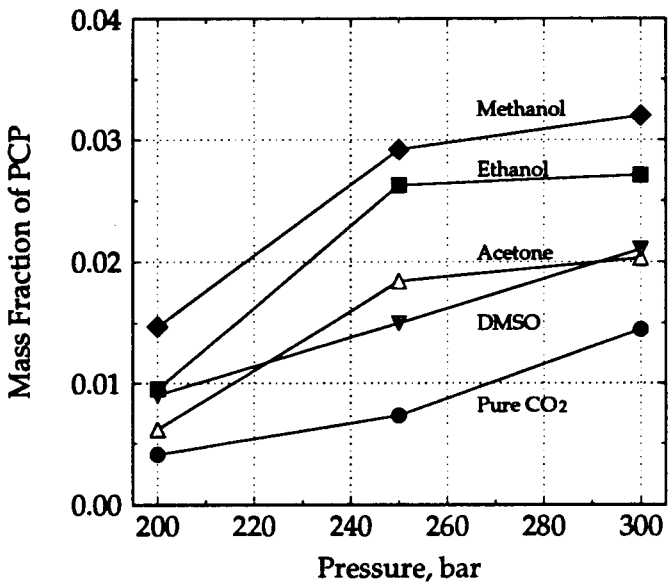

Figure 3.15 Solubility of pentachlorophenol in SC-CO_2 mixed with 3.5 mole % of a cosolvent at 353 K and selected pressures.

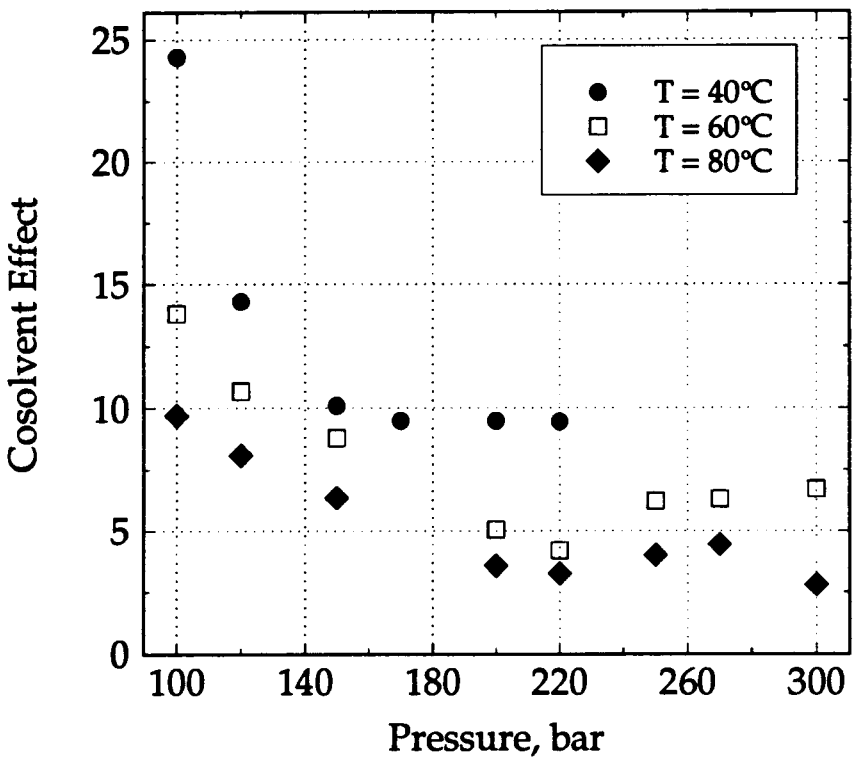

Figure 3.16 Cosolvent effect on pentachlorophenol solubility as a function of pressure for CO_2/3.5 mole % methanol mixture.

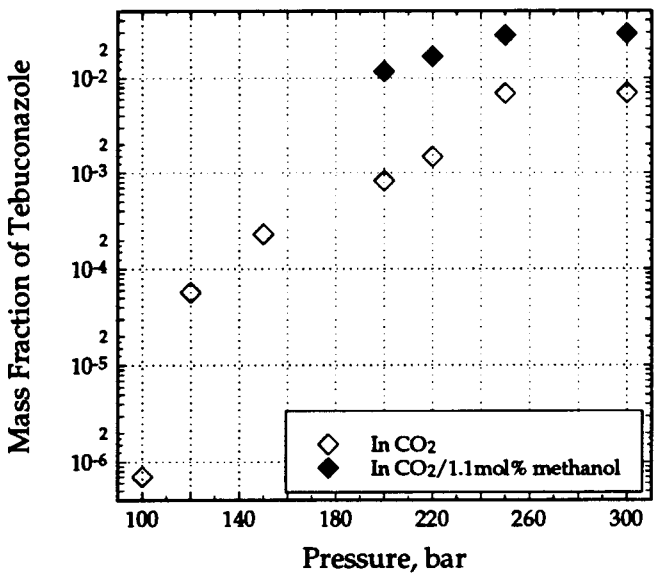

Figure 3.17 Solubility of tebuconazole in SC-CO_2 and in SC-CO_2 /1.1 mole % methanol at 55°C and selected pressures.

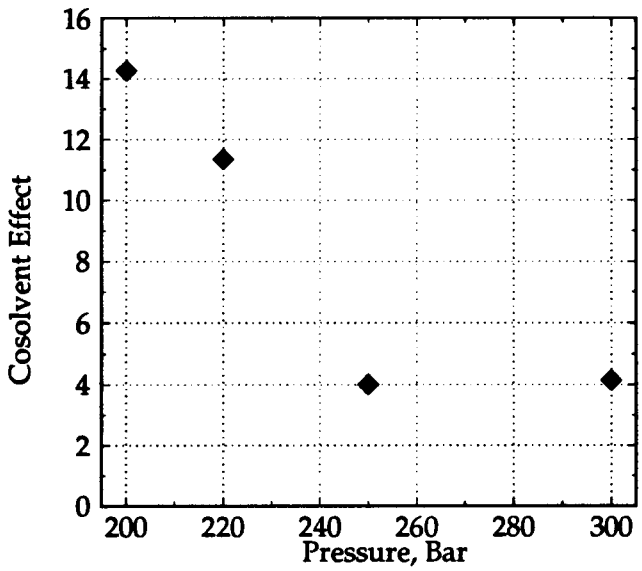

Figure 3.18 Cosolvent effect on tebuconazole solubility as a function of pressure for SC-CO_2 / 3.5 mole % methanol mixture at 55°C.

IPBC

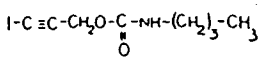

Solubilized in:

CO_2

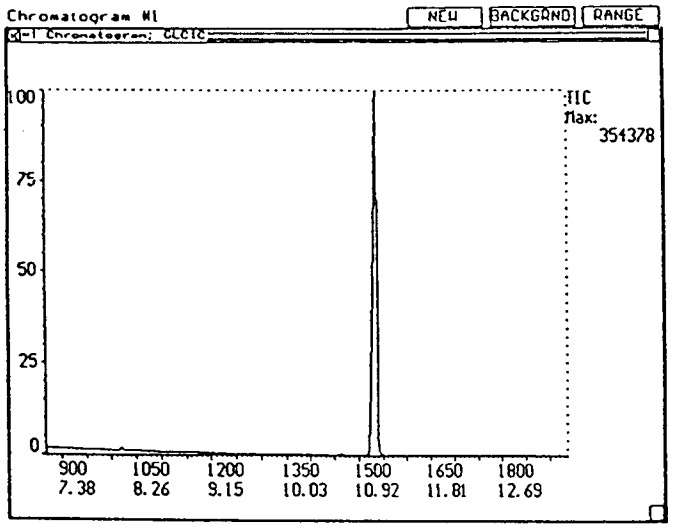

CO_2 + Acetone

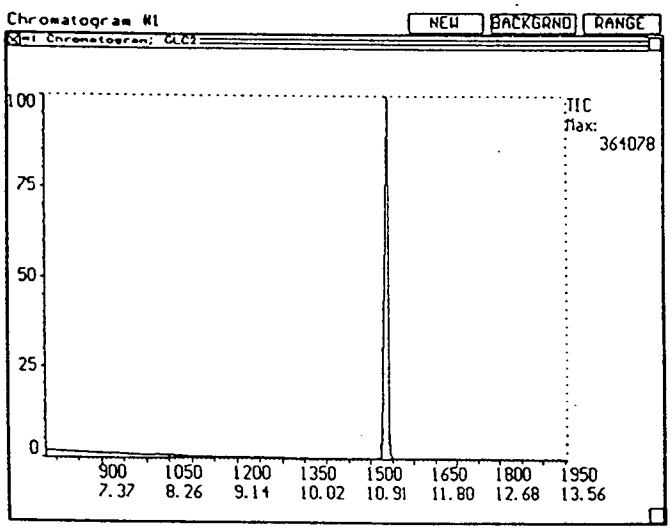

Figure 3.19 Gas chromatograms of IPBC solubilized in (a) SC-CO_2, or (b) in SC-CO_2/ acetone

IPBC Solubilized in:

CO_2

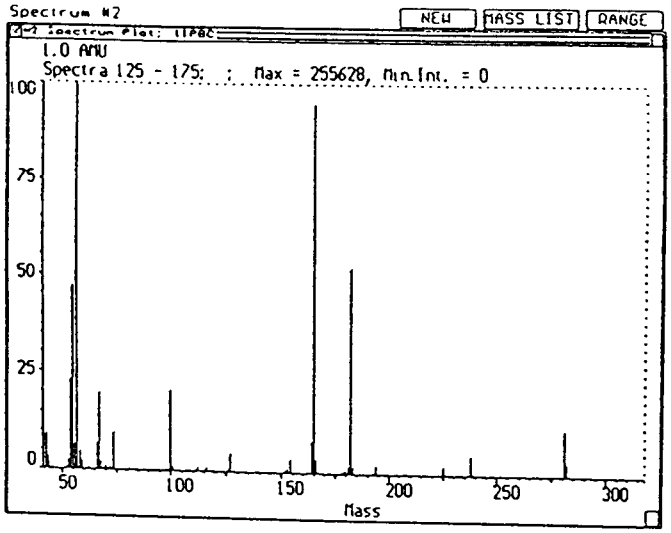

CO_2 + Acetone

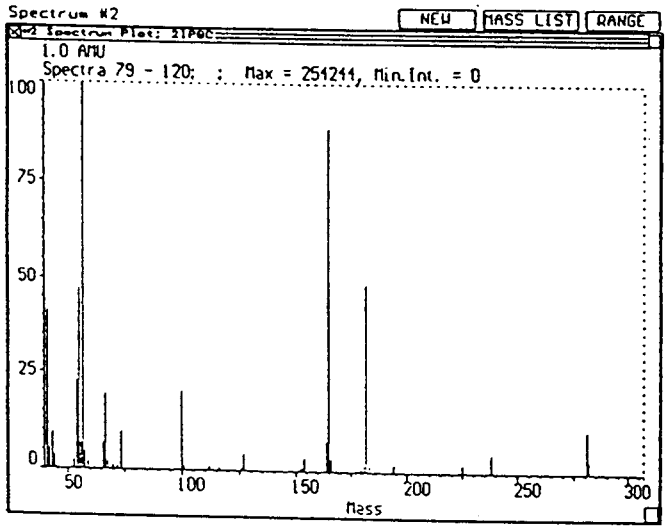

Figure 3.20 Mass spectra of IPBC ($C_8H_{12}INO_2$ mol wt = 281) solubilized (a) in SC-CO_2, (b) in SC-CO_2 / acetone

Tebuconazole

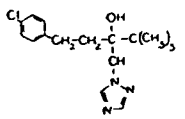

Solubilized in:

CO_2

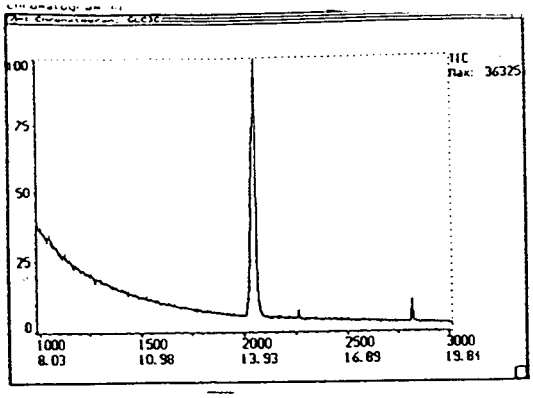

CO_2 + Acetone

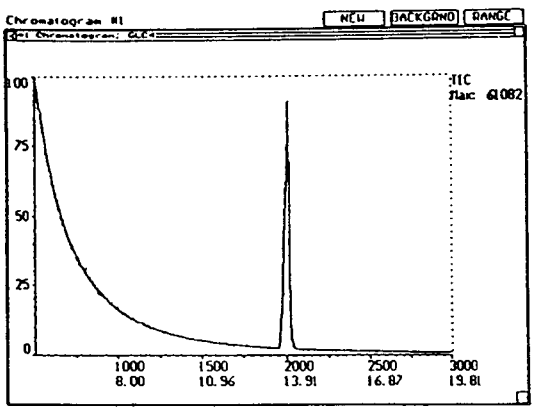

CO_2 + Methanol

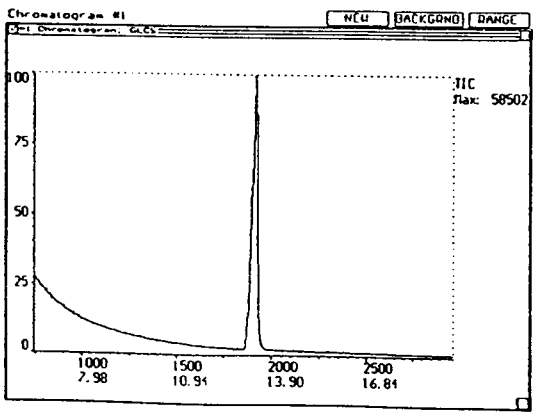

Figure 3.21 Gas chromatograms of tebuconazole solubilized in (a) SC-CO_2, (b) in CO_2 + acetone, and (b) in CO_2 + methanol

Tebuconazole Solubilized in CO_2

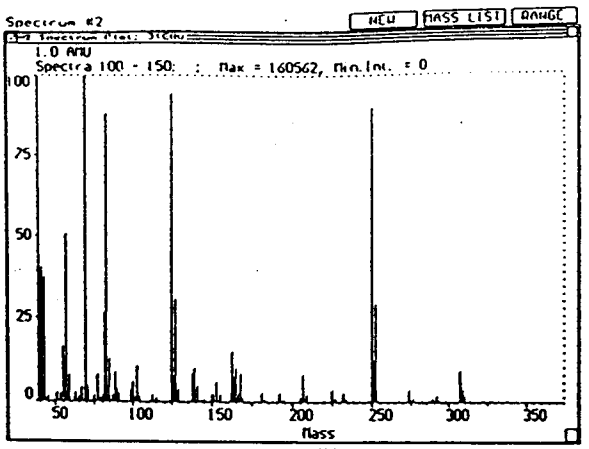

CO_2 + Acetone

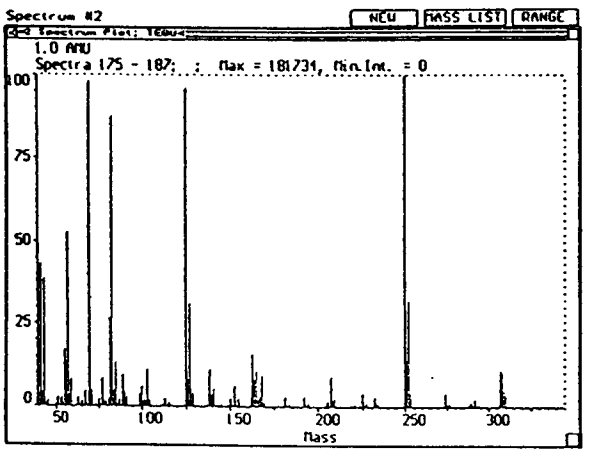

CO_2 + Methanol

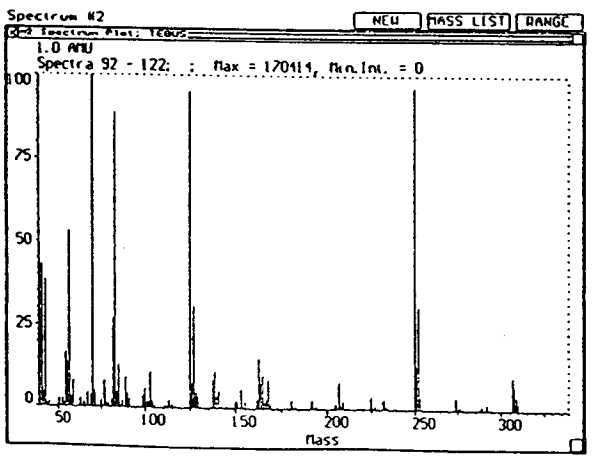

Figure 3.22 Mass spectra of tebuconazole ($C_{16}H_{22}ClN_3O$, mol wt = 308) solubilized (a) in SC-CO_2, (b) in SC-CO_2 / acetone, or (c) in SC-CO_2 / methanol.

3.5 Conclusion

The solubility of nine organic compounds in pure and modified CO_2 has been experimentally studied over a pressure range of 100 - 300 bar and temperature of 35 - 80°C. Solubilities varied over a range of more than three orders of magnitudes. Five of the biocides showed maximum solubilities greater than 2 wt%. The vapor pressure of the biocides appears to be an important factor to influence solubility, since biocides with higher vapor pressures or lower melting points showed higher solubilities. Solubilities of biocides, which have low vapor pressure and high molecular weight, such as Amical-48 or Cu-8-quinolinolate, were very low in both pure or modified SC-CO_2. Adding 3.5 mol % of methanol in SC-CO_2 increased solubility of tebuconazole by 1100% and pentachlorophenol by 500% over pure CO_2 at 200 bar. The cosolvent effect, i.e. the enhancement of solubility by adding cosolvent, increased with cosolvent amount and decreased with increases in pressure and temperature. Cosolvent effects indicate the affinity of the solute for the cosolvent and were independent of fluid density at higher pressures. Cosolvent effect ratios were comparable to retention time ratios (RTR) obtained using GC screening studies reported in Section 3.2. For example, for chlorothalonil the RTR and cosolvent effect values were both close to 1. However, for TCMTB, RTR values were 11 times higher than the measured cosolvent effects, which indicate that biocide-cosolvent association measured

via the GC method do not always correlate with higher solubilities at supercritical conditions.

CHAPTER 4

SOLUBILITY MODELING AND DATA CORRELATION

4.1 Introduction

The solubility of substances in a SCF can be increased by several orders of magnitude over that expected from pure component vapor pressure data and Dalton's law. From Dalton's law, we expect that the mole fraction of a dissolved solute in a gas is given by P^{sat}/P, where P^{sat} is the vapor pressure of the solute at a given temperature. Usually P^{sat} is much smaller than P, and experiments show large deviations from the law at high pressures. The enhanced solubility is due to the solvating power of the SCF, whose properties are directly related to solvent density, and primarily reflects interactive forces between the molecules of the solute and those of the gas.

Reliable models of SCF phase behavior are vital to the design and evaluation of supercritical fluid processes. However, the high compressibility, the asymmetry of the systems, and the mathematically singular nature of the critical point make modeling efforts challenging.

An ideal model would use easily measured physical properties to predict phase equilibria at all conditions and would be theoretically based. Current models, which use equations of state (EOS) to calculate the fugacity of

the solute in the fluid phase or treat the SCF as an expanded liquid, do not fit these criteria. Existing correlations of phase equilibria data contain many regressed parameters, are semi-empirical at best, and may succeed in accurately fitting the data in only portions of the phase diagram. On the other hand, predictive models attempt to theoretically justify a link between the model parameters and real physical phenomena. However, these theoretical based models are forced to fit the data by introducing adjustable parameters, which makes them no better than the semi-empirical models.

Various approaches have been used to describe the solubility behavior of pure solids and liquids in supercritical solvents. These include the solubility parameter approach (Allada, 1984; Vetere, 1979), lattice models (Kumar et al., 1987; Vezzetti, 1982, 1984;), perturbed hard-sphere equations of state (Johnston et al, 1982; Wong et al., 1985; Johnston et al., 1989; Ghonasgi et al, 1991), Monte Carlo simulation (Shing and Chang, 1987), Kirkwood-Buff solution theory (Cochran et al., 1987; Pfund et al., 1988) and cubic equations of state (Mackay and Paulaitis, 1979; Kurnik et al., 1981; Debeneditti and Kumar, 1986). Two major approaches have been used with cubic EOS modeling. The fluid may also be treated as a compressed gas (Adachi, 1983; D'Avila, 1976, Johnston and Eckert, 1981, Kurnik and Reid, 1982; Mart et al., 1985) or as an expanded liquid (Mackay and Paulaitis, 1979).

The most straight-forward and thermodynamically consistent method for calculating high-pressure phase equilibrium is the use of an equation of

state to model the equilibrium dense phase and SCF. For a solid-fluid system to be at equilibrium, the phases must be at the same temperature, pressure and the chemical potential for each component must be the same in both phases. By equating the fugacities of the solute as it exists in each phase, an equivalent but more useful criterion can be obtained (Prausnitz et al. 1986):

$$\hat{f}_2^s = \hat{f}_2^F \tag{4.1}$$

where are f_2^s and f_2^F are fugacities of the solute in the dense and fluid phases. Equation (4.1) can be written in terms of a pure component fugacity by neglecting the solubility of fluid in the solid phase. From the definition of the isothermal pure component fugacity in terms of the Gibbs function, f_2^s ,can be

$$d\ \ln f_2^s = V_2^s \frac{dP}{RT} \tag{4.2}$$

expressed in terms of molar volume and pressure:

At constant molar volume, the integration of equation (4.2) from an arbitrarily chosen reference pressure, P^o, to a desired pressure gives:

$$f_2^s = f_2^{os} \exp\left[\frac{V_2^S(P-P^o)}{RT}\right] \tag{4.3}$$

where $f^{os}{}_2$ is a function of pressure.

By selecting the vapor pressure of the solute as the reference pressure in equation (4.3):

$$f_2^s = f_2^{sat} \exp\left[\frac{V_2^s(P-P^o)}{RT}\right] \tag{4.4}$$

Since f_2^{sat} is usually small, Equation (4.4) can be simplified replacing f_2^{sat} by P_2^{sat}. The fugacity coefficient for the solute in solution is defined by:

$$\hat{\phi}_2^F = \frac{\hat{f}_2^F}{y_2 P} \tag{4.5}$$

Substituting equations (4.4) and (4.5) into equation (4.1), solving for y_2 the equilibrium mole fraction of the solute yields:

$$y_2 = \frac{P_2^{sat} \exp\left[\frac{V_2^s(P-P_2^{sat})}{RT}\right]}{P\,\hat{\phi}_2^F} \tag{4.6}$$

where:

$$\ln \phi_2 = \frac{1}{RT}\int_0^P \left(\bar{V}_2 - \frac{RT}{P}\right) dP \tag{4.7}$$

$$\bar{V}_2 = \left(\frac{\partial v}{\partial n_2}\right)_{T,P,n_1} \tag{4.8}$$

The assumptions made for solid-fluid systems to obtain Equation (4.6) are:

1. The solid phase has a vapor pressure sufficiently small so that $\phi_2^s \approx 1.0$.
2. The solid is incompressible.
3. The solubility of the fluid solvent in the solid solute is negligible.

The dependence of solubility on density cannot readily be seen from equation (4.6). Kumar and Johnston (1988) defined the product of fugacity coefficient and compressibility factor (Z) as, $\psi_2 \equiv \phi_2 Z$, to relate the fugacity coefficient with density. The equation relating solid solubility in SCF as a function of solvent density can then be written as:

$$y_2 = \frac{P_2^{sat}}{\rho RT\psi_2} \exp\left[\frac{V_2^s(P - P_2^{sat})}{RT}\right] \tag{4.9}$$

where

$$\ln \psi_2 = \int_0^P \left[1 - \frac{\bar{V}_2}{RT\kappa_T}\right] dP \tag{4.10}$$

and V_2 is the partial molar volume of the solute 2 in the SCF phase and $\kappa_T \equiv (1/\rho)(\partial\rho/\partial P)_{T,y2}$ is the isothermal compressibility of the SCF. Although

solubility appears to be inversely proportional to density in Equation (4.9), ψ_2 decreases as ρ increases and the product $\rho\psi_2$ decreases as ρ increases. Fugacity coefficients decrease by three orders of magnitude as reduced density increases from 0.3 to 1.2.

Differentiating equation (4.10):

$$\left(\frac{\partial \ln\psi_i}{\partial \ln\rho}\right)_{T,y_1} = -\left(1 - \frac{\bar{V}}{RT\kappa_T}\right) \qquad \textbf{(4.10b)}$$

In the case of equilibrium between a liquid solute and a supercritical fluid, the thermodynamic analysis is considerably more complicated than for the SCF-solid system because both components exist in each phase. This leads to a composition dependence of the chemical potential of the system that is far removed from Henry's law. Therefore, one must sample or otherwise determine the composition of all phases when studying SCF-liquid systems.

4.2 Density - Based Correlations

Correlations of solute concentration with solvent density were derived by Chrastil (1982) using two different approaches: an association law or from the entropy of components in the mixture. The analysis was based on the assumption that a solute molecule A associates with *n* molecules of the solvent B to form a solvato complex AB_n, which is in equilibrium with the system. From equilibrium considerations and the approximation of the

Clausius-Clapeyron equation, which estimates the vapor concentration of the solute, A, the following theoretical equation was derived:

$$\ln y = (n-1)\ln\rho + \frac{\gamma}{T} + Y \qquad \textbf{(4.11a)}$$

where y is the mass fraction of solute in the SCF, ρ is the density of the SCF, γ is $\Delta H/R$, ΔH is $\Delta H_{solvation} + \Delta H_{vaporization}$, $Y = q - n\ln M_B + \ln (M_A + M_B)$, q = constant, M_A, M_B = molecular weights of solute and solvent, respectively The association constant, n, was found to range between 1 and 13 (Chrastil, 1984).

Although, the linear ln y *vs* ln ρ correlation (Eqn. 4.11) was based on empirical observations, it was later shown using equation(4.10b) that the linearity is a manifestation of V_1/κ_T being a constant and independent of density near the critical point (Kumar and Johnston 1988). Kumar and Johston (1986) correlated the solubilities of non-volatile solutes in SCF as a function of solvent density and showed that solubility and solvent density were linear when plotted on log-log or log-linear scales.

$$\ln y = C_o - \left(\frac{\bar{V}_1}{RT\kappa_T}\right)_{\rho_r=1} \ln \rho_r \qquad \textbf{(4.11b)}$$

The slope of this plot is thus dependent on isothermal compressibility of the solvent (κ_T) and the partial molar volume of the solute.

4.3 log E vs ρ relationship

Solubilities and also selectivities in SCFs are governed primarily by vapor pressure and only secondarily by solute-solvent interactions in the SCF phase (Johnston, 1989). This secondary effect of increased solute solubility can be described using an enhancement factor (E), the ratio of true mole fraction in a SCF solution to the mole fraction predicted from ideal gas behavior from the vapor pressure. From Dalton's law, solubility in an ideal gas is:

$$(y_2)_{id} = \frac{P_2^{sat}}{P} \tag{4.12}$$

Equation (4.9) can thus be written as:

$$y_2 = \frac{P_2^{sat}}{P} E \tag{4.13}$$

y_2 can be predicted using equation (4.6) and the predicted enhancement factor then becomes:

$$E = \frac{\exp\left[\frac{V_s^2(P - P_2^{sat})}{RT}\right]}{\hat{\phi}_2^F} \tag{4.14}$$

This factor is a normalized solubility, because it removes the effect of the vapor pressure, and can provide a measure of the interactions in the SCF phase. In carbon dioxide the predicted values of E do not exceed 3.5 orders of

magnitude for substances with a variety of polar functional groups (Dobbs and Johnston, 1987). However, the actual values of E vary up to eight orders of magnitude.

There is a semi-log empirical relationship between the enhancement factor and density (Johnston and Eckert, 1981). Plots of log E versus pure solvent density (or reduced density) show a set of parallel lines at selected temperatures. Schmit and Reid (1985) suggested that these enhancement isotherms can be made to collapse into a single line by the following empirical equation:

$$\log E = \alpha\rho_r + \beta + \sigma(T - T_{ref}) \tag{4.15}$$

where α and β represent the slope and the intercept of the line at log E vs ρ_r, respectively for $T = T_{ref}$, and σ (K^{-1}) is the isotherm spacing constant determined from the plot of the log E vs T at a chosen solvent density T and T_{ref} are the system and reference temperatures, respectively. The reference solubility isotherm is arbitrarily chosen. Schmit and Reid (1985) used equation (4.15) to correlate experimental data and to predict solubilities at other temperatures and pressures based on their limited data.

4.4 The Ziger and Eckert Relationship

The solubility of solid solutes in a supercritical fluid as a function of pressure as shown in equation (4.6) can be written as:

$$\ln E = -\ln \phi_2 + V_2^s \left(\frac{P - P_2^{sat}}{R} \right) \tag{4.16}$$

Considering the lighter component, i.e., the SCF phase, as an expanded liquid and the condensed solute as a subcooled liquid the fugacity of component i in a liquid solution is related to its mole fraction y_2 by the equation:

$$\hat{f}_i^L = \gamma_i y_i f_i^o \tag{4.17a}$$

where γ_i is the activity coefficient and f_i^o is the fugacity of i at arbitrary standard condition. From equations (4.13) and (4.17) E can be written in terms of the activity coefficient:

$$\ln E = \ln \frac{f_2^2}{f_2^o} - \ln\gamma + \ln \frac{P}{P^{vap}} \tag{4.17b}$$

Regular solution theory (RST) from Scatchard-Hildebrand has been used to predict activity coefficients for liquid-vapor equilibrium of nonpolar solvents:

$$RT \ln \gamma_2 = v_2^L \Phi_1^2 [\delta_1 - \delta_2]^2 \tag{4.18}$$

From Equations (4.17b) and (4.18), Prausnitz (1965) suggested applying RST to solid-fluid equilibria:

$$\ln E = \ln \frac{f_2^L}{f_2^o} - \frac{v_2^L}{RT} \Phi_1^2 [\delta_1 - \delta_2]^2 + \ln \frac{P}{P_2^s} \tag{4.19}$$

Ziger and Eckert (1983) proposed a semi-empirical correlation using the vdW EOS and mixing rule to determine the fugacity coefficient of the solute in the fluid phase in terms of the solubility parameters of the solvent and solute δ_1 and δ_2 respectively:

$$\ln \phi_2 = \ln \left(1 + \frac{\delta_1^2}{P}\right) - \zeta_2^* \Delta(2 - \Delta) + \frac{v_2^L P}{2.3 RT} \tag{4.20}$$

where:

$$\zeta_2^* = \frac{\delta_2^2 V_2^L}{2.3 RT}$$

and Δ is a reduced solubility parameter defined by δ_1 / δ_2 and V_2^L is the molar volume of the solute treated as a subcooled liquid. The Hilderbrand solubility

parameter, δ, defined as the square root of the cohesive energy density, was introduced to relate solubility enhancement of the solute with pressure, temperature and its molecular nature. The solubility parameter of the solvent may be calculated by the relationship (Giddings, 1969):

$$\delta_1 = 1.25\, P_c^{1/2} \frac{\rho_r}{\rho_{r,liquid}} \tag{4.21}$$

where P_c is the fluid critical pressure, while $\rho_{r,SF}$ and $\rho_{r,liquid}$ are reduced densities of the fluid in the supercritical state and in the liquid state respectively. Solubility parameters of the dissolved solutes (δ_2) are available from a number of literature sources or may be computed from group contribution methods based on their molecular structures (Fedors, 1974).

Inserting equation (4.21) into equation (4.16) and assuming the subcooled liquid volume is about the same as the solid, the enhancement factor can be related to the solute solubility parameter as:

$$\log E = \eta \left[\zeta_2^* \frac{\Delta}{y_1} \left(2 - \frac{\Delta}{y_1} \right) - \log \left(1 + \frac{\delta_1^2}{p} \right) \right] + \omega \tag{4.22}$$

ln E was converted to log E for simplicity of obtaining the slope and intercept. The two parameters, η and ω, were incorporated to account for the inadequacy of regular solution theory and the van der Waals equation and they were regressed from experimental data.

4.5 Results and Discussion

The experimental binary and ternary solute-solvent equilibrium data presented in Chapter 3 were evaluated using three correlation procedures. The solvent density for each system was obtained from the modified BWR equation of state developed for pure carbon dioxide (Ely, 1986). Calculated densities showed an average of 0.2% deviation when compared to IUPAC data (Angus, 1976).

The plots of log-log relationships between solute solubility mass fraction and solvent molar density are shown for chlorothalonil, Amical-48 and pentachlorophenol in Figures 4.1, 4.2 and 4.3 respectively. The log of solubilities in all cases was a linear function of the solvent density. Increased solubility with increasing temperature at constant density was observed seen in all systems. For all binary systems, the fitted correlations indicted formations of solvato complexes with a temperature dependent association constant, n. The association constant decreased with increases in temperature (Table 4.1). Near the critical point the fluid is highly compressible and solvent density is a sensitive function of temperature and pressure, causing clustering of molecules and resulting in larger solvato complexes (Gurdial et al., 1989). A similar solubility-density correlation was proposed by Kumar and Johston (1988) (Eqn. 4.11b). The slope of this relationship was used to calculate the solute partial molar volume. The estimated partial molar volumes of five biocide were found to be very large negative numbers which suggests that

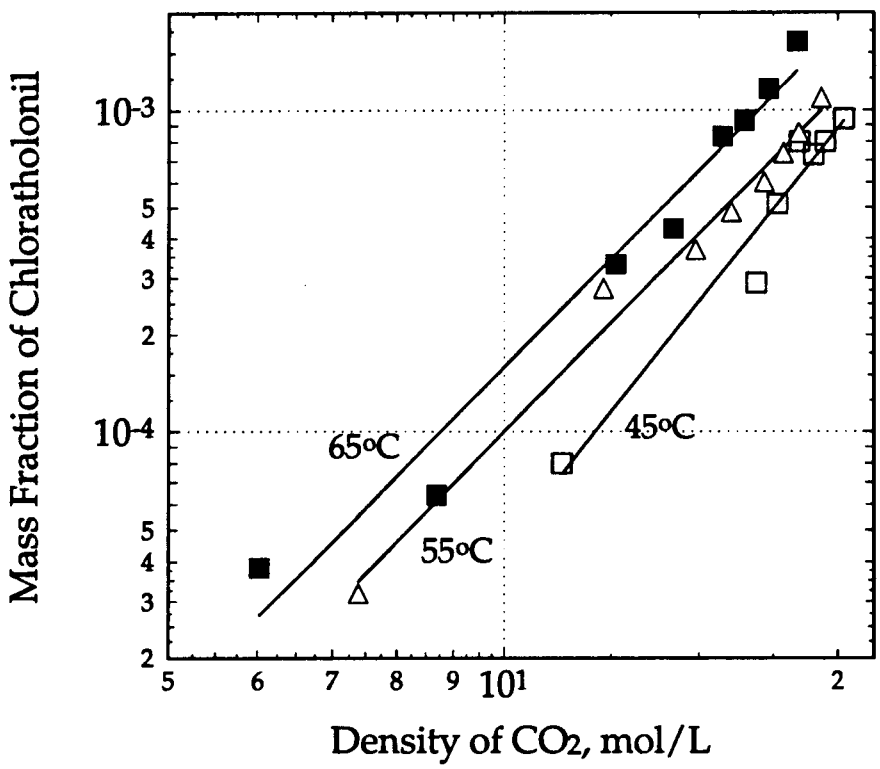

Figure 4.1 Solubility isotherms of chlorothalonil *vs* density of CO_2. Lines represent best fits for the three temperatures tested.

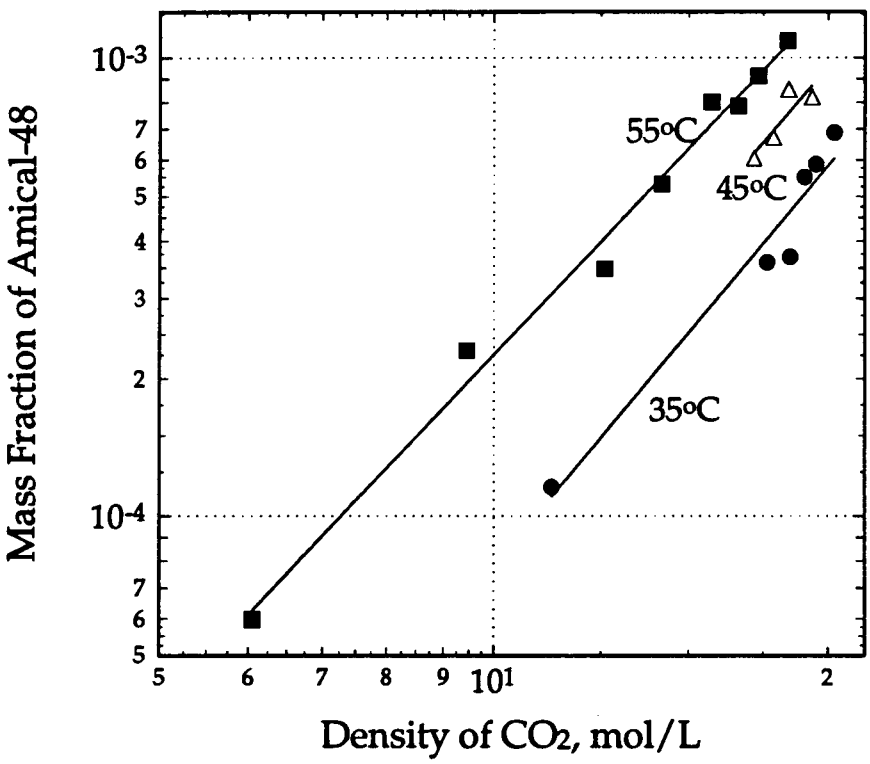

Figure 4.2. Solubility isotherms of Amical-48 *vs* density of CO_2. Lines represent best fit the three temperatures tested.

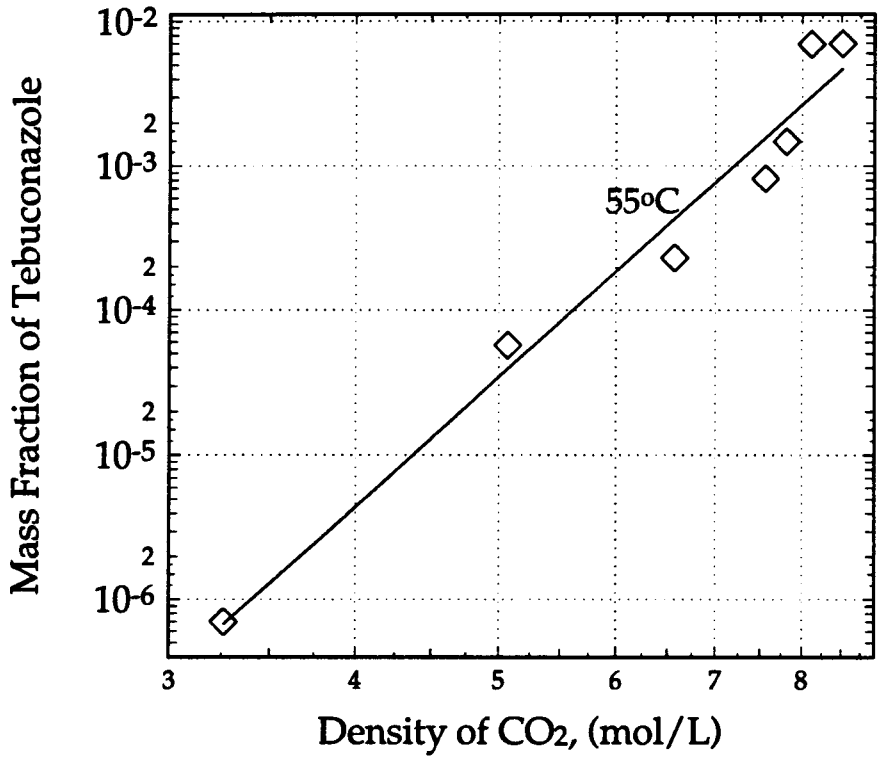

Figure 4.3 Solubility of tebuconazole *vs* density of carbon dioxide at 55°C.

Table 4.1 Association constants for selected biocides using density-based correlation

Biocide	Temperature °C	Solvato complex constant, *n*	R^2 *
Chlorothalonil	45	3.84	0.95
	55	3.59	0.99
	65	3.42	0.96
AMICAL-48	35	2.91	0.94
	45	2.84	0.78
	55	2.55	0.99
PCP	40	7.95	0.92
	60	5.02	0.99
	80	4.08	0.98
Tebuconazole	55	9.23	0.96
TCMTB	50	9.13	0.99
	65	5.95	0.99

* Correlation constant for linear fit in Figure 4.1.

"condensation" of solvent molecules about a solute molecule creating clusters (Brennecke and Eckert, 1989) (Table 4.2). These values have to be compared with experimental observations, which are currently unavailable.

When small amounts of methanol (3.5 mole %) were added in CO_2 the solubility isotherms were not clearly parallel, however the fitted association constant was nearly independent of solvent density (Figure 4.4). To determine the density of modified CO_2, the density of dilute mixtures of methanol and SC-CO_2 and density of pure SC-CO_2 were calculated using Peng-Robinson equation of state (PR-EOS). The ratios of the two densities were multiplied by a more accurate density of pure CO_2 using modified BWR EOS.

Dissolving a solute molecule in a SCF can be characterized as evaporation or dissolution involving solute vapor pressure and the non-ideality of the solvent. An enhancement factor (or the normalized solubility) is utilized to decouple these two effects. The log of the enhancement factor for pentachlorophenol was almost a linear function of the CO_2 density (Figure 4.5). Based on a fit to the correlation of E in equation (4.15), the predicted solubility mass fractions of pentachlorophenol are compared to data in Figure 4.6. This correlation considers the effect of temperature on both the solute and the solvent. They indicate the temperature effects on the solute-solvent interactions in the fluid phase.

To employ the Ziger-Eckert correlation of equation (4.22), a number of solute and solvent pure component thermodynamic parameters were required.

Table 4.2 Estimated partial molar volumes of selected biocides

Biocide	Temperature K	Solvato complex	Isothermal compressibility	Partial molar volume
Chlorothalonil	318	3.84	0.01743	-1769
	328	3.59	0.00966	-945
	338	3.42	0.00656	-630
Amical-48	308	2.91	0.06699	-4991
	318	2.84	0.01743	-1308
	328	2.55	0.00966	-671
PCP	313	7.95	0.0280	-5792
	333	5.02	0.0078	-1084
	353	4.08	0.0043	-514
Tebuconazole	328	9.23	0.00966	-2431
TCMTB	323	9.13	0.01249	-3062

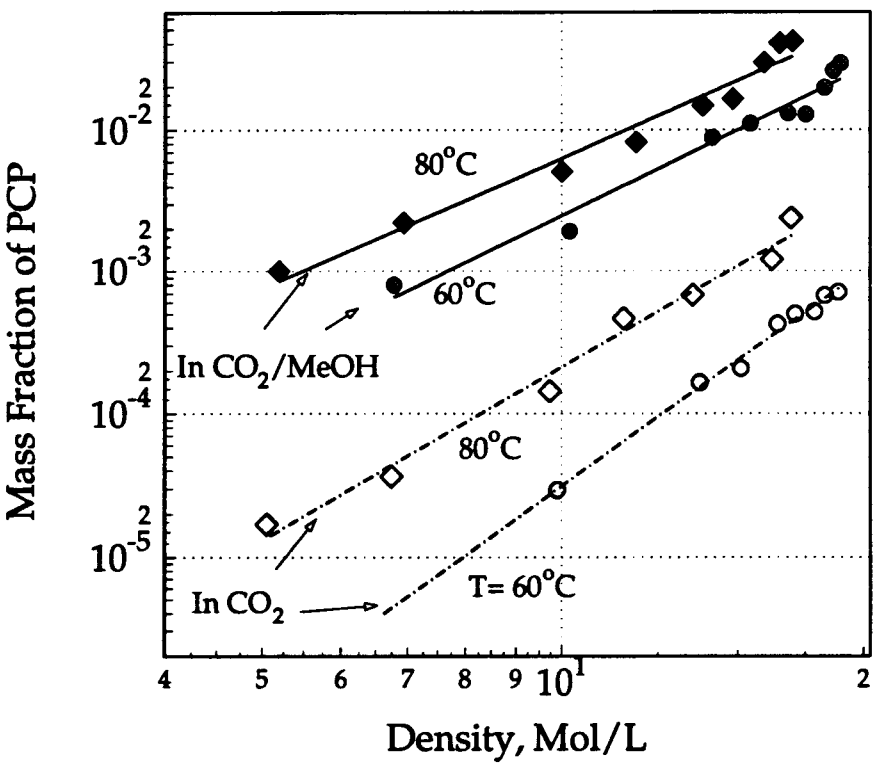

Figure 4.4 Solubility of pentachlorophenol in CO_2 or in CO_2 + 3.5 mole % methanol *vs* CO_2 density. Lines represent best fits for the respective temperatures.

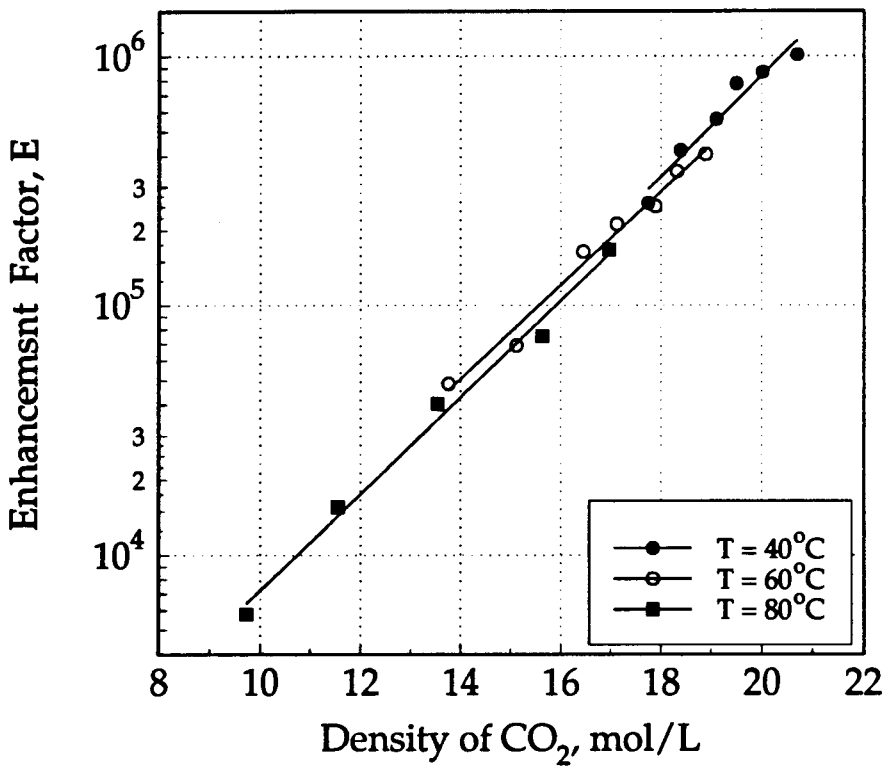

Figure 4.5 Enhancement of pentachlorophenol solubility *vs* CO_2 density. Solid lines represents best fit for the selected temperatures.

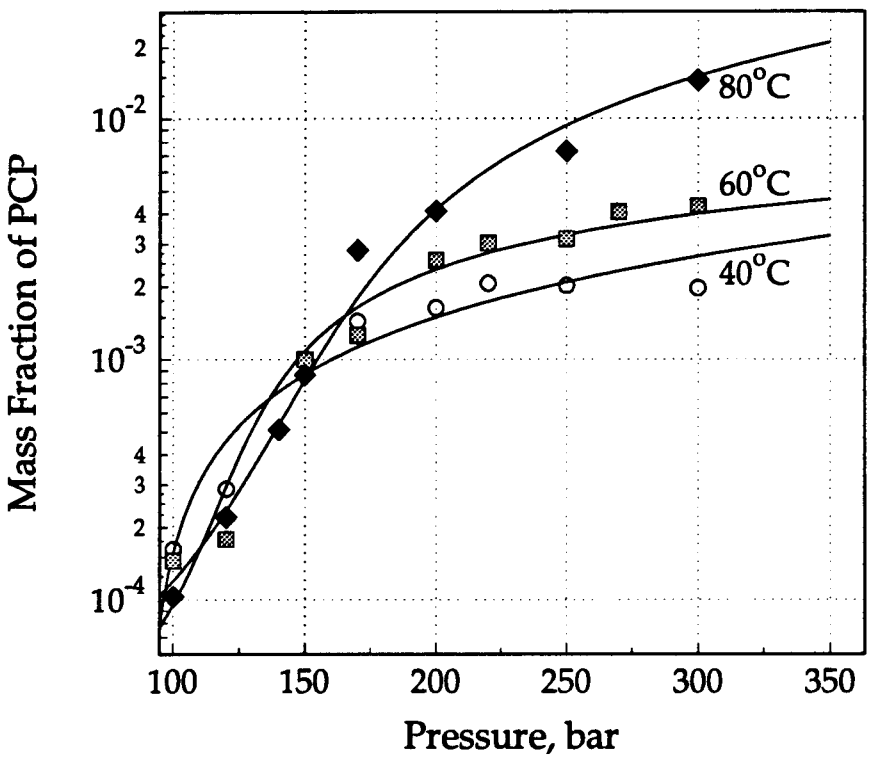

Figure 4.6 Correlated solubility of pentachlorophenol in SC-CO_2 at selected pressures and temperatures.

The solute solubility parameter and volume were calculated using the atomic and group contribution approach suggested by Fedros (1974) (Appendix D) from the structural formula of the biocides. The solubility parameter of CO_2 was calculated as a function of density using equation (4.21). This method of calculating the solubility parameters overcome the difficulty of obtaining thermal properties and molar volume of the solute and has been successfully used previously(Gurdial et al., 1989, Gurdial and Foster, 1991).

The linear relation of solubility correlations for pentachlorophenol (Figures 4.7) and tebuconazole (Figures 4.8) using the semi-empirical correlation of Ziger and Eckert provided a valuable qualitative measure of behavior of the SCF mixtures. The solubility isotherms collapsed to a single line with a slope (η) equal to 0.34 for PCP at three temperatures. For tebuconazole at one temperature the slope was equal to 0.502. The slope of the solubility data indicates solvent-solute interactions (Ziger and Eckert,1985). A slope of 0.497 was found for non-polar solute-CO_2 systems (Ziger and Eckert,1985) and 0.42 for o-hydroxybenzioc acid-CO_2 system (Gurdial and Foster, 1991). A slope of 0.34 for PCP could be as a result of the hydroxylic group which has a inhibiting effect on the rate at which solubility increases with changes in solubility parameters (Gurdial and Foster, 1991).

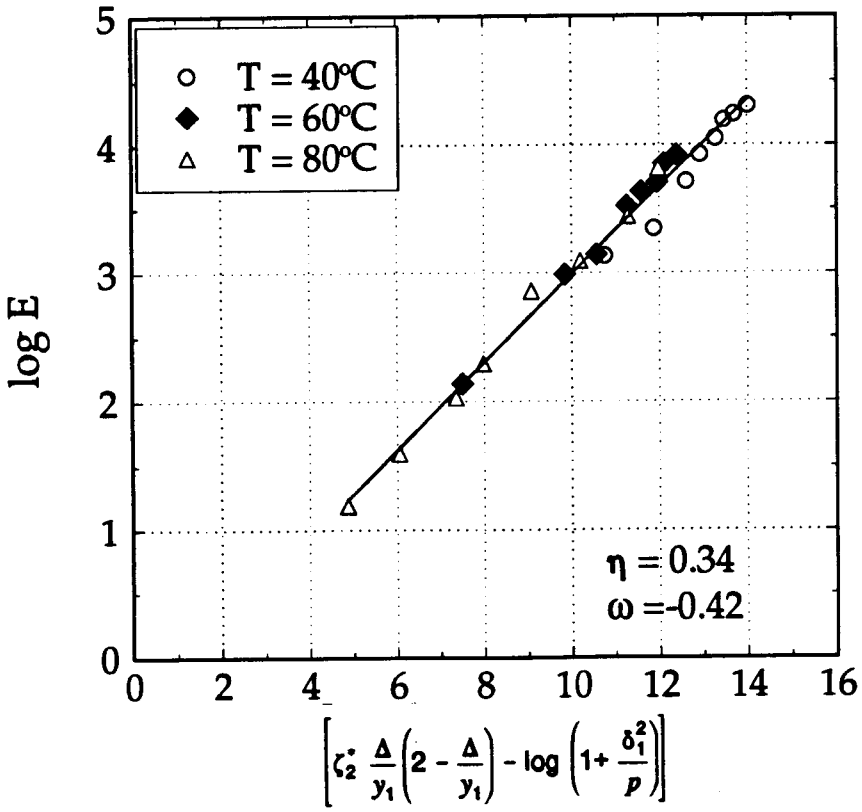

Figure 4.7 Plot of the Ziger-Eckert model for pentachlorophenol in SC-CO_2 at selected temperatures.

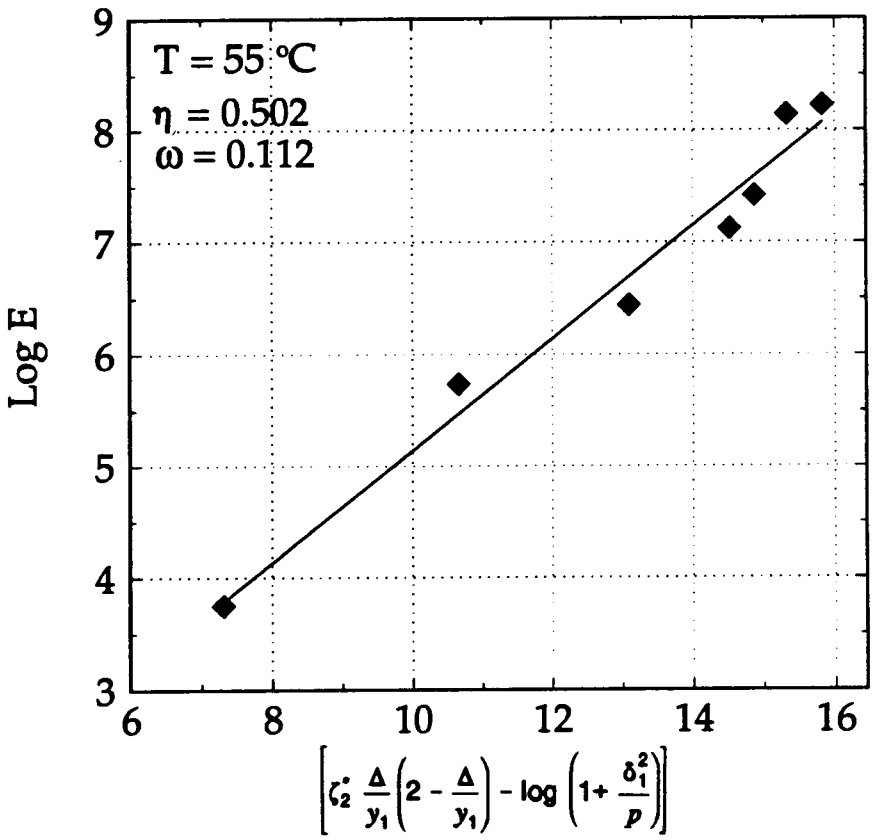

Figure 4.8 Plot of the Ziger-Eckert model for system of tebuconazole SC-CO_2 at 55°C.

CHAPTER 5

DEPOSITION OF CHEMICALS WITHIN WOOD USING SUPERCRITICAL FLUIDS: Bench Scale Studies

5.1 Introduction

Impregnation of wood with polymers, preservatives, fire retardants or silicon compounds can greatly improve its basic properties (Mott and Rotariu, 1968) and can overcomes some service limitations (Bodig and Jayne, 1982). Many characteristics of porous solids, including thermal conductivity, hardness, and chemical resistance, can be significantly improved by impregnation of appropriate modifiers (Volk et al., 1962; Harper, 1961; Dalton and McCann,1968).

Solid wood can also be modified by physical means such as densification under heat or pressure, but more commonly wood is treated using combinations of vacuum, pressure and temperature to force chemicals into the wood. These treatments can merely fill the cell voids, or can react with the wood polymers to render the wood less susceptible to moisture uptake or enzymatic attack.

In wood preservation, the performance of treated wood depends mainly on the treatment process and biocide used. Treatment results are measured by the penetration, retention and distribution of biocides. Penetration measures

how deep a treatment fluid flowed into the treated solid from the surface. Retention is the mass of chemical deposited per unit volume of the porous solid, whereas distribution describes where in the porous solid the chemicals were retained. The macrodistribution is a measure of gross chemical retention at locations within a piece of wood, whereas distribution of chemicals on a microscopic scale, such as on the wood cell-wall level, is known as microscopic distribution. The initial flow of biocides during a treatment process is mainly through the major openings of the cell lumens, to achieve macrodistribution. Further movement of the biocide into the cell wall can result in variable microdistribution. The retention of biocide is the most important factor influencing the ability to extend service life of the treated wood. The retention level required for a given biocide depends on the toxicity of the biocide and the conditions under which the wood is to be used. It is also important that the biocide be injected to a depth adequate for a particular application.

The fluids employed for wood treatment are usually either liquid resins, solutions or solid-fluid suspensions that are forced into the interstices of the porous material. Penetration depends on the permeability of the wood, the properties of the fluid and the treatment schedule. Most conventional techniques use viscous fluids and suspensions that may not flow uniformly through wood, resulting in uneven distribution and shallow penetration. The heartwood of many wood species becomes less permeable as pits, which connect parallel lumens, aspirate and become encrusted. In addition,

geographic areas within the growing ranges of some species produce wood which is more difficult to treat. Thin sapwood species and treatment difficulties some species limit the use of some wood species for wood poles and create long-term maintenance problems. Various pretreatment steps, such as incising, through-boring, radial drilling and kerfing, can improve treatment, but they cannot completely overcome the inherent treatment difficulties associated with many species.

As an alternative, the characteristics of treatment fluids or the treatment conditions can be varied. Altering fluid properties to reduce viscosity could reduce impregnation difficulties. This idea has been employed in the Cellon process, which used liquefied petroleum gas (LPG) as a carrier for pentachlorophenol and did improve penetration. Unfortunately, solvent characteristics rendered the treated wood susceptible to surface decay and the process is no longer used commercially. However, due to their low viscosity, high diffusivities, non-wetting properties, and adjustable solvent characteristics, SCFs should be good candidates for treatment fluids.

In concept, application of SCF technology to wood treatment appears very simple. A known amount of biocide is dissolved in a supercritical solvent and wood is exposed to the supercritical solution until the voids are filled. The operating conditions (pressure/temperature) are altered to decrease solubility, depositing the biocide in wood. The process is expected to be influenced by the solvency of the biocide, operating temperature and pressure,

and the characteristics of the wood. The treated product would ideally be deeply penetrated with biocides, yet have essentially the same appearance as it did prior to treatment and be able to be painted or finished in the same manner as untreated wood. Conventional techniques use liquid carriers, which are characterized by lower diffusivities, higher viscosities and small gas-liquid interfaces in the pores which result in development of backpressure. This may prevent any contact between the wood and preservative except for the cells near surface, thus resulting in higher retentions near the surface and lower retentions further from the surface. Supercritical fluid carriers offer several intrinsic advantages over liquid-phase treatments for depositing "dry" powder in porous solids. First, penetration is more uniform and rapid because of the lack of surface tension effects. Second, SCFs have lower viscosities and higher diffusivities that ease flow and penetration. Third, SCFs can remove extractives that encrust the pit membrane coating, thus increasing wood permeability.

Interactions of biocides with wood can also affect distribution. Inorganic biocides chemically react with wood to form inorganic or organometallic complexes, enabling them to be fixed in the wood. On the other hand, organic biocides undergo simple physical interactions. Organic biocides, like pentachlorophenol, have shown no irreversible fixation with wood (Renze et al., 1988). Biocide interactions can be either confined to the gross structure or can include microdistrubution effects (Nicholas and Preston, 1984).

The development of an SCF wood treatment processes requires identification of the treatment parameters to effectively deliver chemical into the wood in the shortest time with minimal effect on wood properties. Although individual SCF phenomena have been extensively studied, little information exists in the open literature about the delivery of chemicals into semi-porous solid such as wood.

5.2 Objectives

The goal of the deposition study described in this chapter was to identify the main operational parameters that would affect supercritical fluid wood treatment and to determine the effects of those operational parameters on the distribution of biocides in the wood. The specific objectives were to:

- develop methods to analyze retention and distribution of biocides that readily dissolved in supercritical fluids and could be deposited in wood
- experimentally determine the effects of process parameters (pressure, time and temperature) on the distribution of biocides in the wood,
- determine the effect of SCF solvent composition on the distribution of biocides

Bench scale studies were limited because of the size of the treatment vessel and the lack of a separate vessel for producing solutions saturated with biocide. All studies were performed using small Douglas-fir and ponderosa pine wood dowels. Results from the bench scale studies helped to refine the

design of the pilot plant treatment system and allowed more directed research using larger equipment.

5.3 Material and Methods

All bench scale studies were performed using small Douglas-fir and ponderosa pine wood dowels (13 mm diameter by 40 mm long) that were obtained from kiln dried boards with varying ring densities. The wood was conditioned to a uniform moisture content at 23°C and 60% relative humidity by keeping it in a moisture and temperature controlled room for 6 weeks. The dowels were then end-sealed with epoxy resin to restrict longitudinal flow.

Bench scale impregnation studies were preformed using the previously described Isco 2000 series system (Chapter 3.3). A 10 ml treatment vessel was filled with biocide and the wood block, as shown in Figure 5.1. For biocides that were solid at room temperature, the ground biocide was placed into the vessel above the wood. Copper naphthenate, which was a liquid formulation, was diluted in dichloromethane and coated onto diatomaceous earth that was then placed into the vessel. The pressure in the vessel was raised in 15 bar increments and equilibrated for five minutes at each step to minimize mechanical and structural damage. The wood was kept at the desired pressure for the set treatment period with solution flowing downward continuously through the vessel.

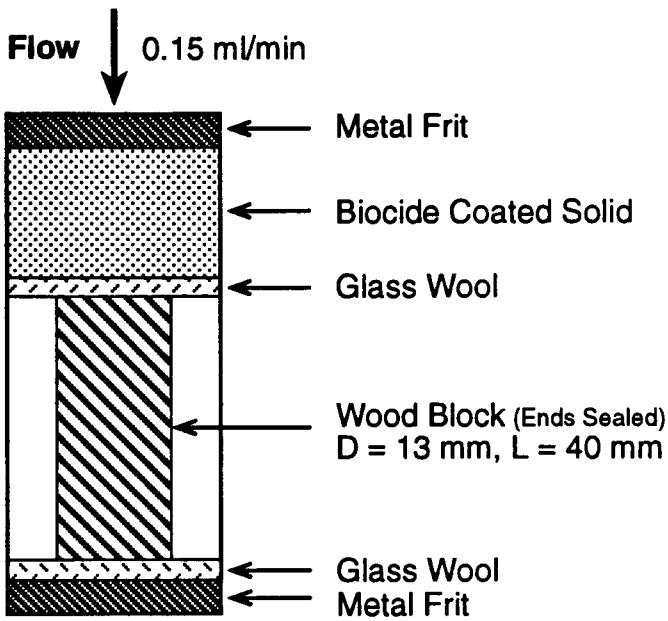

Figure 5.1 Vessel loading configuration for bench scale impregnation of wood dowels.

After the desired treatment period, the SCF was released by venting, which caused an abrupt reduction of pressure that triggered biocide precipitation. A typical pressure program is shown in Figure 5.2. The effects of the various interacting factors that influence impregnation (temperature, pressure and treatment period) were studied using four replicates at each treatment condition.

5.3.1 Analysis of Retention

The measurement technique used for the biocide retention in the wood matrix depends on the nature of the molecule and the concentration level. Macrodistributions of biocides were determined using techniques appropriate for each biocide. The biocides used for this study and the methods of retention analysis are listed in Table 5.1. For IPBC, a 2 x 10 x 36 mm long wafer was cut from the center of each dowel. These wafers were then analyzed for iodine by neutron activation analysis. To do this the sample was kept in a nuclear reactor irradiated with neutron flux (Ecole Polytechnique, Quebec, Canada). A known fraction of the iodine atoms captured neutrons and were converted to radioactive I-128. The samples were removed from the reactor and placed on a germanium semiconductor gamma-ray detector connected to a multichannel analyzer. I-128 emits gamma-rays of energy 422 keV and the number of gamma-rays detected at this energy, corrected for background interferences, was proportional to the total amount of iodine in the sample. The amount of

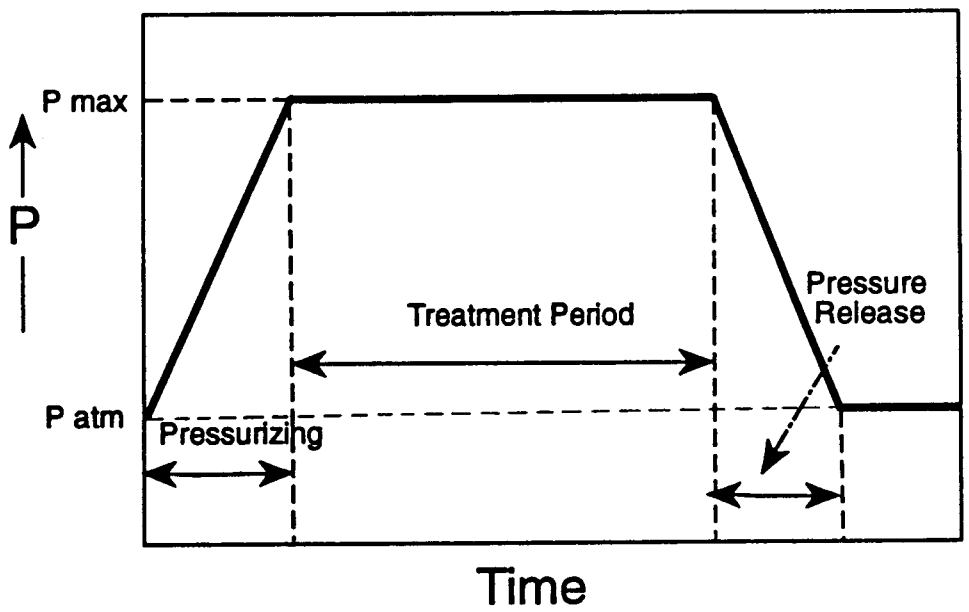

Figure 5.2 A typical single cycle pressure program used for supercritical fluid treatment of wood.

Table 5.1 Methods for retention analysis of selected biocides

	Biocide	Quantitative - (Qualitative) Analysis
1	IPBC	NAA* (n.a.)**
2	Tebuconazole	HPLC (n.a.)
3	TCMTB	HPLC (n.a.)
4	Chlorothalonil	HPLC (n.a.)
5	Propiconazole	HPLC (n.a.)
6	PCP	X-ray (stain)
7	Cu-naphthenate	X-ray (visual)

! X - ray fluorescence spectroscopy

* Neutron Activation Analysis

** No available qualitative spot test at present.

iodine was then calculated by comparing with a standard. This method has a detection limit of 0.1µg per cm^2 of exposed surface with a 5% precision of measured value.

Tebuconazole treated blocks (10 x 10 x 20 mm) were analyzed by dividing the blocks into an outer 2 mm region and an inner 6 mm region. The samples were ground to pass a 20 mesh screen and then extracted with methanol for 3 hours in a 60°C sonicator bath. The extract was then analyzed using High Performance Liquid Chromatography (Shimadzu Model LC-6A). The HPLC column used was a Spherisorb ODS-2 (250 mmx4.6 mm i.d.) (Alltech) at room temperature. A mixture of 55% acetonitrile and 45%water was used for the mobil phase at a flow rate of 1.5 ml/min. After each run a 95% acetonitrile solution was passed through the column for 2 minutes to wash the column. The detector wavelength was 280 nm (0.02 AU). Blocks treated with TCMTB, chlorothalonil or propiconazole were analyzed using similar sample preparation technique as used for tebuconazole but at detector wave lengths of 275, 254 and 268 nm, respectively. Distribution of TCMTB was measured by spraying zinc powder followed by hydrochloric acid in the section of treated blocks. A bright red color was indicative of TCMTB penetration. The remaining biocides were not visible in the wood nor were indicators available to detect them in the wood.

Samples treated with pentachlorophenol or Cu-naphthenate were also ground and then analyzed with x-ray fluorescence spectroscopy using an

Asoma 8620 analyzer. Retention of pentachlorophenol and Cu-naphthenate were determined by cutting the dowels in half and spraying the cut transverse face with penta-check or chrome azurole S.

The threshold retention depended on the physical characteristics of the biocide, the severity of the biological environment and the depletion of the biocide with time (Nicholas, 1973). The minimum required solubility values to obtain threshold retentions were determined based on the following assumptions. The wood is assumed to be inert with a constant porosity, the treatment fluid fills all pore volumes and all the biocide carried into the wood matrix is retained. For Douglas-fir blocks having a density of 450 kg/m^3 and moisture of 15 %, the porosity is estimated to be 0.55. The required concentration of an SCF solution to fill the porous space to obtain the threshold amount of retention was compared with measured solubilities (Table 5.2). All biocides except chlorothalonil had sufficient solubility to develop the required retentions.

Table 5.2 Solubility levels required to produce target retention levels

	Biocide	Threshold Retention* kg/m^3	Minimum Rqd. Solubility wt %	Maximum Observed Solubility wt %
1	IPBC	0.3	0.06	10.8
2	Propiconazole	0.85	0.15	4.9
3	Tebuconazole	1	0.2	4.7
4	Cu-naphthenate	1	0.2	3.0
5	PCP	3.2	0.64	2.9
6	TCMTB	1.2	0.24	2.2
7	Chlorothalonil	2.6	0.5	0.16

* Against fungal organisms, (Nicholas, Vol. 1, 1973)

5.4 Results and Discussion

Developing an impregnation process involves understanding the dynamics of solubility changes and the unsteady-state flow through the semi-porous wood. This study focused on the effects of three basic factors that influence retention: (1) the operating conditions, (2) the treatment solution composition, and (3) wood characteristics.

5.4.1 Effects of Operating Conditions

All of the biocides used for this study were delivered to the dowels in measurable quantities, although the levels varied widely. For treatment with tebuconazole, two Douglas fir blocks (1 x 1 x 2 cm) were loaded per charge and pure CO_2 was allowed to flow through the vessel for the given period. Tebuconazole was delivered into the wood at retention levels ranging from 0.94 to 1.82 kg/m^3, depending on the conditions employed (Table 5.3). Prolonging the pressure period did not affect retention at the lower pressure tested (207 bar). The use of higher pressure produced marked increases in retention. This effect was greatest when the temperature or treatment period was also increased. For example, raising pressure and lengthening the treatment period from the base case A (90 minutes and 207 bar) to Case D (120 minutes and 241 bar) resulted in a 94% increase in retention, while increasing only pressure, Case C, or only treatment period, Case B, resulted in

Table 5.3 Tebuconazole levels in Douglas-fir dowels following SCF treatment at varying temperatures and pressures

Case	No. of Runs*	Conditions			% Tebuc.	Retention kg/m^3
		P bar	*T* °C	*t* min		
A=base	3	207	45	90	0.152	0.936 ± 0.123
B	3	207	45	120	0.160	0.96 ± 0.342
C	2	241	45	90	0.193	1.158 ± 0.378
D	3	241	45	120	0.303	1.818 ± 0.329
E	2	241	65	90	0.287	1.722 ± 0.389

* Two blocks per run
Threshold retention value for Tebuconazole = 1 kg m^{-3}

marginal increase. When both temperature and pressure were raised, Case E, the increased solubility levels resulted in an increased retention by 84% over Case A.

Cu-naphthenate retentions were generally higher than those found for tebuconazole. Retention generally increased with longer treatment periods, although again there were some exceptions to these trends (Table 5.4 and Figure 5.3). The reasons for variations with treatment period are unclear, since equilibrium solubility was assumed to depend only on pressure, temperature and solvent composition.

Treatments with IPBC produced the highest retentions of all biocides evaluated (Table 5.5) and reflected the high solubility of IPBC in SC-CO_2. Retention was sensitive to the percentage of methanol used as a cosolvent, increasing 3 to 4 fold with a 2 % increase in methanol. This effect declined with increasing treatment period, perhaps because longer treatment periods depleted the packed biocide and resulted in unsaturated flow. Increasing the pressure from 207 to 275 bar increased retention.

Pentachlorophenol (PCP) retentions were lower than those of IPBC under similar conditions (Table 5.6). Higher pressures produced increases in retention in almost all cases at both 50 and 80 °C. Increased temperature also increased retention. The effects of temperature and pressure were expected, since solubility increased at higher pressures and temperatures. The logarithm of the retention of PCP was approximately linear with solubility (Figure 5.4).

Table 5.4 **Retention of Cu-naphthenate in Douglas-fir dowels following treatment using SC-CO_2 at selected temperatures and pressures**

P bar	*T* °C	Treatment period hr	Average Retention % Cu	Average Retention kg/m³
207	50	0.5	0.036 ± 0.017	0.216
		1.0	0.097 ± 0.110	0.546
		1.5	0.074 ± 0.042	0.444
		2.0	0.138 ± 0.094	0.829
207	80	0.5	0.068 ± 0.016	0.361
		1.0	0.049 ± 0.040	0.294
		1.5	0.205 ± 0.108	0661
		2.0	0.253 ± 0.201	1.518
275	50	0.5	0.008 ± 0.007	0.048
		1.0	0.164 ± 0.057	0.984
		1.5	0.067 ± 0.040	0.402
		2.0	0.177 ± 0.116	1.062
275	80	0.5	0.064 ± 0.060	0.384
		1.0	0.067 ± 0.014	0.403
		1.5	0.103 ± 0.100	0.618
		2.0	0.203 ± 0.157	1.218

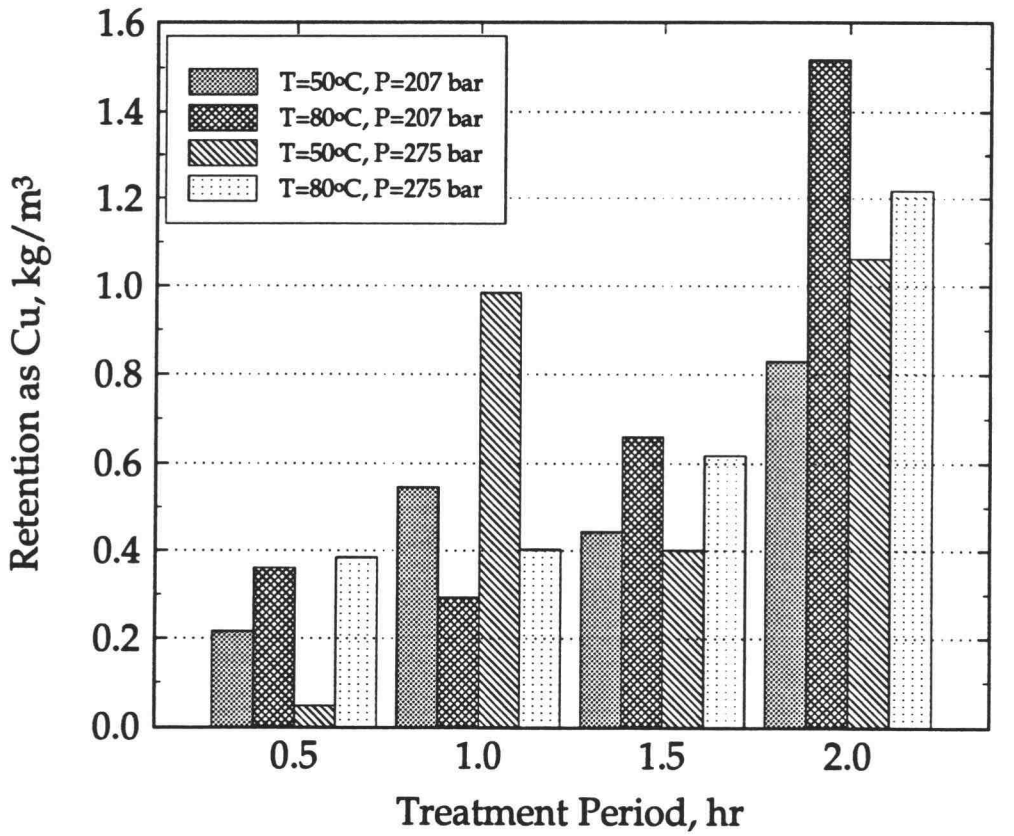

Figure 5.3 Retention of Cu-naphthenate in Douglas-fir dowels (as Cu) *vs* treatment period using SC-CO_2.

Table 5.5 IPBC levels in Douglas-fir dowels following SCF treatment at varying temperatures and pressures

Species	Pressure bar	Methanol mol %	Time hr	Retention * kg/m^3
S. pine	207	8	1	8.6 ± 2.1
S. pine	207	8	1.5	5.7 ± 1.4
S. pine	207	10	1	23.2 ± 3.2
S. pine	207	10	1.5	19.2 ± 3.4
S. pine	275	8	1	28.2 ± 5.2
S. pine	275	8	1.5	26.1 ± 4.9
D-fir	275	5	0.5	13 ± 3.2
D-fir	275	5	2	2.6 ± 0.53

* Average of four individual dowels

Threshold value for IPBC = 0.1 kg/m^3 (Nicholas, 1984)

Table 5.6 Effects of process parameters on retention of PCP in Douglas-fir dowels treated using SC-CO_2

Treatment Time min	Pressure bar	Temperature °C	Average* Retention kg/m³
10	207	50	0.977
	207	80	2.501
	275	50	3.409
	275	80	10
30	207	50	1.48
	207	80	5.81
	275	50	3.92
	275	80	4.12
60	207	50	0.461
	207	80	3.687
	275	50	0.873
	275	80	5.029
90	207	50	0.588
	207	80	1.878
	275	50	1.100
	275	80	8.120
120	207	50	1.474
	207	80	2.210
	275	50	0.906
	275	80	7.704

* Average of five dowels

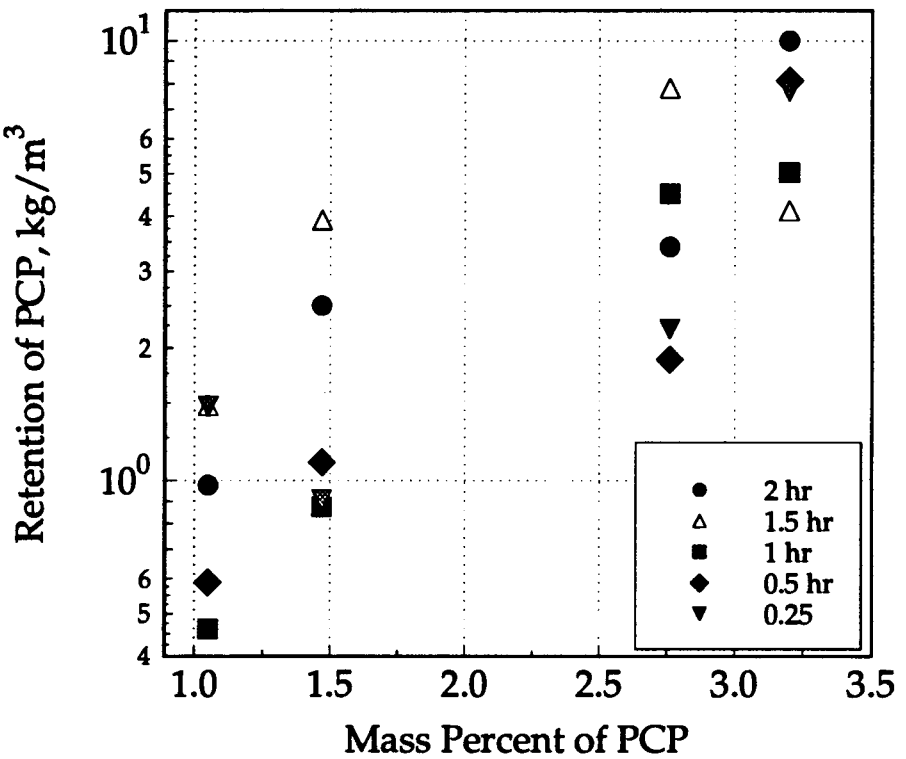

Figure 5.4 Retention of PCP in Douglas-fir dowels *vs* PCP solubility in CO_2 + 3.5 mol % methanol.

use of longer treatment periods produced more variation in results. Increasing the treatment period at 207 bar and at 80 °C produced no consistent pattern of changes on retention. For example, an exceptionally large value for t=60 min.

5.4.2 Effects of Cosolvents on Chemical Distribution

Cosolvents can have dramatic effects on biocide solubility, and improving the potential for delivering effective biocide levels into the wood. The cosolvents used varied in polarity and were hydroxylic and nonhyroxylic. Effects of cosolvents were evaluated at 207 or 275 bar and 50 or 80 °C.

Because pentachlorophenol was generally less soluble in supercritical carbon dioxide than other biocides, it is useful for testing the effects of cosolvent addition. A of the effects of cosolvents on retention of pentachlorophenol is shown in Table 5.7 and Figure 5.5. Dimethylformamide (DMF) and dimethyl sulfoxide (DMSO) produced the greatest increases in retention for a given set of operating variables. Beside their strong polarity, DMF and DMSO were selected because they can cause high volumetric swelling, since they swell the carbohydrate-type polymers in the cell wall Comparison of relative polarity of cosolvents and levels of solubility and retentions of PCP is shown in Table 7.8.

The distribution of pentachlorophenol across the dowel sections was extremely variable (Table 5.9, Figure 5.6 and 5.7). These variations suggest that some type of cosolvent/wood interaction may have interfered with

Table 5.7 **Effects of cosolvent on retention of PCP in Douglas-fir dowel following SC-CO_2 treatment.**

P bar	*T* °C	Cosolvent 3.5 mol %	Avg. Retention* wt %
207	60	DMF	4.27 ± 0.61
		DMSO	3.92 ± 1.54
		Acetone	2.87 ± 2.04
		Methanol	1.15 ± 0.59
		Ethanol	0.29 ± 0.03
207	80	DMSO	6.96 ± 2.06
		DMF	5.05 ± 1.67
		Methanol	2.55 ± 1.50
		Ethanol	0.55 ± 0.19
		Acetone	0.13 ± 0.06
248	60	Methanol	4.77 ± 3.27
		DMSO	4.18 ± 1.94
		DMF	3.91 ± 0.54
		Ethanol	1.38 ± 0.37
		Acetone	1.12 ± 1.02
284	80	DMF	6.55 ± 1.08
		DMSO	4.77 ± 0.67
		Methanol	2.43 ± 2.15
		Ethanol	0.59 ± 0.12
		Acetone	0.51 ± 0.14

* Average of five individual dowels

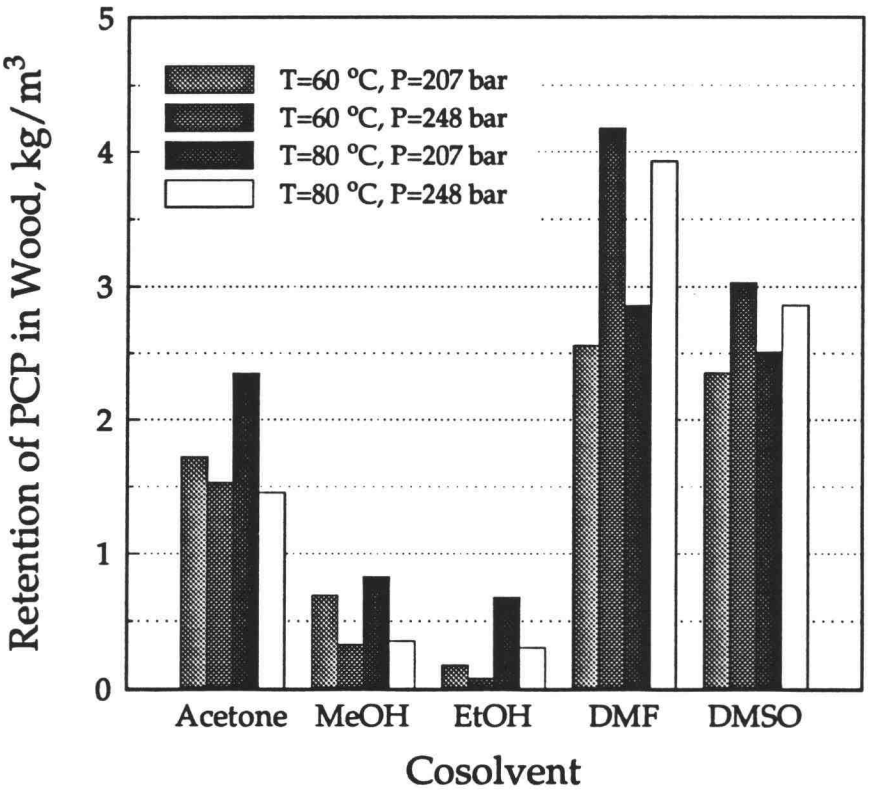

Figure 5.5 Effects of cosolvents on retention of PCP in Douglas-fir dowels treated with SC-CO_2 + 3.5 mol % cosolvent for 30 minutes.

Table 5.8 **Comparison of relative polarity, solubility and retention of PCP for selected cosolvents.**

(Each column arranged in decreasing order for that property)

Polarity	Solubility	Retention
DMSO	Methanol	DMSO
Methanol	Ethanol	Methanol
Ethanol	Acetone	Ethanol
Acetone	DMSO	Acetone

Table 5.9 **Effect of cosolvents on distribution of PCP in Douglas-fir dowels following SC-CO_2 treated at 60 or 80 °C and 207 or 248 bar**

Cosolvent	Average Retention kg/m³	Outer Shell Retention kg/m³	Inner Core Retention kg/m³	Avg. of Reten. Ratios[a] (outer/inner)[a]
DMSO	2.98	4.12	0.35	11.6 (6 - 21)
DMF	2.96	5.46	0.04	124 (50.2 - 231)
Methanol	1.63	2.87	0.168	12.6 (11.1 - 13.8)
Acetone	0.69	0.59	0.17	3.5 (2.1 - 8.3)
Ethanol	0.44	0.82	0.17	4.9 (2.0 - 13.8)

[a] Values in parenthesis represent ranges of ratios for 5 individual dowels

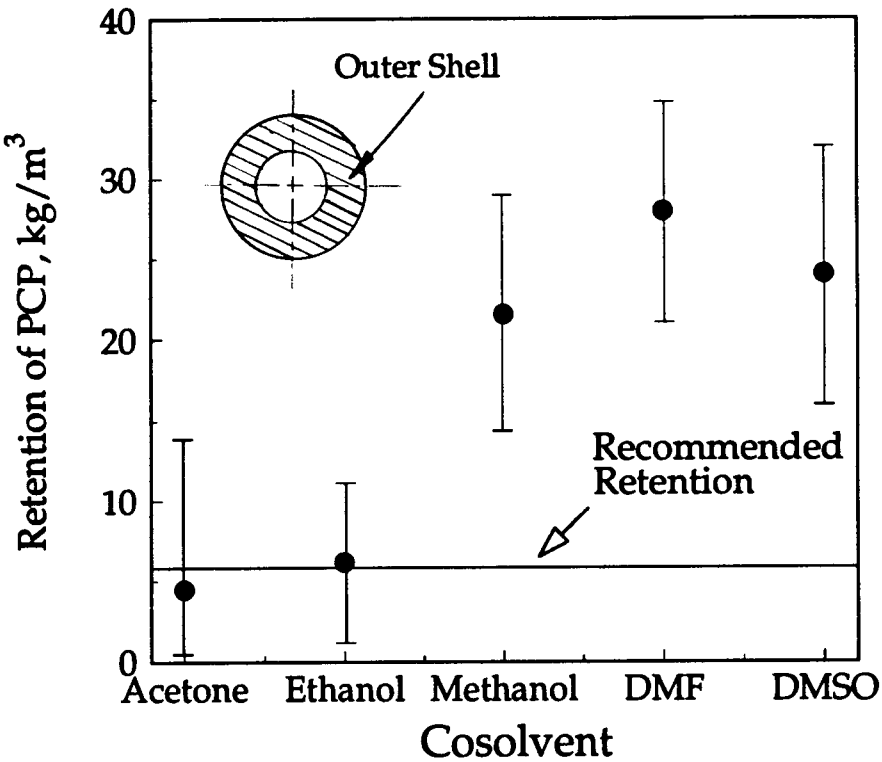

Figure 5.6 Retention of PCP in the outer shell of Douglas-fir dowels treated with PCP using SC-CO_2 + 3.5 mole % cosolvent. (Error bars show ranges of measured retentions).

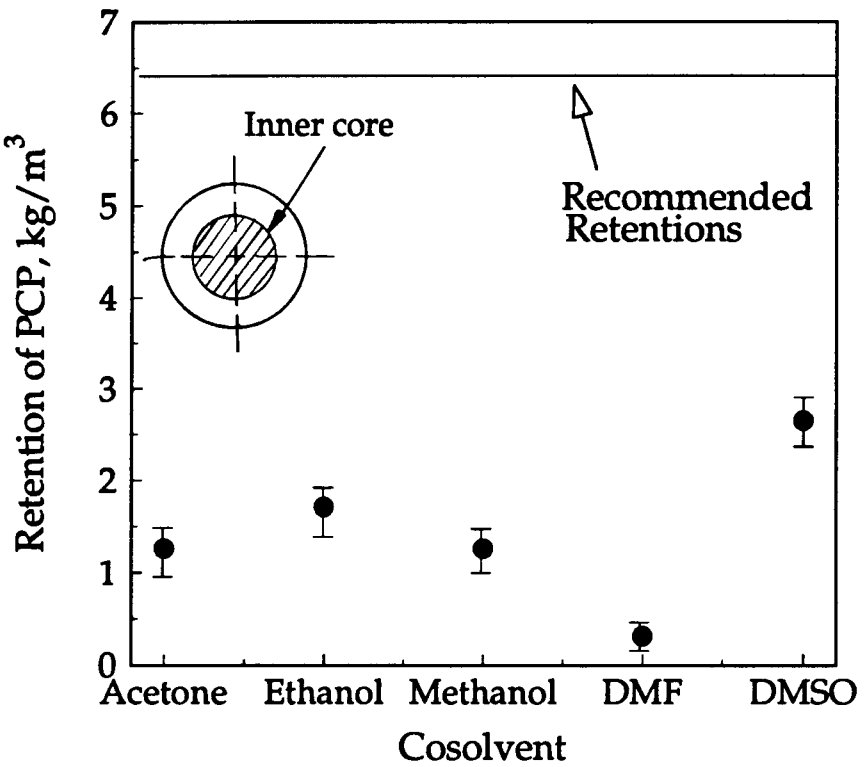

Figure 5.7 Retention of PCP in the inner core of Douglas-fir dowels treated with PCP using SC-CO_2 + 3.5 mole % cosolvent. (Error bars show ranges of measured retentions).

biocide solubility, resulting in uneven deposition. Under some conditions, methanol produced results which approached those produced with DMSO and DMF. Higher temperatures improved retention substantially for methanol at 207 bar, but had an opposite effect at the higher pressure (248 bar). A similar trend was noted with ethanol, while retention using acetone as the cosolvent declined with increased temperature at both pressures. Increased methanol levels resulted in increased PCP retention in southern pine dowels, with a maximum retention at 5 mole %. Further increases in methanol levels were associated with decreased retentions (Figure 5.8).

The results indicate that a variety of biocides can be efficiently delivered into Douglas-fir heartwood using short treatment cycles. These retentions generally increased with increased pressure and temperature. The wide variation in the retention associated with different biocides reflects the differences in solubility of the biocides in SCF. These trials were performed on small wood specimens. Although these samples were end-sealed, they may not accurately reflect conditions found in larger wood members. For example, as volatile cosolvents vaporize, they can redistribute or carry biocides to the wood surface causing surface blooming. This effect can increase for larger wood pieces.

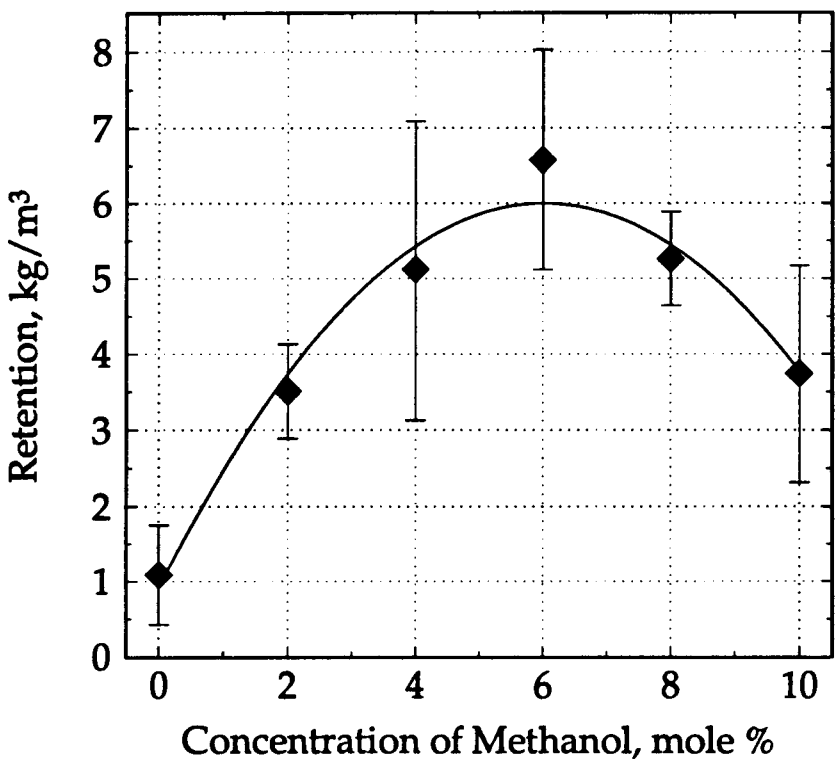

Figure 5.8 PCP Retention in southern pine dowels as a function of amount of methanol mixed with SC-CO_2 at 80°C, 207 bar treated for 30 minutes.

CHAPTER 6

DEPOSITION OF CHEMICALS WITHIN WOOD: Pilot Plant Scale Treatment

6.1 Introduction

Experience in using the smaller bench scale equipment (Isco Series 2200 system) provided useful data on the effects of temperature, pressure and solvent composition on distribution of selected biocides in wood. However, the small dimensions of the samples and the absence of a separate saturator (mixing) vessel limited the usefulness of the system. The two problems encountered in preservative treatment of refractory wood are the inability to obtain even distribution of the biocide and the difficulty in achieving a desired overall level of biocide retention. The conventional treatment uses pressures up to 14 bar. Although higher pressures can increase penetration, the concern for possible wood damage has precluded development of a process. Whether higher pressures in liquid treatments cause wood collapse is a matter of controversy (Walter and Whittington, 1970; James, 1961). The reason for collapse could be the pressure gradient across the grain instead of the total pressure. To study treatment characteristics of hard-to-treat wood with larger cross sections, a larger treatment vessel was required. Studies with larger scale equipment help to validate bench scale results and identify critical scale-up parameters. The pilot plant was also used to treat large numbers of samples

are required for the statistical analysis of effects of treatment on strength and decay resistance.

The objective of this pilot plant study was to confirm and verify those factors that influence impregnation of wood samples. These factors include operating variables, wood characteristics, and solvent composition. The pilot plant allowed much more flexible operations and better monitoring of the process to identify factors associated with scaling up the process. The goal of pilot plant treatments were to ensure an even distribution of chemicals within the charge, to achieve the required specification and to be reproducible between charges.

6.2 Experimental

6.2.1 Pilot Plant System

The pilot plant system was a modified Newport Scientific, Inc. apparatus that was originally designed for extraction (Figure 6.1). Carbon dioxide flowed from a commercial cylinder with a dip-tube through a 5μm filter at about 60 bar to a double-end diaphragm compressor (Newport, 46-133320-2) with a capacity of 690 bars and an average flow of 60 to 80 l/min at treatment conditions. Pressure control was achieved using a pressure regulator (Tescom, 26-1721-44-092) to direct excess fluid back into the compressor's suction-end.

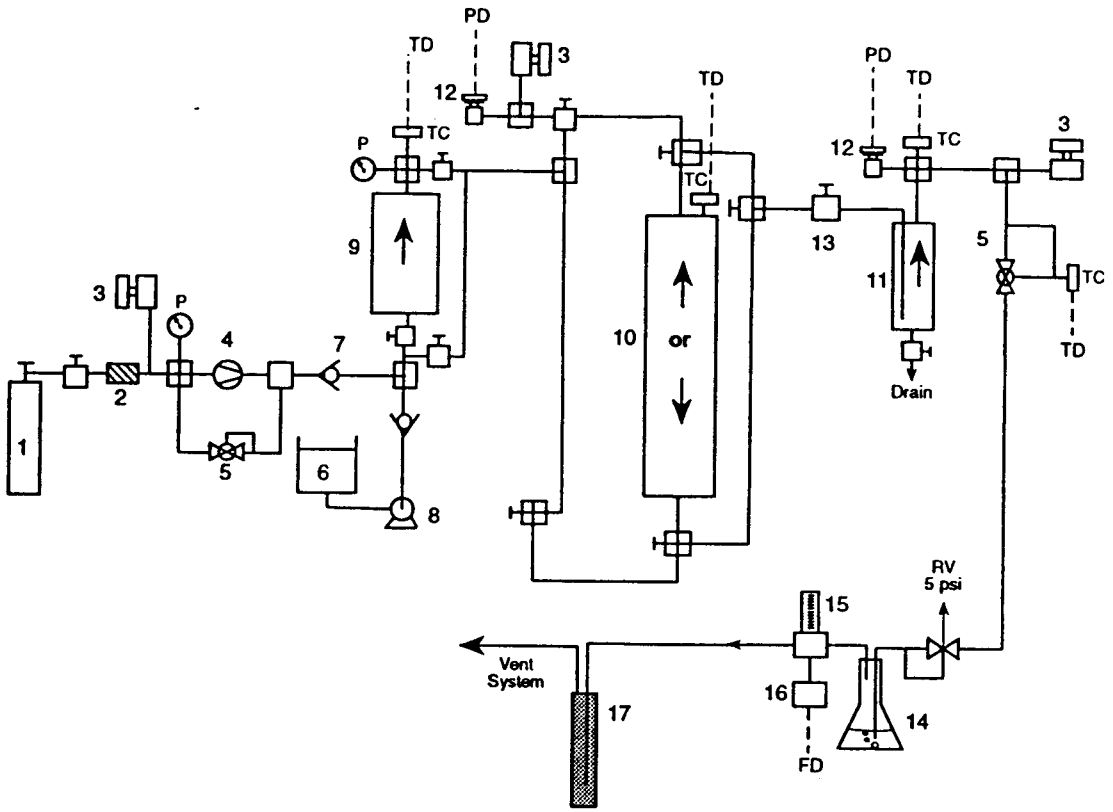

1. Liquid CO_2 cylinder
2. Relief Valve
3. Filter
4. Compressor
5. Back pressure regulator
6. Cosolvent tank
7. Check valve
8. Mini pump
9. Saturator
10. Treatment vessel
11. Separator
12. Pressure transducer
13. Metering valve
14. Cold trap
15. Digital flow meter
16. Digital totalizer
17. Entrainment trap

P - Pressure gauge
PD - Pressure transmitter to personal computer
TD - Temperature transmitter to personal computer
FD - Flow transmitter to personal computer

Figure 6.1 Schematic of the pilot plant impregnation system

Cosolvent was added using a metering duplex pump (LDC Analytical, 2396-57) which had variable flow rate 0.48 cm^3/min to 9.7 cm^3/min, which was adjusted using calibrated stroke length microdials. The CO_2 / cosolvent mixture flowed into the saturator vessel (6.5 cm diameter, 845 cm^3 volume) where biocide was solubilized by the supercritical solvent. The saturated solution then flowed through heated tubing into the treatment vessel (6.5 cm in diameter and 53.3 cm length) which was equipped with four hand-operated valves that provided the ability to change the flow direction through the vessel. The treatment vessel had both heating and cooling capacity for an operational range of -35 to 300 °C. This system permitted the study of a variety of temperature and pressure conditions.

The flow rate of the CO_2/cosolvent mixture in the system was adjusted by a solid stem micrometering valve placed after the treatment vessel. A back pressure regulator was used to maintain the desired pressure in the separator vessel (3.8 cm diameter, 26.7 cm length). A second separation at atmospheric pressure was accomplished in the "cold trap" before the gas stream passed through a flow meter indicator (McMillan Co., 310-3) and was vented to the atmosphere. The flow meter was connected to a flow totalizer (Kessler-Ellis Co., INT-69). Temperature and pressure readings from the saturator, the treatment and separator vessels and the flow meter were collected using a personal computer for data acquisition (National Instrument, PC-LPM-16).

6.2.2 Treatment Techniques

There are three techniques for making a supercritical treatment solution and introducing it to the treatment vessel:

1. Carbon dioxide and cosolvent mixed and this mixture flows through a packed bed of biocide maintained at constant temperature. Solid solutes were packed with glass beads while liquid solutes were coated on filter paper or cellulose sponge. Solute-solvent contact occurred above the critical conditions for a sufficient time to solubilize the biocide. The solution then flowed into the treatment chamber which was kept at a constant pressure. This technique required loading a large amount of solute in the saturator to ensure the presence of a saturated solution over the course of treatment.

2. Solute is dissolved in a liquid cosolvent before pumping that solution to a mixing vessel where the CO_2 is added above the critical conditions of the ternary mixture. The mixing vessel must be designed to produce good contact between the two streams.

3. The solute is loaded with the porous solid in the treatment vessel. The CO_2-cosolvent mixture flows through the treatment vessel and dissolves the solute chemical, thereby eliminating the need for a separate mixing vessel. A mechanical mixer or circulation pump would be necessary to produce uniform solutions within the vessel.

6.2.3 Materials

Douglas-fir heartwood blocks (10 cm long and square sides of 3.8, 2.5 or 1.9 cm) were chosen for most of this study, since this refractory species has a low average permeability of 3.5×10^{-13} cm^2 (s.d. 1.08×10^{-14} cm^2, Appendix H). Measured densities and permeabilities of the three species of wood used are listed in Table 6.1. The surface of the blocks was carefully smoothed to avoid blocking of the pores. The blocks were end sealed by double coating with epoxy resin to minimize longitudinal flow and conditioned to a 12% moisture content.

6.2.4 Treatment Procedures

Defect free, end matched, Douglas-fir heartwood blocks (3.8x3.8x10 cm) were cut from kiln dried boards and end sealed with coats of epoxy resin to restrict longitudinal flow. These blocks were used to evaluate impregnation with TCMTB using supercritical fluids. The first and the second impregnation techniques discussed above were acceptable, while the third method was only marginally effective since the high retentions of IPBC obtained in the bench scale runs could not be replicated with the pilot plant treatments.

Supercritical impregnation was carried out as an empty cell treatment using pressure programming discussed in Chapter 5. The saturator vessel was filled with the supercritical solvent under isothermal conditions. The mixture

Table 6.1 Experimental conditions evaluated for treatment with TCMTB

Solvent:	TCMTB - Supercritical CO_2 Methanol
Treatment System	
Saturator:	
Diameter:	6.5 cm
Height:	25.4 cm
Volume:	850 cm^3
Impregnator	
Diameter:	6.5 cm
Height:	53.3 cm
Volume:	1770 cm^3
Separator	
Diameter:	3.81 cm
Height:	26.7 cm
Volume:	304 cm
Treatment Parameter:	
Temperature (°C):	45 - 80
Inlet pressure (bar)	50 - 65
Maximum pressure (bar):	140 - 275
Pressure increase rate (bar/min)	~ 15 - 25
Pressure release rate (bar/min)	~ 20 - 25
Flow Rate (l/min) at room conditions:	20 - 30
Residence Time	
saturator (min):	10
impregnator (min):	20
Wood Blocks	
Douglas-fir heartwood	
Specific permeability (cm^3/s.cm.bar)	0.111 ± 0.067
Density (kg/m^3)	505 ± 15
Porosity	0.541
Ponderosa Pine	
Specific permeability (cm^3/s.cm.bar)	6.719 ± 0.045
Density (kg/m^3)	626 ± 88
Porosity	0.469
Cross section (cm)	1.9 to 3.8 square block
Southern Pine	
Specific permeability (cm^3/s.cm.bar)	3.877 ± 0.925
Density (kg/m^3)	444 ± 14
Porosity	0.582
Cross section (cm)	1.9 square block

was allowed saturate for about 20 minutes and the treatment cylinder containing the timber was brought to the required temperature before being filled with treatment solution was allowed to fill. Some initial loss of the biocide from the solution can occur since the pressure on the solution drops as it enters the non-pressurized treatment chamber, producing an unsaturated solution. Pressure and temperature variations in the treatment vessel for typical run is shown in Figures 6.2 and 6.3. Solvent outlet flow of from the separator indicated that the flow had rapid oscillations (Figure 6.4). Typical density - pressure changes during the experiment are given in Figure 6.5.

The vessel was pressurized to a predetermined value isothermally (line A - B) followed by isochoric - isothermal dissolution with increasing pressure to a maximum (line B - C). The vessel was maintained at the maximum pressure for a given treatment period (unless pressure oscillation was used) while the SC solution swept along the treated blocks at an average flow rate of 62 ml/min.

At the end of the pressure period, the vessel was depressurized isothermally (line C - A). Venting reduced both pressure and vessel temperature by 5 to 8°C. However, the vessel attains its original temperature in a few minutes. As the result of decrease in pressure the SC-solvent becomes a gas and flows out from the wood leaving the dissolved chemical behind.

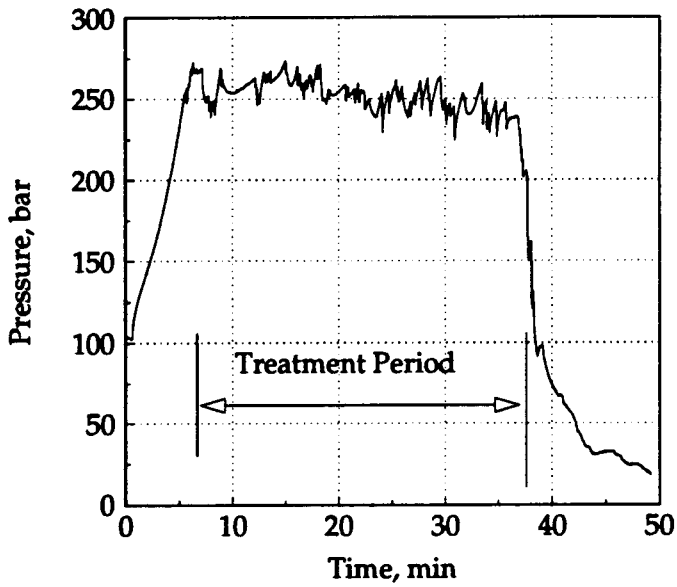

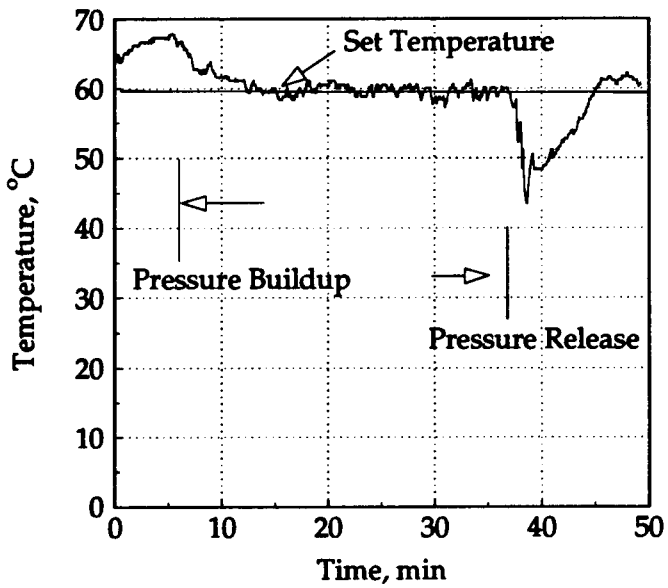

Figures 6.2 and 6.3 Pressure and temperature variations in the treatment vessel during SC-CO_2 treatment of wood with TCMTB.

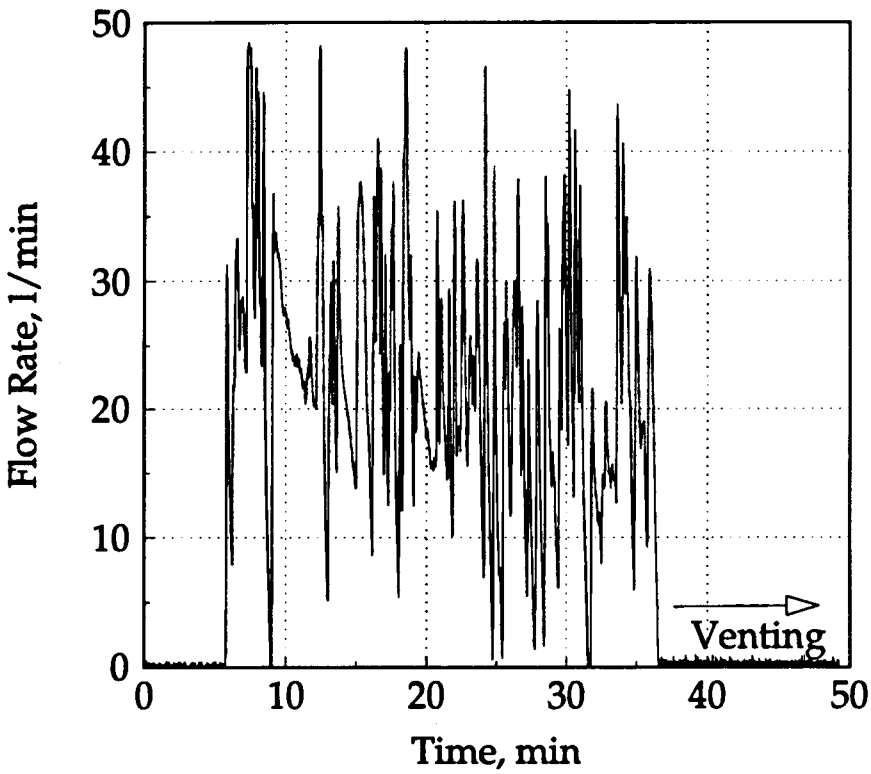

Figure 6.4 Solvent outlet flow from the separator during a SC-CO_2 treatment with TCMTB.

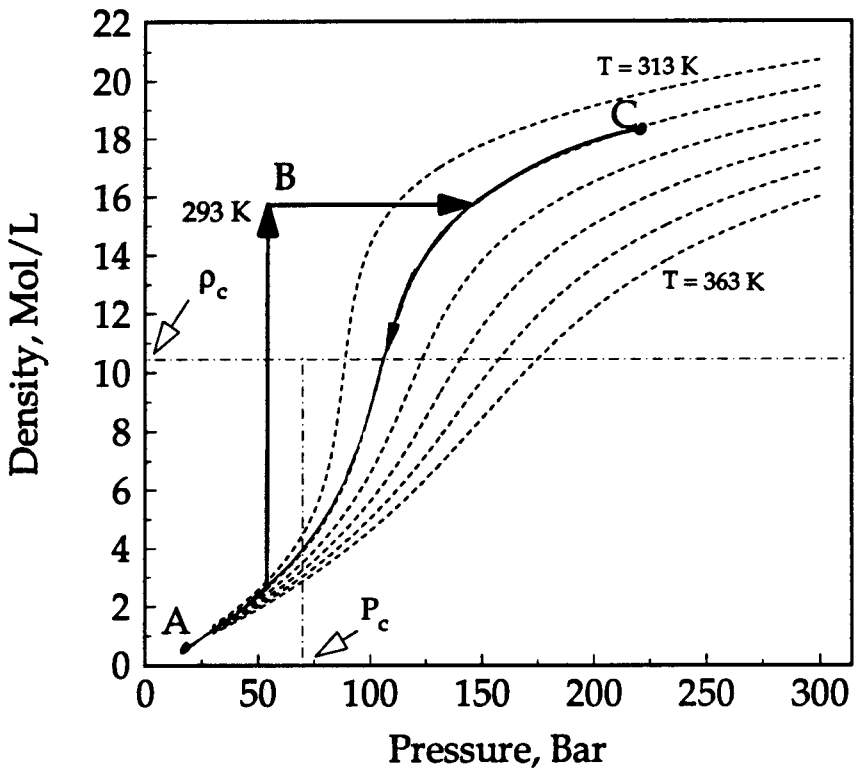

Figure 6.5 Density profile of CO_2 during treatment of wood.

Precautions taken to assure consistency and reproducibility in experiments included:

- End matched samples were used for all treatment conditions and the wood blocks were moisture conditioned (12% MC) before treatment.
- Preliminary runs indicated that precipitation during venting was greater at the ends of the treatment vessel. As a result, the wood blocks were kept in the middle of the treatment vessel (Figure 6.6) and the vessel was vented slowly over a 30 minutes period.
- Higher flow rates (10 - 15 ml/min) were used to enhance mixing and create uniform boundary conditions.

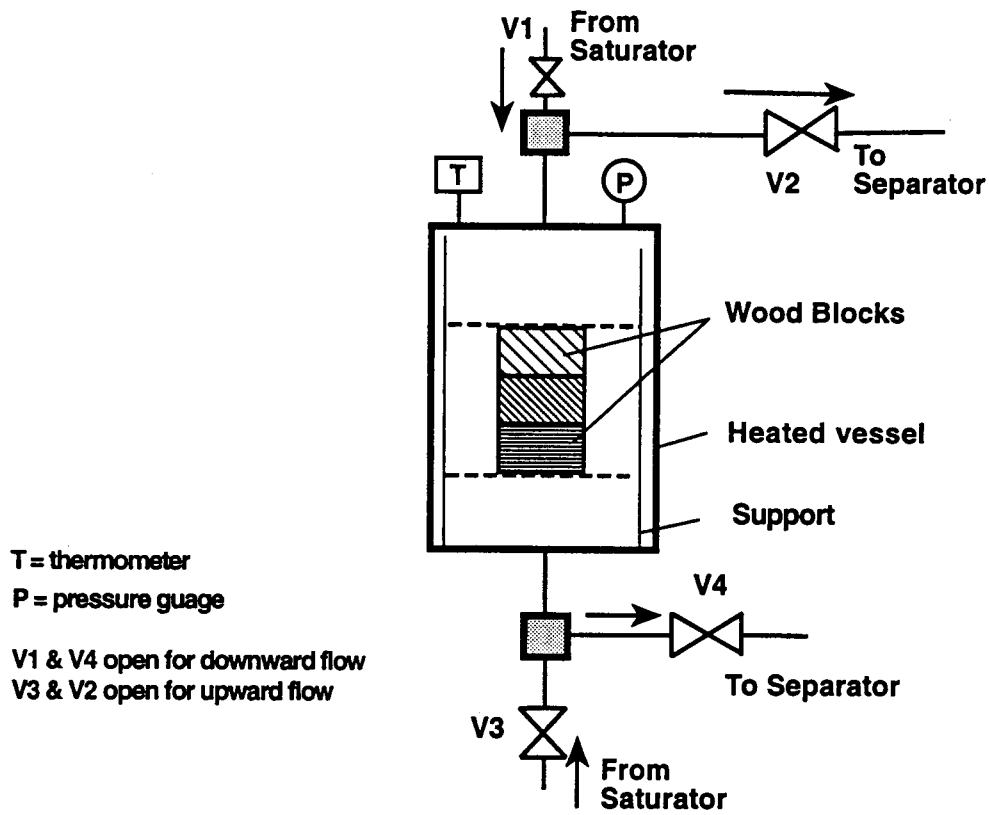

Figure 6.6 Configuration used for loading wood blocks in the treatment vessel.

6.2.5 Experimental Design

Four factors which had significant effects on chemical deposition were selected to study effects of retention and distributions a model biocide, TCMTB. Effects of single variables will be considered.

(a) Pressure Five levels were selected at 138, 172, 206, 241,276 bar. Since the critical pressure of CO_2 and about 2.8 mole % acetone is 82 bar, experiments were conducted above this pressure in order to avoid phase separation.

(b) Treatment Period Four nominal values of 15, 30, 60 and 90 minutes were selected.

(c) Size of Wood Blocks Three sizes (1.9x1.9x10 cm), (2.5x2.5x10 cm), and (3.8x3.8x10 cm) were employed. The three sizes correspond to volume-to-surface area ratio of 1, 1.35 and 2 respectively.

(d) Permeability of Wood Southern pine sapwood and Douglas-fir heartwood blocks (1.9 x 1.9 cm) were treated together to investigate the effect of the large permeability differences (about 100 to 1) on retention.

The fluid composition and treatment temperature will be kept constant for all the runs. The treatment fluid was SC-CO_2 with 2.8 mole % acetone maintained at 50°C. Rates of pressure increase and release at the beginning and end of treatment cycles were the same for all trials. There were three replicates for each trial with two blocks charged per run.

6.2.6 Retention Analysis

Biocide distribution was evaluated using a chemical indication and by chemical analysis.

Staining Technique

TCMTB was dictated on the surface or in the wood cell walls using staining techniques combined with visual and microscopic observations. TCMTB consists of a benzothiazole conjugate ring structure and a single side chain. To detect TCMTB in treated wood the thiocyano group offers potential site for detection. For the spot test system, nacent hydrogen, produced by the reaction of hydrochloric acid and zinc, liberates hydrogen sulphide that reacts with hydrogen cyanide from the thiocyanate to produce a red color (Feigl, F., 1966).

HPLC Analysis

TCMTB at different depths in the treated wood was determined by drilling 10 mm diameter plugs in radial and tangential directions. Four mm discs were then sliced from the plugs to provide retentions at average depths of 2, 6, 14 and 19 mm and ground to pass a 20 mesh screen. The ground wood was well mixed, weighed and mixed with 10 ml of methanol in a screw capped bottle. The mixture was then sonicated for 3 hours in a 60°C water

bath. After extraction the mixture was filtered and diluted to 25 ml. The solution was then analyzed with HPLC (Shimadzu LC-6A) (Appendix H).

6.3 Results and Discussion

6.3.1 Qualitative Analysis: Staining Technique

Staining indicated that TCMTB had thoroughly penetrated the treated blocks. TCMTB appeared to be more concentrated in latewood than in earlywood (Figure 6.7), however, sawing may have displaced the biocide. Attempts to microtome smaller sections for microscopic analysis also appeared to displace biocide from the cell lumen to the cell wall. Although, staining was a good indicator for the presence of TCMTB, it was preliminary, qualitative and can not replace extraction and chemical analysis.

6.3.2 Distribution Studies

The effects of process parameters (temperature, pressure and treatment period), wood characteristics (volume-to-surface ratio of blocks and permeability of the wood) and solvent composition (cosolvent effect) on biocide retention were examined using TCMTB as the primary biocide although some data was also collected with tebuconazole.

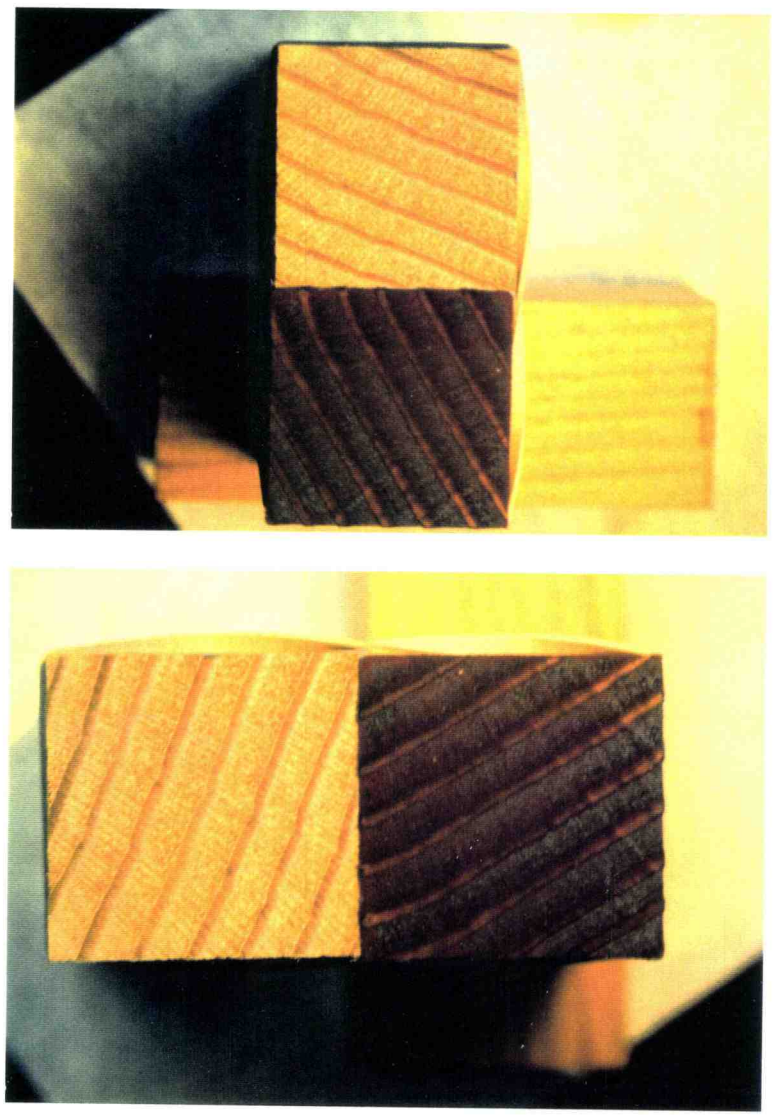

Figure 6.7 Distribution of TCMTB in the cross-section of 3.8 x 3.8 cm Douglas-fir blocks using SC-CO_2. The presence of a dark red color reflects TCMTB treatment.

Effect of Pressure on Impregnation

Douglas fir heartwood blocks (3.8 x 3.8 x 10 cm) were completely impregnated with TCMTB using a supercritical carbon dioxide-acetone mixture. For a treatment period of 30 minutes, as the maximum treatment pressure increased from 140 to 270 bar the retention at center of the blocks increased 7 fold (Figure 6.8). Further pressure increases to 300 bar resulted in much small increases in retention (20%). Higher pressure creates a larger driving force for bulk flow into wood and enhances biocide solubility by increasing the density of the SCF. Biocide solvency in the SC solution must be sufficiently high under the treatment conditions employed to produce the required penetration and retention. Higher pressure also produces more even distribution of TCMTB in the wood.

Effect Treatment Period on Impregnation

Treatment period appeared to have less of an effect on TCMTB retention than pressure. However, for treatment pressure of 250 bar, retention increased an average of 75% when treatment period was extended from 15 to 60 minutes (Figure 6.9). Variations in TCMTB distribution across the blocks appeared to be unrelated to the length of treatment period suggesting that longer treatment periods, which can be used to flatten biocide gradients in conventional liquid processes, may be less useful for this purpose with SCF.

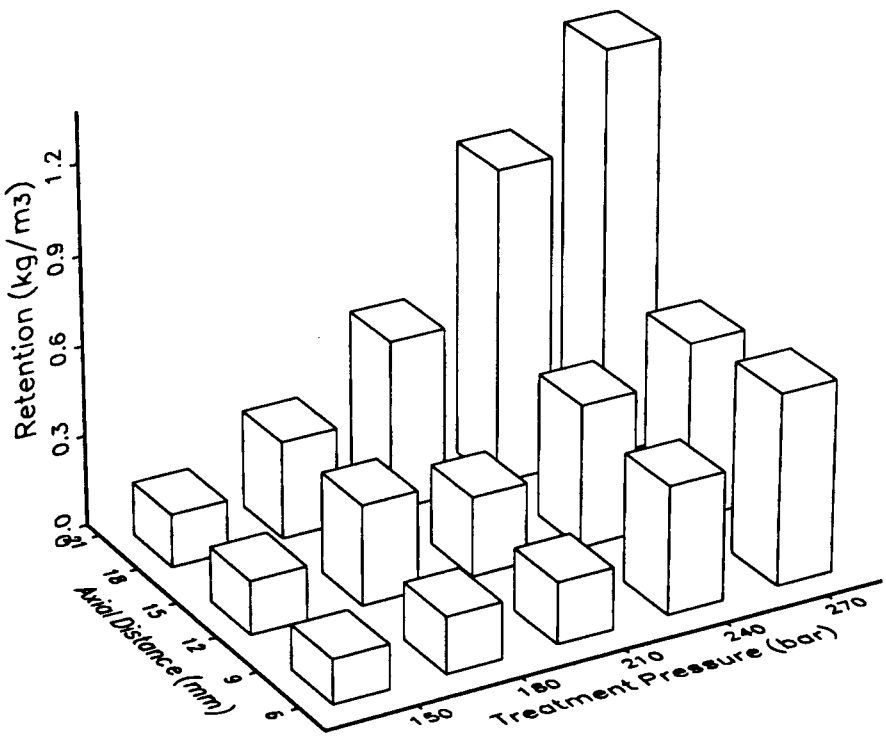

Figure 6.8 Retention of TCMTB at selected depths in Douglas-fir blocks (38x38mm) as a function of treatment pressure.

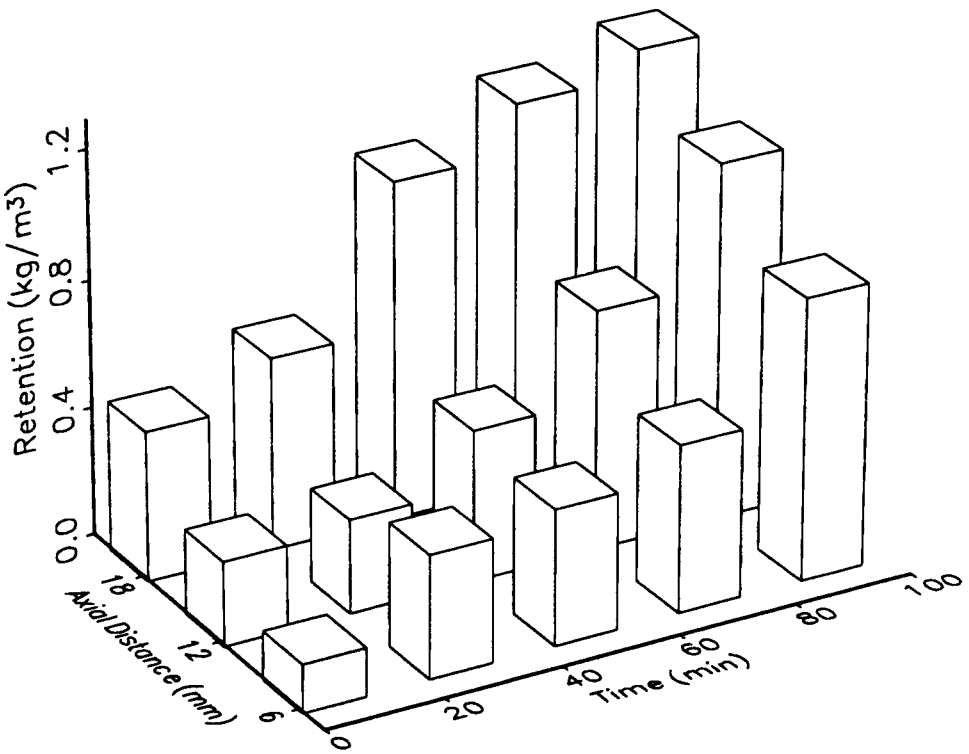

Figure 6.9 Retention of TCMTB at selected depth in Douglas fir blocks as a function of treatment time.

Influence of Specimen Length

The effect of specimen length in the flow direction was investigated by treating blocks of three different sizes (3.8, 2.5 or 1.9 cm square by 10 cm length) in a single change. Average retentions at selected depths indicated that despite high near surface retention, which may have been caused by surface deposition, the inner distribution was uniform for 25 and 19 mm blocks (Figure 6.10, 6.11 and 6.12). Ratios of TCMTB in the inner and outer zones were 1.8 and 2.61 for 19 and 25 mm blocks, respectively. There was, however, a notable concentration gradient along the depth of the larger (38 mm) blocks. Differences in surface-to-volume ratio and the decreased effective permeability with increased specimen size may explain for the differences in distribution (Bramhall,1971; Siau,1984).

TCMTB retention in Southern pine sapwood stakes (19 x 19 mm) treated at 248 bar and 60°C for a period of 30 minutes was 0.88 ± 0.43 kg/m^3 in the inner (7 x 7 mm) core and 3.98 ± 1.58 kg/m^3 in the outer shell (Figure 6.13) . The presence of a high concentration gradient or egg-shell distribution profile, may reflect the deposition of biocide crystals was more on the wood surface rather than in the inner portions. The inner retentions were reproducible over 10 runs including 50 stakes (Figure 6.13), however, the outer portion retentions exhibited wide variations.

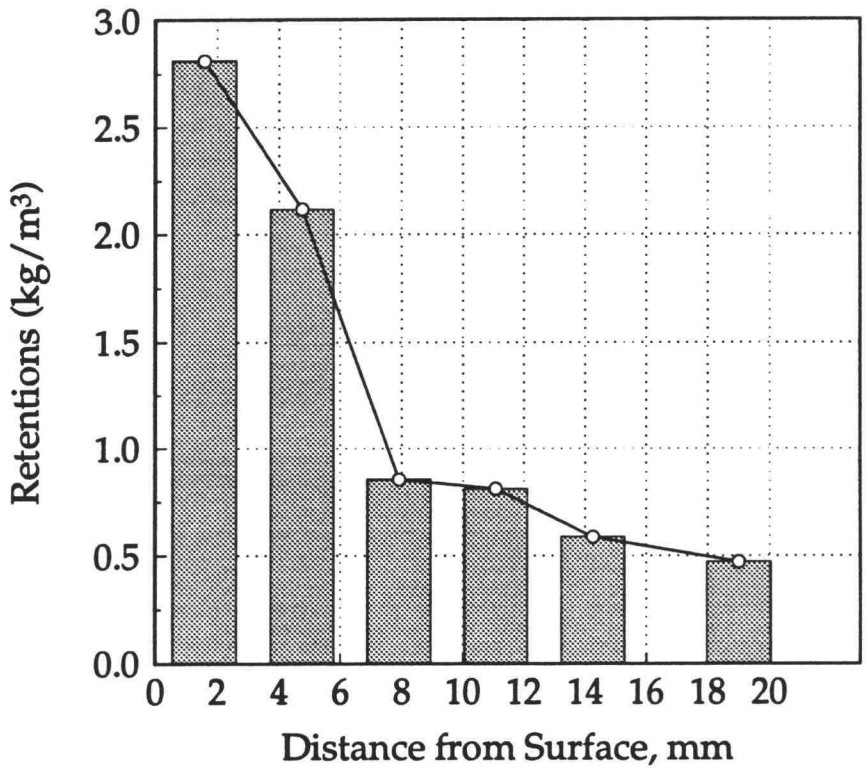

Figure 6.10 TCMTB retentions in Douglas-fir blocks (38 x 38 mm) treated using SC-CO_2 with 2.7 mol % acetone at 248 bar and 50°C for 30 minutes.

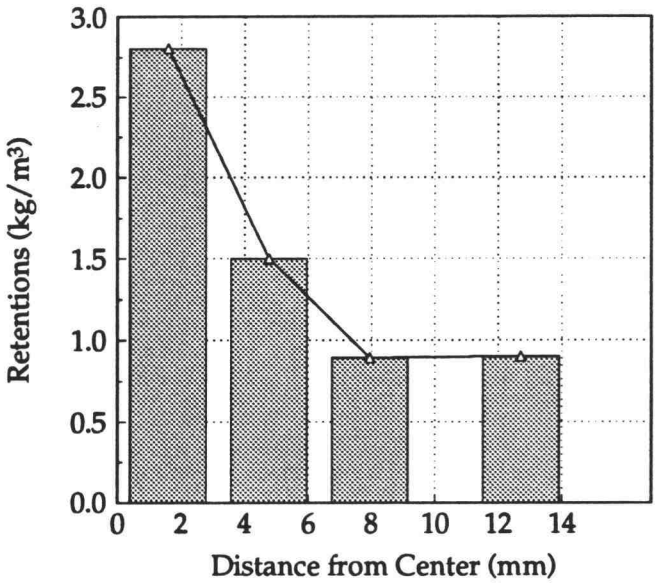

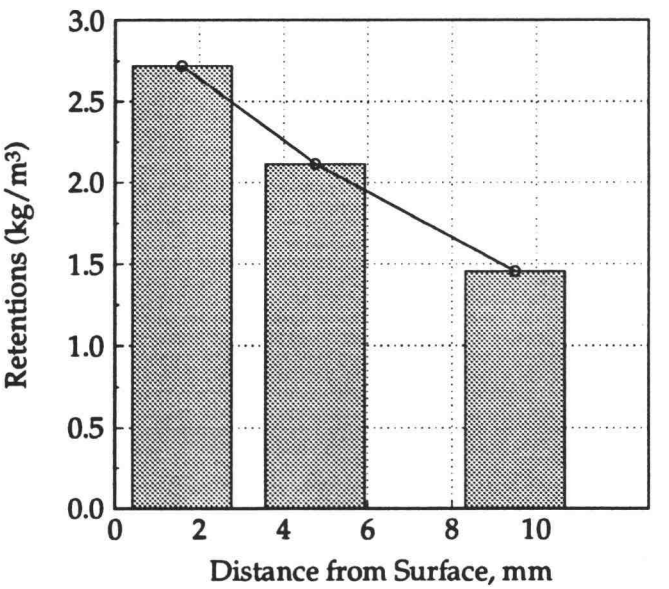

Figure 6.11 and 6.12 Retention of TCMTB in Douglas-fir heartwood blocks measuring (a) 25 x 25 mm or (b) 19 x 19 mm treated at 248 bar for 60 minutes at 50°C

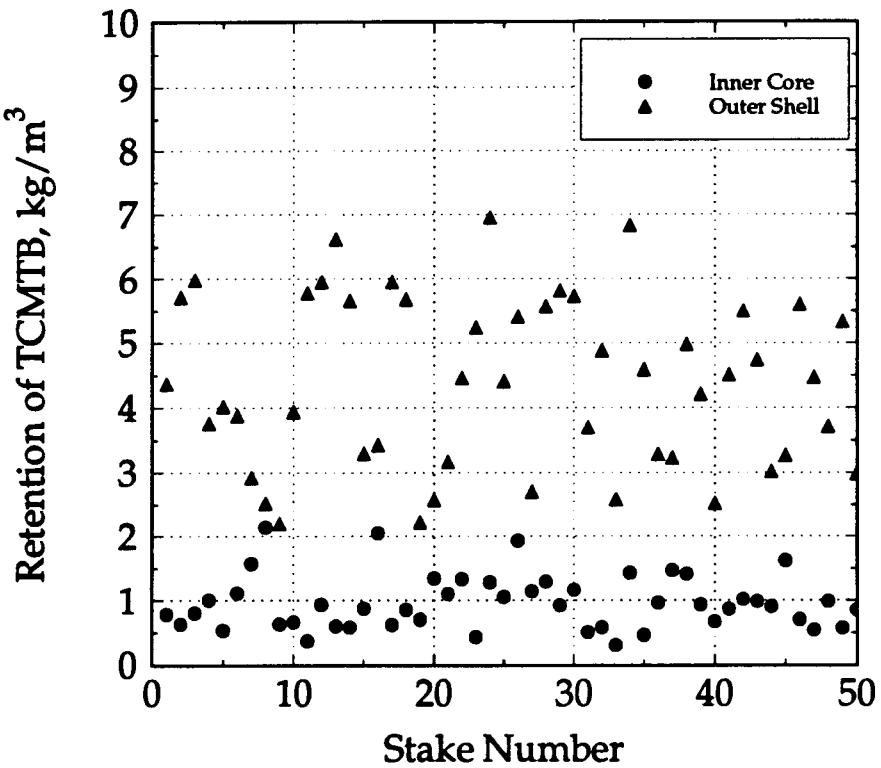

Figure 6.13 Distribution of TCMTB in southern pine blocks (19x19 mm) treated with SC-CO_2 at 248 bar for 30 minutes at 50°C.

Effect of Permeability on Impregnation

The movement of liquids or gases through wood is largely dictated by permeability. Permeability of a porous medium is the ease with which fluids flow through it under a pressure gradient. Permeability of wood strongly depends on the porous ultrastructure, moisture content, degree of pit aspiration and pore size. Ponderosa pine sapwood and Douglas-fir heartwood blocks (19 x 19 x 150 mm), with radial permeabilities of 6.719 ± 0.045 and 0.111 ± 0.067 $cm^3/s.cm.bar$, respectively, were treated with TCMTB at 240 bar for 30 minutes and 50°C. Average inner core (6 x 6 mm) retentions was 0.152 and 0.586 kg/m^3 for Douglas-fir and Ponderosa pine, respectively (Table 6.2). Outer portion retention was 0.693 and 1.595 kg/m^3. Although the permeability of the two species varied by a factor of 60, retentions in Ponderosa pine, the more permeability species, were only 2.4 times higher than those in Douglas-fir. Distribution of biocide in pine samples, however, tend to be more uniform. The differences in retention might have been greater if larger cross section blocks were used, there by increasing the potential for reduced penetration in the less permeable wood.

Effect of Cosolvent on Impregnation

Small amounts of cosolvents produced marked increases in the biocide solubility in supercritical CO_2. Southern pine stakes were treated with

Table 6.2 Distribution of TCMTB in Douglas-fir and Ponderosa pine blocks (1.9x1.9x10 cm) treated with SC-CO_2 at 207 bar for 30 minute at 50°C.

Species	TCMTB Retention, kg/m³		Outer/Inner retention Ratio
	Inner zone[a]	Outer zone	
Douglas-fir	0.1616	0.6066	3.7
	0.0646	0.6863	10.62
	-	0.4965	
	0.1824	0.8370	4.6
	0.2928	0.8020	2.7
	0.0586	0.7318	12.4
P. pine	0.5700	1.4900	2.6
	0.6933	1.9890	2.9
	0.6800	1.350	1.9
	0.4228	1.6310	3.8
	0.5245	1.3140	2.5
	0.6259	1.7530	2.8

[a] Inner 0.6 x 0.6 cm core

tebuconazole using pure CO_2 and CO_2/3 mole % of methanol at 207 bar for 30 minutes at 60°C. Average tebuconazole retentions increased from 0.79 ± 0.25 kg/m^3 to 1.92 ± 0.92 kg/m^3 with the addition of methanol (Figure 6.14). Preliminary solubility data showed that tebuconazole solubility increased by a factor of approximately 3 when 3 mole % methanol was added in SC- CO_2 at 248 bar and 50°C. The apparent lack of a corresponding improvement in retention may reflect in biocide concentration in the treatment vessel was less than saturation.

Effect of Flow Direction

In the pilot plant scale treatments, axial variation in biocide retention was observed, with wood near the bottom of the vessel having much higher retentions than those at the center or the top. These difference were notable for runs with unidirectional flow but could be reduced when flow directions were alternated during the run. This variation was mainly due to lack of adequate mixing in the treatment vessel.

Figure (6.15) shows retentions of pentachlorophenol in 1.9 cm ponderosa pine cubes treated at 60°C using SC-CO_2 with 3 mol % methanol. The result illustrates the effects of flow direction in the treatment vessel and position of samples within the treatment vessel retention / distribution.

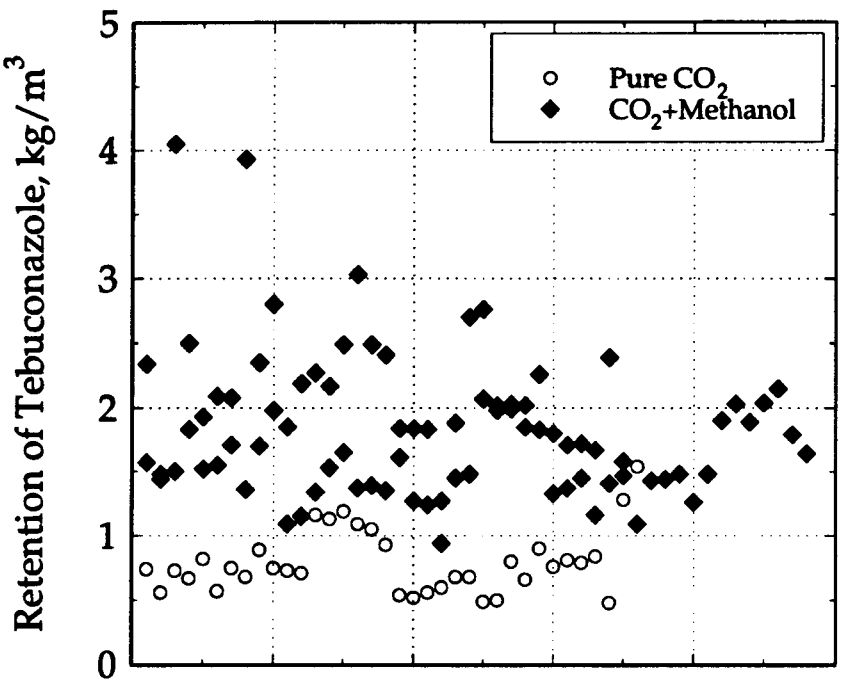

Figure 6.14 Effect of cosolvent on retention of tebuconazole in southern pine stakes (19 x 19 mm) treated at 172 bar for 30 minutes at 60°C.

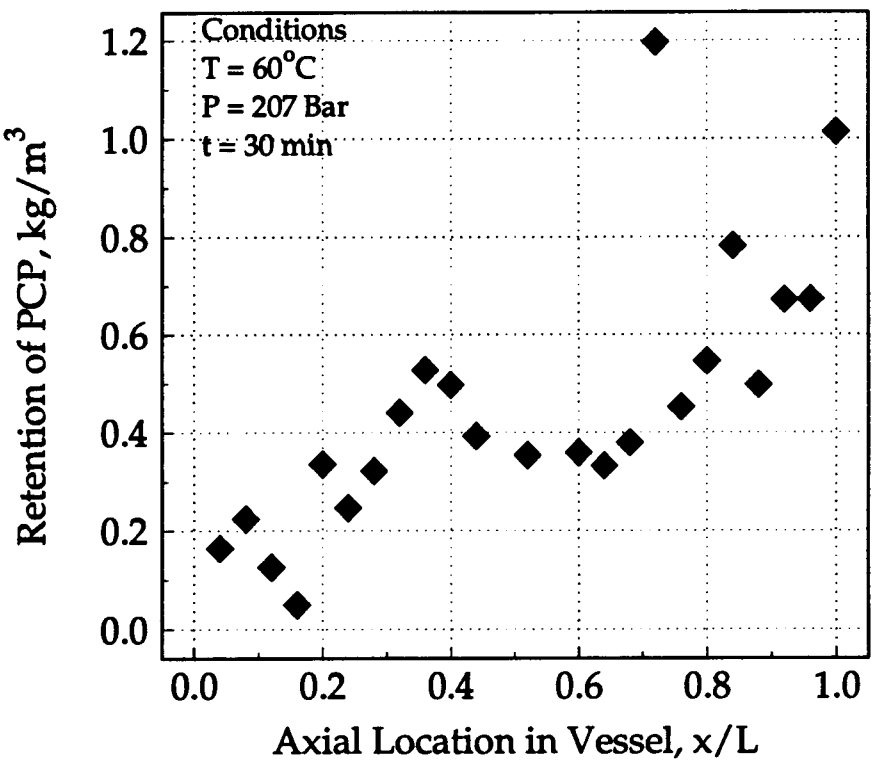

Figure 6.15 Effects of position in the treatment vessel on retention of PCP in 1.9 cm cubes. Location 0 is at the bottom of treatment vessel and 1.0 is the top.

6.4 Crystallization of Biocides from SCF Solution

When a supercritical solution is allowed to expand, either by flowing through an obstruction or depressurizing in a batch crystallizer, the dissolving power of the solvent changes dramatically during its transition from a supercritical fluid, which has a significant dissolving capacity, to a gas having negligible dissolving power. This process encourages rapid nucleation and growth of low vapor pressure solute particles, provided sufficient solute density exists prior to the expansion. Rapid expansion of supercritical solutions (RESS) has been used to produce powders, films and fibers through homogeneous nucleation of the solute species present in the solutions prior to expansion (Smith et al., 1986; Matson et al., 1989, Mohamed et al., 1989). Since nucleation is triggered mechanically by pressure change rather than thermally by temperature change, the solute undergoes rapid uniform supersaturation with respect to the solvent and nucleates within microseconds to produce uniform micro- and nano-scale particle (Peterson et al., 1986; Matson et al., 1987).

Temperature and pressure of the solution prior to expansion, the chemical and physical properties of the solute and the concentration of the solute in the SC before the expansion all affect the size and the morphology of the particles. Solute particle formation during rapid expansion of concentrated supercritical fluid solutions containing low vapor pressure solutes occurs in three stages: supersaturation of solute in the expanding fluid, solute nucleation

and subsequent growth of the particles (Matson et al., 1989). The conditions under which expansion occurs can affect one or more of these stages.

Expansion of a SCF through a flow obstruction produces highly nonequilibrium conditions. Theoretical models have been developed to relate physical properties of the expansion products with saturation, solute nucleation and crystal growth (Debenedetti, 1990). Depending on the conditions at which the expansion occurs, nucleation forms products of various morphologies: droplets, powders, fibers or thin films (Matson et al., 1987, 1989; Lele and Shine, 1992; Brand and Miller, 1991).

Much of the research done on rapid expansion processes has used flow obstruction devices like capillaries (Peterson et al., 1986; Lele and Shine, 1991), valve (Chang and Randolph, 1989) or orifices and nozzles (Mohamed et al., 1989; Brand and Miller, 1991). However, Tavana et al., (1989) used a batch crystallizer to manipulate particle size distribution and found that depressurization processes affected product-size distribution. A narrow crystal size distribution could be obtained by gradual step-wise reduction of pressure to maintain constant supersaturation, since the solid and the SCF were at equilibrium at each stage. These conditions were similar to those used in our experiment where precipitation occurred when the treatment vessel was vented.

When supercritical CO_2 / pentachlorophenol solution was allowed expand by venting the treatment vessel, the dissolved pentachlorophenol

nucleates and crystals grow rapidly as the solvating capacity of the fluid drops. The particles created have long needle shaped morphology (Figure 6.16 and 6.17). Slower venting can be used to create particles that are about 400 times longer than the initial feed material (6.18 and 6.19).

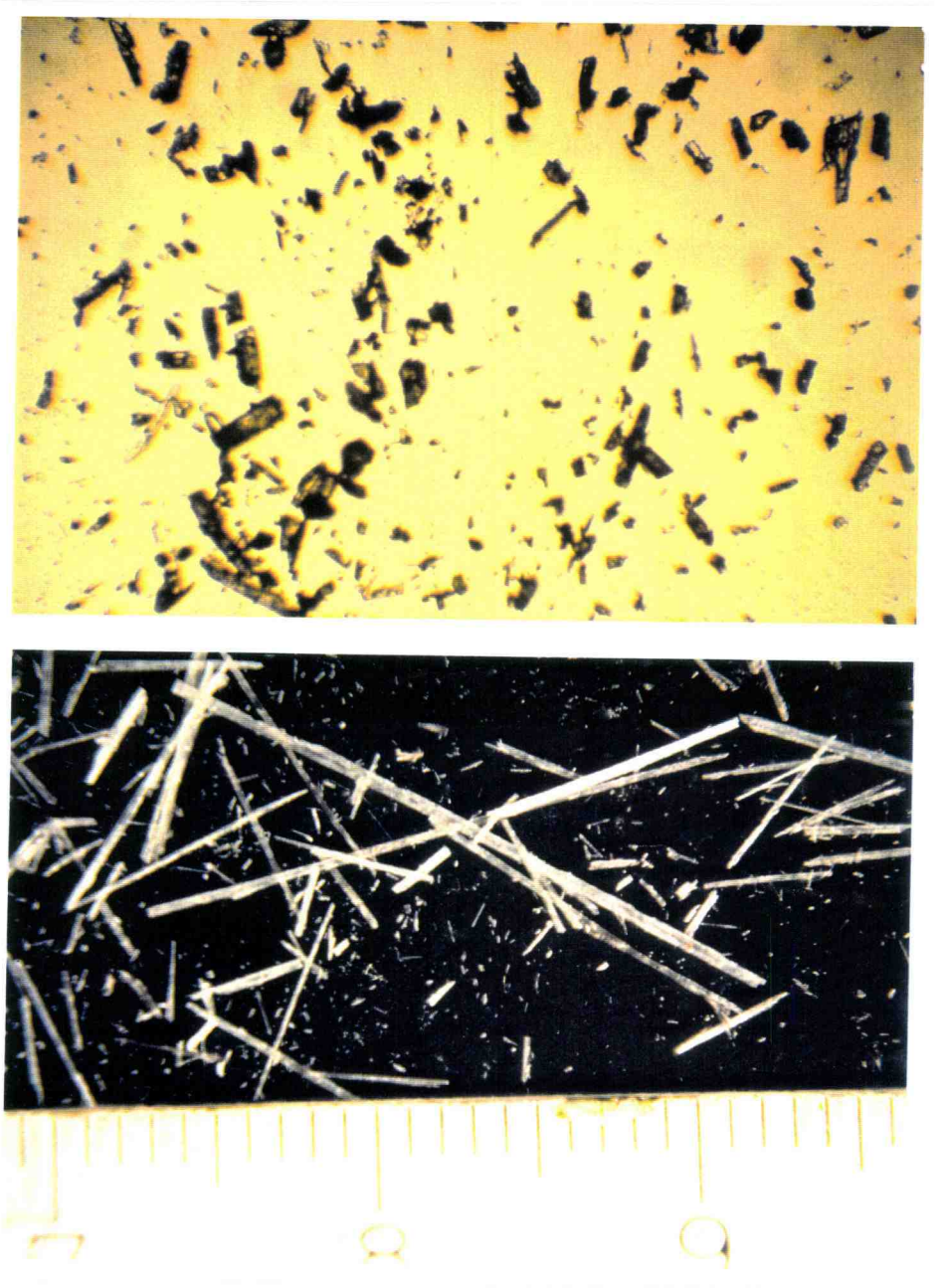

Figure 6.16 and 6.17 Examples of pentachlorophenol particles (a) before being loaded in the saturator (50X) and (b) after deposition from SC-CO_2 (4 X) at 250 bar and 80 °C.

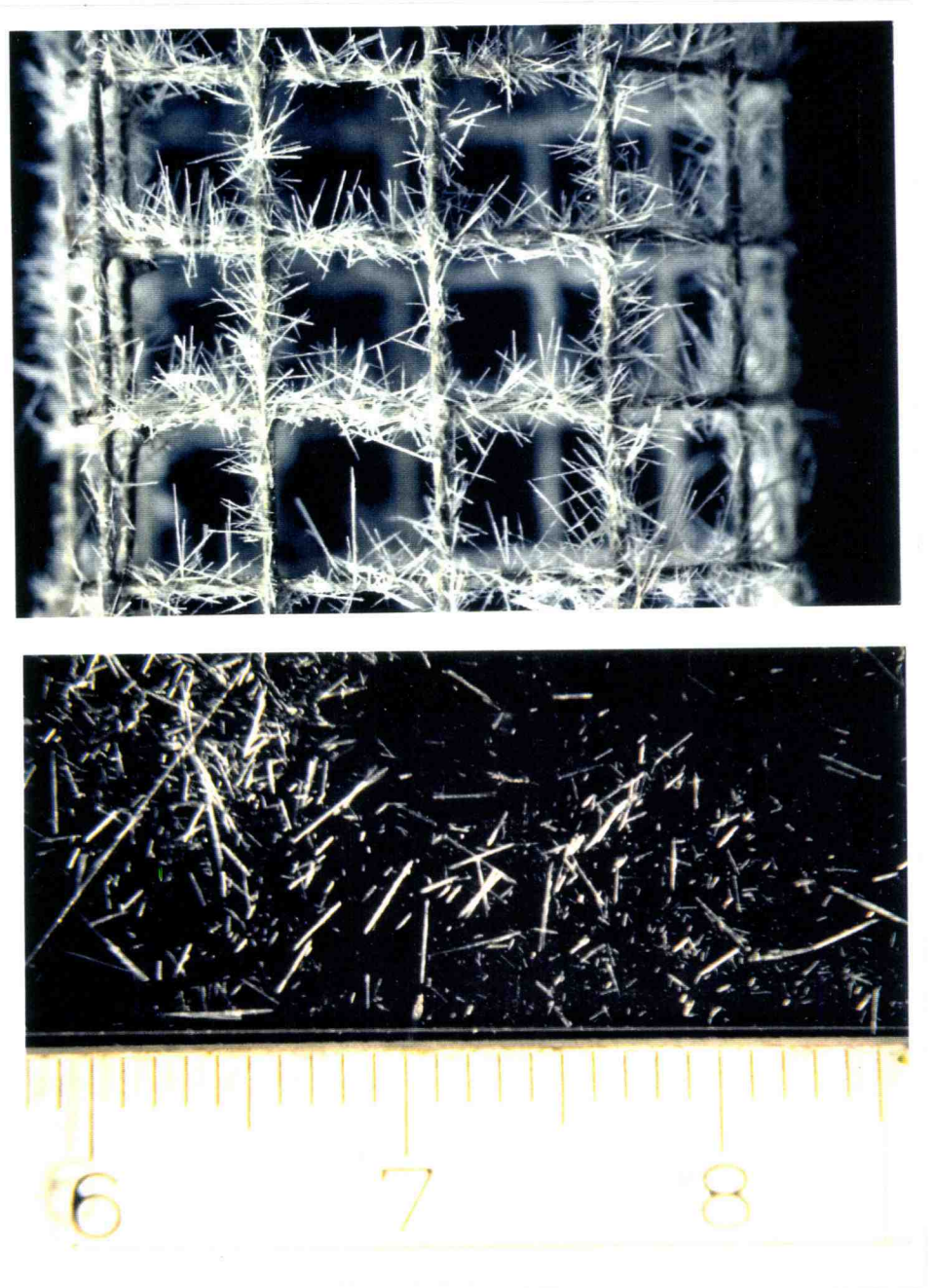

Figure 6.18 and 6.19 Examples of pentachlorophenol crystals (a) deposited on a sample holding cage and (b) deposited in the saturator vessel following solubilization in SC-CO_2

CHAPTER 7

DYNAMICS OF CHEMICAL DEPOSITION IN SEMI-POROUS MEDIA USING SUPERCRITICAL FLUIDS

7.1 Introduction

Semi-porous solids, such as wood, can be modified in various ways to change their physical, chemical and biological properties. Impregnated chemicals may be merely physically deposited in void structures of wood or can be reacted with the wood polymers to enhance various properties. The use of supercritical fluids to deliver biocides into wood is a much more complex process than liquid based impregnation, since solvent density and solute solubility vary with pressure. The current knowledge concerning the mechanism of fluid intrusion into wood and the complex phenomena controlling the supercritical impregnation process is limited. Chemical deposition studies are important for understanding impregnation but are rarely performed. Previous deposition studies were mainly experimental and intended to demonstrate the principle of impregnation. A more complete understanding of the impregnation process will be essential for consistently delivering chemicals into wood at the desired retention level.

A wide array of factors influence deposition of chemicals into a porous solid. Factors that control such transport and deposition are:

1. macroscopic factors, such as the unsteady-state flow dynamics of the treatment solution which depend on the structure of the medium as well as varying properties of the carrier fluid during the process.
2. microscopic factors such as phase behavior, precipitation and chemical association of dissolved biocides with wood functional groups.

Siau and Shaw (1971) attempted a semi-empirical correlation to explain the effects of permeability (K), treatment pressure (P), solution viscosity (μ), treatment time (t) and sample length (L) on retention and penetration of oils in wood. They experimentally found that volumetric retention was directly proportional to the log of $P^{0.42}$, $t^{1.3}$, and K and inversely proportional to $\mu^{0.42}$ and $L^{2.1}$. Siau emphasized the importance of developing a theoretical relationship based on unsteady-state fluid flow into wood.

Ward et al. (1990) presented a combined theoretical and experimental study on the dynamics of delivering a monomer, methyl methacrylate (MMA), into wood to manufacture a wood-polymer composite. Monomer loading could be tailored to a desired level. For example the average MMA loading increased from 16.9 to 33 wt% when the treatment solution concentration increased from 15 to 22 wt%. Measured MMA retentions, based on weight gain of the treated wood, were much higher than predicted values, but the study did not consider monomer distribution within the wood.

Once the SCF solution has permeated and diffused into the porous matrix, retention of the dissolved chemicals may result by precipitation,

deposition and association. Studies on precipitation kinetics of SCF solutions have primarily examined rapid expansion (RESS) across flow obstruction devices like capillaries (Peterson et al., 1986; Lele and Shine, 1991), valves (Chang and Randolph, 1989) and orifices or nozzles (Mohamed et al., 1989; Brand and Miller, 1991). In all these cases, the fluid expands rapidly ($<10^{-5}$ s) causing homogeneous solute precipitation.

Tavana et al., (1989b) used a batch crystallizer to manipulate the size distribution of particles by gradual step-wise reduction of pressure to maintain the solution at constant supersaturation. The rates of pressure change during the expansions were much smaller than in the case of SCF rapid expansion studies. Depressurization did not exceed 12 bar/min and high initial supersaturation levels were required to trigger nucleation.

Chemical interactions of biocides with different wood constituents may be either advantageous, when they result in fixation of the chemicals to prevent depletion, or detrimental, due to biocide inactivation. Chemical fixation of water soluble inorganic salt preservatives within the wood substrate has been partially elucidated by various researchers (Dahlgren and Hartford, 1972; Pizzi,1982). Most of these inorganic salts, however, showed little solubility in pure SC-CO_2. On the other hand, most organic biocides are much less reactive with wood, but they are soluble in SC-CO_2 with cosolvent. However, several of those SCF-soluble biocides show some reaction with

wood (Nicholas and Preston, 1984). For example, TCMTB reacts with wood extractives, particularly at elevated temperature (Daniels and Swan, 1987).

7.2 Objective and Approach

The objective of this study is to develop a theoretical model for the dynamics of supercritical fluid impregnation of semi-porous solids during selected treatment programs. The mathematical model describes the infiltration of the supercritical fluid, the deposition of the dissolved biocides and the evolution of pore geometry with time. Compressible flow dynamics were modeled for flow of pure SC-CO_2 into wood pores. Differential equations were solved for the unsteady-state pressure, density and viscosity changes of CO_2, including the corresponding variations in solubility of the dissolved biocide in wood pores. The equations were solved assuming uniform initial conditions and by utilizing the measured treatment fluid pressure and temperature as time-varying boundary conditions. The model describes the fluid dynamics of the process in the treatment vessel and in the voids of the porous solid. The changes in state variables, especially pressure and density, experienced in the solid pores during the treatment were computed for a given treatment cycle. Simulations were carried out to identify factors that influence retention and distribution of chemicals with the porous solid. These included specimen geometry, permeability, the treatment operating variables and treatment solution concentration. Comparisons with

experimental retention data and estimates of the distribution of biocides within various pieces of wood exposed to different treatment condition have been made.

Before discussing flow modeling, some of the wood characteristics that make this material unique and the basic factors that control fluid movement in wood will be reviewed.

7.3 Structural Characteristics of Softwoods

Fluid flowing through wood, for either impregnation with preservatives or extraction of chemicals with solvents, must overcome combinations of chemical, physical and anatomical restrictions. Wood is a derived porous material, which is mainly composed of cellulose, hemicellulose and lignin. Cellulose is the skeleton, hemicellulose the matrix, and lignin the encrusting substance that binds the cells together and gives rigidity to the cell wall. Low-molecular-weight compounds called extractives are found primarily in the heartwood. Structural and chemical variability of wood are exhibited in physical phenomena such as capillary behavior, permeability, thermal conductivity and diffusion of bound water. Because of their simpler structure, economic importance and uniformity, this study dealt mainly with softwoods. The presence of early and late wood, sapwood and heartwood, and compression / tension wood adds to the difficulty of understanding the structure and permeability of wood. Wood is nonhomogeneous and

anisotropic. Therefore, the structure is described in terms of three coordinate directions: radial, tangential and longitudinal (Figure 7.1).

Most coniferous wood (93%) is composed of vertically arranged, thread-like structure cells called tracheids. Six percent of the wood is present in bands of ray cells that are aligned in the horizontal plane and one percent of the volume of wood consists of resin canals. Differences in distribution of cells in the three coordinate directions helps to explain the high degree of anisotropy of wood. A typical cellular arrangement in soft wood is shown in Figure 7.2.

Fluid conduction in softwoods occurs through longitudinally oriented tracheids. Ray parenchyma cells are oriented from the pith or center of the tree stem to the bark. Fluids pass through the cell cavity, or lumen. These cells have closed ends, and flow between cells occurs through paired openings in adjoining tracheids called pits. The low rates of fluid penetration into wood can be due to the minute size Figure 7.3 of the pit membrane pores connecting tracheids or to their occlusion by debris.

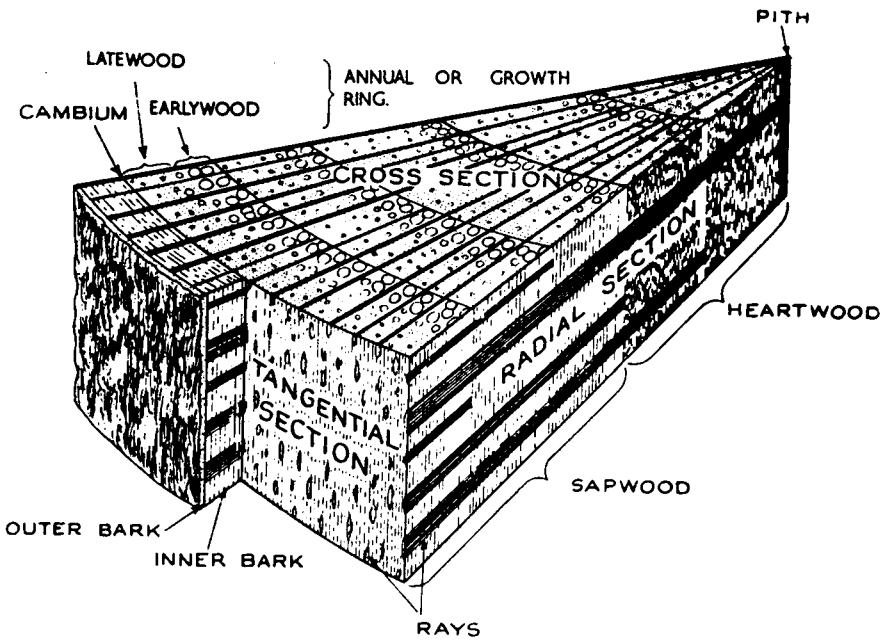

Figure (7.1) Three dimensional view of a hardwood showing different parts and orientations. (Prince Risborogh Laboratory, Building Research Establishment, U.K.)

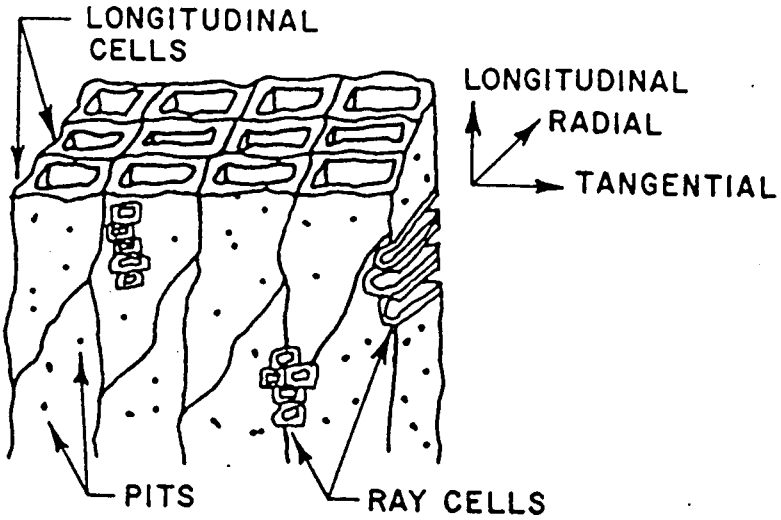

Figure (7.2) Cellular arrangement of a typical softwood (Plumb et al., 1985)

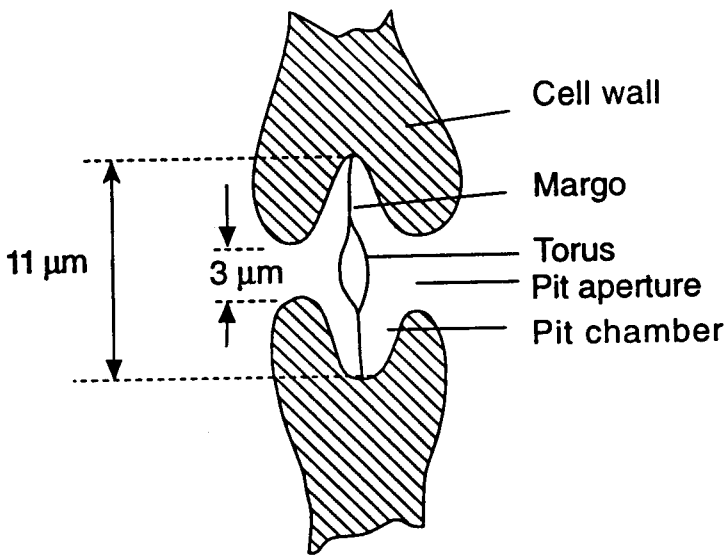

Figure (7.3) Example of a bordered pit (adapted from Petty, 1972)

7.3.1 Pits

Softwoods tracheid lumens are the pathways through which fluids must travel and this movement is largely controlled by pits, although cell wall capillaries can exert limited localized influence. Three different types of pits are present in softwood: bordered, semi-bordered and simple. Bordered pits are restricted to the radial walls of the tracheids, tending to be located toward the ends of the cells. Semi-bordered pits interconnect the vertical tracheids with the horizontal ray parenchyma cells, while simple pits connect adjacent parenchyma cells. The most important pit type is the bordered pit, since it controls inter-tracheid flow. An average tracheid is 0.35 cm long with a diameter of 35 μm and has from 50 to 300 pits connecting adjoining fibers. There are from 50,000 to 100,000 such fibers in a square centimeter cross section (Stamm 1964). Horizontally aligned ray cells are the principal pathway for radial flow, while both longitudinal and transverse flow paths in softwoods are dictated by the permeability of the bordered pits. These differences produce anisotropic permeability, with longitudinal permeability being about 10,000 times greater than transverse or radial.

The membranes of bordered pits are centrally located in living tissue. In this condition the membrane of the bordered pit is permeable and readily allows the flow of fluids and particles. A central thickened disk, called the torus, is supported in the center of a bordered pit chamber by strands of cellulose microfibrils (Figure 7.3). Pressure can push the torus to the pit

aperture of the opposite tracheid or aspirate the pit, effectively seal the opening. This may occur if an air-water meniscus develops within the torus which contacts the overhanging membrane, thereby blocking the permeable portion of the pit membrane. Pit aspiration can also occur during drying, when a sufficient force develops to bring the tori toward the pit border. Permeability in unaspirated pits is a function of porosity, thickness, and area of the membrane. Permeability in aspirated pits depends upon how closely the torus is seated, the area of the membrane and whether resinous material has coated the membrane. Heartwood pits in some species are already aspirated in the green condition (Phillips, 1933).

The shape and size of tracheids, as well as type, number and location of pits, and the presence of rays, all affect directional permeability.

7.3.2 Variability in Structure

There are several aspects of wood structure that account for the variations in permeability, including variation in size, shape and distribution of cell types, pit type and distribution, and the presence of rays. Permeability in the longitudinal or tangential direction is primarily affected by bordered pits on radial walls; whereas, radial flow occurs primarily through ray tracheids (Panshin and de Zeeuw, 1980).

The ratio of longitudinal to transverse permeability varies between 100 - 10,000 for the various species. Permeability also varies between sapwood and

heartwood, between early and late wood and within the same tree. "The effectiveness of the communicating structure," reported Stamm (1946), "not only varies greatly between species and different specimens of the same species, but from one annual ring to the next. This variation of structure that controls flow accounts for the very irregular line of advance of treating material into wood under pressure permeability conditions."

7.3.3 Geometric Representation of Softwood Structure

The pore structure of most solids is exceedingly complex. Gross properties of porous solids such as porosity and permeability are easily measured, but fine measurements are more difficult. For example, techniques used to measure porosity do not provide the means for determining the shape and length of pores. In contrast to the random packing of other porous media, such as sand, wood cells are organized in a regular pattern, making it attractive to use geometric modeling. In that approach one postulates a geometry, which bears some similarity to the wood structure, to identify porous properties, yet is sufficiently simple to allow the governing differential equations to be solved. Figure (7.4) shows a mechanistic model of softwood structure (Comstock, 1970).

The permeability of consolidated porous solids is a direct function of the available passage, or size of the interconnected pores. Permeability of wood depends on the distribution of pit pairs and the number of cell walls

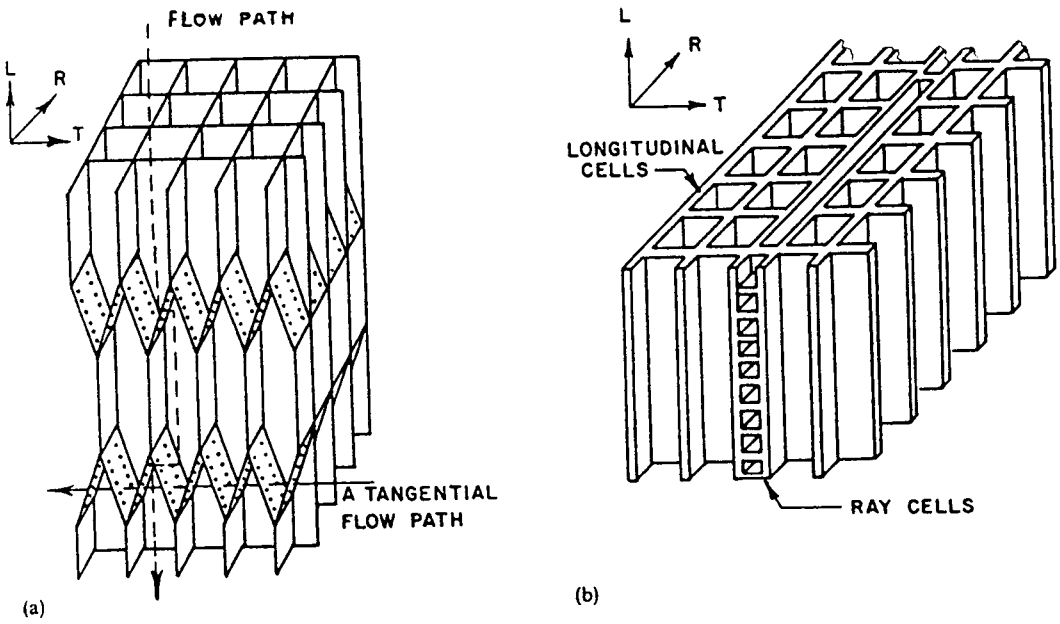

Figure (7.4) A mechanistic model for softwood (Comstock, 1970).

that must be traversed. The porosity of wood (ε) may be calculated from the moisture content of (*W*, wt %, dry basis), the wood density ρ_{wood} (gm/m^3)and assuming the density of the cell wall substance to be 1.49 gm/cm^3(Siau, 1984):

$$\varepsilon = 1 - \rho_{wood}\left(\frac{1}{1.49} + \frac{W}{100\rho_{water}}\right) \qquad (7.1)$$

7.4 Diffusion and Flow of Supercritical Fluids in Porous Solids

Mass transport in porous solids is complex and may involve several mechanisms. Two important mechanisms for the transport of fluids through wood include diffusion (molecular and Knudsen) and bulk flow. Most models for predicting flow of fluids in porous solids are based on well-developed theories of diffusion and flow in capillaries. Capillary theories are adapted to simple geometric models to represent the porous solid structure. These models are not completely fundamental, since they contain adjustable parameters that must be determined experimentally.

7.4.1 Diffusion into Porous Solids

Diffusion is the dominant mode of transport when the system pressure is uniform ($P_{surface}$= P_{center}). The diffusion rate depends on the size and number of pit membrane openings. Hence, the diffusion coefficient is correlated with permeability.

Diffusion consists of: bulk gas diffusion, which includes transfer through gas in the lumen, and diffusion within the cell wall capillaries. If the radius of the capillary (r) and the fluid pressure are such that the mean free path of the solute (Γ) is large compared to the diameter of a pore, the rate of transport of the solute is governed by collisions with the capillary wall. This type of transport is referred to as Knudsen diffusion. Qualitatively, Knudsen diffusion appears to dominate for values $r/\Gamma < 0.1$:

$$N_2 = -D_{K2}\frac{dC_2}{dx} \tag{7.2}$$

where N_2 is the mass flux , m/(s.cm^2), D_{K2} is the Knudsen diffusion coefficient, cm^2/s and C_2 is solute concentration, mole/cm^3.

When the ratio r/Γ is greater than 10, ordinary molecular diffusion predominates. Using fluxes of solvent and solute (N_1 and N_2) relative to a fixed coordinate x, the flux of solute (2) for ordering molecular diffusion is:

$$N_2 = -D_{21}\frac{dC_2}{dx} + y_2(N_2+N_1) \tag{7.3}$$

where the diffusion coefficient D_{21} is independent of capillary size.

For $0.1 < r/\lambda < 10$, the flux can be written:

$$N_2 = -D_N \frac{dC_2}{dx} \tag{7.4}$$

where

$$\frac{1}{D_N} = \frac{1}{D_{K2}} + \frac{1}{D_{21}} \tag{7.5}$$

7.4.2 Flow into Porous Solids

In the presence of a pressure gradient ($P_{surface} \neq P_{center}$), bulk flow is usually the dominant mechanism for mass transfer. Bulk flow depends on the permeability of the wood, i.e. the ease with which a fluid may be made to flow through the material by an applied pressure difference. Permeability is determined solely by the structure of the porous medium (Siau,1984). Although, wood has a porosity ranging from 0.6 to 0.8 (Stamm, 1963), it is not homogeneous and it is not very permeable.

The momentum equation is given by Darcy's law (Darcy, 1856), which is the porous medium analog of the Navier-Stokes equation. Darcy's law implies that the rate of flow of a homogenous fluid within a porous matrix is proportional to the pressure gradient and to the cross sectional area normal to the direction of flow, but inversely proportional to the viscosity of the fluid. Writing this as an equation in terms of specific fluid velocity (u), which is equal to volumetric flow divided by cross sectional area:

$$u = -\frac{K}{\mu}\frac{\partial P}{\partial x} \tag{7.6}$$

where the empirical constant K is the specific permeability of the porous matrix. The value of $K^{1/2}$ is a length scale representative of the effective pore diameter. The values of K for softwoods vary between 10^{-14} - 10^{-12} m^2 for sapwood and heartwood, thus effective pore diameters are 0.1 to 1 μm. A theoretical basis for Darcy's law has been obtained using deterministic (Dullien, 1979) or statistical models (Whitaker, 1986).

Slip flow in gases occurs when the mean free path of the flowing gas becomes an appreciable fraction of the capillary radius through which the gas flows. As a result of this slip flow, the velocity of the gas at the wall of the capillary is finite and the permeability of wood is dependent on pressure.

Slip increases with increasing pressure. Carman, (1956) noted that slip flow occurs within a transition region between the pure viscous flow of gases, where intermolecular collisions control the rate of flow, and "free molecule" or Knudsen flow of gases, where molecules collide only with the capillary walls and not with one another. When χ, defined as (Perry, 1984):

$$\chi = \frac{\Gamma}{2r}\sqrt{\frac{8}{\pi}} = \frac{\mu}{P_m r}\sqrt{\frac{RT}{M_w}} \tag{7.7}$$

is greater than unity, flow is essentially molecular. When χ it is less than 0.014, flow is primarily molecular. In equation (7.7) P_m is the mean absolute pressure and M_w is the molecular weight of the gas. The mean free path length (Γ) of the gas and the effective radius (r) must be in the same units. For χ between 0.014 and 1.0, both slip and Knudsen flow contribute to the flux. The mean free path for CO_2 at an average pressure of one bar is estimated to be 0.1μm and the corresponding χ value is approximately 0.6 in wood. Thus both Knudsen and viscous flow contribute significantly to total flow. Combining these two components, the superficial gas permeability, K_g, can be determined from the Adzumi equation (1937):

$$K_g = \frac{\pi J r^4}{8\mu} + \frac{3r^3\mu}{\bar{P}}\sqrt{\frac{RT}{M_w}} \qquad (7.8)$$

where J is number of parallel capillaries per unit area, R is the universal gas constant, T is the temperature, K and M_w is the molecular weight of the gas. Substituting Equation (7.7) in Equation (7.8) and rearranging it the relationship between permeability and pressure, called the Klinkenberg effect (Klinkenberg, 1941) :

$$K_g = K\left(1 + \frac{3.8\lambda}{r}\right) = K\left(1 + \frac{b}{P_m}\right) \qquad (7.9)$$

where $b = 4c\Gamma P_m/r$ and c is a constant. From equation (7.9) it is clear that the superficial permeability at higher pressures, where Γ is very small, K_s, is not significantly larger than specific permeability, K.

Darcy's law is valid for laminar flow, where the fluid is homogenous and incompressible and has no interaction with the solid substrate (Musket,1946; Scheidegger,1974). Bramhall, (1971), suggested a correction to Darcy's law where the length factor was raised to an exponent, corresponding to the exponential decrease of the available cross-sectional area of the conducting trachieds. The available flow area was exponentially related to pore size (Hosli and Orfila, 1985).

It has been shown that Darcy's law is valid for flow of gases through wood (Siau,1971). For flow of SCFs through wood, Darcy's law is assumed to be valid with uniform permeability.

7.4.3 Combined Diffusion and Viscous Flow

The combined flux due to viscous flow and diffusion in a porous matrix obtained from equations (7.2) and (7.6) can be expressed as:

$$N_2 = -D_e\frac{\partial C_2}{\partial x} - C_2\frac{K\,dP}{\mu\,dx} \qquad (7.10)$$

where D_e is the effective diffusivity which is equal to D/ε and K is permeability. Although diffusion is the mechanism utilized in certain

waterborne preservative treatments of lumber, penetration is very slow. Fluid flow through the interconnected voids of the wood structure is much more rapid than diffusion and provides greater opportunities to control penetration and retention. The relative importance of diffusion and flow can be compared by computing the characteristic times for each mechanism assuming an effective diffusion coefficient, in SC-CO_2 equal to $10^{-4}cm^2/s$ (Paulaitis et al., 1983) and tortuosity of one, the characteristic time for a compound to diffuse through SC-CO_2 to the center of a 3.8 cm Douglas-fir block is calculated to be 10 hours using:

$$t_{cD} = \frac{L^2}{4D_e} = \frac{(3.8\,cm)^2}{4 \cdot 10^{-4} cm^2/s} \tag{7.11}$$

However, the characteristic time for a supercritical solution to flow into a 3.8 cm Douglas-fir block a assuming pressure difference of 20 bar and permeability (K) of $5x10^{-13}cm^2$, viscosity (μ) of $8x10^{-5}$ Pa.s and porosity (ε) equal to 0.6 is about 3 minutes:

$$t_{cF} = \frac{L^2 \mu \varepsilon}{4KP} = \frac{(3.8\ cm)^2 8.10^{-5}\,Pa\,s.0.6}{4\,(5 \cdot 10^{-13}\,cm^2)\ 20^5\,Pa} \tag{7.12}$$

Thus viscous flow of the supercritical solution is about two orders of

magnitude faster than molecular diffusion, and viscous flow is considered the dominant factor for the net flux of chemicals into wood when there is a pressure gradient.

7.5 Model Development

7.5.1 Process Constraints

The process of chemical deposition into a porous solid involves increasing the pressure to a maximum by adding a supercritical treatment solution, maintaining that static maximum pressure for a required period and then venting the solution out of the treatment vessel. There are three operational and physical limitations that are characteristic of a treatment system.

1. The pressure build-up rate depends on the compressor capacity and the volume of the treatment system. The capacity of a constant speed compressor depends on the cylinder size and compression ratio. In this study a pressure increase rate of 24.9 bar/min was assumed.

2. The initial mass present and the mass rate of venting determines how fast the density decreases in the treatment vessel, which decreases the solubility of dissolved solutes. The limit for the venting velocity is sonic flow through the outlet lines. The maximum rate of mass venting also depends on the outlet diameter.

3. When a highly anisotropic porous solid like wood is exposed to extreme pressure gradients, it can become damaged or collapse. For moderately strong wood, the tensile strength parallel to the grain is 1000 bar, whereas the tangential and radial direction tensile strength are only 35 bar and 530 bar respectively (Dietz et al., 1980). This difference in strength can be attributed to microfibril orientation in the cells. Rapid venting of the treatment vessel contents can create high tangential and radial stresses which can crack the wood.
   Conversely, the compressive stress perpendicular to the grain may cause failure by collapsing the wood cell. The stress level at which flattening occurs is about 400 bar for softwood.

The pressurizing and depressurizing rates of the treatment vessel used in the following simulations were based on these limits.

7.5.2 The System

The model is based on a finite, two dimensional square block, ($0 \leq x \leq$L $0 \leq z \leq$ L), matrix that is permeable at both faces (Figures 7.5a 7.5b). Initially the medium has uniform permeability and no solute is present. At $t \geq 0$, the matrix is exposed to a supercritical solution with an increasing pressure at the surface of 24.9 bar/min until a maximum pressure is reached.

When the treatment chamber attains a final maximum value, the composition at the boundaries ($x = 0$, $x = L$ and $z = 0$ and $z = L$) is specified

as saturated, and the solution begins to flow into the matrix. After a treatment time, t_{tr}, the chamber pressure is reduced below the critical value at a given rate of depressurization. Supercritical fluid flows smoothly out of the interior of the solid matrix, causing precipitation and deposition of chemicals.

7.5.3 Assumptions

Supercritical deposition of solutes in a porous matrix depends on dissolution, compressible fluid flow through porous media and heterogenous crystallization. Since we are interested in the qualitative behavior of the system, a number of simplifying assumptions were made.

1) The matrix is a three dimensional uniform block, with longitudinal ends sealed. Pressure gradients in the longitudinal direction were assumed to be negligible since the ends of the blocks are sealed.

2) The volume fraction of the precipitated solute is negligible compared to the void volume, thus the matrix porosity and permeability are constant.

3) The solvent has no effect on the porous matrix, i.e. the matrix does not swell.

4) Permeabilities in radial and tangential directions are the same,

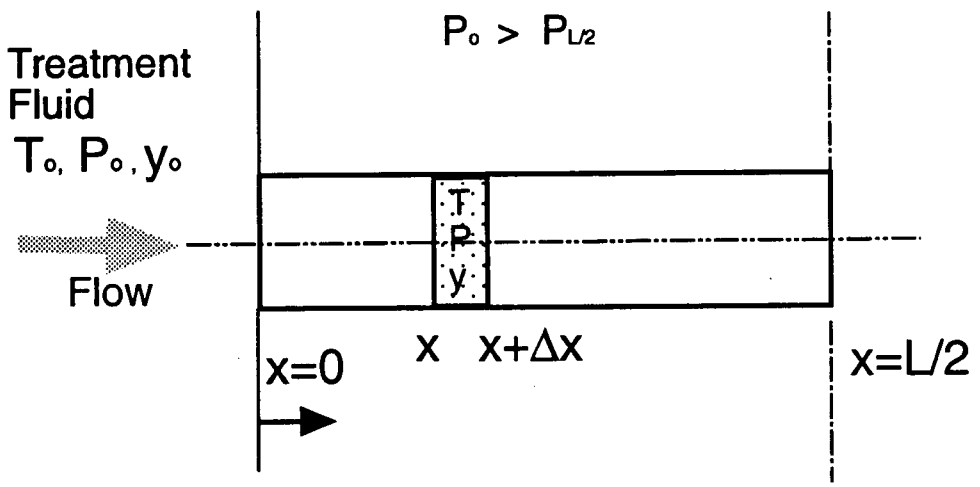

Figure (7.5) Schematic of a model pore.

although in wood slight differences have been noted (Panshin and de Zeeuw, 1980).

5) The main transport is by viscous flow and diffusion transport is relatively small.

6) Fluid within the matrix is always in equilibrium with a deposited solute phase. During venting the pressure at the interior surface of the matrix is assumed to be atmospheric. Thus essentially all solute in the SCF solution within the matrix at the onset of venting remains some where in the matrix.

7) Pressure within the bulk fluid in the vessel is uniform during the treatment process, since pressure differences can cause rapid mixing.

7.5.4 Mathematical Formulation

Total Mass Balance Equations

Equations of continuity and motion for flow of a pure isothermal fluid through a porous medium can be developed from the basic equation of continuity (Bird et al., 1960):

$$\varepsilon \frac{\partial \rho}{\partial t} + (\nabla \cdot \rho \underline{u}) = 0 \tag{7.13}$$

and Darcy's law. Combining equations (7.6) and (7.13) yields:

$$\varepsilon \frac{\partial \rho}{\partial t} = \nabla \cdot (\frac{K}{\mu} \rho \nabla . p) \tag{7.14}$$

Density can be expressed in terms of pressure and the compressibility factor (Z) using an equation of state:

$$\rho = \frac{p}{RTZ} \tag{7.15}$$

where R is the universal gas constant. .

Assuming the permeability, K, and porosity, ε, constant and using normalized pressure, $P = p/p_o$ the flow equation for two dimensional cartesian coordinates (x, z) becomes:

$$\varepsilon \frac{\partial}{\partial t}\left(\frac{P}{Z}\right) = p_o\left[\frac{\partial}{\partial x}\left(\frac{K}{\mu Z} \cdot \frac{\partial P^2}{\partial x}\right) + \frac{\partial}{\partial z}\left(\frac{K}{\mu Z} \cdot \frac{\partial P^2}{\partial z}\right)\right] \tag{7.16}$$

where p_o is the initial pressure. For a real compressed gas, μ and Z are functions of pressure and for a homogenous porous matrix, equation (7.16) can be rearranged to:

$$\frac{\partial P}{\partial t} + PZ\frac{\partial Z^{-1}}{\partial t} = \frac{\zeta}{\mu_R}\left[\frac{\partial^2 P^2}{\partial x^2} + \frac{\partial P^2}{\partial x}\left(Z\frac{\partial Z^{-1}}{\partial x} + \mu\frac{\partial \mu^{-1}}{\partial x}\right)\right] + \frac{\zeta}{\mu_R}\left[\frac{\partial^2 P^2}{\partial z^2} + \frac{\partial P^2}{\partial z}\left(Z\frac{\partial Z^{-1}}{\partial z} + \mu\frac{\partial \mu^{-1}}{\partial z}\right)\right] \tag{7.17}$$

where:

$$\zeta = \frac{Kp_o}{\varepsilon \mu_c} \tag{7.18}$$

ζ is a flow parameter similar to the diffusivity and is expressed in units of m^2/s and μ_c and μ_R are the critical and reduced viscosity of the solvent.

Dimensionless time and dimensionless distance are defined as:

$$\tau = \frac{\zeta}{L^2} t = \Omega t \tag{7.19}$$

$$\acute{x} = \frac{x}{L} \tag{7.20}$$

$$\acute{z} = \frac{z}{L} \tag{7.21}$$

where Ω is the dynamic flow coefficient, which is equivalent to the inverse of the characteristic time, and p_o is the initial pressure used as a reference pressure. Using the above dimensionless variables, Equation (7.17) becomes:

$$\frac{\partial P}{\partial \tau} + PZ\frac{\partial Z^{-1}}{\partial \tau} = \frac{1}{\mu_R}\left[\frac{\partial^2 P^2}{\partial \acute{x}^2} + \frac{\partial P^2}{\partial \acute{x}}\left(Z\frac{\partial Z^{-1}}{\partial \acute{x}} + \mu\frac{\partial \mu^{-1}}{\partial \acute{x}}\right)\right] + \frac{1}{\mu_R}\left[\frac{\partial^2 P^2}{\partial \acute{z}^2} + \frac{\partial P^2}{\partial \acute{z}}\left(Z\frac{\partial Z^{-1}}{\partial \acute{z}} + \mu\frac{\partial \mu^{-1}}{\partial \acute{z}}\right)\right] \tag{7.22}$$

The initial conditions at $\tau = 0$ are:

$$P = 1, \quad T = 1 \tag{7.23}$$

The boundary conditions are:

$$\text{At } \acute{x} = 0, \text{ and } \acute{x} = 1, \quad P = P_{vessel} \tag{7.24}$$

Since most biocides had low solubility in SC-CO_2 (< 10^{-3} mole fraction), the compressibility of pure carbon dioxide is assumed to accurately model the SCF solution properties. This compressibility is used in Equation (7.20) as given by the modified Benedict-Webb-Rubin equation of state (Ely, 1986).

$$Z(T,\rho) = \frac{1}{RT}\left[\sum_{n=1}^{9} a_n(T)\rho^{n-1} + e^{-\gamma\rho^2}\sum_{n=10}^{15} a_n(T)\rho^{2n-18}\right] \tag{7.25}$$

The set of constants, $\{ a_n \}$ are given in Appendix B. The equation of Yoon and Thodos (1970) for non-polar compounds was used to estimate the viscosity of SC-CO_2 as a function of pressure. At low pressures the viscosity of gases may be approximated (Yoon and Thodos, 1970) by:

$$\mu\xi = 4.610 T_R^{0.618} - 2.04 e^{-0.449 T_R} + 1.94 e^{-4.058 T_R} + 0.1 \qquad (7.26)$$

and for dense fluids ($0.1 < \rho_R < 3$) the following relationship was used (Jossi et al., 1962):

$$[(\mu - \mu^o)\xi + 1]^{0.25} = 1.0230 + 0.23364\ \rho_R + 0.58533\ \rho_R^2 - 0.40758\ \rho_R^3 + 0.093324\ \rho_R^4 \qquad (7.27)$$

where μ^o is the viscosity at atmospheric pressure (shown Appendix D) and at the same temperature and ξ is given by:

$$\xi = T_c^{1/6}\ M^{-1/2}\ P_c^{-2/3} \qquad (7.28)$$

Equations (7.15), (7.25) and (7.26) or (7.27) can be used with equation (7.22) to solve for pressure in a porous matrix at any given time and location.

Solute Balance Equation

Consider a medium with a porosity of ε and permeability of K through which a homogeneous supercritical solution is flowing. As the solution flows through the medium, simultaneous permeation and retention caused by

adsorption and deposition occurs. The solute concentration in the porous medium satisfies the following equation:

$$\varepsilon \frac{\partial w_2}{\partial t} + \frac{\partial (w_2 u)}{\partial x} + \frac{\partial (w_2 u)}{\partial z} + \acute{\varepsilon} \frac{\partial w_{2s}}{\partial t} = 0 \qquad (7.29)$$

where w_2 is mass of solute per volume of solvent, t is the time, u is the interstitial velocity of the fluid through the porous medium, x and z the coordinates, w_{2s} is the solute concentration deposited on unit area of the pore surface, and ε' is the specific surface area per unit volume. The term $\partial w_{2s} / \partial t$ in equation (7.13) represents the net local association and deposition rate of solute particles onto the surface of the porous medium at a position (x, z) and time t. A theoretical formulation of this term is given below.

Chemical Deposition Rate

In the process of SCF deposition, pore surfaces are covered with the retained solutes. Dissolved solutes precipitate when conditions change and become physically or chemically adsorbed. In addition the dissolved solute may react with a component of the matrix in a fluid-solid reaction. The average deposition rate (per unit surface area) of the particle onto the pore surface can be expressed in a general form as:

The first term on the right side of the equation represents the primary

$$\frac{\partial w_{2s}}{\partial t} = \kappa_1 \exp\left(\frac{-\kappa_2}{\log^2 S}\right) + \kappa_3 w_2 \qquad (7.30)$$

The first term on the right side of the equation represents the primary nucleation rate for supersaturation $S = w/w^*$, where w^* is the saturated concentration (Mullin, 1972). The nucleation rate is sensitive to supersaturation. When conditions in the vessel change, small pressure perturbations arise and the large surface area may enable many small particles to nucleate. The second term accounts for the chemisorption and reaction between the solute and the matrix. The reaction rate may depend on the concentration of dissolved solute and on the available functional groups of the matrix per unit surface area. The constants κ_1, κ_2 and κ_3 depend on the properties of solvent, solute and the matrix.

The mass balance for solute can be obtained by combining equations (7.29) and (7.30):

$$\varepsilon\frac{\partial w_2}{\partial t} + \frac{\partial (w_2 u)}{\partial x} + \frac{\partial (w_2 u)}{\partial z} = -\acute{\varepsilon}\left[\kappa_1 \exp\left(\frac{-\kappa_2}{\log^2 S}\right) + \kappa_3 w\right] \qquad (7.31)$$

The solute concentration and SCF density can be related as (from Chapter 4):

$$\ln w_2 = n \ln \rho + \frac{\gamma}{T} + Y \tag{7.32}$$

where γ and$Y$ are constants related to heats of solvation and molecular weight. The current knowledge of kinetics for heterogenous nucleation of solids from SCFs and reactions of biocides with wood is very limited. For practical convenience two limiting cases which result in equivalent depositions were considered for a typical operation:

Case 1) the association between the solute and matrix is strong enough to retain all the solute carried into the matrix

Case 2) the association between the dissolved solute and the porous matrix is negligibly weak. However, during pressure release, the rate of pressure drop at a point in the porous medium is larger than the rate of pressure drop with the flowing fluid, causing particles to precipitate and remain in the pore voids instead of being carried out with the flow. That is:

$$\left| \frac{\partial P}{\partial t} \right|_x \leq \left| u_f \nabla P \right|_t \tag{7.33}$$

An alternative expression in the literature is the dimensionless Strouhal number (Bear and Buchlin, 1991), defined as:

$$St = \frac{L/u}{t} \tag{7.34}$$

The Strouhal number expresses the ratio between the rate of pressure change seen by an observer moving at the superficial velocity and the rate of pressure change at a given point.

The assumption contained equation (7.16) can be written in terms of a Strouhal number as:

$$St \left| \left(\frac{\partial p}{\partial t} \right) \right| > |u \cdot (\nabla P)| \tag{7.35}$$

This assumption was found to be valid for the rate of pressure release we used here at all positions in the treated wood except near the surface. For example, consider a 4x4 cm Douglas-fir hearwood block kept for a long time in a vessel filled with saturated SC-CO_2 solution at a constant pressure of 250 bar and 50°C. When the vessel is depressurized at rate of 50 bar/min, the pressure drop rate at any point in the cross section 30 seconds after depressurization started becomes almost 50 bar/min. For comparisons, the pressure drop moving with the flow remains less 18 bar/min at all points except near the surface.

Retention Calculation

Based on the description of either Case 1, or Case 2 retentions of a chemical with known solubility can be computed based on equation (7.22) for typical operating conditions using:

$$R^* = \int_{x=x_i}^{x=x_j} \int_{z=z_i}^{z=z_j} \rho(x,t)\ w(x,t) \in L\ dx dz \qquad (7.36)$$

where R^* is the retention (in gm) in a volume of $(x_f-x_i)(z_f-z_i)L$ after time t.

Model Parameters

In order to evaluate the influence of the process conditions on deposition profiles in a semi-porous medium, TCMTB was chosen as the solute since its solubility was low enough to be one-tenth of the amount required to close a pore with a diameter of 0.5 μm. This means that the maximum amount of deposited material would not change porosity and permeability of the media. The rate of pressure increase rate was chosen to be 24.9 bar/min and all simulations were performed at constant temperature. The precipitation and association of the delivered material was estimated to be high enough to ensure retention. Model parameters for the simulation are given in Table 7.1.

7.5.5 Numerical Procedure

The nonlinearity of the dynamic balance equations (7.15) and (7.24) necessitates the use of a digital computer to generate an approximate solution. Approximate solutions of differential equations can be obtained by evaluating the derivatives in terms of finite differences and integrating numerically by means of the resulting difference equations. To formulate a difference equation for equations (7.15) and (7.26), a net of mesh-width $\Delta x'$, $\Delta z'$ and $\Delta \tau$ would be established. Subscripts i , j and k are used to denote distance and time positions, respectively, as $P_{i,j,k}$. Approximations to x-derivatives at i, j, k were found by the Taylor central expansions of P^2 about point i, j,k.

At each time increment, the nodal values of the fluid properties (P, μ, ρ, Z, w_v) were solved iteratively and convergence was checked on both variables. Initially, the fluid properties were set to be equal at all nodes at the values. The boundary condition values were based on experimental conditions. The results presented in the following sections are from a one dimensional model solved using an Intel 486 personal computer. Typical time increments were 2 seconds, while typical spatial increments were 0.1 cm.

Table 7.1 Model parameters for deposition of biocide in a Douglas-fir block

Symbol	*Parameter*	*Values Employed for a base case*
Constants		
T	temperature	50°C
$\partial p/\partial t$	pressure change rate	24.9 bar/min
Variables		
K	specific permeability	$5.10^{-13}cm^2$
$r_e = K^{1/2}$	effective pore radius	0.3 - 7 μm
$P(x,z)$	pressure	250 bar
P_{max}	maximum pressure	140 - 300 bar
L	length of solid	4 cm
z, x	position	0 - 4 cm
w	solute bulk concentration	2 gm/cm^3
ρ	density of solvent	700 $kg.m^{-3}$
ζ	flow coefficient	$7.5x10^{-4}$ - $7.5x10^{-2}$ cm^2/s
Ω	dynamic flow coefficient	$5x10^{-5}$ - 0.03 min^{-1}

7.6 Results and Discussion

The supercritical deposition of a solute in semi-porous media is a complex process in which both the solute and solvent undergo dramatic changes during the treatment process. Individual phenomena such as solute solubility, precipitation dynamics, and assumptions associated with these process are poorly understood. Currently there is no quantitatively predictive mathematical model. The development of such a model requires a better understanding of the individual processes. The present work is part of an on-going SCF deposition study that includes experimental and simulation research. The current modeling study was intended to identify the variables and relationships which most influence treatment in order to design future experiments to for a more complete understanding of the physical process of impregnation.

The following comparisons between experimental results and model predictions are not intended to accurately estimate model parameters but were developed to study qualitative predictions of the simplified model. The following is a discussion of predicted general trends and experimental observations for retention of TCMTB in Douglas-fir blocks after treatment using pure SC-CO_2.

Factors Influencing Retention

There are three kinds of factors that affect retention of a solute deposited in a semi-porous matrix from a supercritical fluid: operating variables, solute characteristics and matrix characteristics. Pressure and treatment time were the process variables investigated, while the matrix was characterized by the term $\Omega = \zeta/L^2$. Solubility of TCMTB in pure SC-CO_2 as a function of the pressure was included. The rate of pressure build up in a porous media and the corresponding density and solubility changes are shown in Figures 7.6 to 7.8. For a 3.8 x 3.8 cm Douglas-fir blocks the Ω value is about 1.4 $x10^{-4}$ sec^{-1}. Figure 7.6a and 7.6b show pressure profiles for different treatment periods in a cross section of blocks with flow coefficients of 5 x 10^{-5} s^{-1} and 10^{-4} s^{-1}, respectively. For Douglas-fir treated at 250 bar and 50°C, the pressure at an axial position of x/L= 0.3 increased from 50 to 210 bar when the treatment time increased from 15 to 45 minutes. This pressure increase corresponds to a 7.5 fold increase in density and a solubility increase of about 7 orders of magnitude. Therefore, longer treatment periods are necessary to load a significant level of material in less permeable solids. As the treatment pressure increases biocide solubility increases and the distribution from surface to center becomes more uniform (Figure 7.7 and 7.8).

The influence of pressure and treatment period is better shown in Figure 7.9. Total retention in a block with an Ω of $10^{-4}s^{-1}$ increases 6.3 times as pressure increases from 200 to 300 bar for a 20 minute treatment period.

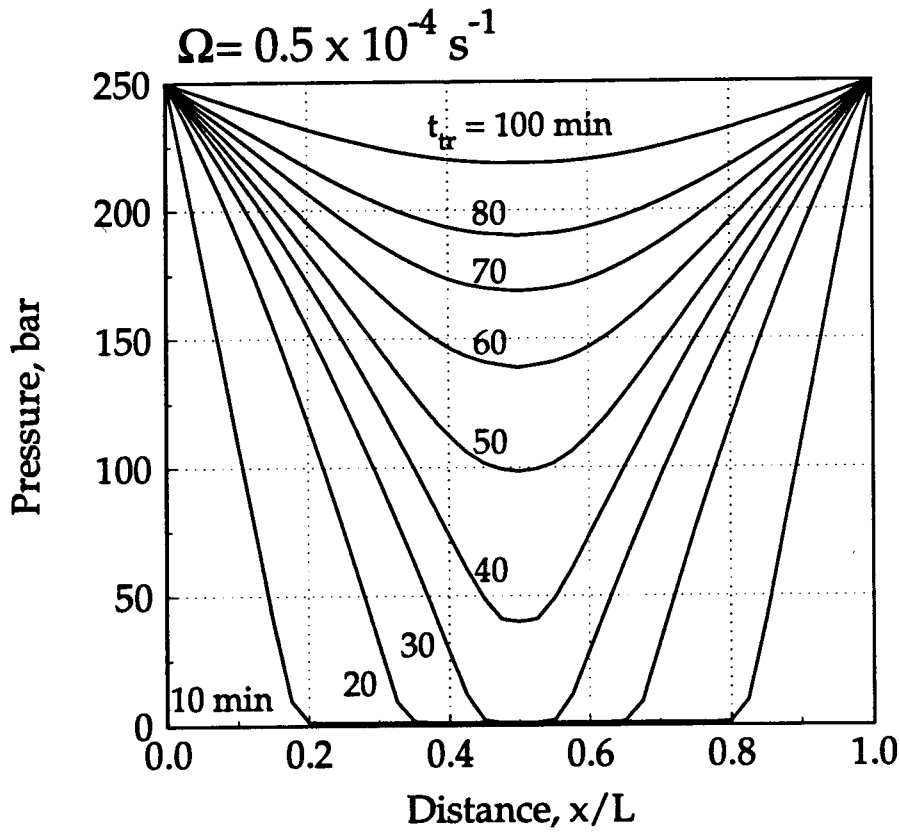

Figure 7.6a Time evolution of pressure profile in wood treated at 250 bar, 50°C and having $\Omega = 0.5 \times 10^{-4}$.

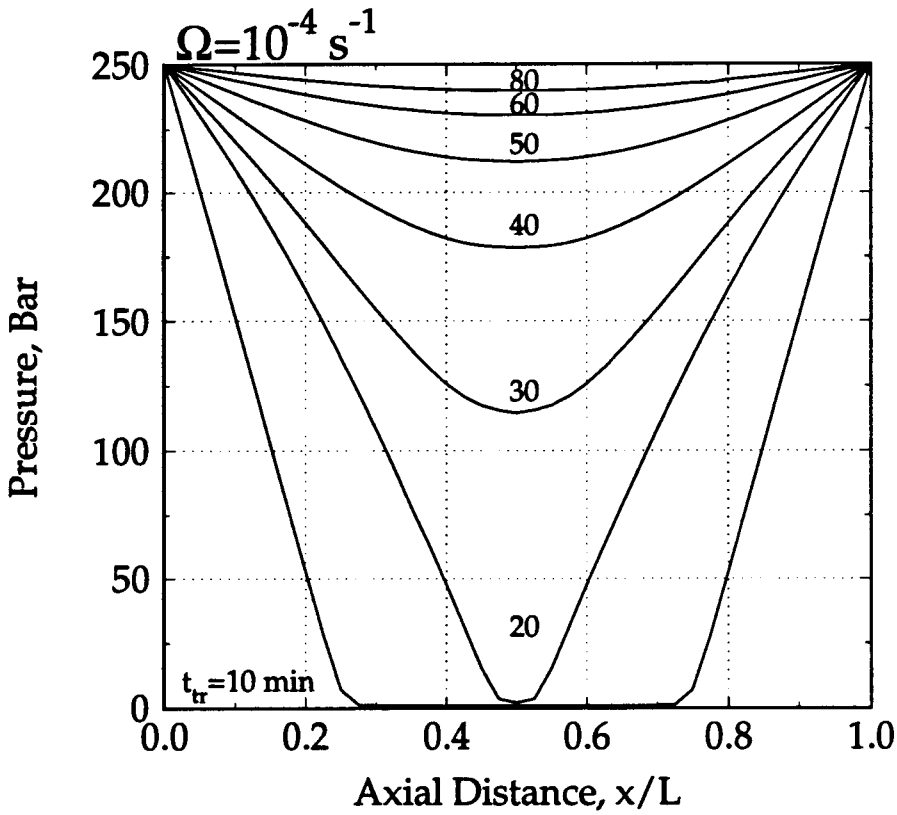

Figure 7.6b Time evolution of pressure profile in wood treated at 250 bar, 50°C and having $\Omega = 10^{-4}$.

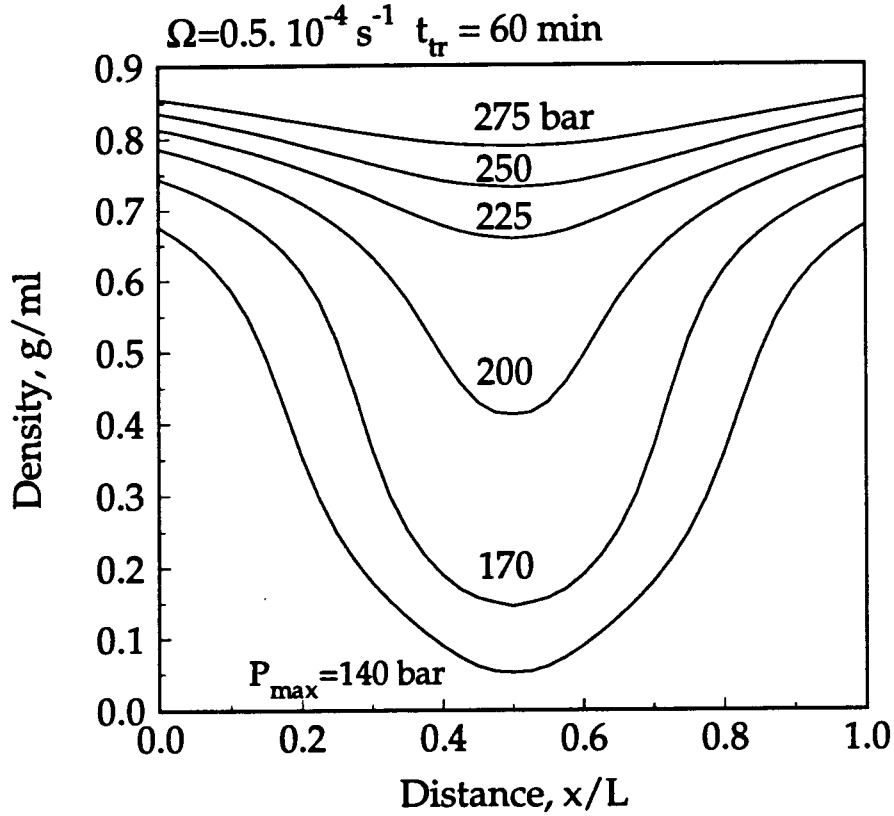

Figure 7.7 Density profiles in wood pores for different vessel pressure after 60 minutes of treatment period at 50°C.

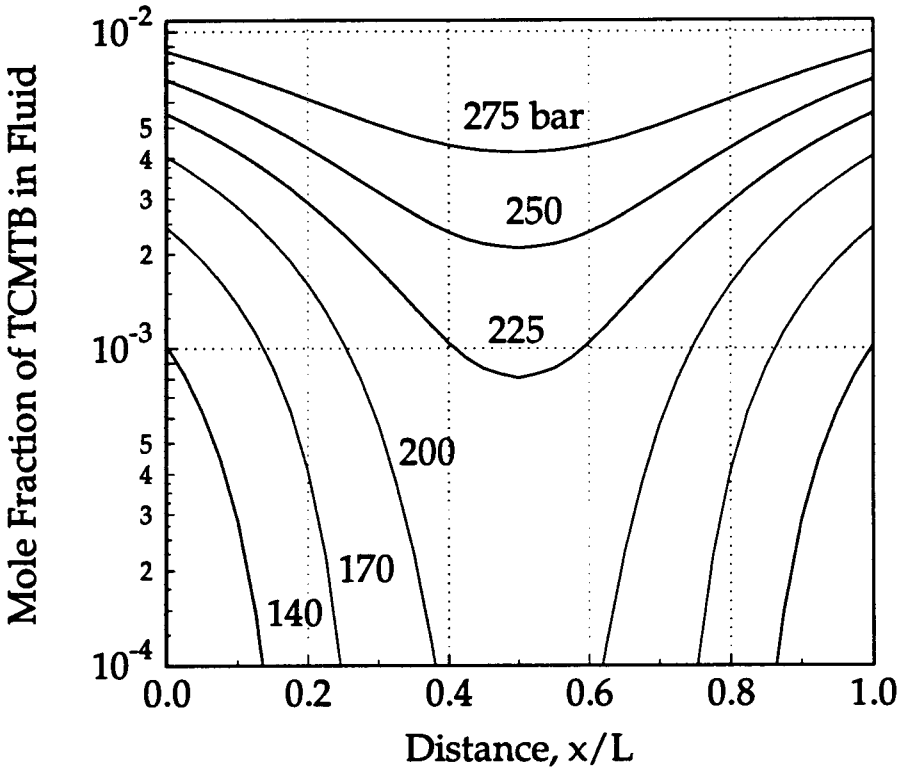

Figure 7.8 Relationship between pressure and TCMTB solubility at various depths in wood treated for 60 minutes at 50°C.

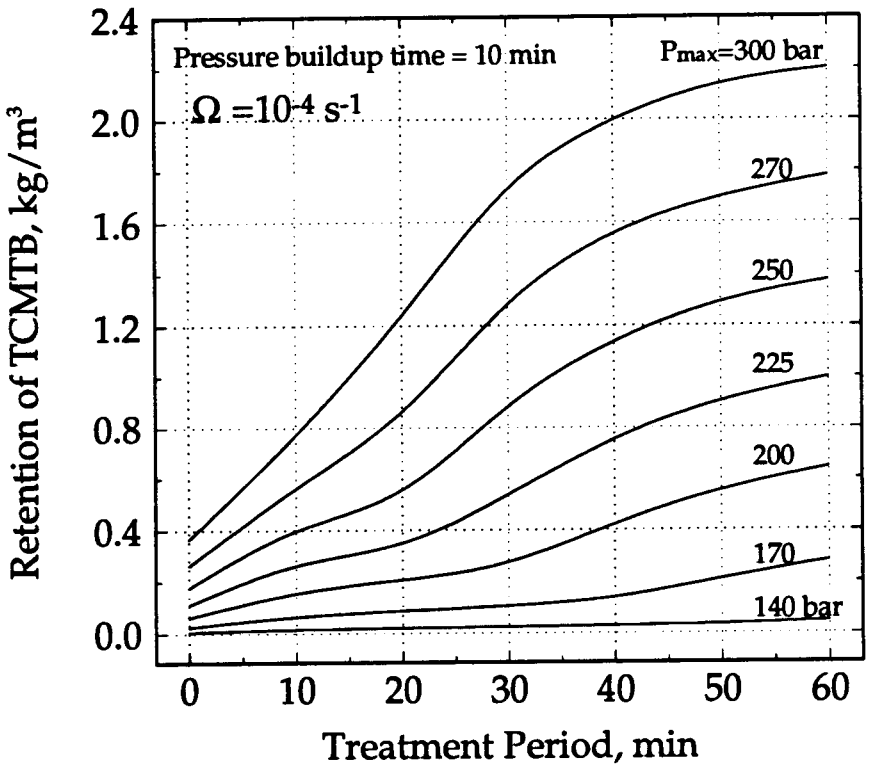

Figure 7.9 Effects of treatment period and maximum pressure on TCMTB retentions in wood blocks having an $\Omega = 10^{-4}$ s^{-1}.

However, the retention improvement ratio is only to 3.3 when the treatment period is 60 minutes (Figure 7.9). Figure 7.10 shows that total retention depends more strongly on pressure than treatment period. In addition, total retention is much more sensitive to the value of Ω than to pressure or time. Porous solids with an Ω value of 5.10^{-4} s^{-1} retain 4 times more biocide than those with Ω value of 5.10^{-5} min^{-1} following a 30 minute treatment period (Figure 7.11).

For a given maximum treatment pressure there is a corresponding maximum retention which would be similar to that delivered using a conventional full cell treatment process. Retention corresponds to the saturated solubility of the solute at the treatment temperature and pressure, assuming that all pores are at the same pressure and nothing diffuses into the wood cell wall. Retention increases linearly with solubility for a given treatment time and pressure (Figure 7.12), which follows from assumption six in the model formulation.

Biocide Deposition Profiles in a Douglas-fir Block

Retention profiles were constructed for TCMTB assuming complete retention of the delivered material (Figures 7.13, 7.14 and 7.15). Deposition profiles have a general exponential-decay shape, with a maximum at the surface of the solid and steep gradients for short treatment periods or low Ω values (Figures 7.13 and 7.14). Shorter treatment periods resulted in an egg-

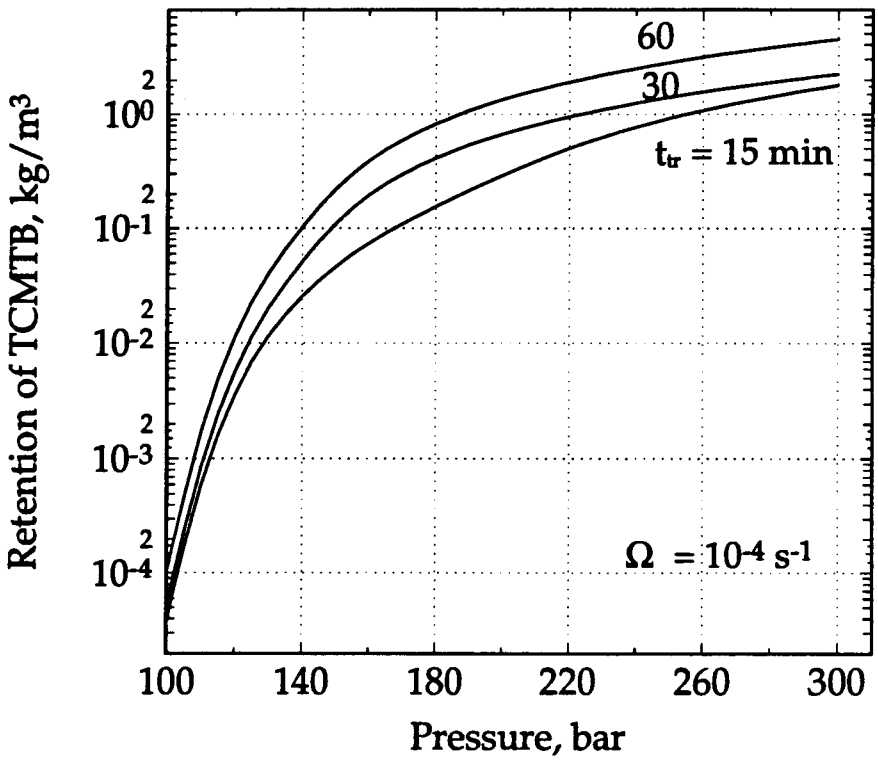

Figure 7.10 Relationship between treatment pressure and total retention of TCMTB in a wood block.

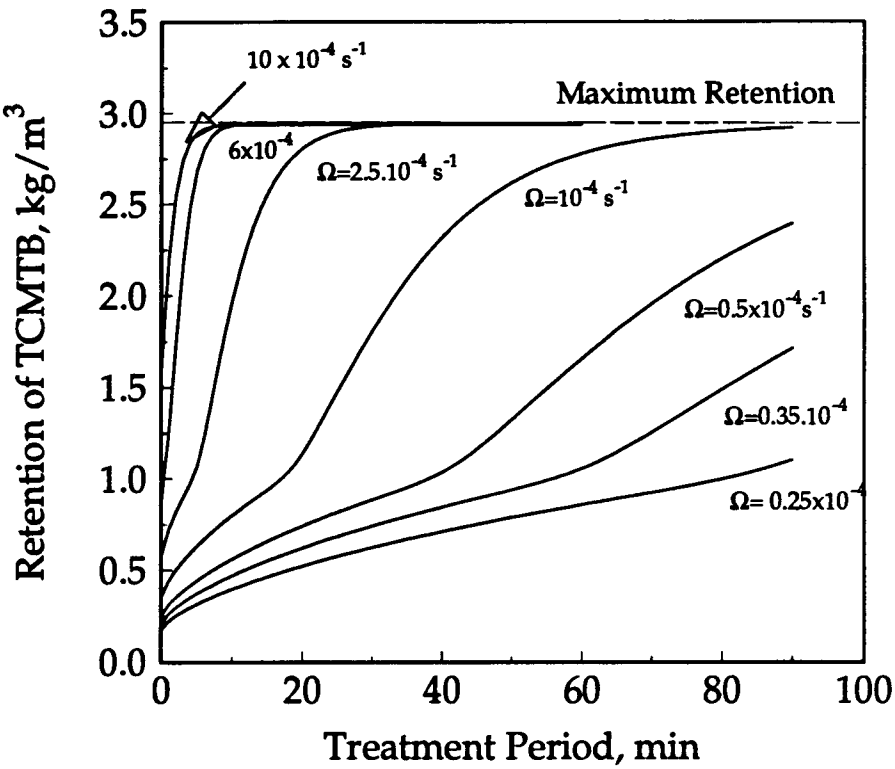

Figure 7.11 Effect of treatment period and Ω on retention of TCMTB in a wood block treated at 250 bar and 50°C.

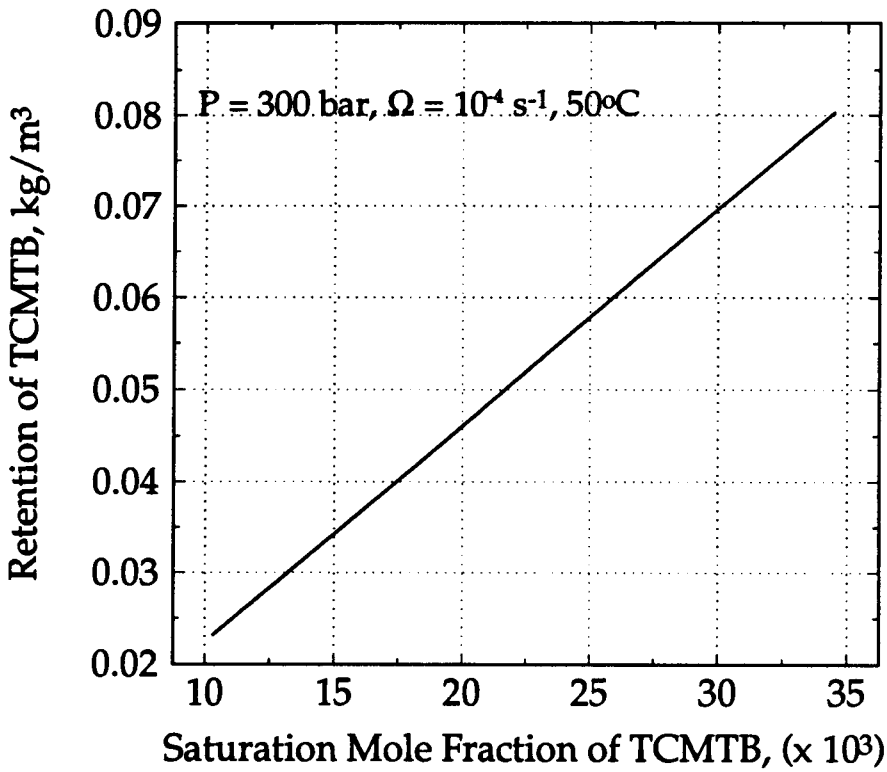

Figure 7.12 Effect of enhanced solubility in the SCF on retention of TCMTB at P_{max}=300 bar for 30 minutes.

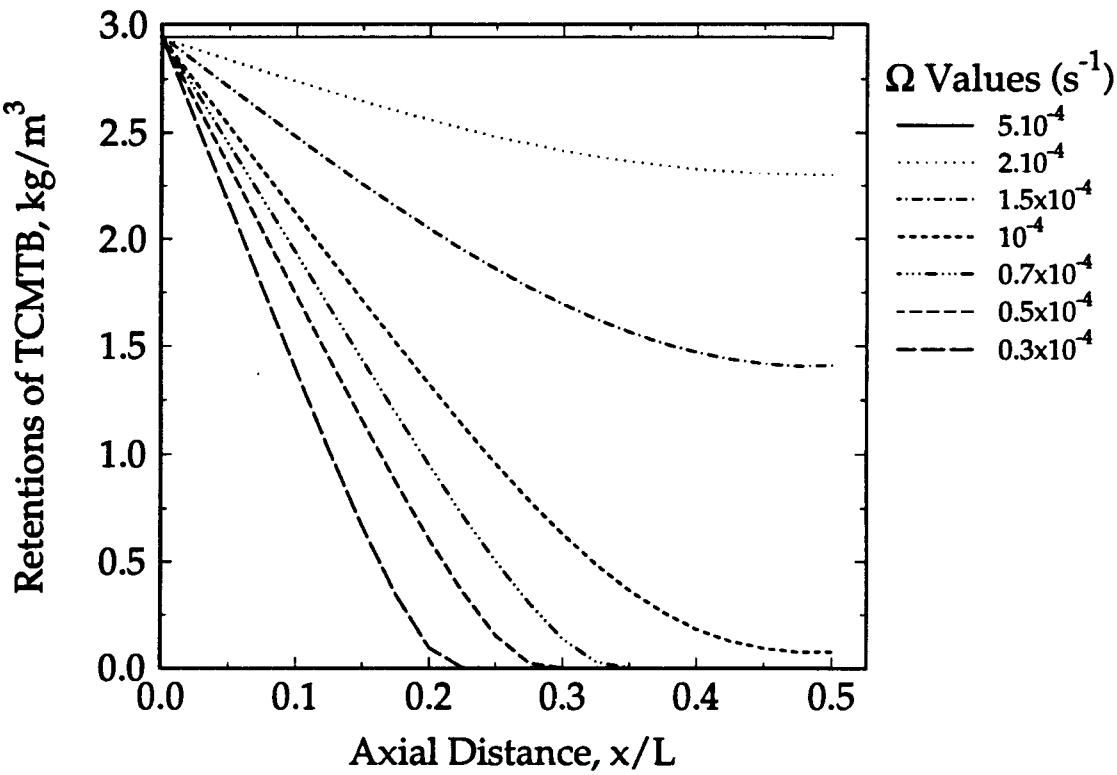

Figure 7.13 Simulated deposition profiles of TCMTB in a Douglas-fir heartwood block treated for 30 min. at 250 bar and 50°C using Ω values ranging form $0.3.10^{-4}$ to 5.10^{-4} s^{-1}.

shell type distribution while longer treatment periods resulted in more homogeneous retention. The bulk concentration was assumed to be a saturated concentration and maximum retention near the surface rose as the treatment pressure increases (Figure 7.15). Depositions of TCMTB at three axial locations (x' = 0, 0.25 and 0.5) in Douglas-fir heartwood block treated for 60 minutes at 150 to 300 bar are shown in Figure 7.16. Lower-pressure-treatments resulted in smaller total retentions with higher deposition gradients from surface to center of the block.

Comparison with Experimental Data

Results obtained from the one-dimension model solved in this study were compared with the experimental data collected for TCMTB treatment of Douglas-fir heartwood blocks presented in Chapter 6.

Theoretical calculations using the model were carried out for the same process variables as in the experimental studies (Table 7.1). The effects of pressure on biocide retention and distribution for a 30 minute treatment period are shown in Figure 7.17. Actual retentions in a 38 mm square block at four depths were compared with model predictions using Ω values of 10^{-4} and 5.10^{-5} s^{-1}. Actual retention values near the block surface were high because of surface depositions. Although calculated values were not based on optimal parameters, they agree fairly well with measured values. Measured and calculated retentions of TCMTB for Douglas-fir blocks treated at 250 bar for

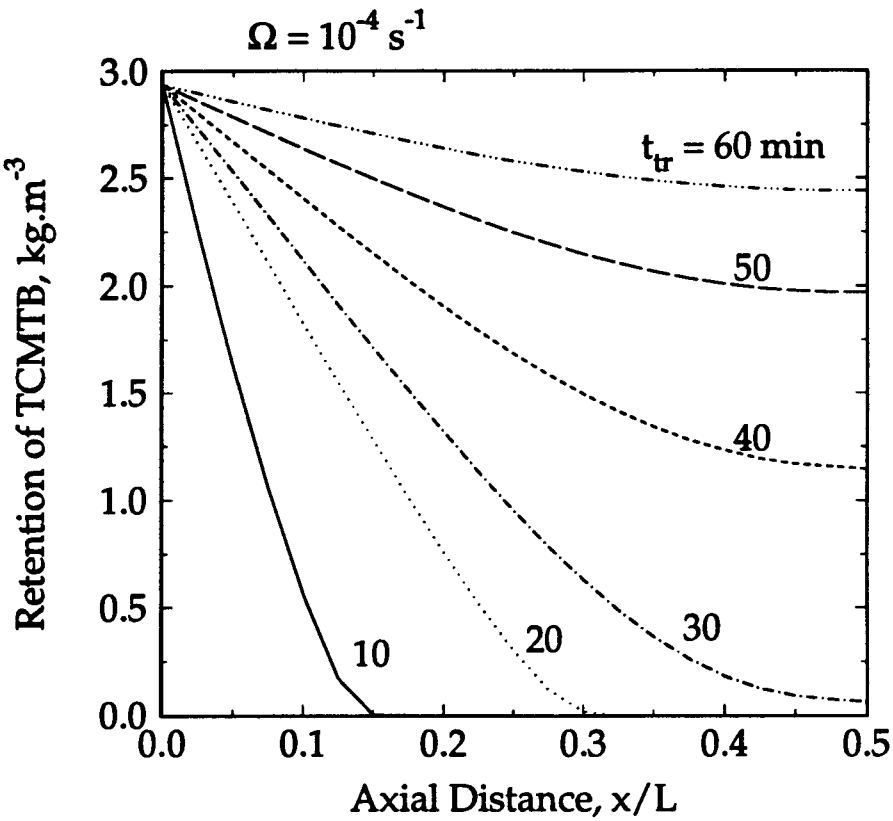

Figure 7.14 Simulated deposition profiles of TCMTB in a Douglas-fir block treated for 10 to 60 minutes at 250 bar.

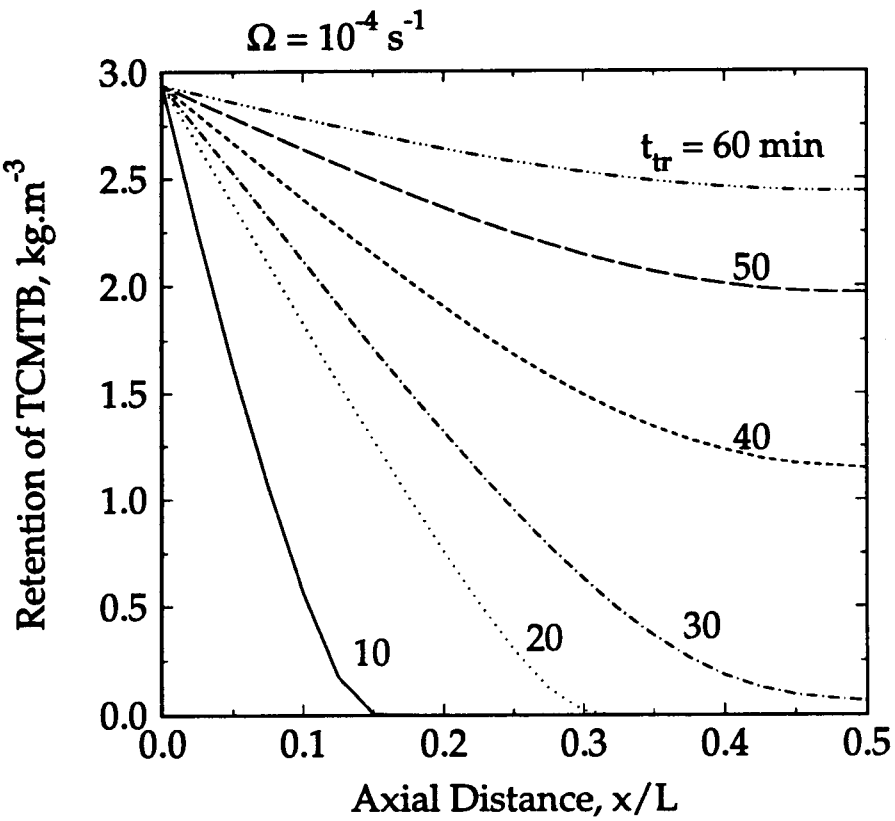

Figure 7.15 Simulated deposition profiles of TCMTB in Douglas-fir block treated for 30 minutes at 140 to 250 bar.

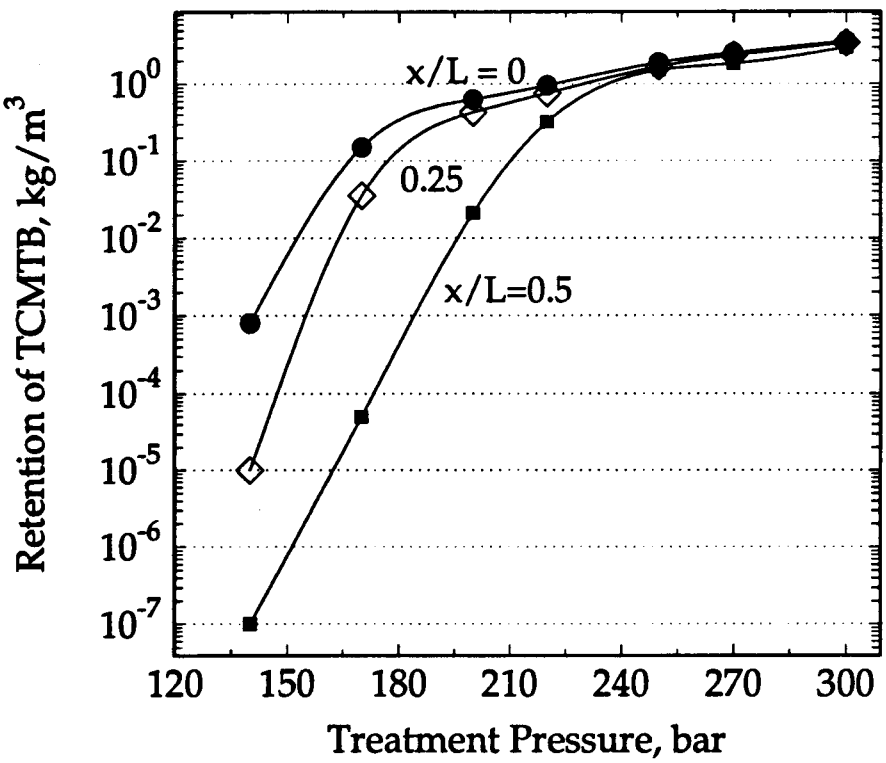

Figure 7.16 Simulated deposition of TCMTB at three loactions in a Douglas-fir heartwood block treated for 30 minutes at 170 to 300 bar.

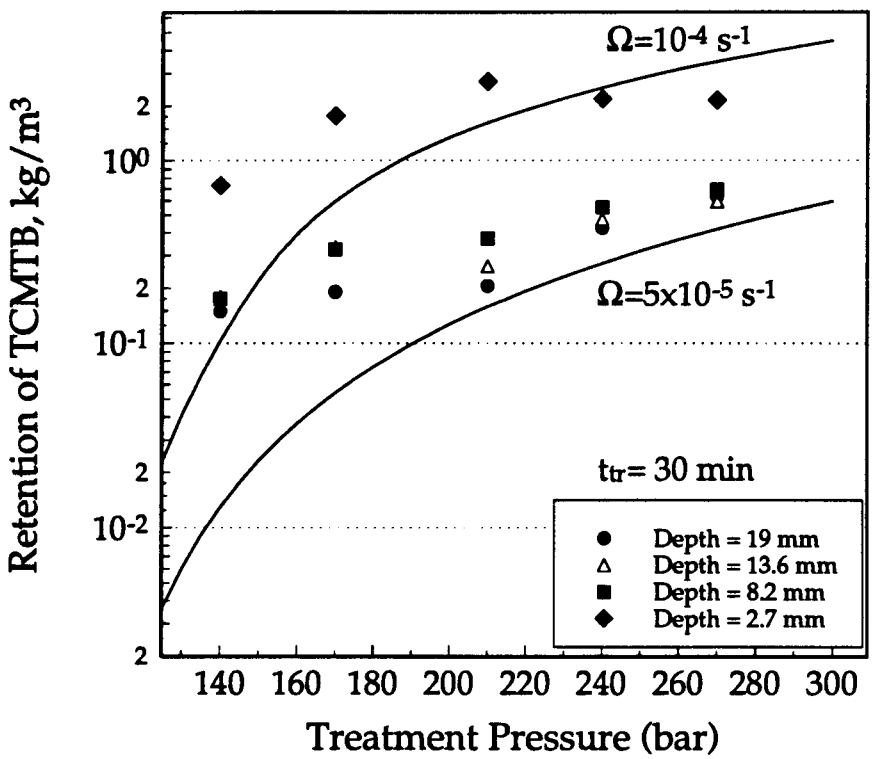

Figure 7.17 Comparison between simulated and measured retentions of TCMTB at selected depths in a Douglas-fir heartwood block treated for 30 minutes at 140 to 270 bar.

different treatment periods were generally in agreement (Figure 7.18). Similarly, calculated and experimental axial deposition profiles of TCMTB in Douglas-fir blocks (19, 25 and 25 mm) treated at 250 bar for 60 minutes were similar for values of Ω between 10^{-4} and $1.5x10^{-4}$ (Figure 7.19). These results suggest that impregnation of SC-CO_2 solubilized biocides into wood can be predicted with a reasonable degree of certainty. Given the wide array of potential variables which might otherwise need to be experimentally, this method should make it far easier to optimize treatments with a given biocide.

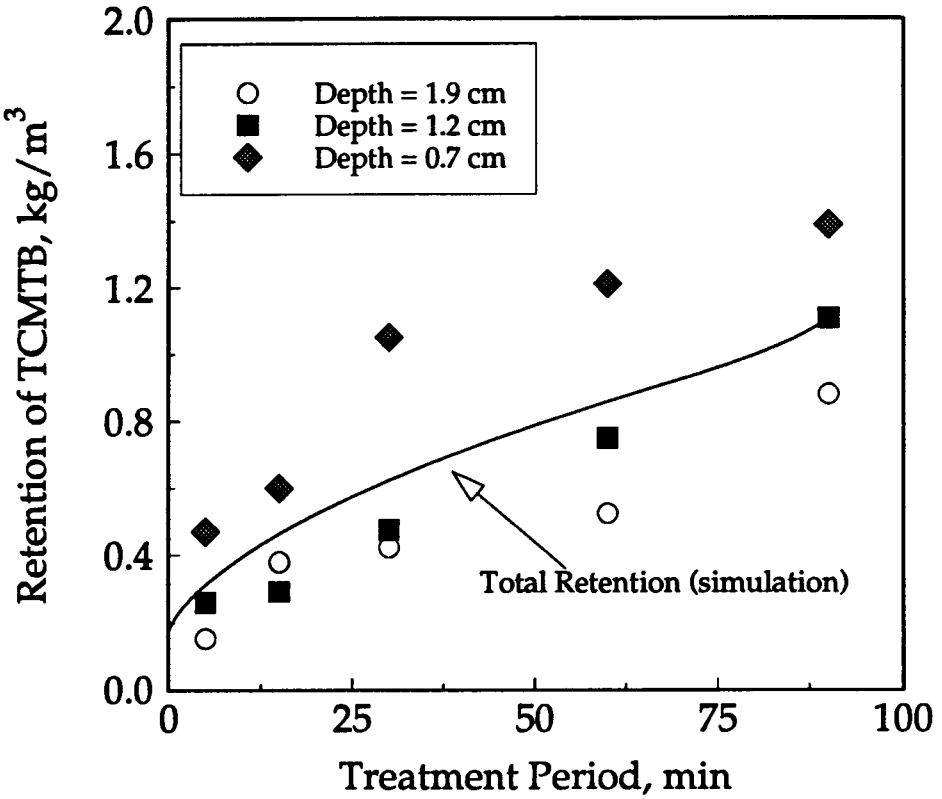

Figure 7.18 Comparison between simulated and measured TCMTB retentions at selected depths in a Douglas-fir heartwood block as a function of treatment period.

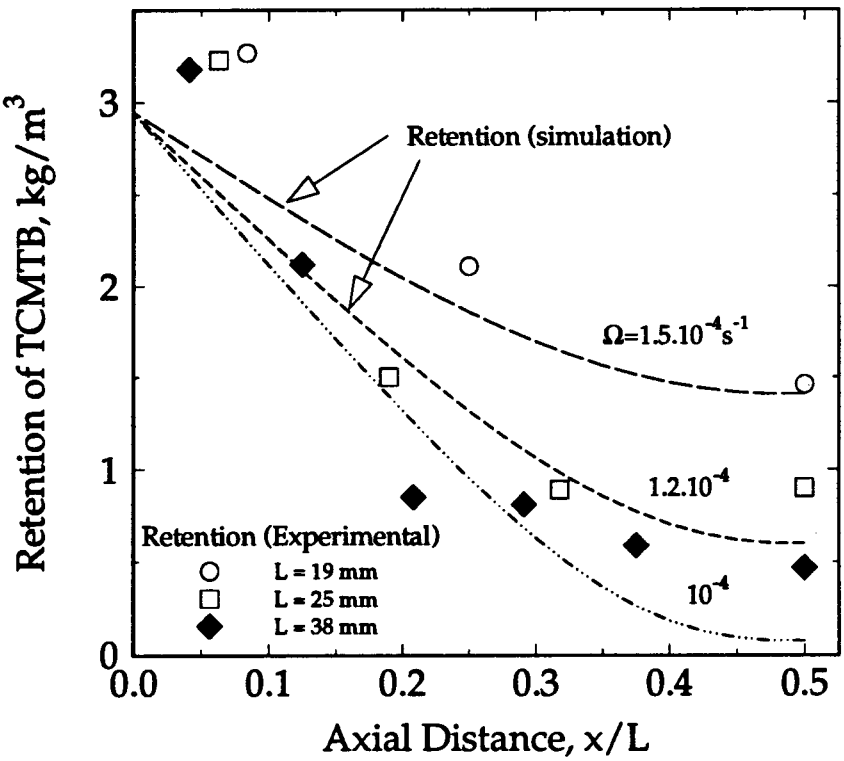

Figure 7.19 Effect of Ω on retentions of TCMTB in 19, 25, or 38 mm square Dougls-fir heartwood blocks treated for 30 minutes at 250 bar.

7.7 Summary and Conclusion

A theoretical model for simulating the dynamics of deposition of materials in porous matrix was developed which emphasized the importance of macroscopic flow dynamics of the process and microscopic interaction and nucleation of solutes. The key features of this model include: (1) the consideration of solvent and solute properties as a function of process parameters, time and position in the porous solid and (2) during venting rates of density change at a point are much higher than density changes with the flow out of the wood. This results in local solute deposition at the locations where solubility has been decreased, i.e. no supersaturation occurs and no precipited solute is entrained in the venting solvent.

Pressure and porous solid characteristic are the most significant variables in treatment. The treatment period is less important although an egg-shell type distribution profile results from short treatment periods in less permeable solids. Longer treatment periods result in more uniform biocide distributions. Deposition profiles may be altered if the solute has strong interactions with the porous matrix or if the porous solid is more permeable. The derived model adequately described experimental data of material deposition from supercritical solutions under physical and chemical conditions described earlier.

While the model reasonably described the test conditions, more experimental data must be gathered to more fully understand solute

interactions with the porous media and crystallization kinetics. These variables can have marked effects on retention and distribution of biocides in a porous matrix.

In conclusion, the lack of complete understanding of heterogenous crystallization from supercritical solutions and the interactions of solutes with the porous matrix limits the ability to produce distribution profiles for various solutes under a wide array of treatment conditions. This study demonstrated the possibility of obtaining these profiles under the assumption that rates of precipitation and association are rapid. A better characterized solute-solvent system, a more uniform porous matrix, and a process with better defined kinetics would allow more controlled deposition and more complete optimization of the impregnation process.

CHAPTER 8

CONCLUSIONS AND RECOMMENDATIONS

8.1 Conclusions

This work presented in this thesis shows that the use of supercritical fluids to deliver substances into porous solids is a promising technique with numerous applications. Advantages of the technology include: flexibility, the ability to penetrate deeply into pores within a short period, the complete elimination of liquid solvents and the use of recyclable solvents such as CO_2. Studies to develop supercritical deposition processes must address both phase equilibria and rate phenomena.

Solubility data were developed for 10 commercially available organic and organo-metallic biocides in pure and modified SC-CO_2. Biocides with lower boiling points and higher vapor pressures were more soluble in pure SC-CO_2. The measured solubilities were correlated with either reduced solvent density or the solute enhancement factor. Tebuconazole, propiconazole, TCMTB, IPBC and isothiazolone showed solubilities higher than 3 wt %. Adding a small amount of modifier, such as acetone, methanol or ethanol, enhanced solubility of most biocides. The size of this increase depended strongly on the structure of the biocide as well as the nature of the cosolvent.

Adding 3.5 mol % of methanol to SC-CO_2 increased solubility of tebuconazole by about 1100% and pentachlorophenol by 500 % over pure CO_2 at 200 bar, however, this effect for pentachlorophenol must be viewed with caution, since its solubility was low in pure CO_2. The cosolvent effect on solubility increased with cosolvent amount and decreased with increases in pressure or temperature. At higher pressures, the cosolvent effects were independent of fluid density. Possible mechanisms for this enhancement include association effects, such as hydrogen bonding or dipolar coupling between biocide and cosolvent, or the polarizability of the supercritical solvent mixture. For many of the biocides evaluated, the use of a cosolvent increased the solubility above the estimated minimum levels required for successful wood impregnation.

Various qualitative and quantitative methods were developed to measure the distribution of biocides retained in wood. Supercritical fluid treatments resulted in complete TCMTB penetration of Douglas-fir blocks. Deposition of chemicals from supercritical fluids can be influenced by the solvent properties (e.g. density and temperature), solute chemistry, the porous solid characteristics and the treatment time. Distribution was strongly affected by the solvent pressure, wood permeability and sample dimensions. Total retention increased with increased solvent density, solute concentration and wood permeability; whereas it decreased with increases in sample dimensions. For a given treatment pressure, there was an asymptotic total retention level

that could be achieved depending on the porous solid permeability and dimensions.

A mechanistic model for the dynamics of the supercritical deposition of a material into a porous solid was developed which combined macroscopic balances and ideal microscopic behavior. The model assumed equilibrium in the fluid phase - no supersaturation was allowed. The simulations indicated that the resultant deposition profiles had exponential-decay shapes with maximum deposition at the surface and minimum at the center of the porous matrix piece. The maximum (surface) retention increased with pressure and solubility. The absence of knowledge of the precipitation kinetics of the solute and its chemical association with the porous matrix limits a better understanding of the supercritical deposition process.

8.2 Recommendations

Although this work was preliminary and exploratory in nature, some basic questions related to the phenomena of impregnation were answered. Nevertheless, a wide range of additional studies will be required to better define the complete process including:

1. Identification of partition coefficients or equilibrium relationships for a given set of biocide-supercritical fluid combinations in porous solids.

2. Determination of precipitation kinetics and porous solid characteristics on deposition. Studies of this nature must be performed with a controlled, well-characterized system of solute-solvent and porous media to minimize variability.

3. Development of an improved general model and design of an experimental progress for use in parameter estimation in order to evaluate the true effects of the various treatment factors.

4. Further exploratory studies to identify other factors that were not examined in this study. For example solutes that precipitate as liquids appear to distribute more evenly than those that precipitate as solids. This could have important implications in performance of SCF-treated wood against biological agents. Other factors that may be considered are effects of moisture content of the wood, rates of pressure rise or venting, the use of time-varying temperature and / or pressure.

REFERENCES

Abbot, M. M., "Cubic Equation of State," *AIChE Journal*, **19** (3): 596-601, 1973.

Adachi, Y. and B. Lu "Supercritical Fluid Extraction with Carbon Dioxide and Ethylene," *Fluid Phase Equilibria*, **14**, 147-156, 1983

Adzumi, H., "Studies on the Flow of Gaseous Mixtures Through Capillaries. III. The Flow of Gaseous Mixtures at Medium Pressure," *Bull. Chem. Soc. Japan*, **12**(6) : 292-303, 1937.

Adzumi, H. "On the Flow of Gases Through a Porous Wall," *Bull. Chem.Soc. Japan*, **12**(6): 304-312, 1937.

Allada, S. R., Solubility Parameters of Supercritical Fluids, *Ind. Eng. Chem. Process Des. Dev* , **23**( ):344-348, 1984.

Angus, S. and B. Armstrong and K. M. deReuck, *Carbon Dioxide, International Thermodynamics Table of Fluid State*, IUPAC, 1976

Aranafsky, J.S., and R. Jerkins, "Unsteady Flow of Gas Through Porous Media, One-Dimensional Case," *Proc. 1st Nat. Congr. Appl. Mech.*, 763, 1952

Aranow, R. H., "Statistical Approach to Flow Through Porous Media," *Phys. Fluids*, **9** 1721, 1966.

Bailey, I. W. "The Preservative Treatment of Wood. II. The structure of pit membranes in the tracheids of conifers and their relation to the penetration of gases, liquids, and finely divided solids into green seasoned wood," *Forest Quart.*, **11**(1):12-20, 1913.

Bailey, P. J., and R. D. Preston, "Some Aspects of Softwood Permeability I, Structural Studies with Douglas-fir Sapwood and Heartwood," *Holzforschung*, **23**(4):113- 120, 1969.

Baines, E. F., and J. M. Saur, "Preservative Treatment of Spruce and Other Refractory Wood," *Proc. Amer. Wood Preserv. Assoc.*, **81**, pp 136-147, 1985.

Baines, E. F., and J. M. Saur, "Preservative Treatment of Spruce and Other Refractory Wood," *Proceedings American Wood Preserver's Association*, 1985.

Bartman, D., and G. M. Schneider, "Experimental Results and Physico-Chemical Aspects of Supercritical Fluid Chromatography With Carbon Dioxide as Mobile Phase, *J. Chromatog.*, **83**, 135-45, 1973.

Belenovic, Z., M. M. Mayers and J. C. Giddings, " Binary Diffusion in Dense Gases to 1360 atm by Chromatographic Peak-Broadening Method, *J. Chem. Phys.*, **52**, 912-22, 1970.

Berand, M. J., *Statistical Continuum Theory*, Interscience, N.Y., New York, 1968.

Berneburg, P. L., V. Forest, and V. J. Krukonis, "Method for Densification of Ceramic Materials", US Patent 4552786, 1985

Blew, J. O., H. G. Roth, and H. L. Davidson, "Preservative Retention and Distribution in Several Western Conifers," *Proc. Amer. Wood Preserv. Assoc.*, **63**, pp 30-43, 1967.

Boding, J., and B. A. Jayne, *Mechanics of Wood and Wood Composites*, Van Norstrand Reinhold Comp., N. Y., 1982.

Booth, H. S. and Bidwell, R. M., "Solubility Measurement in the Critical Region, *Chem. Rev.*, **44**, 477-513,1949.

Brand, J. I., and D. R. Miller, "Thin Films form the Free-Jet Expansion of Supercritical Water-Alumina Solutions," *AIChE Annual Meeting*, Los Angels, 1991.

Bramhall, G., "The Validity of Darcy's Law in the Axial Penetration of Wood," *Wood Science and Technology*, **5**, pp 21-134, 1971.

Brennercke, J. F., and C. A. Eckert," Phase Equilibria for Supercritical Process Design," *AIChE J.*, **35**(9): 1409 - 1427, 1989.

Brennercke, J. F., D. L. Tomasko, J. Peshin, and C. A. Eckert,"Fluorescence Spectroscopy Studies of Dilute Supercritical Solutions," *Ind. Eng. Chem. Res.*, **29**, 1682, 1990

Brooks, C.S., and W. R. Purcell, Trans. *AIME*, 195: 289, 1952.

Bruno, T.J. and J.F. Ely, *Supercritical Fluid Technology: Reviews in Modern Theory and Applications*, CRC Press, Ann Arbor, 1991

Brunner, G., and S. Peter, "Gas Extraction in the Presence of an Entrainer," 2nd World Congress of Chemical Engineering, Montreal Canada, Oct. 5, 1982

Brunner, G., "Selectivity of Supercritical Compounds and Entrainers with Respect to Model Substances," *Fluid Phase Equilibria*, **10**, 289-98, 1983

Calimli, A. and Olcay, A.;"Supercritical Dioxane Extraction of Spruce Wood and Dioxane-Lignin and Comparison of the Extracts with the Pyrolysis Products," *Separation Sci. and Technol.*, **17**(1): 183-197, 1983.

Carman, P. C., *Flow of Gases Through Porous Media*, Academic Press Inc. Publishers, London, 1956.

Casey, J.P. Pulp and paper, vol. 1, pp. 280:285, 2nd ed. Interscience Publishers, New York, 1960

Chang, C. J. and A. D. Randolph, "Precipitation of Microsize Organic Particles from Supercritical Fluids," *AIChE J.*, **35**, 11, 1876-1882, 1989

Chang, H. and D. G. Morell, "Solubilities of Methoxy-1-tetralone and Methyl Nitrobenxoate Iomers and Their Mixtures in Supercritical Carbon Dioxide," *J. Chem. Eng. Data.*, **30**, 74-78, 1985

Chrastll, J., "Solubility of Solids and Liquids in Supercritical Gases," *J. Phys. Chem.*, **86**, 3016 - 3021, 1982.

Cochran, H.D., L. L. Lee and D. M. Pfund, "Application of Kirkwood-buff Theory of Solutions to Dilute Supercritical Mixtures," *Fluid Phase Equilib.*,**34**, 219, 1987

Cochran, H. D., and L. L. Lee, "Solvation Structure in Supercritical Fluid Mixtures Based on Molecular Distribution Functions," *ACS Symp. Ser.*, **406**, 27, 1989

Collins, R. E., *Flow of Fluids Through Porous Materials*, Rein Hold Publishing Corporation, New York, 1991.

Comstock, G. L., "Longitudinal permeability of Wood to gases and nonswelling liquids," *Forest Product Journal*, **17**(10):41-46, 1967

Comstock, G. L., "Directional Permeability of Softwoods," *Wood and Fiber*, 1:283-289, 1970

Côté, W. A. Jr. and R. L. Krahmer, "The Permeability of coniferous pits demonstrated by electron Microscopy," TAPPI **45**(2): 119-122, 1958.

Dahlgren, S. E. and W. H. Harford, *Hlzforschung*, **26**(2), 62-69, 1972

Dalton, F. L., and J. D. McCann,"Radiation Engineering in the Polymerization of Monomers in Fibrous Materials: Accelerators, In *Impregnated Fibrous Material*, International Atomic Energy Agency, Vienna, 1968.

Dandge, D. K., J. P. Heller and K. V. Wilson, "Structure solubility Correlation: Organic compounds and Dense Carbon Dioxide Binary Systems," *Ind. Eng. Chem. Prod. Res. Dev.*, **24**: 162-166, 1985.

Darcy, H., *Les Fontaines Publiques de la Ville de Dijou*, Dalmont, Paris, 1856.

D'Avila, S.G., B.K. Kaul and J.M. Prausnitz, "Solubilities of Heavy Hydrocarbons in Compressed Methane and Nitrogen," *J. Chem. and Eng. Data*, **21**(4), 1976.

David, A. W., "Wood Preservative Treatments For Crossties and Potential Future Treatments," *Crossties*, Jan. 1991.

Davies, D. L. "Durability of Poles Treated with Penta in an LP Gas System," *Proc. Amer. Wood Preserv. Assoc.* **67**: 37-45, 1971.

Davolio, F., G. C. Penrosa and M. Katz,"Vapor-Liquid Equilibrium for the p-Dioxane-Acetonitrile System at 298.15K.," *J. Chem.Eng. Data*, **26**: 26-27, 1982.

Debenedetti, P. G. and S. K. Kumar, "Infinite Dilution Fugacity Coefficients and the General Behavior of Dilute Binary Systems," *AIChE Journal*, **32**(8), 1986.

Debenedetti, P. G., "Clustering in Dilute, Binary Supercritical Mixtures: A Fluctuation Analysis," *Chem. Eng. Sci.*, **42**(9), 2203, 1987.

Debenedetti, P. G., I. B. Petsche, and R. S. Mohamed,"Clustering in Supercritical Mixtures: Theory, Applications and Simulations. *Fluid Phase Equilib.* **52**, 347, 1989

Debenedetti, P. G., "Homogeneous Nucleation in Supercritical Fluids," *AIChE Journal*, **36**(9), 1990.

de Fillipi,R.P., V. j. Krukonis, R. J. Robey, and M. Modell, Supercritical fluid regeneration of activated carbon for adsorption of pesticides. Report EPA-600/2-80-054, March, 1980.

Diepen, E.A. and Scheffer, F.E.C. *J. Phys. Chem.*, **57**, 575, 1953

Dietz, A. G., E. L. Schaffer, and D. S. Gromala, *Wood As a Structural Material*, Forest Products Laboratories, USDA, University of Wisconsin-Extension, 1980

Dobbs, J. M., J. M. Wong, R. J. Lahiere and K. P. Jonston, "Modification of Supercritical Fluid Phase Behavior Using Polar Cosolvents," *Ind. Eng. Chem. Res.*, **26**, 56-65, 1987.

Dobbs, J. M., J. M. Wong and K. P. Johnston, "Nonpolar Co-solvents for Solubility Enhancement in Supercritical Fluid Carbon Dioxide, *J. Chem. Eng. Data*, **31**: 303-308, 1986.

Dooley, K. M., K. Chien-Ping, R. P. Gambrell, The Use of Entrainers in the Supercritical Extraction of Soils Contaminated with Hazardous Organics, *Ind. and Eng. Chem. Res.*, **26**: 2058-2062, Oct. 1987.

Dorek, M., and L.H.Allen, "Kraft mill pitch problems: Chemical changes in wood resin during pulping," *TAPPI* 61(7):47-51, 1978

Dullien, F.A.L., "Single Phase Flow Through Porous Media and Pore Structure," *Chem. Eng. J.*, **10**:1-34, 1975.

Dullien, F. A. L. *Porous Media Fluid Transport and Pore Structure,* Academic Press, New York, 1979.

Eckert, C. A.; D. H. Ziger, K. P. Johnston,and S. Kim, "Solute Partial Molar Volumes in Supercritical Fluids. *J. Phys. Chem.*, **90**, 2738, 1986

Ely, J. F., "Application of the Extended Corresponding States Modeling to Hydrocarbon Mixtures," Proc, 63 rd Gas Processors Association Annual Convention, New Orleans, **9**, 1984.

Ely, J.F., An Equation of State Model for Pure CO_2 and CO_2 Rich Mixtures, Proceedings of 65th Gas Processors Association, Denver, 1986

Feder, J, K.C. Russell, J. Lothe and G. H. Pound, "Homogeneous Nucleation and Growth of Droplets in Vapors," *Adv. Phys.*, **15** (11), 1966.

Fedors, R. F., A Method for Estimating Both the Solubility Parameters and Molar Volumes of Liquids, *Polymer Eng. and Science*, **14**(2):147-154, 1974.

Feigl, F, A. Vinzenz, R. E. Oesper, *Spot Test in Inorganic Analysis*, 7th Ed. Elsevier Publishing Co. Amsterdam 772p, 1966.

Ferlazzo, D.E. and M. J. Kennedy, "A Reliable Spot Test for TCMTB in Wood," *The International Research Group on Wood Preservation*, IWG/WP/2391-92,1992

Finholt, R. W., Maurice W., and Clayton H.: New theory on Wood Preservation, *Ind. Eng. Chem.*, **44**: 101-105, 1955

Flores Luna, J. L., and F. Barnes de Castro, "Evaluation of Various Modifications of the Redlich-Kwong Equation, International Chemical Engineering," **18**(4): 611 - 626, Oct. 1978.

Francis, A. W. "Ternary System of Liquid Carbon Dioxide,"**58**, 1099-114, Dec. 1954.

Fredenslund, A., R. L. Jones and J. M. Prausnitz, "Group-Contribution Estimation of Activity Coefficients in Nonideal Liquid Mixtures," *AIChE Journal*, **21**(6): 1086, Nov. 1975.

Froment, H. A. U. S. Patent 43088200, Dec 28, 1981

Giddings, J. C., M. N. Myers, and J. W. King, "Dense Gas Chromatography at Pressure to 2000 Atmospheres," *J. Chromatographic Science*, **7**, 276, 1969

Gjovik, L. R., "Treatability if Southern pine, Douglas-fir, and Englemann Spruce Heartwood with Ammoniacal Copper Arsenate and Chromated Copper Arsenate Water Borne Preservatives," *Proceedings American Wood Preservers Association*, **79**, pp. 18-30,1983.

Gründlinger, R. and Otto Exner, "Tebuconazole - a new triazole for wood preservation,"*The International Research Group on Wood Preservation*, May 1990

Gurdial, G. S. and N. R. Foster, "Solubility of O-Hydroxybenzoic Acid in SC-CO_2," *Ind.and Eng. Chem. Res.* **30**: 575-580, 1991.

Gurdial, G. S., P. A. Wells, N. R. Foster, R. P. Chaplin, "The Role of Polarity on Correlations os Solid-Supercritical Fluid Phase Systems," *J. Supercritical Fluids*, **2**, 85, 1989.

Hannay, J. B. and J. Hogarth, "On the Solubility of Solids in Gases," *Proc. Roy. Soc.* (London), Ser. A., **29**, 324-326, 1879.

Hannay, J. B.; On the Solubility of Solids in Gases, II, *Proc. Roy. Soc.* (London), **30**, 484, 1880.

Hansen, S.M and April, G. C., *Ind. Eng. Chem. Prod. Res. Dev.*, **21**, 621, 1982

Harper, C. A. *Electronic Packaging with Resins*, McGraw-Hill Book Co., Inc., New York, 1961.

Hills, W. E. *Wood extractives and their significance to the pulp and paper*, in Academic Press, New York, 1980

Hoyer, G. G.; "Extraction with Supercritical Fluids: Why, How, and So What," *Chemtech*, July : 440-448, 1985.

Hubert, P. and O. G. Vitzthum, "Fluid Extraction of Hops, Spices, Tobacco with Supercritical Gases," *Angew. Chem. Int. Ed. Engl.*, **17**: 710-715, 1978.

Hunt, G. M., and G. A. Garratt, *Wood Preservation*, New York, N.Y., McGraw-Hill, 1967.

Ito, N.T., T. Someya, M. Taniguchi, and H. Imamura, Japanese Patent 59-1013111, 1984

James, R.E., "A Prelimenary Experiment with High Pressure Preservative Treatements," *Amer. Wood-Preserv. Assoc. Proc.* **57**:108-144, 1961

Johnston, K. P. and C. A. Eckert, "An Analytical Carnahan-Starling-van der Waals Model for Solubility of Hydrocarbon Solids in Supercritical Fluids," *AIChE Journal*, **27**(5): 773, 1981.

Johnston, K. P., D. H. Ziger and C. A. Eckert, "Solubility of Hydrocarbon Solids in Supercritical Fluids. The Augmented van der Waals Treatment," *Ind. and Eng. Chem. Fundam.*, **21**: 191 - 197, 1982.

Johnston, K. P., In *Encyclopedia of Chemical Technology*, suppl. Vol. 2., 3rd ed., Wiley, New York, 1984.

Johnston, K. P., "New Directions in Supercritical Fluid Science and Technology," *ACS Symposium Series*, 406, 1989

Johnston, K. P., S. E. Barry, N. K. Read, and T. R. Holcomb, "Separation of Isomers Using Retrograde Crystallization from Supercritical Fluids," *Ind. Eng. Chem. Res.*, **26**: 2372-2377, 1987.

Jossi, J. A., L. I. Stiel and G. Thodos, AIChE, J. **8**, 59, 1962.

Kajimoto, O. M. Futakami, T. Kobayashi, and K. Yamasaki, "Charge Transfer-State Formation in Supercritical fluids: (N,N-Dimethylamino)benzonitrile in CF_3H," *J.Phys. Chem.*, **92**, 1347, 1988

Kamlet, M.J., J. M. Abboud, M.H. Abraham and R.W. Taft, "Linear Solvation Energy Relationships. π^*, α, and β and Some Methods for Simplifying the Generalized Solvatochromic Equation," *J. Org. Chem.*, **48**, 2877, 1983

Kantrowiz, A., "Nucleation in Very Rapid Vapor Expansions," *J. of Chemical Physics*, **9** (9), 1951.

Kayihan, F.,"Method of Perfusing a Porous Workpiece with a Chemical Composition using Cosolvents," US Patent 5094892, 1992

King Jr., A. D., and W. W. Robertson, "Solubility of Naphthalene in Compressed Gases," *J. of Chemical Physics*, **37** (7): 1453-1455, 1962.

King, M. B., D. A. Alderson, F. H. Fellah, D. M. Kassim, K. M. Kassim, J. R. Sheldon and R. S. Mahmud, In *Chemical Engineering at Supercritical Conditions*, edited by M. E. Paulaitis, et al., Ann Arbor Science, Ann Arbor, MI, pp 31 - 80, 1983.

King, M. B., and T. R. Bott, "Problems Associated with the Development of Gas Extraction and Similar Process," *Separation Science and Techn.*, **17**(1), 119-150,1982

Kiran, E.,"Supercritical Pulping: A New Concept," *Amer. Papermaker*, Nov.1987.

Kleintjens, L. A., and R. Koningsveld, Mead-Field Lattice-Gas Description of the System CO_2/H_2O, *Separation Science and Technology*, **17** (1): 215-233, 1982.

Klesper, E., "Chromatography With Supercritical Fluids," Angew, Chem. *Int. Ed. Engl.*, **17**: 738 - 746, 1978.

Klinkenberg, L. J., A.P.I. Drilling Prod. Proc., 200, 1941.

Klincewicz, K. M., and R. C. Reid, "Estimation of Critical Properties with Group Contribution Methods," *AIChE Journal*, **30** (1): 137, 1984.

Koll. P., Bronstrup, B., and Metzger, J. O., "Liquification of Biomass with Supercritical Fluids in High Pressure/ High Temperature Flow Reactor." In *Chemical Engineering at Supercritical Fluid Conditions*; Paulaitis, M. E., Penninger, J. M. L., Gray, R.D., Jr. P. Davidson, P., Ed.; Ann Arbor Science: Ann Arbor , MI, 1983.

Kollmann, F. F. P., Côté, "Principles of Wood Science and Technology I," Springer Verlag, New York, 1975.

Kollmann, F. F. P., E. W. Kuenzi, A. J. Stamm, *Principles of Wood Science and Technology II*, Springer-Verlag, New York, 1975.

Kozeny, J. S., Ber. Weiner Akad. Abt, IIa, 136: 271, 1927.

Krukonis, V. J., "Processing with Supercritical Fluids: Overview and Applications," *ACS Symposium Series*, **366**: 27- 43, 1988.

Krukonis, V. J. and R. T. Kurnik, "Solubility of Solid Aromatic Isomers in Carbon Dioxide," *J. Chem. Eng. Data*, **30**: 247, 1985.

Kumar, S. K.; K. P. Johnston, "Modeling Solubility of Solids in Supercritical Fluids with Density as an Independent Variable," *J. Supercritical Fluids*, **1**, 15, 1988.

Kumar, S. K.; R. C. Reid and U. W. Suter, "A Statistical Mechanics Based Lattice Model Equation of State: Applications to Mixture With Supercritical Fluids," *ACS Symposium Series*, **329**, 1987.

Kumar, S. and J.J. Morrel, "Effects of Surfactants on Penetration and Absorption of Chromated Copper Arsenate in Douglas-fir," Forest Product Jouranal, **42**, 5, 1992.

Kurnik, R. T., S. J. Holla and R. C. Reid, "Solubility of Solids in Supercritical Carbon Dioxide and Ethylene," *J. Chem. Eng. Data*, **26**: 47-51, 1981.

Kurnik, R. T., and R. C. Reid, "Solubility of Solid Mixtures in Supercritical Fluids," *J. Fluid Phase Equilibria*, **8**:93, 1982

Labrecque, R., S. Kallagulne, and J. L. Grandmalson, "Supercritical Gas Extraction of Wood with Methanol," *Ind. Eng. Chem. Prod. Res. Dev.*, **23**: 177-182, 1984.

Langsdorf Jr., A., "Nucleation form Gases: The Diffusion Cloud Chamber," *Ind. Eng. and Chem.*, **44**(6): 1298, 1952.

La Mer, V. K., "Nucleation Theory, Review: Nucleation in Phase Transition," *Ind. Eng. and Chem.*, **44**(6): 1252, 1952.

Lawson, J. R. and Klein, M. T., *Ind. Eng. Chem. Fundamentals*, **24**, 337, 1985.

Lele, A. K. and A. D. Shine, "Morphology of Polymers Precipitated from a Supercritical Solvent," *AIChE J.*, **38**, 5, 742-752, 1992

Li, L, and E. Kiran, "Interaction of Supercritical fluids with Lignocellulosic Materials," *Ind. Eng. Chem. Res.*, **27**, 1301 -1312, 1988.

Li, L, and E. Kiran, "Gas-Liquid Critical Properties of Methylamine + Nitrous Oxide and Methylamine + Ethylene Binary Mixtures," *J. Chem. Eng. Data*, **33**: 342-344, 1988.

Li, L, and E. Kiran, "Supercritical Fluid Extraction of Lignin for Wood," *ACS, Symposium Series*, **397**, 1989.

Lin, Ho-Mu, and K.C. Chao, "Correlation of Critical Properties and Acentric Factor of Hydrocarbons and Derivatives," *AIChE J.*, **30** (6): 981, 1984.

Lira, C. T., "Physical Chemistry of Supercritical Fluids: A Tutorial," *ACS Symposium Series*, **366**, 1987.

Lory, T. H., and K. S. Richardson, *Mechanism and Theory of Organic Chemistry*, 2nd Ed., Harper & Row Publishers, New York, 1981.

Lyderson, A.L, "Estimation of Critical Properties of Organic Compounds," Univ. Wisconsin, Coll. Eng., *Eng. Exp. Stn. Rep.* **4**, Madison, WI, 1955.

Mackay, M. E. and M. E. Paulaitis, "Solid Solubilities of Heavy Hydrocarbons in Supercritical Solvents," *Ind. Eng. Chem. Fund.*, **18**(2): 149-153, 1979.

Mart, C. J. and K. D. Papadopoulos, "A Modification of the Random-Fluid Approximation for Solid-Supercritical Fluid Equilibria," *Supercritical Fluid Technology*, J. M.L. Penniner et al., eds., Elsevier, New York, **67**, 1985

Matson, D. W., K. A. Norton, R. D. Smith, "Making Powder and Film from Supercritical Fluid Solutions," *Chemtech*, **19**: 480-486, 1989.

Matson, D. W., J. L. Fulton, and R. L. Petrson, Rapid Expansion of Supercritical Fluid Solutions: Solute Formation of Powders, Thin Films, and Fibers, *Ind. and Eng. Chem. Res.*, **26**: 2298-2306, 1987.

Matson, D. W. and R. D. Smith, "Supercritical Fluid Technologies for Ceramic-Processing Applications," *J. Amer. Ceram. Soc.*, **72**(6): 871-881, 1989.

McDonald, E. C., J. Howard and B. Bennett, "Chemicals from Forest Products by Critical Fluids Extraction," ENFOR Project C-51, Phase III. Canadian Forestry Services, Department of Environment, Quebec, Canada, 1982.

McDonald, E. C., J. Howard and B. Bennett, "Chemicals from Forest Products by Critical Fluids Extraction," *Fluid Phase Equilibria*, **10**(2-3): 337-344. 1983.

McDonald, R. A., S. A. Scrader and D. R. Stull,*J. Chem. Eng. Data*, **4**, 311, 1959

McHugh, M. A. and M. E. Paulatis, "Solid Solubilities of Naphthalene and Biphenyl in Supercritical Carbon Dioxide," *J. Chemical Eng. Data*, **25**: 326 - 329, 1980

McHugh, M. A., A. J. Seckner and T. J. Yogan, "High-Pressure Phase Behavior of Binary Mixtures of Octacosane and Carbon Dioxide," *Ind. Eng. Chem. Fund.*, **23** (4), 1984.

McHugh, M.A. and T. J. Yogan, "A Study of Three-Phase Solid-Liquid-Gas Equilibria for Three Carbon Dioxide-Solid Hydrocarbon Systems, Two Ethane-Hydrocarbon Solid Systems, and Two Ethylene-Hydrogen Solid System," *J. Chem. Eng. Data*, 29, 112, 1984

McKinley, C., J. Brewer and E. S. J. Wang, "Solid-Vapor Equilibria of the Oxygen-Hydrogen System," *Advances in Cryogenic Engineers*, **7**, Plenium Press, N. Y., 1982.

Mohammed, R. S., D. S. Halverson, P. Debenedetti, and R. K. Prud'homme, "Solid Formation After the Expansion of Supercritical Mixtures," *ACS Symposium Series*, **406**, 357, 1989.

Moradinia, I. and A. S. Teja, "Solubility of Five Solid n-Alkanes in Supercritical Ethane," *ACS Symposium Series*, **329**, 1987.

Morita, A., O. Kajimoto, "Solute-Solvent Interaction in Nonpolar Supercritical Fluid: A Clustering Model and Size Distribution," *J. Phys. Chem.*, **94**, 6420, 1990

Mullin, J.W., *Crystallization*, 2nd ed., CRC Press, 1972.

Murphy, H. R.; D. R. Miller, *J. Phys. Chem.* **88**, 4474, 1984.

Muskat, M., *The Flow of Homogeneous Fluids Through Porous Media*, Edwards, Ann Arbor, 1941.

Nicholas D. D., and A. F. Preston, "Evaluation of Alkyl Ammonium Compounds as Potential Wood Preservatives," *Amer. Wood Preservers' Assoc. Proc.*, **77**, 13-18, 1980.

Nicholas D. D., *Wood Deterioration and Its Prevention by Preservative Treatments*, Vol. I, and Vol. II, Syracuse Wood Science Series, Syracuse University Press, 1973.

Nicholas D. D. and Parikh, S.V., "The Efficacy of a Primer Biocide System against Wood Decay Fungi," Mississippi State University, Report Feb. 1982.

Orfila, C., and J. P. Hösli, "Pressure Development in Low Permeable Woods During the Intrusion of Air," *Amer. Wood Preservers' Assoc. Proc.*, **82**, 1985

Panshin, A.J., Carl de Zeeuw, *Textbook of Wood Technology*, McGraw-Hill, New York, 4th Ed., 1980

Paulaitis, M. E., K. P. Johnston and C. A. Eckert, "Measurement of Partial Volume at Infinite Dilution in a Supercritical Fluid Solvent Near Its Critical Point," *J. Phys. Chem.*, **85**: 1770-1771, 1981.

Paulaitis, M. E., V. J. Krukonis, R. T. Kurnik and R.C.Reid, "Supercritical Fluid Extraction," *Reviews in Chemical Engineering*, **1,2**, 179-250, 1983

Peng, Ding-Yu, and D. B. Robinson, "A New Two-Constant Equation of State," *Ind. Eng. Chem. Fundam.*, **15** (1), 1976.

Perry, R. H., and D. Green, *Perry's Chemical Engineering's Handbook*, McGraw Hill Publish, New York, 6th edn., 1984.

Peter, S. and G. Brunner, "The Separation of Nonvolatile Substances by Means of Compressed Gases in Counter Current Processes," *Angew. Chem. Int. Ed. Egl.*, **17**: 746-750, 1978.

Peter, S. and G. Brunner, and Riha, R., Phasengleichewwichte bei hohen Drucken und Möglichkeiten ihrer technischen Anwendung. *Chem.-Ing. Tech.*, **46**: 623, 1974.

Petersen, R. C., Matson, D. W., Smith, R. D., "The Formulation of Polymer Fibers From the Rapid Expansion of Supercritical Fluid Solutions," *Polymer Engineering and Science*, **27**, 1697, Dec. 1987.

Pfund, D. M.; L. L. Lee, and H. D. Cohchran, "Application of the Kirkwood-Buff Theory of Solutions to Dilute Supercritical Mixtures II. The Excluded Volume and Local Composition Models," *Fluid Phase Equilibria*, **39**, 161, 1988.

Phillips, E. W. J., "Movement of Pit Membrane in Coniferous Woods with Special Reference to Preservative Treatment," *Forestry* **7**: 109-120, 1933

Pitzer, K. S., and R. F. Curl, "The Volumetric and Thermodynamic Properties of Fluids, III. Empirical Equation for the Second Varial Coefficient," *J. Amer. Chem. Soc.*, **79**: 2369, 1957.

Pizzi, A. J. *Polym. Sci., Polym. Chem. Ed.* 20,739-64, 1982

Plumb, O. A., G.A. Spolek and B. A. Olmstead, "Heat and Mass Transfer in Wood During Drying," *Int. J. Heat Mass Transfer*, **28**(9), pp 1669-1678, 1985

Pound, G. M., "Liquid and Crystal Nucleations," *Ind. and Eng. Chem.*, **44**(6): 1278, 1952.

Poirier, M. G., A. Ahmed, J. L. Grandmaison, and S. C. F. Kaliaguine, "Supercritical Gas Extraction of Wood with Methanol in a Tubular Reactor," *Ind. Eng. Chem. Res.*, **26**: 1738-1743, 1987.

Prausnitz, J.M., Lichtenthaler, R.N. and de Azevedo, E.G. *Molecular Thermodynamics Fluid-Phase Equilibria*, Englewood Cliffs: Prentice Hall Inc., 1986.

Probstein, R. F., "Time Lag in the Self-Nucleation of a Supersaturated Vapor," *J. Chemical. Physics*, **19**(5), 1951.

Puri, V. P., and H. Haners, "Explosive Pretreatment of Lignocellulosic Residues with Pressure Carbon Dioxide for the Production of Fermentation Substrates," *Bioengineering and Technology*, **25**, 3149-3161, 1983.

Randall, L. G., "The Present States of Dense (Supercritical) Gas Extraction and Dense Gas Chromatography: Impetus for DGC/MS Development," *Separation Science and Technology*, **17**(1): 1-118, 1982.

Redlich, O., and A. T. Kister, "On the Thermodynamic of Solutions, VII. Critical Properties," *The Journal of Chemical Physics*, **36**(8), April, 1962.

Reichenberg, D., "The Viscosities of Gases at High Pressures," *NPL Rep. Chem.* 38, National Physical Laboratory, Teddington, England, Aug., 1975.

Reid, R. C., J. M. Prausnitz, T. K. Sherwood, *The Properties of Gases and Liquids*, 3rd Edition, McGraw-Hill Book Company, N.Y., 1977.

Reynolds, W. C. *Thermodynamic Properties in SI: Graphs, Tables, and Computational Equations for Forty Substances*, Stanford University Mechanical Engineering Department: Stanford, CA:122-154, 1979.

Riedel, L., "Eine Neue Universelle Damfdruckformal," *Chem. Ing. Tech.*, **26** (83) 1954.

Ritter, D. C., and A. G. Campbell, "Supercritical Carbon Dioxide Extraction of Southern Pine and Ponderosa Pine," *Wood and Fiber Science*, **23**(1): 98-113, 1991.

Robin, S. and B. Vodar, "Solubility in Compressed Gases," *Discussions of the Faraday Society*, **15**, 1953.

Rowlinson, J. S., and M. J. Richardson, "The Solubility of Solids in Compressed Gases," *Adv. Chem. Phys.*, **2**, 85, 1958.

Ruddick, J. N. R.; "Preservative Treatment of White Spruce Poles," Western Forest Product Information Report VP-X-176, 26p., 1978.

Ruddick, J. N. R.; "Treatability of Lodge Pole Pine Lumber With ACA and CCA," *Forest Products Journal*, **30**(2): 28-32, 1980.

Saad, H. and Gulari, E., "Diffusion of Liquid Hydrocarbons in Supercritical $C0_2$ by Photon Correlation Spectroscopy," *Ber. Bunseges, Phys. Chem.*, **88**, 834-841, 1984.

Scheidegger, A. E., *The Physics of Fluid Through Porous Media*, 3rd, Ed., University of Toronto Press, Toronto, 1974.

Scheidegger, A. E., "Statistical Theory of Flow Through Porous Media," *Trans. Soc. Rheol.*, **9**, 313, 1965.

Schmitt, W. J., and R. C. Reid, "Solubility of Monofunctional Organic Solids in Chemically Divers Supercritical Fluids," *J. Chem. Eng. Data*, **31**: 204-212, 1986.

Schneider, G. M.,"Physicochemcal Principles of Extraction With Supercritical Gases," *Angew. Chem. Inter. Ed. Engl.*, **17**: 716-727, 1978.

Sebastian, L. P., W. A. Côté Jr., C. Skaar, "Relationship of Gas Phase Permeability to Ultrastructure of White Spruce Wood," *Forest Product J.*, **15**(9): 394-404, 1965.

Shing, K. S., and S. T. Chung, "Computer Simulation Methods for the Calculation of Solubility in Supercritical Extraction Systems," *J. Phys. Chem.*, **91**: 1674-1681, 1987.

Siau, J. F., *Transport Process in Wood*, Springer-Verlag, Berlin, 1984.

Siau, J. F., J. A. Petty, "Correction for Capillaries in Permeability of Wood. In:

Nicholas, D. D., Wood Deterioration and Its Prevention by Preservative Treatments, II," *Preservatives and Preservative Systems*, Syracuse Univ. Press Syracuse: 299-343, 1973.

Smith, R. D., J. L. Fulton, R. C. Petersen, A. J. Kopriva, and B. W. Wright, "Performance of Capillary Restrictors in Supercritical Fluid Chromatography," *Anal. Chem.*, **58**, 2057, 1986

Sonnefeld, W.J., W.H. Zoller, and W.E. May, *Anal.Chem.*, **55**, 275, 1983.

Stahl, E., W. Schilz, E. Schutz, and E, Willing, "A Quick Method for the Microanlytical Evalution of the Dissolving Power of Supercritical Gases," *Angew. Chem. Int. Ed. Engl.*, **17**: 731-738, 1978.

Stamm,A.J, "Passage of Liquids, Vapors, and Dissolved Materials through Softwoods," *U.S.D.A., Technical Bul.* 929, Oct, 1946

Stamm,A.J., *Wood and Cellulose Science*, Roland New York, 1964

Stephen, K. and K. *Lucas, Viscosity of Dense Fluids*, Plenum Press, New York, 1979.

Stephan, K. and K. H. Schaber, "High pressure Phase Equilibria for Vapor Phase Extraction Process," *Separation Science and Technology*, **17**(1): 235-260, 1982.

Stephan, K; Lucas, K. "Viscosity of Dense Fluids," Plenum Press, New York,1979

Sucoff, E. I., P. Y. S. Chen, and R. L. Hossfeld, "Permeability of Unseasoned Xylem of Northern White Cedar," *Forest Product Journal*, **15** (8): 321-324, 1965.

Sunol, A. K., P. Richey, "Supercritical Fluid-Aided Treatment of Porous Materials", US Patent, 4992308, 1991.

Swaid, I. and G.M. Schneider, "Determination of Binary Diffusion Coefficients of the Benzene and Some Alkylbenzenes in Supercritical CO_2 between 308 and 328 K in the Pressure Range 80 to 160 bar with Supercritical Fluid Chromatography (SFC)," *Ber. Bunsenges. Phys. Chem.*, **83**, 969, 1979

Tavana, A., J. Chang, A. D. Randolph and N. Rodriguez, Scanning of Cosolvents for Supercritical Fluids Solubilization of Organics, *AIChE Journal*, **35**(4): 645-648, April 1989a.

Tavana, A., and A. D. Randolph, "Manipulating Solid CSD inSupercritical Fluid Christallizer: CO2-Benzoic Acid," AIChE J., **35**, 10, 1625, 1989b

Thompson, W. S. and P. Kock, Preservative Treatment of Hardwoods: A Review, U.S.D.A. Southern Forest Experiment Station General Technical Report SO-35, 47p., 1981.

Tolley, W. K., and L. S. Tester, Supercritical CO_2 Solubility of $TiCl_4$, Report of Investigations, 9216, *Bureau of Mines*, 1989.

Tsekhanskaya, Y. V., Iomtev, M. B. and Mushkina, E. V., Solubility of Diphenylamine and Naphthalene in Carbon Dioxide Under Pressure, *Russ. J. Phys. Chem.*, **36**(10):1177-1181, 1962.

Tsekhanskaya, Y. V., M. B. Iomtev, and E. V. Mushkina,,"Solubility of Naphathalene in Ethylene and Carbon Dioxide Under Pressure," *Russ. J. Phys. Chem.*, **38**, 9, 1173, 1964..

Tsekhanskaya, Y. V., "Diffusion of Naphthalene Solution in Carbon Dioxide Near the Liquid-Gas Critical Point," *Russ. J. Phys. Chem.*, **45**,744, 1971

Yoon, P., and G. Thodos, "Viscosity of Nonpolar Gaseous Mixtures at Normal Pressures," *AIChE. J.*, **16**, 300, 1970.

Van Alsten, J.G., Structural and Functional Effects in Solutions with Pure and Entrained-Doped Supercritical Solvent, PhD dissertation, Ill. Inst. Tech., 1986.

Van Everdinger, A. F., and N. Hurst, "The Application of the Laplace Transformation to Flow Problems in Reservoirs," *Journal of Petroleum Technology*, AIME, Dec. 1949.

Vetere, A., "A Predictive Method for Calculating the Solubility of Solids in Supercritical Gases Application to Apolar Mixtures," *Chem. Engr. Science.*, **34**, 1393-1440, 1979

Vezzetti, D. J.,"Solubility of Solids in Supercritical Gases," *J. Chem. Phys.*, **77** (3): 1512-1516, Aug. 1982.

Vezzetti, D. J.,"Solubility of Solids in Supercritical Gases. II. Extension to Molecule of Differing Sizes," *J. Chem. Phys.*, **80** (2), Jan. 1984.

Vicky Roy, J. R.., and A. D. Converse ," In Supercritical Fluid Technology," Penninger, J.M. L., Radosz, M., McHugh, M. A., Krukonis, V. J.., Eds., Elsevier: New York, 1985

Volk, M. C. and J. W. Lefferge, and R. Stetson, *Electrical Encapsulation*, Reinhold Publishing Co., Inc. N.Y., 1961.

Walters, C. S., and J. A. Whittington, "The Effect of Treating Pressure on Preservative Absorption and on the Mechanical Properties of Wood, II Douglas Fir," Amer. Wood-Preserv. Assoc. Proc. **66**:798-193, 1970

Ward, D., T. Dinatelli, and A. K. Sunol, "Supercritical Fluid Aided Wood-Polymer Composite Manufacture," AIChE Meeting, Orlando, Fl, Spring, 1990

Whitaker, S., "Advances in Theory of Fluid Motion in Porous Media, In " Flow Through Porous Media, ACS Sixth State-of-the-Art Symposium, June 9-11, 1969.

Williams, D. F., "Extraction with Supercritical Gases," *Chemical Engineering Science*, **36**(11): 1769-1788, 1981.

Won, K. W., and J. M. Prausnitz, "High-Pressure Data. Thermodynamic Consistency," *Ind. Eng. Chem. Fundam.*, **12**(4): 459-463, 1973.

Wong, J. M., and K. P. Johnston, "Solubilization of Biomolecules in Carbon Dioxide Based Supercitical Fluids," *Biotechnology Progress*, **2**(1), March 1986.

Wong, J. M., R. S. Pearlman, and K. P. Johnston, "Supercritical Fluid Mixtures: Prediction of the Phase Behavior," *J. Phys. Chem.*, **89**, 2671-2675, 1985.

Worster, H.E., M. E. Bartels, and A.J. Horning, *"Effects of some kraft black liquor components of poorly washed pulp on lineboard properties,"* TAPPI 63(11):63-65, 1986

Ziger, D. H. and C. A. Eckert, "Correlation and Prediction of Solid-Supercritical Fluid Phase Equilibria," *Ind. Eng. Proc.Des. Dev.*, **22**: 582-588, 1983.

Zosel, K. "Separation With Supercritical Gases: Practical Applications," *Angew. Chem. Int. End. Engl.* **17**: 702-709, 1978.

Appendices

Appendix A

Solubility data

Table A.1 Solubility of naphthelene in supercritical carbon dioxide at (A) 35°C and (B) 45°C

(A)

P bar	ρ mol/L	y^a, mol % 10^4	y^b, mol % 10^4	Error %
121.59	17.53	125	124.4	0.5
141.87	18.29	139	148.4	6.7
162.14	18.87	151	152	0.7
192.54	19.49	163	171	4.9

(B)

P bar	ρ mol/L	y^a, mole % 10^4	y^b, mole % 10^4	Error %
126.67	15.56	154	159	3.2
141.87	16.51	183	148.4	3.1
155.04	17.11	197	202	2.4
202.67	18.55	245	245.7	0.3

a = Tsekhanskaya, et al., 1964
b = This work

Table A.2 Solubilities of biocides in pure carbon dioxide at gauge pressure 250 bar and selected temperatures.

Biocide	Solubility, wt %		
	T = 40°C	T = 55°C	T = 80°C
Amical-48*	0.078	0.085	0.16
Chlorothalonil*	0.094	0.162	0.165
Cu Naphthanate	0.298	0.972	1.933
Cu-8-Quinolinolate	0.0010	0.002	0.009
Tebuconazole	0.23	0.83	1.20
IPBC	1.67	4.20	7.50
Propiconazole	-	2.08	2.50
PCP	0.201	0.314	0.729
TCMTB	0.320	0.63	0.710

* Solubility measured at 45, 60, 80 °C

Table A.3 Solubilities of selected biocides in SC-CO_2 + 3.5 mole % acetone at gauge pressure 250 bar and selected temperatures

Biocide	Solubility, wt %		
	T = 40°C	T = 55°C	T = 80°C
Amical-48*	0.138	0.165	-
Chlorothalonil*	0.090	0.112	-
Cu Naphthanate	0.834	-	3.860
Cu-8-Quinolinolate	0.0048	0.005	-
Tebuconazole	2.08	2.51	3.53
IPBC	7.890	-	8.870
Propiconazole	3.570	4.28	4.40
PCP	1.095	1.690	2.860
TCMTB	1.400	1.568	2.250

* Solubility measured at 45, 60, 80 °C

Table A.4 Solubilities of selected biocides in SC-CO_2 + 3.5 mole % methanol at gauge pressure 250 bar and selected temperatures

Biocide	Solubility, wt %		
	T =40°C	T = 55°C	T = 80°C
Amical-48*	0.090	0.080	0.124
Chlorothalonil*	0.090	0.162	0.224
Cu Naphthanate	1.120	1.040	3.040
Cu-8-Quinolinolate	0.010	0.021	-
Tebuconazole	3.770	4.590	4.700
IPBC	8.200	9.100	10.800
Propiconazole	3.900	6.24	6.900
PCP	1.100	1.950	2.920
TCMTB	1.50	1.940	2.200

* Solubility measured at 45, 60, 80 °C

Table A.5 Solubilities of selected biocides in SC-CO_2 + 3.5 mole % ethanol at gauge pressure 250 bar and selected temperatures

Biocide	Solubility, wt %		
	T = 40°C	T = 55°C	T = 80°C
Amical-48*	0.145	0.090	0.125
Chlorothalonil*	0.100	0.157	-
Cu Naphthanate	1.526	2.129	1.880
Cu-8-Quinolinolate	0.008	0.010	-
Tebuconazole	2.140	2.560	3.510
IPBC	3.350	6.680	8.840
Propiconazole	2.800	3.62	3.950
PCP	-	2.180	2.163
TCMTB	2.134	2.003	2.610

* Solubility measured at 45, 60, 80 °C

Table A.6 Solubility of chlorothalonil in carbon dioxide

Pressure gauge, bar	Mass Fraction (x 10^4)		
	T = 45°C	T = 55°C	T = 80°C
100	0.80	0.318	0.383
125	-	2.79	0.64
150	2.90	3.68	1.31
170	5.13	4.83	3.28
200	8.00	6.00	8.30
225	7.30	7.38	9.30
250	8.00	8.50	11.6
300	9.40	10.9	16.2

Table A.7 Solubility of Amical-48 in carbon dioxide

Temperature, K	Pressure gauge, bar	Reduced Density, ρ_r	Mole Fraction, ($x10^5$)
318.15	100	1.065	1.22
	125	1.455	-
	150	1.593	-
	170	1.666	3.80
	200	1.745	3.90
	225	1.799	5.81
	250	1.841	6.20
	300	1.913	7.26
328.15	100	0.698	-
	125	1.163	-
	150	1.403	-
	170	1.514	-
	200	1.620	6.38
	225	1.686	7.07
	250	1.741	8.98
	300	1.826	8.66
338.15	100	0.571	0.63
	125	0.892	2.43
	150	1.189	3.67
	170	1.339	5.60
	200	1.484	8.45
	225	1.569	8.29
	250	1.636	9.63
	300	1.737	1.15

Table A.8 Solubility of tebuconazole in SC-CO_2 and SC-CO_2 + 1.1 moel % methanol

Pressure guage bar	Solubility in CO_2, $x10^4$ wt fraction	Solubility in CO_2+ 1.1mol % methnol, $x10^4$
100	0.001	-
120	0.094	-
150	0.38	-
200	1.36	16.884
220	2.42	24.350
250	11.42	40.534
300	11.52	42.334

Table A.9 Solubility of TCMTB in supercritical carbon dioxide at (A) T = 50°C and (B) T = 65°C

(A)

Pressure bar	Density g/cm^3	Solubility wt %	Solubility mole%
110	0.5049	0.00682	0.00126
125	0.6166	0.03807	0.00704
150	0.7029	0.18748	0.03471
200	0.7858	0.49730	0.09151
250	0.8354	0.64839	0.12051
300	0.8715	0.85396	0.15898

(B)

Pressure bar	Density g/cm^3	Solubility wt % x10^3	Solubility mole% x10^3
100	0.2657	0.0094	0.00175
110	0.3206	0.0353	0.0066
125	0.4169	0.1246	0.02363
150	0.5568	0.6038	0.1143
200	0.6945	3.3672	0.6376
300	0.8097	7.6751	1.4533

Table A.10 Solubility of pentachlorophenol in carbon dioxide

Temperature K	Pressure gauge, bar	Reduced Density, ρ_r	Mass Fraction, ($x10^4$)	Enhancement Factor, E
313.15	100	1.356	1.62	3375
	120	1.547	2.88	7200
	150	1.679	10.0	31250
	170	1.737	14.4	51000
	200	1.805	16.3	67916
	220	1.842	20.6	94416
	250	1.889	20.2	105208
	300	1.955	19.7	123125
323.15	120	0.936	1.78	834
	150	1.304	2.00	5859
	170	1.433	12.6	8367
	200	1.558	25.7	20078
	220	1.618	30.2	25953
	250	1.691	31.4	30664
	270	1.722	40.7	42925
	300	1.782	43.0	50390
333.15	100	0.475	1.03	93
	120	0.636	2.20	240
	140	0.824	5.10	649
	150	0.919	8.7	1186
	170	1.091	28.2	4358
	200	1.281	41.0	7454
	250	1.477	72.9	16568
	300	1.602	144.7	39463

Table A.11 Solubility of penthachlorophenol in SC-CO_2 with cosolvents (A) at T = 333 K and (B) at T = 353 K

(A)

Solvent	Mass fraction ($x10^3$)		
	200 bar	250 bar	300 bar
Pure CO_2	2.57	3.14	3.04
CO_2 + Acetone	6.80	15.90	21.50
CO_2 + Methanol	13.00	23.00	26.90
CO_2 + Ethanol	7.70	21.80	25.90
CO_2 + DMSO	7.65	12.20	13.70

(B)

Solvent	Mass fraction ($x10^3$)		
	200 bar	250 bar	300 bar
Pure CO_2	4.10	7.29	14.47
CO_2 + Acetone	6.14	18.40	20.30
CO_2 + Methanol	14.70	29.20	32.00
CO_2 + Ethanol	7.70	21.80	25.9
CO_2 + DMSO	7.65	12.20	13.70

Table A.12 Solubility of penthachlorophenol in SC-CO_2 /methanol mixture

Temperature K	Pressure guage, bar	Mass Fraction in CO_2($x10^4$)	Mass Fraction in CO_2/MeOH ($x10^4$)	Cosolvent Effect
313.15	100	1.62	39.37	24.30
	120	2.88	41.00	14.30
	150	10.01	101.1	10.10
	170	14.40	136.8	9.50
	200	16.30	155.0	9.51
	220	20.60	191.1	9.46
	250	20.20	-	-
	300	19.70	-	-
				-
323.15	120	1.78	8.0	13.81
	150	10.0	88.1	10.67
	170	12.60	110.0	8.80
	200	25.70		-
	220	30.20	130.4	5.06
	250	31.40	127.0	4.20
	270	40.70	195.0	6.21
	300	43.02	257.0	6.31
			289	6.72
333.15	100	1.030	10.0	9.70
	120	2.20	51.0	8.10
	140	5.10	82.0	6.35
	150	8.70	147.1	-
	170	28.20	163.0	3.58
	200	41.03	292.	3.26
	250	72.90	400	4.00
	300	144.47	410	4.40

Table A.13 Solubility of tebuconazole in pure and modified SC-CO_2

Pressure guage bar	Wt Fraction in CO_2, 10^4	Wt Fraction in CO_2 + in 1.1 mole% MeOH, 10^4	Cosolvent Effect
100	0.007	-	-
120	0.570	-	-
150	2.300	-	-
200	8.200	117.0	18.9
220	14.800	168.0	18.10
250	69.100	227.0	3.97
300	6.970	289.0	3.20

Appendix B

Density Calculation Using Modified Benedict-Webb-Rubin Equation of State and CO_2 Viscosity Calculation at Atmospheric Pressure

B.1 Calculation of CO_2 Density

A modified Benedict-Webb-Rubin equation of state with 32 terms was proposed for CO_2 and CO_2 rich mixtures (Ely, J.F., 1986). This equation is essentially a polynomial in density and temperature and it is much simpler and more accurate than the widely used IUPAC model (Angus et al., 1976). Generally the equation reproduced density to within 0.3%, pressure to 2%, heat capacity to 2%. The functional form of Modified Benedict-Webb-Rubin equation of state:

$$Z = \frac{1}{RT}\left[\sum_{n=1}^{9} a_n(T)\,\rho^{n-1} + e^{-\gamma\rho^2}\sum_{n=10}^{15} a_n(T)\,\rho^{2n-18}\right]$$

$a_1 = R\,T$

$a_2 = b_1T + b_2T^{1/2} + b_3 + b_4/T + b_5/T^2$

$a_3 = b_6 + b_7 + b_8/T + b_9/T^2$

$a_4 = b_{10}T + b_{11} + b_{12}/T$

$a_5 = b_{13}$

$a_6 = b_{14}/T + b_{15}/T^2$

$a_7 = b_{16}/T$

$a_8 = b_{17}/T + b_{18}/T^2$

$a_9 = b_{19}/T^2$

$a_{10} = b_{20}/T^2 + b_{21}/T^3$

$a_{11} = b_{22}/T^2 + b_{23}/T^4$

$a_{12} = b_{24}/T^2 + b_{25}/T^3$

$a_{13} = b_{26}/T^2 + b_{27}/T^4$

$a_{14} = b_{28}/T^2 + b_{31}/T^3 + b_{32}/T^4$

Coefficients for carbon dioxide:

Parameter	**CO_2**
P_c [bar]	0.7384325000 E + 2

T_c [K]	0.3042100000 E +2
ρ_c [mol/L]	0.1060000000 E +2
b(1)	-0.9818510658 E -2
b(2)	0.9950622658 E +0
b(3)	-0.2283801603 E +2
b(4)	0.2818276345 E +4
b(5)	-0.3470012627 E +6
b(6)	0.3947067091 E -3
b(7)	-0.3255500001 E +0
b(8)	0.4843200831 E +1
b(9)	-0.3521815430 E +6
b(10)	-0.3240536033 E +4
b(11)	0.4685966847 E -1
b(12)	-0.7545470121 E +1
b(13)	-0.3818943540 E -4
b(14)	-0.4421929339 E -1
b(15)	0.5169251681 E +2
b(16)	0.2124509852 E -2
b(17)	-0.2610094748 E -4
b(18)	-0.8885333890 E -1
b(19)	0.1552261794 E -2
b(20)	0.4150910049 E +6
b(21)	-0.1101739675 E +8
b(22)	0.2919905833 E +4
b(23)	0.1432546065 E +8
b(24)	0.1085742075 E +2
b(25)	-0.2477996570 E +3
b(26)	0.1992935908 E -1
b(27)	0.1027499081 E +3
b(28)	0.3776188652 E -4
b(29)	-0.3322765123 E -2
b(30)	0.1791967071 E -7
b(31)	0.9450766278 E -5
b(32)	-0.1234009431 E -2
γ	0.8899964400 E -2

B-2 Viscosity Calculation at Lower Pressures

Viscosity of carbon dioxide is given at atmospheric pressure and at selected temperatures (Perry and Green, 1984):

Table B.1 Viscosity of CO_2 at atmospheric pressure and selected temperatures

Temperature, K	Viscosity (μ_o), 10^{-4}Pa.s
250	0.126
300	0.150
400	0.196
500	0.239
600	0.278

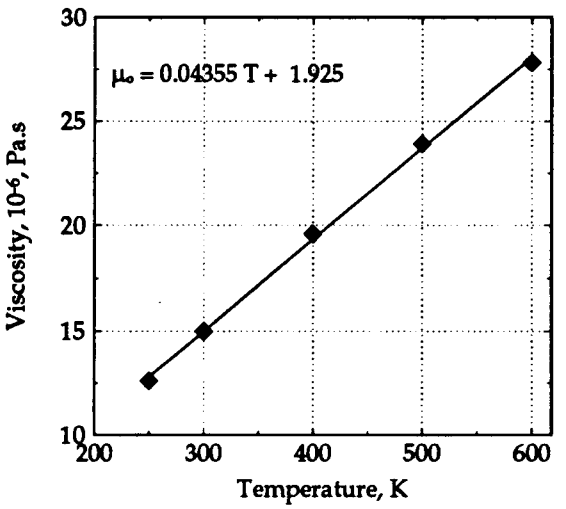

Figure B.1 Viscosity *vs* temperature for CO_2 at atmospheric pressure.

Appendix C

Molecular Structure and Solubility in SCF

Most thermodynamic correlations for the solubility of solids and liquids in supercritical fluids require extensive physicochemical data to characterize solute-solvent interactions and have been applied mostly to a limited number of structurally-simple solutes dissolved in a pure supercritical fluid. Most of the biocides studied in this thesis were molecularly complex and very little physical properties data was available on these molecules.

There have been various attempts to formulate structure-solubility correlations in organic compounds SC-CO_2 systems (Dange et al., 1985). One of the methods used classification of compounds by functional groups and structures. Structural features include, chain length, branching, type and position of substitutes on the rings and aromaticity. Correlation of a solute's molecular structure with its solubility in a SCF based on micro extraction studies was first employed by Stahl et al., (1978). They formulated several extraction rules based on changes in a solute's molecular structure to qualitatively predict the extent of solute dissolution in SC-CO_2. Qualitative trends in solute solubilities have also been summarized by various researchers (Hyatt, 1984; Dandge et al.,1985; and Rizvi et al., 1986).

Condensed states (liquids or solids) have considerable cohesive energy between the molecules, which are said to have a large negative potential energy compared to their vapor states. If we define U as the molar internal

energy of the molecules, then $-U$ will be the energy associated with the net attraction of the

material, which is the molar cohesive energy.

$$-U = \nabla_l^g + \nabla_g^{\infty} U \qquad \text{(C-1)}$$

where

∇_l^g = the molar vaporization energy required to vaporize a mole of the liquid to its saturated vapor,

∇_g^{∞} = the energy required to expand the saturated vapor to infinite volume at constant temperature, i.e. the energy required to completely separate the molecules.

Hildebrand (1950) considered internal pressure as a basis for comparing the likeness of molecular forces. The Hildebrand solubility parameter (δ) is the square root of the molar cohesive energy density, or energy per volume:

$$\delta = \left(-\frac{U}{V}\right)^{1/2} = \left(\frac{\nabla_L^g U}{V}\right)^{1/2} \qquad \text{(C-2)}$$

There is a relationship between the cohesive energy densities of liquids and their miscibility. Therefore, the Hildebrand solubility parameter can be

calculated directly if the molar volume and the molar enthalpy have been determined at a prescribed temperature. Barton (1983) reported values of δ for various liquids. For other liquids, polymers, solids and surfaces, δ values must be estimated.

King and Fredirch (1990) suggested the concept of the reduced solubility parameter, Δ, to correlate solubilities and distribution coefficients in SCFs.

$$\Delta = \frac{\delta_1}{\delta_2} \qquad \text{(C-3)}$$

where δ_1 is solvent solubility parameter, which can usually be obtained from standard sources, and δ_2 is the solute solubility parameter, which is calculated using Fedro's group contribution method (1974). This method permits us to estimate solute solubilities from knowledge of the solute's molecular structure.

At a given pressure and temperature the solubilities of the biocides were found to vary widely (Figure C.1). The log of the solubility appears to have linear correlation with δ. King and Fredrich(1990) reported that for reduced solute solubility parameters above 0.5 there is a substantial increase in solubility.

Table C.1 Estimated values of δ for eight biocides

(δ_{co2} = 6.775 $(cal/cm^3)^{1/2}$ at 250 bar and 40°C)

Biocide	δ_{biocid} $(cal/cm^3)^{1/2}$	$\delta_{co2}/\delta_{biocid}$
Amical-48	11.88	0.57
Chlorothalonil	14.49	0.46
IPBC	11.32	0.59
PCP	14.31	0.47
Propiconazole	9.39	0.71
Tebuconazole	13.93	0.48
TCMTB	12.98	0.52

Table C.2 Estimated biocide densities using group and atomic contribution method

Biocide	Specific Volume cm^3/mol	Molecular weight g/mol	Density estimated g/cm^3	Density measured g/cm^3	Deviation %
Amical-48	167.5	417	2.48	NA	-
Chlorothalonil	136.4	266	1.95	1.7	-5.1
IPBC	161	281	1.74	1.6	-8.7
PCP	126.4	266	2.10	1.98	-6.2
Propiconazole	346.8	342	1.27	0.98	29.6
Tebuconazole	170.6	308	1.80	NA	-
TCMTB	145	238	1.64	1.38	-18.8

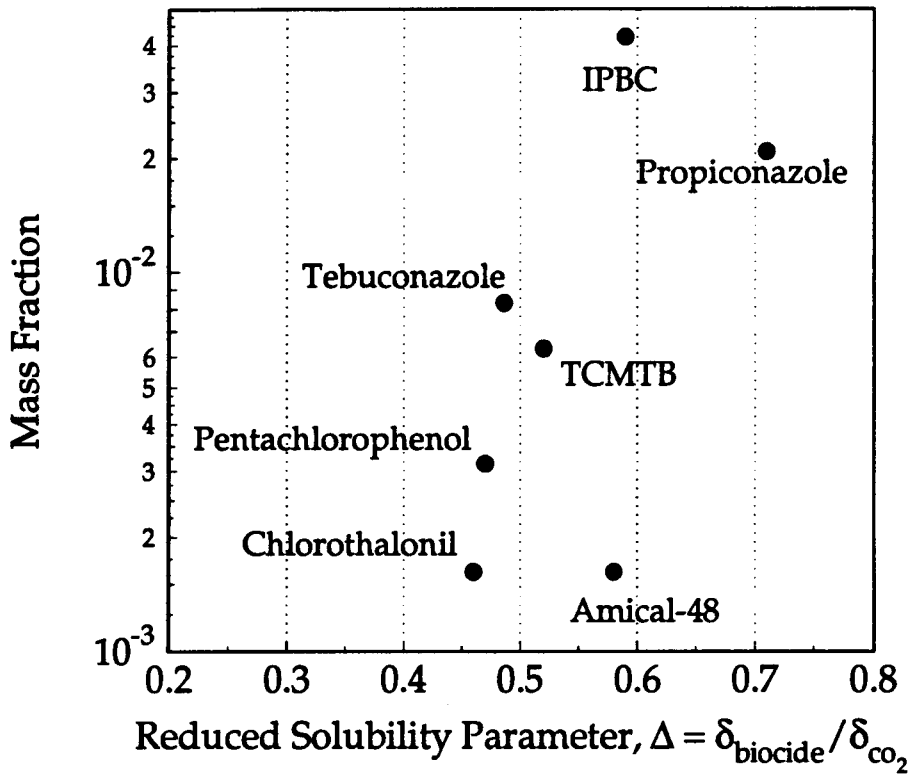

Figure C.1 Biocide weight fraction in SC-CO_2 at 250 bar and 60°C *vs* biocide reduced solubility parameter.

Appendix D
Solubility Parameter Estimation from Group and Atomic Contribution Method (Fedors, 1974)

Amical-48 *(diiodomethyl p-tolyl sulfone)*

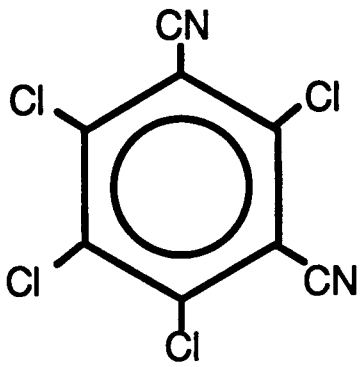

Group	Δe_i (cal/mol)	Δv_i
(cm^3/mol)		
2 -C=	2(1030) = 2060	2(-5.5) = -11
4 = CH	4(1030) = 4120	4(13.5) = 54
$-CH_3$	1125	33.5
S	3380	2
2 O	2(800) = 1600	2(3.8) = 7.6
2 I	2(4550) = 9100	2(31.5) = 63
-CH	8200	-1.0
Conj. double bond	1200	-6.6
6-membered ring closure	250	16
	23,655	167.5

$$\delta = \left(\frac{\sum e_i}{\sum V_i}\right)^{1/2} = 11.8 \left[\frac{cal}{cm^3}\right]^{1/2}$$

Chlorothalonil *(tetrachloroisophthalonitrile)*

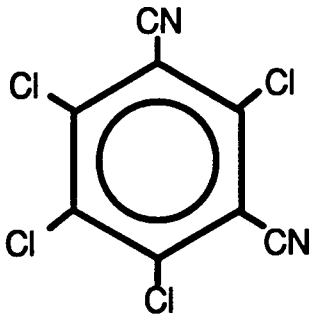

Group	Δe_i (cal/mol)	Δv_i (cm^3/mol)
6 -C=	6(1030)=6180	6(-5.5)= -33
2 CN	2(6100)=12200	2(24)=48
4 Cl	4(2700) = 11040	4(24) = 98
4 Cl (attached to -C=)	4(552)= -2208	4(4) = 16
3 conjugated double bond	3(400)= 1200	3(-2.2) = -6.6
6-membered ring	250	16
Total	28662	136.4

$$\delta = \left(\frac{\sum e_i}{\sum V_i}\right)^{1/2} = 14.49 \left[\frac{cal}{cm^3}\right]^{1/2}$$

IPBC *(3-Iodo-2-propynyl butyl carbamate)*

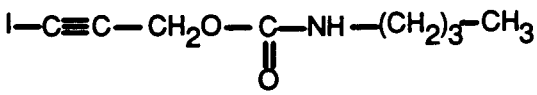

Group	Δe_i (cal/mol)	Δv_i (cm^3/mol)
4 $-CH_2$	4(1180) = 4720	4(16.1) = 64.4
-CH3	1125	33.5
-NH	2000	4.5
-O-	800	3.8
2 -C≡	2(1690)	2(6.5)
I	4550	31.5
CO	4150	10.8
	Total 20725	161

$$\delta = \left(\frac{\sum e_i}{\sum V_i}\right)^{1/2} = 11.32 \left[\frac{cal}{cm^3}\right]^{1/2}$$

Pentachlorophenol

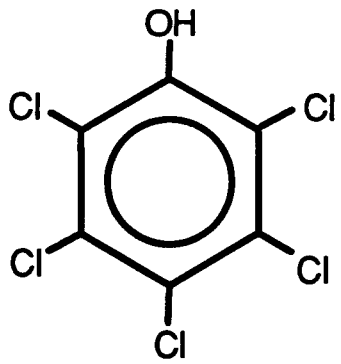

Group	Δe_i (cal/mol)	Δv_i (cm^3/mol)
5(-Cl)	5(2760) = 13800	5(24)=120
6(-C=)	6(1030)= 6180	-33
- OH	7120	10
5(-Cl) attached to C=	5(552)= - 2760	20
3 Conjugated double bond	1200	-6.6
Ring Closure	250	16
Total	25790	126

$$\delta = \left(\frac{\sum e_i}{\sum V_i}\right)^{1/2} = 14.31\left[\frac{cal}{cm^3}\right]^{1/2}$$

Propiconazole ((*RS*)1-(2-(2',4'-dichlorophenyl)-4-propyl-1, 3-dioxolan-2-methyl)-1H-1,2,4 triazole)

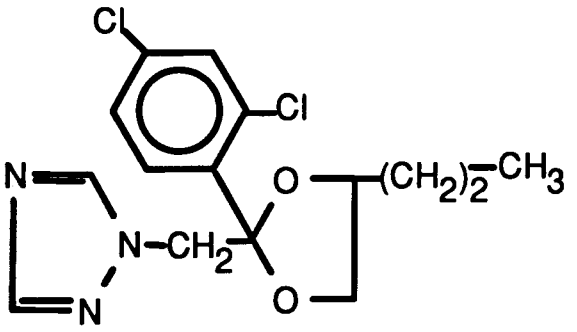

Group (cm^3/mol)	Δe_i (cal/mol)	Δv_i
5 = CH-	5(1030)= 5150	5(33.5)=167.5
2 -N=	2(2800)= 5600	2(5.0) = 10
-N-	1000	-9.0
4 $-CH_2$	4(1180)= 4720	2(16.1)=32.2
3 C=	3(1030) = 3090	3(-5.5) = -16.5
C	350	-19.2
$-CH_3$	1125	33.5
-CH-	820	-1.0
2 O	2(800)=1600	2(3.8)= 7.6
2 Cl	2 (2760) = 5520	2(24) = 48
2 Cl attached to C=	2(-552)= -1140	2(40) = 8.0
3 Ring closure	3(250) = 750	3(16)= 48
5 Double bond	5(400)= 2000	5(-2.2)= -11
	Total= 30585	346.8

$$\delta = \left(\frac{\sum e_i}{\sum V_i}\right)^{1/2} = 9.39 \left[\frac{cal}{cm^3}\right]^{1/2}$$

TCMTB *(2-(Thiocyanomethylthio) benzothiazole*

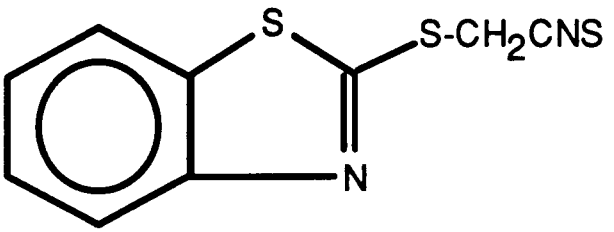

Group	Δe_i (cal/mol)	Δv_i (cm^3/mole)
4 HC=	4(1030) = 4120	4(13.5)= 54
3 -C=	3(1030) = 3090	3(-5.5) = -16.5
$-CH_2$	1180	16.1
2 -S-	2(3380) = 6760	2(12) = 24
-N=	2800	5.0
-CNS	4800	37
2 ring closure	2(250) = 500	2(16) = 32
3 conjugation in ring	3(400) = 1200	3(-2.2) = -6.6
	Total= 24450	145

$$\delta = \left(\frac{\sum e_i}{\sum V_i}\right)^{1/2} = 12.98 \left[\frac{cal}{cm^3}\right]^{1/2}$$

Tebuconazole *(α-[2-(4-chlorophenyl) ethyl]-α-(1,1-dimethylethyl)-1H-1,2,4-triazole-1-ethanol)*

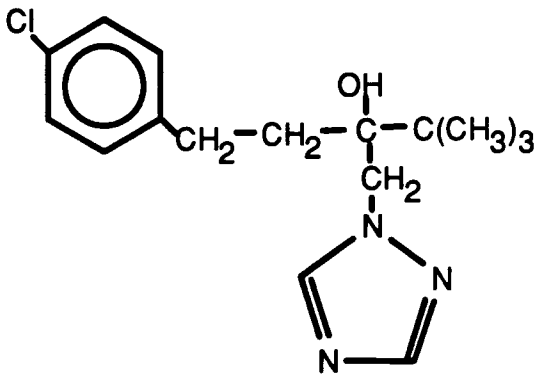

Group	Δe_i (cal/mol)	Δv_i (cm^3/mol)
6 HC=	6180	81
-N=	2800	5.0
N	1000	-9.0
3 CH_3	3375	100.5
4 C=	4120	-22
3 CH_2	3540	48.3
3 C	1050	-57.6
OH	7120	-9.0
Cl	2760	24
Cl (attached to C=)	-552	4.0
3 ring closure	500	32
conjugated ring	1200	-6.6
	Total= 33093	170.6

$$\delta = \left(\frac{\sum e_i}{\sum V_i}\right)^{1/2} = 13.93 \left[\frac{cal}{cm^3}\right]^{1/2}$$

Appendix E

Vapor Pressure of Biocides

Vapor pressure is one of the most important physical parameters required to correlate phase equilibria data. Vapor pressure of most substances can be approximated from the semi-empirical Antoine Equation (Antoine, 1888):

$$\log_{10} P^{vap} = A - \frac{B}{T + C} \qquad \text{(E-1)}$$

where P^{vap} is the vapor pressure (kPa) and T is temperature (°C).

- For pentachlorophenol (McDonald et al., 1959):

A = 7.22246 B = 2846.009 C= 230.000

T (°C)	P exptl.(kPa)	P calcd. (kPa)	Percent dev.
200	4.133	4.111	-0.52
215.51	6.759	6.827	1.01
233.07	12.279	12.221	-0.47

The deviation between experimental and calculated values is higher at lower temperatures. For example, at 20 °C the measured vapor pressure of pentachlorophenol is 2 Pa, whereas, calculated value is 68 Pa.

-For Tebuconazole Antoine constants are not available, however, two experimental points have been reported (Gründlinger and Exner, 1990):

T, K	P^{vap} (bar)
293	7.2×10^{-12}
333	4.5×10^{-9}

Using a two paramter relationship for vapor and temperature:

$$\ln P^{vap} = A - \frac{B}{T} \qquad \text{(E-2)}$$

For a two-parameter form of P^{vap} - T relationship the constants A and B will be 27.937 and 15703.12.

Vapor pressure for biocides can be measured using the gas saturation method (Sonnefeld, et al, 1983) where a known mass of nitrogen flows through a saturator for a long period. The dissolved solute is collected in a liquid solvent and the concentration is analyzed using a GC. The concentration is used in a mass balance to evaluate the vapor pressure.

APPENDIX F

Distribution of TCMTB in SCF-Treated Douglas-fir Blocks

Table F.1 Retentions of TCMTB in Douglas-fir blocks (38x38x100 mm) treated for 30 minutes at 50°C and selected pressures

Pressure bar	Retentions at an Average Depth, mm (average of 6 blocks)				Estimated* surface-center retention ratio
	19	12	7	2	
140	0.067 ± 0.038	0.134 ± 0.076	0.131 ± 0.10	1.173 ± 0.61	30.8
170	0.190 ± 0.073	0.334 ± 0.121	0.324 ± 0.071	1.76 ± 0.676	9.26
210	0.205 ± 0.09	0.262 ± 0.070	0.570 ± 0.100	2.25 ± 0.80	10.8
240	0.423 ± 0.108	0.475 ± 0.121	1.050 ± 0.094	2.18 ± 0.74	5.17
270	0.634 ± 0.270	0.593 ± 0.127	1.690 ± 0.184	2.14 ± 0.88	3.37

* Averages of 6 individual outermost / innermost retentions

Table F.2 **Retention of TCMTB in Douglas-fir blocks (38x38x100 mm) treated at 240 bar and 50°C for selected treatment periods**

Time min	Retentions at an Average Depth, mm (average of 6 blocks)				Surface-Center Retention Ratio
	19	12	7	2	
5	0.153 ± 0.073	0.261 ± 0.080	0.467 ± 0.04	1.193 ± 0.035	7.8
15	0.380 ± 0.070	0.292 ± 0.148	0.603 ± 0.012	1.95 ± 0.36	5.2
30	0.423 ± 0.108	0.475 ± 0.121	1.050 ± 0.094	2.18 ± 0.74	5.17
60	0.515 ± 0.160	0.750 ± 0.124	1.218 ± 0.180	1.948 ± 0.68	3.79
90	0.896 ± 0.247	1.106 ± 0.538	1.388 ± 0.345	4.92 ± 0.98	4.22

Table F.3 Retentions of TCMTB in different size blocks treated for 60 min at 248 bar and 50°C.

Size mm	Retentions at an Average Depth, mm (average of 8 blocks)						Surface-center retention estimated ratio
	19	**14.25**	**11.08**	**7.91**	**4.75**	**1.58**	
38	0.472 ± 0.216	0.588 ±0.301	0.811 ± 0.466	0.855 ± 0.398	2.121 ± 0.429	2.81 ± 1.81	5.95
25.4	**12.7**	**7.94**	**4.76**	**1.58**			S/C Ratio
	0.902 ± 0.341	0.894 ± 0.361	1.549 ± 0.179	2.805 ± 1.82			3.10
19	**9.5**	**4.75**	**1.58**				S/C Ratio
	1.456 ± 0.387	2.115 ± 0.307	2.72 ± 3.37				1.86

Appendix G

Measuring Density and Permeability of Wood Samples

G-1 Density of Wood

Blocks from three different species were conditioned to a moisture content of 12 % before their density and permeabilities were measured. The densities of the blocks were obtained from their weight and their volume (Table H-1).

G-2 Permeabilities of Wood

Steady-state flow of fluids through wood obeys Darcy's law. Darcy's law (Darcy, 1856) relates the volumetric flow rate, Q, of a fluid flowing linearly through a porous medium directly to the energy loss, inversely to the length of the medium, and proportionally to a factor called the permeability, K. Darcy's law is expressed for gases as:

$$K_g = \frac{\mu Q L P}{A \Delta P \bar{P}}$$

where P is pressure at which the flow rate Q is measured, ΔP is pressure difference, $\bar{P}$ is arithmetic average pressure in the specimen, A and L are area and length of the specimen and μ is the fluid viscosity.

Table G.1 Estimating densities of wood samples

Species	Volume, cm^3	weight, g	Density, g/cm^3
Douglas-fir	36.419	16.471	0.452
	37.302	15.864	0.432
	36.101	16.104	0.439
	36.220	15.915	0.439
	36.525	15.915	0.436
	37.283	17.865	0.479
	36.496	16.216	0.439
	36.537	15.853	0.434
			0.444 ± 0.014
Loblolly Pine	37.305	19.801	0.530
	37.784	19.820	0.524
	37.991	19.420	0.511
	36.489	17.512	0.480
	37.089	18.314	0.494
	37.532	18.552	0.494
	35.823	18.491	0.496
	37.705	19.318	0.512
			0.505 ± 0.015
Southern Pine	36.992	26.012	0.703
	37.302	20.334	0.545
	37.672	20.246	0.537
	36.488	20.421	0.559
	37.921	19.862	0.524
	37.430	26.950	0.720
	36.568	24.702	0.675
	34.849	26.140	0.752
			0.626 ± 0.088

Darcy's law is considered to be valid for creeping or highly viscous flow through the pores of a permeable structure, where $K^{1/2}$ is the length scale representative of the effective pore diameter (Bejan, 1984). Using $K^{1/2}$ as a length scale to define Reynolds number

$$Re = \frac{u \rho K^{1/2}}{\mu}$$

Darcy's law is considered to be valid at O(Re) < 1 where the resistance to flow is due to viscous forces only.

Apparatus

A schematic drawing of the flow-measurement apparatus is shown in Figure G-1. Air flows at constant pressure from a storage cylinder via a two stage pressure regulator. A differential mercury manometer was connected to the gas line to measure the initial pressure on the inlet side and the pressure drop across the test sample. The pressure at the outlet side was measured using water manometer. The test cell consisted of a rubber stopper that hold the specimen. Flow rate was measured using a soap film flow meter (HP 0101-0113) similar to that used by Siau (1971). Calibrated with digital flow meter (McMillan, model 310-3). Bubble flow meters are accurate for steady state flow but are not recommended for unsteady state flow where the pressure changes as the bubble rises in the tube.

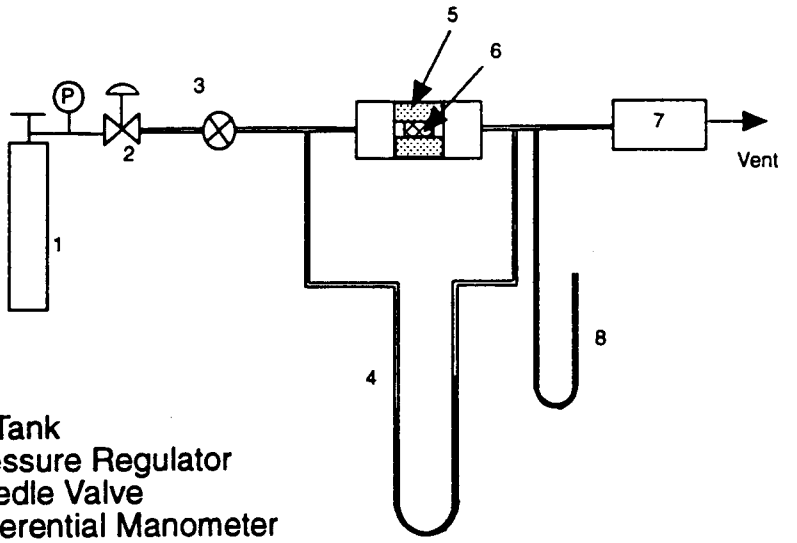

1 AirTank
2. Pressure Regulator
3. Needle Valve
4. Differential Manometer
5. Rubber Stopper
6. Test Sample
7. Flow Meter
8. Water Meter

Figure G-1 Schematics of permeability measurement apparatus

Table G-2 Permeability of southern pine samples

Dowel number	Permeability $cm^3/cm\ atm.s$	Darcy
1	0.8922	0.000692
2	1.6999	0.000556
3	0.1488	4.87×10^{-4}
4	0.2076	6.79×10^{-4}
5	0.8941	0.000292
6	1.5967	0.000722
7	0.5581	0.000183

Average = 0.06719 ± 0.045 cm3/s.cm.bar

Table G.3 Permeability of Douglas-fir samples

Permeabiity of Douglas -fir dowels								
Dowel #	Permeab.	Variance	Dowel #	Permeab.	variance	Dowel #	Permeab.	variance
	Darcy			Darcy			Darcy	
1	0.000551	2.1E-06	36	0.002232	5.45E-08	71	0.001081	8.42E-07
2	0.001587	1.69E-07	37	0.002254	6.53E-08	72	0.001135	7.46E-07
3	0.000908	1.19E-06	38	0.00228	7.92E-08	73	0.001192	6.5E-07
4	0.002207	4.35E-08	39	0.002289	8.44E-08	74	0.001331	4.46E-07
5	0.001043	9.13E-07	40	0.002452	2.06E-07	75	0.001465	2.85E-07
6	0.002034	1.26E-09	41	0.002522	2.74E-07	76	0.001455	2.95E-07
7	0.001889	1.2E-08	42	0.002116	1.38E-08	77	0.001483	2.66E-07
8	0.00122	6.06E-07	43	0.002547	3.01E-07	78	0.001561	1.91E-07
9	0.000842	1.34E-06	44	0.002601	3.63E-07	79	0.001581	1.74E-07
10	0.000956	1.09E-06	45	0.002616	3.81E-07	80	0.001604	1.56E-07
11	0.001097	8.13E-07	46	0.002819	6.73E-07	81	0.001894	1.09E-08
12	0.002788	6.23E-07	47	0.002859	7.4E-07	82	0.001826	2.98E-08
13	0.000343	2.74E-06	48	0.002879	7.75E-07	83	0.001817	3.29E-08
14	0.00399	3.97E-06	49	0.002925	8.58E-07	84	0.001888	1.22E-08
15	0.004917	8.52E-06	50	0.002962	9.28E-07	85	0.001885	1.29E-08
16	0.001205	6.3E-07	51	0.000487	2.28E-06	86	0.001653	1.19E-07
17	0.000807	1.42E-06	52	0.000512	2.21E-06	87	0.001671	1.07E-07
18	0.000955	1.09E-06	53	0.000513	2.21E-06	88	0.001676	1.04E-07
19	0.004374	5.64E-06	54	0.00533	1.11E-05	89	0.001755	5.93E-08
20	0.001857	2E-08	55	0.000614	1.92E-06	90	0.001817	3.29E-08
21	0.004664	7.1E-06	56	0.00069	1.71E-06	91	0.002971	9.46E-07
22	0.002348	1.22E-07	57	0.000695	1.7E-06	92	0.003002	1.01E-06
23	0.000936	1.13E-06	58	0.00715	2.65E-05	93	0.003013	1.03E-06
24	0.001831	2.81E-08	59	0.000719	1.64E-06	94	0.003024	1.05E-06
25	0.00159	1.67E-07	60	0.000746	1.57E-06	95	0.003061	1.13E-06
26	0.002124	1.58E-08	61	0.000749	1.56E-06	96	0.002641	4.13E-07
27	0.000735	1.6E-06	62	0.000752	1.55E-06	97	0.001192	6.5E-07
28	0.000844	1.33E-06	63	0.000753	1.55E-06	98	0.003457	2.13E-06
29	0.001378	3.85E-07	64	0.000852	1.31E-06	99	0.003503	2.26E-06
30	0.002758	5.77E-07	65	0.000852	1.31E-06	100	0.003695	2.88E-06
31	0.001937	3.78E-09	66	0.000854	1.31E-06	101	0.003858	3.46E-06
32	0.001966	1.06E-09	67	0.000884	1.24E-06	102	0.003971	3.89E-06
33	0.001961	1.41E-09	68	0.000913	1.18E-06	103	0.004324	5.41E-06
34	0.001986	1.56E-10	69	0.000948	1.1E-06	104	0.004691	7.25E-06
35	0.002011	1.56E-10	70	0.001053	8.94E-07	105	0.000594	1.97E-06
					avg= 0.001998			
					sd=0.001229			

Appendix H

Instrument and Pump Calibration

Calibration procedures and tables for cosolvent pump, pressure gauges, flow meters and thermocouple used in this study are presented below.

Cosolvent Pump

Cosolvent was delivered using a reciprocating duplex plunger pump (miniPump Model 2396) which was designed to produce liquid flow in the in precise quantities (1% cylinder volume) against positive pressure up to 324 bar. The pump was equipped with two micrometer dials that controled stroke length of the two plungers, which in turn controled the flow rate. Discharge rate of the pump was measured at different dial positions, by collecting the discharge flow for a given period. Calibration result using methanol are shown (Table H.1 and Figure H.1). The flow rate was approximated by the dial position using the calibration equation provided below.

$$Flow = 0.132x - 0.287 \quad (1)$$

where x is the microdial position.

Table H.1 Calibration of metering pump (miniPump Model 2396-57)

Dial Position	Collection Time min	Volume ml	Flow rate ml/min
0	24	1.1	0.048
5	12.5	6.1	0.49
10	14.0	19	1.36
20	6.0	9	1.50
30	6.0	20.5	3.42
40	5.0	22.5	4.50
50	5.1	32	6.32
70	4.0	36.5	9.10
80	2.5	26	10.4
100	3.0	24	8.0

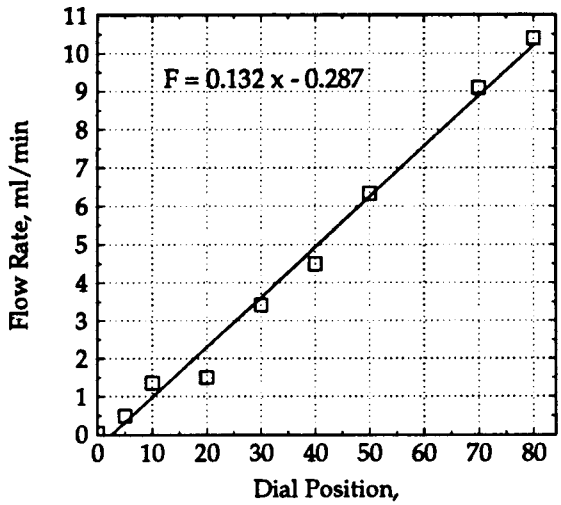

Figure H-1 Cosolvent flow rate *vs* pump dial position.

Pressure

The treatment vessel and separator of the pilot plant were equipped with pressure transducers (Ashcroft Model K2) that were connected to digital displays (Omega DP41-V). The transducers had a range of 0 - 650 bar with accuracies of 1% of the scale. The transducers were calibrated using a Heise pressure gauge (Heise Model 901), that was calibrated by the manufacturers according to the National Bureau of Standard. The calibration for treatment vesssel gauge (Table H.2) shows the treatment vessel pressure transducer was off by a constant amount of 4.5 bar.

Temperature

Calibration of thermocouples was made using thermocouple calibrator (Omega HH20-CAL) connected to Omega Microprocessor thermometer (HH23). The calibrator has an accuracy of 0.3% rdg. The calibration results are shown in Table H.2. The average deviation for all the thermocouples were about 1°C.

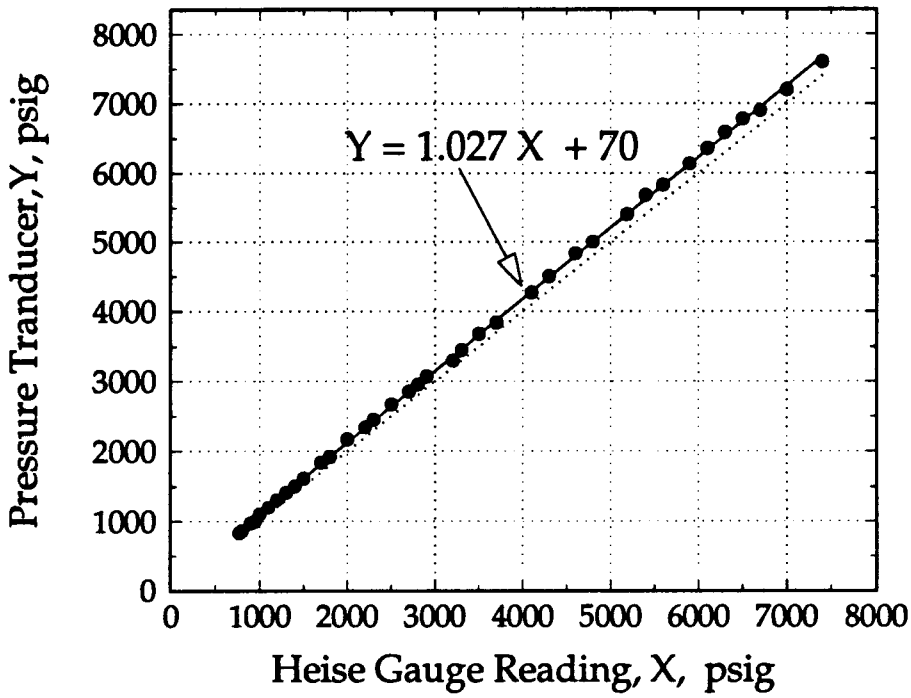

Figure H.2 Calibration of treatment vessel pressure gauge.

Table H.2 Calibration of thermocouples used in the pilot plant

Calibrator temperature °C	Thermocouple 1* °C	Thermocouple 2 °C	Thermocouple 3 °C
12	13	12	12
16	17	17	16
20	18	20	20
25	24	25	25
30	30	30	30
35	36	35	35
50	55	50	49
60	66	60	59
70	70	70	70
75	74	75	75
80	79	80	80

* Thermocouple 1,2 and 3 are J type thermocouples used in the saturator, the separator and treatment vessels.

Appendix I

Listing of Computer Programs

A computer program to calculate retention of a chemical within a solid matrix is presented in Table K.1. The program solves transient compressible flow of carbon dioxide through a semi-porous solid of constant permeability and porosity. The porous media was assumed to be at constant temperature through out the process. Initially the pressure in the cross section of the media was assumed to be constant and uniform. The pressure variation the vessel was as given in Figure 5.2 was considered as boundary conditions to solve the governing differential equation. Modified BWR equation of state (Ely, 1986) was used to compute transient variations of density and compressibility of the treatment fluid and changes in viscosity were computed using equation by Yoon and Thodos, 1970. Approximate solution of the differential equations was obtained by evaluating the derivatives in terms of finite differences and integrating numerically by means of the resulting difference equations. To solve the equation 7.17, a difference equation was established by dividing the solid matrix using a mesh width $\Delta x'$ and $\Delta y'$, and integrating in time steps of $\Delta\tau$. For the computed density equilibrium solubility of the TCMTB was calculated using the fluid density-based correlation as shown in Section 4.2. Deposition of the chemical was estimated based on the assumption that precipitation was fast to prevent supersaturation.

```
      PROGRAM DEPOSITION
C
C     THIS PROGRAM CALCULATES THE UNSTEADY STATE VARIATION OF PRESSURE
C     IN  POROUS MEDIUM . FOR THE FLOW OF DENSE GASES
C     CONTINUITY EQUATION AND DARCY'S LAW WERE SOLVED WITH
C     REDLICH-KWONG STATE TO RELATE PRESSURE AND DENSITY. THE MEDIUM
C     PERMEABILTY AND POROSITY ARE TAKEN TO BE CONSTANT.
C     THE SYSTEM IS ASSUMED TO BE AT CONSTANT TEMPERATURE.
C
C
c .....................................................................
C
C     DEFINITION OF VARIABLES
C          CON1 AND CON2 = CONSTANTS FOR REDLICH-KWONG EQUATION
C
C          T = TEMPERATURE
C          TCR = CRITICAL TEMPERATURE
C          PCR = CRITICAL PRESSURE
C          WTMOL= GRAM MOLECULAR WEITGHT
C          POR = POROSTIY OF THE MEDIUM
C          R  = UNIVERSAL GAS CONSTANT FOR CO2
C          DEN = DENSITY OF THE GAS
C          DENCR = CRITICAL DENSITY OF THE GAS
C          DERD = REDUCED DENSITY FO THE GAS
C          DBC  = BOUNDARY DENSITY
C          PERM = PERMEABILITY OF THE MEDIUM
C          VISC = VISCOSITY OF THE FLUID
C
C
      IMPLICIT DOUBLE PRECISION (A-H,O-Z)
      DIMENSION P(50,50), VINV(50,50), ZINV(50,50)
      COMMON /HIN/  ZINV, VINV, ROCR, ZIV, VNV
      CHARACTER*10 FNAME1, FNAME2
      WRITE(*,*) 'DO YOU WANT TO USE DEFAULT VALUES, YES= 1,NO=2'
      READ(*,*) KCH
      IF(KCH .EQ. 1) THEN
       GO TO 5
      ELSE
       GO TO 6
      END IF
C
C      WRITE(*,*) 'ENTER TEMPERATURE OF THE SYSTEM'
C      READ(*,*)  T
 6    WRITE(*,*) 'ENTER INITIAL PRESSURE TREATEMENT CHAMBER'
      READ(*,*)  PIN
      WRITE(*,*) 'ENTER RATE OF PRESSURE INCREASE, Bar/Min'
      READ(*,*)  PC
      WRITE(*,*) 'ENTER THE INTEGRATION TIME INTERVAL, TOU IN MIN'
      READ(*,*)  TOU
      WRITE(*,*) 'ENTER THE TIME FOR PRESSURE BUILD UP IN MIN'
      READ(*,*)  TON
```

```
      WRITE(*,*) 'ENTER THE TIME FOR CONSTANT PRESSURE IN MIN'
      READ(*,*)  TPROC
      WRITE(*,*) 'ENTER RATE OF DEPRESSURIZATION AFTER Pcon,bar/min'
      READ(*,*)  CP
      WRITE(*,*) 'ENTER THE DEPRESSURIZATION TIME AND TOTAL IN MIN'
      READ(*,*)  TDEPR, TFINAL
      WRITE(*,*) 'ENTER D/L^2 = PHI VALUE'
      READ(*,*)  PHIA
      WRITE(*,*) 'ENTER THE OUT PUT FILE NAME'
      READ(*,1)  FNAME1
    1 FORMAT(A)
C
      T = 323
      TOU = PHIA*TOU
      PC  = PC/PHIA
      CP  = CP/PHIA
      TON = PHIA*TON
      TPROC = PHIA*TPROC
      TDEPR = PHIA*TDEPR
      TFINAL= PHIA*TFINAL
      XL = 1.0
      DELX = 0.025
      GO TO 7
    5 TON = 10
      TRPOC  = 40
      CP     = 24.9
      TDEPR  = 50
      TFINAL = 60
      XL     = 4
      DELX   = 0.2
      PERM = 5E-14
C
    7 POR  = 0.6
      PVAP  = 2.56E-5
      PHI  = PERM/(2*POR)
         TIME  = 0.
         ITR   = 0.
         ICOUNT = 1
         IK   = INT(XL/DELX)
         RO   = 2
         ROCR = 10.6
         TCR  = 304.21
         PCR  = 73.84325
         R    = 0.08314
C
      OPEN (2, FILE=FNAME1, STATUS='NEW')
C*********************************
C    INITIAL CONDITIONS                    *
C*********************************
C
      CALL DENSITY (T,PIN,RO)
```

```
      CALL VISCOS (T,RO)
       WRITE(*,*) 'LINE 104', VNV,ZIV
      DO 10    IP   = 1, IK+1
        DO 11  JP   = 1, IK+1
             P(IP,JP) =  PIN
             ZINV(IP,JP) = ZIV
             VINV(IP,JP) = VNV
   11 CONTINUE
   10 CONTINUE
C
C ***********************************
C     BOUNDARY CONDITIONS                    *
C ***********************************
C
30       ITR = ITR + 1
      IF (TIME .LE. TON) THEN
        DO 12 I = 1, IK+1
          P(I,1)   = P(I,1)   + PC*TOU
          P(I,IK+1)= P(I,IK+1)+ PC*TOU
   12   CONTINUE
        DO 13 J = 1, IK+1
          P(1,J)   = P(1,J)   + PC*TOU
          P(IK+1,J)= P(IK+1,J)+ PC*TOU
   13   CONTINUE
      ELSE IF(TIME .GT. TON .AND. TIME .LE. TPROC) THEN
        DO 14 J = 1, IK+1
          P(1,J) = P(1,J)
          P(IK+1,J)= P(IK+1,J)
   14   CONTINUE
        DO 15 I = 1, IK+1
          P(I,1)   = P(I,1)
          P(I,IK+1)= P(I,IK+1)
   15 CONTINUE
      ELSE IF(TIME .GT. TPROC .AND. TIME .LE. TDEPR) THEN
        DO 16 I = 1, IK+1
          P(I,1)   = P(I,1) - CP*TOU
          P(I,IK+1)= P(I,IK+1)- CP*TOU
   16 CONTINUE
        DO 17 J = 1, IK+1
          P(1,J)   = P(1,J) - CP*TOU
          P(I,IK+1)= P(IK+1,J)- CP*TOU
   17 CONTINUE
      ELSE
        DO 18 I = 1, IK+1
          P(I,1)   = PIN
          P(I,IK+1)= PIN
   18 CONTINUE
        DO 19 J = 1, IK+1
          P(1,J)   = PIN
          P(IK+1,J)= PIN
   19 CONTINUE
```

```
      ENDIF
C
      PBND1 = P(1,1)
      CALL DENSITY (T,PBND1,RO)
      CALL VISCOS (T,RO)
      DO 20 J = 1, IK+1
         ZINV(1,J)    = ZIV
         ZINV(IK+1,J) = ZIV
         VINV(1,J)    = VNV
         VINV(IK+1,J) = VNV
   20 CONTINUE
      DO 21 I = 1, IK+1
          ZINV(I,1)    = ZIV
          ZINV(I,IK+1) = ZIV
          VINV(I,1)    = VNV
          VINV(I,IK+1) = VNV
   21 CONTINUE
C
   32 DO 39 IY = 2, IK
      DO 35 IX = 2, IK
           IXP1 = IX + 1
           IXM1 = IX - 1
           IYP1 = IY + 1
           IYM1 = IY - 1
C
C ********************************************************
C     START THE FINITE DIFFERENCE APPROXIMATION OF THE PDE *
C ********************************************************
C
      YLAMDA = TOU/(DELX**2)
      TERM2 = YLAMDA
      PTRM1 = P(IXM1,IY)**2 - 2*P(IX,IY)**2 + P(IXP1,IY)**2
      PTRM2 = P(IXP1,IY)**2 - P(IXM1,IY)**2
      ZTRM1 = ZINV(IXP1,IY) - ZINV(IXM1,IY)
      VIS1  = VINV(IXP1,IY) - VINV(IXM1,IY)
      VISR  = 210*VINV(IX,IY)
      write(*,*) ziv, vinv(ix,iy)
      TERM3 = TERM2*VISR*(PTRM1+PTERM2*(ZTRM1/ZIV+VIS1/VINV(IX,IY)))
      WRITE(*,*) 'LINE 194'
C
C     CRITICAL VISCOSITY IS 210 MILLIPOIS (mP)
C
      PTRM3 = P(IX,IYM1)**2 - 2*P(IX,IY)**2 + P(IX,IYP1)**2
      PTRM4 = P(IX,IYP1)**2 - P(IX,IYM1)**2
      ZTRM2 = ZINV(IX,IYP1) - ZINV(IX,IYM1)
      VIS2  = VINV(IX,IYP1) - VINV(IX,IYM1)
      TERM9 = TERM2*VISR*(PTRM3+PTERM4*(ZTRM2/ZIV+VIS1/VINV(IX,IY)))
C
      PTT   = TERM3 + TERM9 + P(IX,IY)
      ZT0   = ZIV
   33 CALL DENSITY (T,PTT,RO)
```

```
      ZDIF = (ZIV-ZINV(IX,IY))/ZT0
C     WRITE(*,*) 'ZT0,ZIV',ZT0,ZIV
      PIT = PTT - ZDIF
      IF(ABS(P(IX,IY)-PIT) .LT. 0.01) THEN
         GO TO 34
       ELSE
         P(IX,IY) =  PIT
         GO TO 33
       ENDIF
   34 P(IX,IY) = PIT
       CALL DENSITY (T,PIT,RO)
       CALL VISCOS (T,RO)
       ZINV(IX,IY) = ZIV
       VINV(IX,IY) = VNV
       WRITE (*,*) 'LINE 219'
   35 CONTINUE
   39 CONTINUE
C
      XDF =  FLOAT(ITR/10)*10
      IF(XDF .EQ. FLOAT(ITR) ) THEN
       TM = TIME/PHIA
       WRITE(*,50) TM, (P(I,20), I = 1,10)
       WRITE(*,50) TM, (P(I,20), I = 11,20)
      ENDIF
   50 FORMAT(2X, F9.6, 10(1X,F5.1))
   36 FORMAT(2X,'TIME=',F10.5,2X,'P0=', F12.5,2X,'PM=',F12.5,2X,F12.5)
C
      IF (TM .GT. TON .AND. ABS(TM-(JK+10)) .LT. 0.1) THEN
        CALL RETENTION (P,T,RO,TM,RETEN)
       WRITE(2,144) TM,RETEN
  144   FORMAT(2X, 2(F8.4,2X))
       JK = JK + 1
      ENDIF
      TIME   = TIME + TOU
      IF (TIME .GT. TFINAL) THEN
      GO TO 40
      ELSE
      GO TO 30
      END IF
C
      CLOSE(2)
   40 DO 45 I = 1, IK+1
        DO 49 J = 1, IK+1
      XLOC = FLOAT(I-1)/IK
      CALL DENSITY (T, P(I,J), RO)
   46 FORMAT(3(2X,F11.4),2X,E6.2 )
   49 CONTINUE
   45 CONTINUE
      WRITE(*,47) T,PIN,PC,TOU,TON,TPROC,TDEPR,TFINAL,XL,DELX
   47 FORMAT(2X, 'SYSTEM TEMPRETURE      =', F12.5,/
     &       2X, 'INITIAL PRESSURE       =', F12.5,/
```

```
     &      2X, 'RATE OF PRES. INCREASE = ',F12.5,/
     &      2X, 'INTIGRATION TIME       = ',F12.5,/
     &      2X, 'PRESSURE INCREASE TIME = ',F12.5,/
     &      2X, 'CONSTANT PRESSURE TIME = ',F12.5,/
     &      2X, 'DEPRESSURIZATION TIME  = ',F12.5,/
     &      2X, 'TIME TO STOP           = ',F12.5,/
     &      2X, 'BLOCK LENGTH           = ',F12.5,/
     &      2X, 'SPATIAL INTERVAL       = ',F12.5)
      STOP
      END
C
C

      SUBROUTINE DENSITY (T,PRES,RO)
C     THIS PROGRAM USES MODIFIED BENEDICT-WEBB-RUBIN EQUATION
C     COMPRESSIBILITY FACTOR. THE COEFFICIENTS FOR EQUATION
C     FOR CARBON DIOXIDE.  THE RANGE OF APPLICATION IS
C     TEMP= 215 - 1100K, PRES= UP TO 3000 BAR
C
C
      IMPLICIT DOUBLE PRECISION (A-H,O-Z)
      DIMENSION B(32), A(15),P(50,50), VINV(50,50), ZINV(50,50)
      COMMON /HIN/  ZINV, VINV, ROCR, ZIV, VNV

C
C.... UNITS DENSITY     MOL/L
C           TEMPERATURE K
C           PRESSURE    BAR
C           GAS CONST   BAR.L/MOL.K
C.....CRITICAL CONSTANTS
C
      TCR  = 304.21
      PCR  = 73.84325
      R    = 0.08314
      ESP1  = 0.00001
      NITER1= 100
      NC1 = 0
c     WRITE(*,*)  '         RO       XP1         ERROR'
c     write(*,*) 'subroutine density called'
C.... Parameters and coefficients
C
      B(1) = -0.9818510658E-2
      B(2) =  0.9950622673E+0
      B(3) = -0.2283801603E+2
      B(4) =  0.2818276345E+4
      B(5) = -0.3470012627E+6
      B(6) =  0.3947067091E-3
      B(7) = -0.3255500001E+0
      B(8) =  0.4843200831E+1
      B(9) = -0.3521815430E+6
      B(10)= -0.3240536033E-4
```

```
      B(11)=  0.4685966847E-1
      B(12)= -0.7545470121E+1
      B(13)= -0.3818943540E-4
      B(14)= -0.4421929339E-1
      B(15)=  0.5169251681E+2
      B(16)=  0.2124509852E-2
      B(17)= -0.2610094748E-4
      B(18)= -0.8885333890E-1
      B(19)=  0.1552261794E-2
      B(20)=  0.4150910049E+6
      B(21)= -0.1101739675E+8
      B(22)=  0.2919905833E+4
      B(23)=  0.1432546065E+8
      B(24)=  0.1085742075E+2
      B(25)= -0.2477996570E+3
      B(26)=  0.1992935908E-1
      B(27)=  0.1027499081E+3
      B(28)=  0.3776188652E-4
      B(29)= -0.3322765123E-2
      B(30)=  0.1791967071E-7
      B(31)=  0.9450766278E-5
      B(32)= -0.1234009431E-2
      GAMA =  0.8899964400E-2
C
C
      A(1) = R*T
      A(2) = B(1)*T + B(2)*T**0.5 + B(3) + B(4)/T + B(5)/T**2
      A(3) = B(6)*T + B(7) + B(8)/T + B(9)/T**2
      A(4) = B(10)*T + B(11) + B(12)/T
      A(5) = B(13)
      A(6) = B(14)/T + B(15)/T**2
      A(7) = B(16)/T
      A(8) = B(17)/T + B(18)/T**2
      A(9) = B(19)/T**2
      A(10) = B(20)/T**2 + B(21)/T**3
      A(11) = B(22)/T**2 + B(23)/T**4
      A(12) = B(24)/T**2 + B(25)/T**3
      A(13) = B(26)/T**2 + B(27)/T**4
      A(14) = B(28)/T**2 + B(29)/T**3
      A(15) = B(30)/T**2 + B(31)/T**3 + B(32)/T**4
C
    5 NC1 = NC1 + 1
      SUM1 = 0.0
      SUM2 = 0.0
      SUM3 = 0.0
      SUM5 = 0.0
      DO 100 I = 1, 9
            TERM1 = A(I)*RO**I
            TERM2 = A(I)*I*RO**(I-1)
            SUM1= SUM1 + TERM1
            SUM2= SUM2 + TERM2
```

```
  100 CONTINUE
      DO 110 I = 10, 15
           TERM3 = A(I)*RO**(2.*I-17.)
           TERM5 = A(I)*(2.*I-17.)*(RO**(2.*I-18.))
           SUM3 = SUM3 + TERM3
           SUM5 = SUM5 + TERM5
  110  CONTINUE
       SUM3 = EXP(-GAMA*RO**2.)*SUM3
       SUM4 = 2.*RO*GAMA*SUM3
       SUM5 = EXP(-GAMA*RO**2.)*SUM5
C
       FOFX = PRES - SUM1 - SUM3
       FOFDX= -SUM2 + SUM4 - SUM5
       ROP1 = RO - FOFX/FOFDX
       ERROR = ROP1 - RO
       IF (ABS(ERROR) .GT. ESP1 .AND. NC .LT. NITER1) THEN
       RO = ROP1
       GO TO 5
       ELSE
       GOTO 120
       ENDIF
c      WRITE(*,*) 'NUMBER OF ITERATIONS',NC
  120  NC = 0
       Z = PRES/(RO*R*T)
c      WRITE(*,121) T, PRES,RO,Z
       ZIV = 1/Z
       write(*,*) 'line385', ziv
  121  FORMAT(2X, 4F12.4)
C  122 FORMAT(2X, 'T=',F10.3,2X,'PRES=',F10.3,2X,'RO=',
C     &   F10.3,1X,'Z=',F10.3)
C
       RETURN
       END
C
C
       SUBROUTINE VISCOS (T,RO)
C      THIS PROGRAM USES MODIFIED BENEDICT-WEBB-RUBIN EQUATION
C      COMPRESSIBILITY FACTOR. THE COEFFICIENTS FOR EQUATION
C      FOR CARBON DIOXIDE.  THE RANGE OF APPLICATION IS
C      TEMP= 215 - 1100K, PRES= UP TO 3000 BAR
C
C
       IMPLICIT DOUBLE PRECISION (A-H,O-Z)
       DIMENSION P(50,50), VINV(50,50), ZINV(50,50)
       COMMON /HIN/  ZINV, VINV, ROCR, ZIV, VNV

C
C.... UNITS DENSITY     MOL/L
C           TEMPERATURE K
C           PRESSURE    BAR
C           GAS CONST   BAR.L/MOL.K
```

```
C.....CRITICAL CONSTANTS
      TCR  = 304.21
      PCR  = 73.84325
      R    = 0.08314
      TR   = T/TCR
      WM   = 44.009
      ESP  = 0.00001
      NITER= 100
c      write(*,*) 'subroutine viscous called'
C
C     VICOSITY CALCULATIONS
C
      DENS = RO
      ETA0 = 0.435488*T + 19.25
      PCR  = PCR*0.986923
      ROCR = 10.59
      PSIA = (TCR**0.16666)*(WM**(-0.5))*(PCR**(-0.66667))
      RORD = DENS/ROCR
      IF (RORD .LE. 0.1) THEN
        TERM1 = 4.610*TR**0.618 - 2.04*DEXP(-0.449*TR)
     &    + 1.94*DEXP(-4.058*TR) + 0.1
        ETA = TERM1/PSIA
       ELSE
        TERM2 = 1.023 + 0.23364*RORD + 0.58533*RORD**2 -
     &          0.40758*RORD**3 + 0.093324*RORD**4
        ETA   = (TERM2**4 - 1)/PSIA + ETA0
        ENDIF
        DENSTY = RO*WM
       WRITE(*,*) ' LINE 435',ETA, DENSTY
       VNV = 1/ETA
C
      RETURN
      END
C
C
      SUBROUTINE RETENTION (P,T,RO,TM,RETEN)
C
C     THIS PROGRAM USES MODIFIED BENEDICT-WEBB-RUBIN EQUATION
C     COMPRESSIBILITY FACTOR. THE COEFFICIENTS FOR EQUATION
C     FOR CARBON DIOXIDE.  THE RANGE OF APPLICATION IS
C     TEMP= 215 - 1100K, PRES= UP TO 3000 BAR
C
C
C
      IMPLICIT DOUBLE PRECISION (A-H, O-Z)
      DIMENSION B(32),A(15),P(100),XL(40),DENS(100),SOL(100),RETN(100)
      CHARACTER*10 FNAMEi
C      WRITE(*,*) 'ENTER THE CONSTANT OF SOLUBILITY EQUATION'
C      READ(*,*)   ALPHA, BETA
      ALPHA = 9.12869
      BETA  = -3.3139
```

```
C
      DO 7 I = 1,21
      WRITE(*,6) P(I)
   6  FORMAT(1X,F5.3,1X,7(2X,F6.2))
   7  CONTINUE
C
C.... UNITS DENSITY    MOL/L
C        TEMPERATURE K
C        PRESSURE   BAR
C        GAS CONST  BAR.L/MOL.K
C.....CRITICAL CONSTANTS
     ROCR = 10.6
     TCR  = 304.21
     PCR  = 73.84325
     R    = 0.08314
     ESP  = 0.00001
     NITER= 100
     NC = 0
     WRITE(*,*)  '        PRES     RO      XP1       ERROR'
C.... Parameters and coefficients
C
     B(1) = -0.9818510658E-2
     B(2) =  0.9950622673E+0
     B(3) = -0.2283801603E+2
     B(4) =  0.2818276345E+4
     B(5) = -0.3470012627E+6
     B(6) =  0.3947067091E-3
     B(7) = -0.3255500001E+0
     B(8) =  0.4843200831E+1
     B(9) = -0.3521815430E+6
     B(10)= -0.3240536033E-4
     B(11)=  0.4685966847E-1
     B(12)= -0.7545470121E+1
     B(13)= -0.3818943540E-4
     B(14)= -0.4421929339E-1
     B(15)=  0.5169251681E+2
     B(16)=  0.2124509852E-2
     B(17)= -0.2610094748E-4
     B(18)= -0.8885333890E-1
     B(19)=  0.1552261794E-2
     B(20)=  0.4150910049E+6
     B(21)= -0.1101739675E+8
     B(22)=  0.2919905833E+4
     B(23)=  0.1432546065E+8
     B(24)=  0.1085742075E+2
     B(25)= -0.2477996570E+3
     B(26)=  0.1992935908E-1
     B(27)=  0.1027499081E+3
     B(28)=  0.3776188652E-4
     B(29)= -0.3322765123E-2
     B(30)=  0.1791967071E-7
```

```
      B(31)=  0.9450766278E-5
      B(32)= -0.1234009431E-2
      GAMA =  0.8899964400E-2
C
      A(1) = R*T
      A(2) = B(1)*T + B(2)*T**0.5 + B(3) + B(4)/T + B(5)/T**2
      A(3) = B(6)*T + B(7) + B(8)/T + B(9)/T**2
      A(4) = B(10)*T + B(11) + B(12)/T
      A(5) = B(13)
      A(6) = B(14)/T + B(15)/T**2
      A(7) = B(16)/T
      A(8) = B(17)/T + B(18)/T**2
      A(9) = B(19)/T**2
      A(10) = B(20)/T**2 + B(21)/T**3
      A(11) = B(22)/T**2 + B(23)/T**4
      A(12) = B(24)/T**2 + B(25)/T**3
      A(13) = B(26)/T**2 + B(27)/T**4
      A(14) = B(28)/T**2 + B(29)/T**3
      A(15) = B(30)/T**2 + B(31)/T**3 + B(32)/T**4
C
       DO 130 IP = 1, 21
    5  NC = NC + 1
      SUM1 = 0.0
      SUM2 = 0.0
      SUM3 = 0.0
      SUM5 = 0.0
      DO 100 I = 1, 9
            TERM1 = A(I)*RO**I
            TERM2 = A(I)*I*RO**(I-1)
            SUM1= SUM1 + TERM1
            SUM2= SUM2 + TERM2
  100 CONTINUE
      DO 110 I = 10, 15
            TERM3 = A(I)*RO**(2.*I-17.)
            TERM5 = A(I)*(2.*I-17.)*(RO**(2.*I-18.))
            SUM3 = SUM3 + TERM3
            SUM5 = SUM5 + TERM5
  110  CONTINUE
       SUM3 = EXP(-GAMA*RO**2.)*SUM3
       SUM4 = 2.*RO*GAMA*SUM3
       SUM5 = EXP(-GAMA*RO**2.)*SUM5
C
      FOFX = P(IP) - SUM1 - SUM3
      FOFDX= -SUM2 + SUM4 - SUM5
      ROP1 = RO - FOFX/FOFDX
      ERROR = ROP1 - RO
      DENS(IP) = RO*44/1000
C
      IF(DENS(IP) .GT. .1) THEN
      SOL(IP) = (DENS(IP)**ALPHA)*EXP(BETA)
      ELSE
```

```
      SOL(IP) = 0.0
      END IF
      RETN(IP)= SOL(IP)*DENS(IP)*0.5*1000
C       WRITE(*,*) 'PRE, DEN, SOL',PRES(IP,JP),DENS(IP,JP),ERRR
 99   FORMAT(2X, 3F12.5)
      IF (ABS(ERROR) .GT. ESP .AND. NC .LT. NITER) THEN
      RO = ROP1
      GO TO 5
      ELSE
      GOTO 120
      ENDIF
 120    NC = 0
 135 CONTINUE
 130 CONTINUE
C
       SUM = 0
       DO 143 I = 1, 20
       RET = RETN(I) - (RETN(I) - RETN(I+1))/2
 143   SUM = SUM + RET
       SUM = SUM*0.025
       WRITE(*,*) 'TIME', TM,'RETENTION =', SUM
       RETEN = SUM
       RETURN
C
      END
```